TECHNISCHE UNIVERSITÄT MÜNCHEN

Fachgebiet für Obstbau

Mass Spectrometry Compatible Enzymatic Assays: Miniaturisation, Automation and Applications

Romy Katharina Scheerle

Vollständiger Abdruck der von der Fakultät Wissenschaftszentrum Weihenstephan für Ernährung, Landnutzung und Umwelt der Technischen Universität München zur Erlangung des akademischen Grades eines

Doktors der Naturwissenschaften

genehmigten Dissertation.

Vorsitzender:		Univ.-Prof. Dr. D. R. Treutter
Prüfer der Dissertation:	1.	Priv.-Doz. Dr. T. Letzel
	2.	Univ.-Prof. Dr. M. Rychlik

Die Dissertation wurde am 31.01.2013 bei der Technischen Universität München eingereicht und durch die Fakultät Wissenschaftszentrum Weihenstephan für Ernährung, Landnutzung und Umwelt am 27.05.2013 angenommen.

Contents

Abbreviations **3**

Abstract **4**

Zusammenfassung **5**

1 Introduction **6**

1.1 Analytical Developments of Enzymological Techniques **6**

1.2 Continuous-Flow Setups with Direct Infusion **9**

1.3 Miniaturised and Automated Setups **10**

1.4 Continuous-Flow Mixing Setups **11**

2 Aims of the Study **14**

3 Material and Methods **15**

3.1 Chemicals **15**

3.2 Measurement of Enzymatic Assays **17**

3.2.1 Photometric Setup 17

3.2.2 Direct Infusion Setup 19

3.2.3 NanoESI Robot Setup 20

3.3 Measurements in Continuous-Flow Mixing Setups **22**

3.3.1 Online Electrochemistry 22

3.3.2 High Temperature Liquid Chromatography 23

3.4 Mass Spectrometric Instrumentation **26**

3.5 Data Analysis **27**

4 Results and Discussion **29**

4.1 Establishment of Mass Spectrometry Compatible Enzymatic Assays **29**

4.1.1 Adaption from Classical Photometric Approaches to Continuous-Flow Mass Spectrometry 29

4.1.1.1 Exemplification with ATPase Assay 30

4.1.1.2 Further Mass Spectrometry Compatible Enzymatic Assays 33

4.1.2 Optimisation of Mass Spectrometry Compatible Enzymatic Assays 35

4.1.2.1 Impact of Organic Solvent on Enzymatic Conversion 36

4.1.2.2 Impact of Multiplexing on Enzymatic Conversion 39

4.1.3 Summary 43

4.2 Automation and Miniaturisation of Mass Spectrometry Compatible Enzymatic Assays 45

4.2.1 Measurement of Enzymatic Assays in the nanoESI Setup 'Infusion' 46
4.2.1.1 Spray Instability 47
4.2.1.2 Impairment of the Enzymatic Activity 48

4.2.2 Measurement of Enzymatic Assays in the Modified nanoESI setup 'Flow-Control' 49

4.2.3 Measurement of Enzymatic Assays in the Modified nanoESI setup 'LC Coupling' 50

4.2.4 Summary 52

4.3 Technical Applications with Mass Spectrometry Compatible Enzymatic Assays 54

4.3.1 Continuous-Flow Assays with Direct Infusion 54

4.3.1.1 Determination of Cleavage Specifities of Chitinases 55

4.3.1.2 Determination of the Hydrolysis Profile of Csn1794 58

4.3.1.3 Investigation of the Myeloperoxidase Assay 61

4.3.2 Continuous-Flow Assays with nanoESI Robot Infusion 66

4.3.3 Continuous-Flow Mixing Assays 67

4.3.3.1 Cleavage Mechanism of Csn1794 68

4.3.3.2 Determination of Enzyme-Regulatory Compounds in House Dust Extracts 70

4.3.4 Summary 75

5 Conclusion 76

6 References 77

Acknowledgements 88

Scientific Communications 89

Curriculum Vitae 91

Appendix 92

Abbreviations

A_2D_2	di-N-acetylchitotetraoses ADAD, ADDA, DDAA, DADA and DAAD with D = GlcN and A = GlcNAc
AChCl	acetylcholine chloride
AChE	acetylcholinesterase
Ala	alanine
AtChiC	chitinase from *Arabidopsis thaliana*
ATCI	acetylthiocholine iodide
ATP	adenosine 5'-triphosphate
ATPase	adenosine 5'-triphosphatase
BcChiA	chitinase from *Bryum coronatum*
ChiC	chitinase from *Streptomyces griseus*
Chy	α-chymotrypsin
CrChiA	chitinase from *Cycas revoluta*
Csn1794	chitosanase from *Paenibacillus* sp. 1794
DTNB	5,5´-dithiobis(2-nitrobenzoic acid)
EGCG	epigallocatechin gallate
ESI	electrospray ionisation
GC	gas chromatography
Glc	D-glucose
GlcN	D-glucosamine
GlcNAc	N-acetyl-D-glucosamine
HEWL	hen egg white lysozyme
HPLC	high performance liquid chromatography
HT-HPLC	high temperature HPLC
Leu	leucine
MMI	multimode ionisation
MPO	myeloperoxidase
MS	mass spectrometry
m/z	mass-to-charge
NE	elastase from human neutrophils
NtChiV	chitinase from *Nicotiana tabacum*
PE	elastase from porcine pancreas
Phe	phenylalanine
pNA	p-nitroanilide
Pro	proline
RSC-c	chitinase from *Secale cereal*
Tyr	tyrosine
Val	valine

Abstract

In recent years, mass spectrometry has become a well-established analytical technique for studying enzymatic reactions. Enzymological applications are of interest in many fields such as food analysis or in pharmaceutical, environmental and clinical research.

The current work presents new technical developments, strategies and applications for studying enzymatic assays by continuous-flow mass spectrometry.

Various enzymatic assays were optimized and established for real-time mass spectrometric measurements: the glycosidases hen egg white lysozyme, chitinases and chitosanases, the proteases chymotrypsin, elastase from pancreas and from neutrophils, ATPase, acetylcholinesterase and myeloperoxidase were adapted and modified from classical spectroscopic detection to mass spectrometric detection. The continuous-flow monitoring of enzymatic assays in a robotic nanoESI setup was realized for the first time and offers a powerful analytical technique. The system enables a miniaturised and automated measuring of enzymatic assays and provides a prospective basis for the efficient and methodological development and investigation of enzymatic assays.

The combination of diverse instrumental modules with enzymatic assays led to beneficial and innovative technological setups for studying enzymological issues in continuous-flow mixing setups. Direct infusion experiments were carried out for characterisation of enzymes regarding reaction cleavage specifities, reaction profiles and investigation of enzyme inhibitors. The combination of enzymatic assays with a high temperature-HPLC module enabled the screening of complex mixtures on enzyme-regulatory effects. The online coupling of an instrument for electrochemical reaction was used to obtain a deeper insight into the enzymatic reaction mechanism.

The current work illustrates research strategies for the establishment and investigation of enzymatic reactions by mass spectrometry and shows possibilities for their appropriate usage in further technological applications. Limitations and benefits of the respective technical setups are presented. The obtained results give important information for using enzymatic assays in environmental, pharmaceutical or medical issues and for the utilization of the enzymes in biotechnology.

Zusammenfassung

Die Massenspektrometrie hat sich in den letzten Jahren zu einer fest etablierten Technik für die Untersuchung von Enzymreaktionen entwickelt. Enzymologische Studien finden in vielen Bereichen Anwendung, z.B. in der Lebensmittelanalytik, in der pharmazeutischen, umweltanalytischen oder klinischen Forschung.

Die vorliegende Arbeit zeigt neue technische Entwicklungen, Strategien und Anwendungsmöglichkeiten für die massenspektrometrische Untersuchung von Enzymreaktionen in kontinuierlichen Flusssystemen.

Ausgehend von klassischen spektroskopischen Methoden wurden diverse Enzymassays an die massenspektrometrische Detektion angepasst und optimiert: Lysozym aus Hühnereiweiß, verschiedene Chitinasen und Chitosanasen, die Proteasen Chymotrypsin, Elastase aus dem Pankreas und aus Neutrophilen, ATPase, Acetylcholinesterase und Myeloperoxidase. In dieser Arbeit wurde die kontinuierliche Messung von Enzymassays in einem nanoESI Robotiersystem zum ersten Mal umgesetzt. Das System bietet eine vielversprechende Messtechnik und dient als Basis für die effiziente und systematische Entwicklung und Untersuchung von Enzymassays.

Innovative technologische Setups, bestehend verschiedenen instrumentellen Messmodulen in Kombination mit Enzymreaktionen, wurden für die Untersuchung von enzymologischen Fragestellungen in kontinuierlichen Flusssystemen herangezogen. Die umfangreiche Chakterisierung von Enzymen erfolgte hinsichtlich Substratspezifität, Reaktionsprofil und Inhibitionsstudien. Das Screening von komplexen Mischungen auf enzymregulatorische Effekte wurde in einer Kombination von Enzymassays mit einem Hochtemperatur-HPLC Modul ermöglicht. Die Anwendung eines Instruments zur elektrochemischen Reaktion direkt im kontinuierlichen Fluss ermöglichte einen weiteren detailierten Einblick in den Enzym-Reaktionsmechanismus.

Die vorliegende Arbeit zeigt Strategien zur Etablierung und Untersuchung von Enzymreaktionen mittels Massenspektrometrie. Möglichkeiten für die geeignete Nutzung in weiterführenden technologischen Anwendungen werden vorgestellt und Grenzen sowie Vorteile der jeweiligen Setups werden aufgezeigt. Die Ergebnisse bieten wichtige Informationen für die Nutzung von Enzymassays in biotechnologischen, umwelt-analytischen, pharmazeutischen oder medizinischen Fragestellungen.

1 Introduction

Enzymes are specialized proteins with a powerful catalytic activity. Manifold biological functions in metabolism are fulfilled and a wealth of chemical reactions is catalyzed by enzymes. They play an important role in industrial applications: food analysis and food technology, e.g. brewing or dairy industry, in the biotechnological, cosmetics and detergents industry as well as in pharmaceutical and medical research (Chaplin and Bucke, 1990; Belitz and Grosch, 1999; Kirk et al., 2002). In recent years studies with enzymatic reactions became an emerging research area, regarding the enzymatic activity, finding new substrates, reaction pathways and inhibition studies.
In this work a number of enzymatic assays was established for mass spectrometric detection and implemented in new technological setups for using them in diverse enzymological applications. Enzymes of different classes and sub-classes were chosen, regarding actual projects and the associated bioanalytical and biotechnological issues. The following section gives an overview of the latest developments in analytical techniques for enzymological research, ranging from classical to more complex and new technological setups. A schematic overview of classical approaches and new technological setups is given in Figure 3 in chapter 2.

1.1 Analytical Developments of Enzymological Techniques

Different classical detection methods have been established for the investigation of enzymatic reactions: spectroscopic, electrochemical or radiometric assays (Eisenthal and Danson, 2002). Most enzymatic assays are based on photometric or fluorescence detection. Numerous applications with spectroscopic detection methods have been described in detail due to the easy handling, moderate costs and the accuracy of the method (Bisswanger, 2007). Thereby, during enzymatic reaction monitoring, chromophores and fluorophores have to be added to or eliminated from the substrate and in most cases the product formation is detected (Figure 3A). The major drawback of such assays is the necessity of artificial substrates which request substrates with optical properties. These substrates may affect the reaction rate and/or kinetics of the enzymatic reaction (Wallenfels, 1962; Bothner et al., 2000; Letzel et al., 2011). In contrast to spectroscopic detection, mass spectrometric detection is independent of chromogenic and fluorogenic labeled substrates.

Moreover it depends on the mass-to-charge (m/z) ratio of the ionized analytes. The simultaneous identification of substrate, intermediates and products, in some cases also the enzyme and enzyme complexes are feasible by their different m/z (Figure 3 F). The differences of photometric and mass spectrometric investigation of enzymatic assays and the respective key benefits of the techniques are summarized in Table 1.

Table 1: Overview of benefits, drawbacks and conditions for the measurement of enzymatic assays with photometric and with mass spectrometric detection.

parameter	***photometry***	***mass spectrometry***
buffer	often use of biological buffer in high concentrations, e.g. 100 mM phosphate buffer (Bisswanger, 2007)	low concentrated volatile buffer required, e.g. 10 mM NH_4Ac (Dennhart and Letzel, 2006)
substrate	substrates with chromophoric group or coupled coloured reactions required	natural substrates possible and often better than labeled substrates (Bothner et al., 2000; Letzel et al., 2011)
pH	pH optimum and also more extreme pH values can be used (Bisswanger, 2007)	pH has to be adjusted regarding the efficient ionization of molecules (Dennhart and Letzel, 2006)
special additives, e.g. salts	normally do not influence the detection	volatile compounds required; high concentrations may lead to signal suppression and cause changes in adduct formation, e.g. $[M + Na]^+$
enzyme and substrate concentrations	no limit when detectable compounds in the absorption range	low concentrations possible, e.g. 10 µM substrate and 1 µM enzyme high concentrations may lead to signal suppression
detectable compounds	only label-containing compound, i.e. substrate depletion or product formation can be monitored	real-time measurement of the enzymatic reaction and detection of multiple compounds, i.e. substrate, product, intermediates (Dennhart and Letzel, 2006)

Recent studies established electrospray ionisation mass spectrometry (ESI-MS) as an appropriate and widespread tool for studying enzymatic reactions. Publications implementing the terms ‘enzyme’ and ‘mass spectrometry’ in the title and/or abstract increased sharply as from 2000, whereas the publications with the terms ‘enzyme’ and ‘photometry’ remained at a constant level (Figure 1).

Mass spectrometry is used in many analytical laboratories and the reader is referred to interesting review articles (Geoghegan and Kelly, 2005; Liesener and Karst, 2005a; de Boer et al., 2007; Greis, 2007; Shipovskov and Reimann, 2007; Letzel, 2008). Studying enzymatic

reactions by mass spectrometry resulted in the determination of kinetic parameters, reaction pathways or regulator identification (Northrop and Simpson, 1997; Ge et al., 2001; Dennhart et al., 2008; Dennhart et al., 2009). Furthermore, mass spectrometric detection is an essential analytical tool in (functional) proteomics. In our days the research of protein functions like detection of covalent and noncovalent complexes uses mass spectrometry (Ganem et al., 1991; Benesch and Robinson, 2006; Weigang et al., 2008) and deals with topics such as protein quantification and sequencing, the location of posttranslational modifications and protein structure (Kouach et al., 1994; Bantscheff et al., 2007; Reinders and Sickmann, 2007; Sharon and Robinson, 2007). In a recently published article we reviewed the progress and the trends in mass spectrometry based enzymological applications (Appendix I).

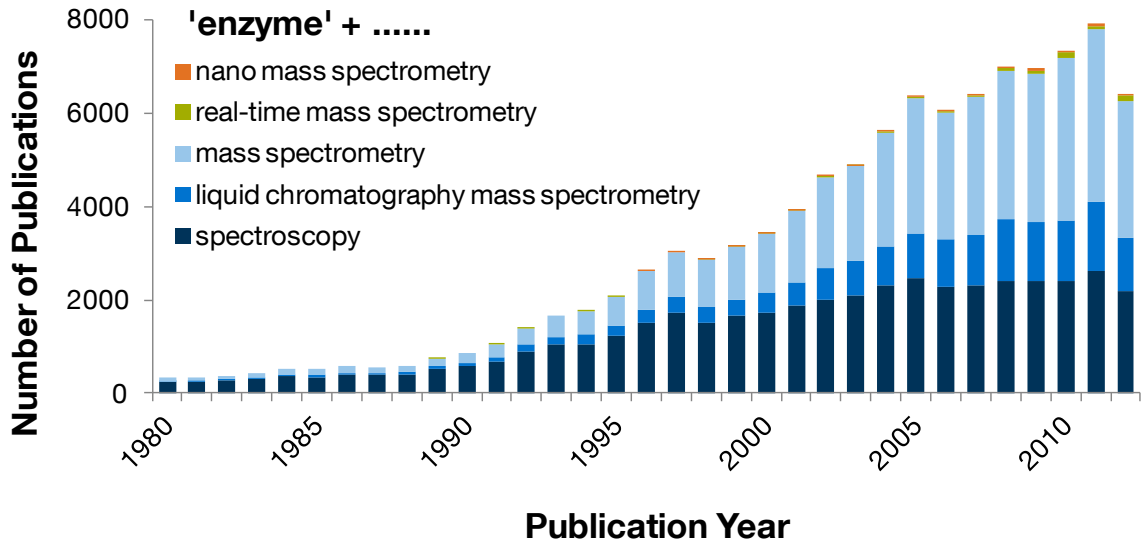

Figure 1: Number of publications with the term 'enzyme' and different detection methods mentioned in the legend. The source for the data from 1980 to 2012 was the 'Scopus' (Elsevier) search in the title and abstract.

The following section presents different technical setups and their applicability for monitoring enzymatic assays by mass spectrometry: continuous-flow measurements with direct infusion, measurements in nanoESI setups and in continuous-flow mixing setups. Table 2 summarizes the versatile areas of applications of the setups and the investigated enzymes with regard to the relevance to the current work.

1.2 Continuous-Flow Setups with Direct Infusion

Typically, enzymatic reactions are conducted either in a single reaction tube or a well plate and after a defined time point the reaction is quenched and the reaction mixture directly analyzed by mass spectrometry (Ge et al., 2001; Pi et al., 2004; Liesener and Karst, 2005a) or after a high-performance liquid chromatographic separation (HPLC) (Fukamizo et al., 1995; Fukamizo et al., 2006). Some recently published reviews discussed high-throughput screening assays which have been conducted in combinations with enzyme, substrate and inhibitors, respectively (Geoghegan and Kelly, 2005; Liesener and Karst, 2005a; de Boer et al., 2007; Greis, 2007; Schluter et al., 2008; Shi et al., 2009). The most notably benefit of the (LC)/MS setup is the information about the concentration of substrate and (intermediate) product(s) at defined time points in one single experiment (Figure 3B). Another promising approach which has been developed is the continuous-flow monitoring of enzymatic reactions in real-time. Publications with the terms ‘enzyme’ and ‘real-time mass spectrometry’ show a distinct and constant increase as of the year 2000 (Figure 2).

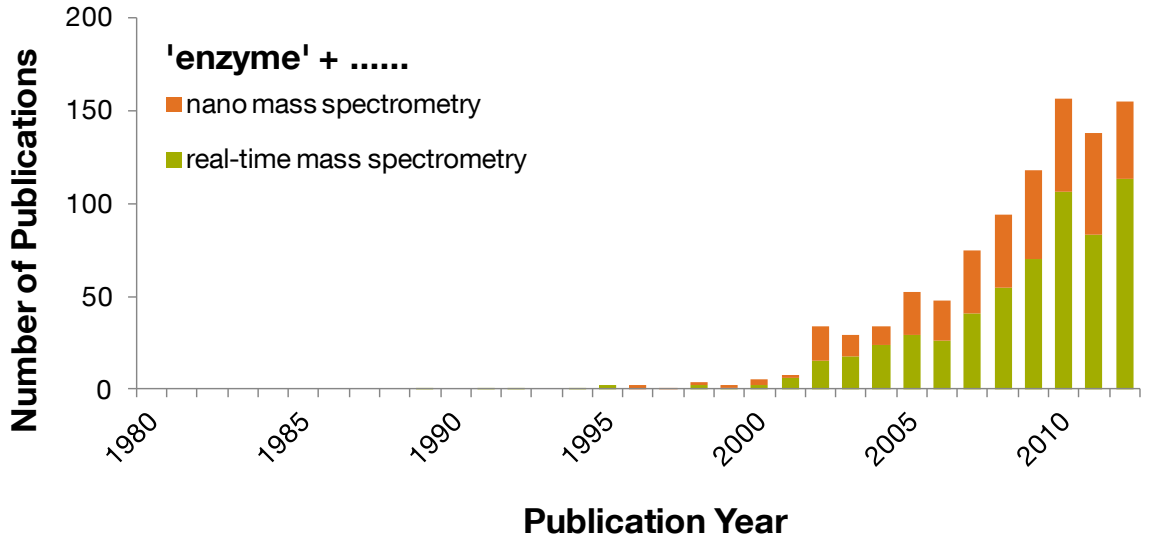

Figure 2: Number of publications with the term 'enzyme' and ‘real-time mass spectrometry’ or ‘nano mass spectrometry’ in the title and/or abstract. The source for the data from 1980 to 2012 was a 'Scopus' search (Elsevier).

The real-time monitoring was developed by Lee and coworkers in 1989, who coupled a continuous-flow system to a mass spectrometer for real-time reaction monitoring of lactase, α-chymotrypsin and leucine aminopeptidase (Lee et al., 1989). The principal setup

for these measurements consists of a direct infusion connection to the mass spectrometer (Figure 3C). A syringe pump constantly delivers the reaction mixture to an ESI source of the mass spectrometer. This kind of measurement is less time consuming than conventional approaches and the reaction solution is measured continuously without additional quenching step. Such continuous-flow assays give information about different enzymatic mechanisms in real-time, are used to investigate kinetic parameters and noncovalent binding complexes and to elucidate the influence of inhibitory substances on enzymatic activity (Ganem et al., 1991; Zechel et al., 1998; Wilson and Konermann, 2004; de Boer et al., 2005c; Gao et al., 2005; Pi et al., 2005; Dennhart and Letzel, 2006; de Boer et al., 2007; Greis, 2007; Dennhart et al., 2008). Using this assay scheme, different sugar hydrolyzing enzymes have been studied, i.e. lysozyme, chitinases and chitosanases (Ganem et al., 1991; Zechel et al., 1998; Clark and Konermann, 2004a; Clark and Konermann, 2004b; Dennhart and Letzel, 2006; Dennhart et al., 2008; Dennhart et al., 2009). Measurements with the glycosidases showed, that the hydrolysis profile of conventional HPLC experiments is basically in agreement with data obtained by ESI-MS experiments. The enzymatic activity in mass spectrometric experiments is typically lower than obtained in HPLC measurements which can be explained by different assay parameters for ESI-MS, e.g. temperature, lower enzyme and substrate concentrations and buffer conditions (Masaki et al., 1981; Fukamizo et al., 1986). Further real-time ESI approaches determined kinetic parameters and the enzymatic hydrolysis of substrates of glutathione S-transferase (Ge et al., 2001), lactase, chymotrypsin, leucine aminopeptidase (Lee et al., 1989) and a thioesterase (Li et al., 2009). In a recently published work, Yu and coworkers monitored the pepsinolysis and trypsinolysis of cytochrome c in real-time using a ‘probe ESI-MS’ system (Yu et al., 2012). The different examples illustrate the widespread opportunities offered by continuous-flow ESI-MS. For a comparison of the main benefits and shortcomings of LC/MS and real-time mass spectrometric measurements the reader is referred to a recently published manuscript (Table 10.1 in Appendix II).

1.3 Miniaturised and Automated Setups

New technologies in automation and miniaturisation of mass spectrometry based analytical techniques provide considerable advantages for studying enzymatic reactions by nanoESI-MS. High sample throughput, timesaving and low sample volume are the most notable benefits of nanoESI-MS systems in comparison to conventional ESI-MS with direct

infusion. Thus, in recent years robotic and chip-based nanoESI-MS systems have been established in mass spectrometry (Wilm and Mann, 1994; Wilm and Mann, 1996; Schultz et al., 2000; Yang et al., 2004b; Svobodova et al., 2010) (Figure 3D). The sharp increase of publications with the term 'enzyme' and ‘real time mass spectrometry’ as of 2002 is clearly recognizable in Figure 2. Studies with nanoESI-MS illustrated the successful application in protein identification (Van Pelt et al., 2002; Zhang et al., 2003a), carbohydrate analysis (Froesch et al., 2004), inhibition studies (Benetton et al., 2003; Jecklin et al., 2009), detection of noncovalent complexes (Keetch et al., 2003; Zhang et al., 2003b; van den Heuvel et al., 2005; Jecklin et al., 2008) or the fundamental applicability for real-time monitoring of enzymatic reactions (van den Heuvel et al., 2005).

The systematic online monitoring of enzymatic reactions with a continuous-flow by a nanoESI-MS robot system was not described in literature up to now. A miniaturised and automated setup for monitoring enzymatic reactions would offer several advantages compared to LC/(MS) or direct infusion experiments. Enzyme, substrate and additional compounds, e.g. cofactors could be mixed automatically. The systematical testing of different combinations and concentrations of all reaction compounds as well as buffer solutions and pH values would be possible. Particularly for expensive or specially produced enzymes which are only available in small amounts those miniaturised systems can pose an interesting setup due to small sample amounts and high sensitivity. A comparison of the benefits and shortcomings of LC/MS, direct infusion with syringe pump and robot measurements is given in a recently published manuscript (Table 10.1 in Appendix II).

1.4 Continuous-Flow Mixing Setups

The screening of large compound libraries (e.g. drugs, pesticides, allergens) or complex mixtures of unknown composition (e.g. natural extracts from plants or environmental material) for potential enzyme regulators is a further emerging research topic. Screening methods might support the exploration of new drug candidates, food ingredients or environmental compounds. Not only the identification of compounds but also the identification of enzyme activities in mixtures (e.g. human plasma, protein fractions or blood) is of interest (Jankowski et al., 2001; Schluter et al., 2003). Advances in separation techniques combined with enzymatic assays and mass spectrometric detection lead to increasing importance of online coupled setups and have already been studied with acetylcholinesterase, phosphodiesterase, cytochrome P450, glutathione-S-transferase and

cathepsin B (Schenk et al., 2003b; de Boer et al., 2004; de Jong et al., 2006; Liesener et al., 2007; Kool et al., 2011) (Figure 3E and G). Different techniques for the online detection of inhibitor activity, identity and the developments in post-column complex mixture screening and the role of mass spectrometry have been reviewed (Shi et al., 2009; Kool et al., 2011). An innovative tool for the effective coupling of chromatographic separation to enzymatic assays was described by De Boer and coworkers who used high-temperature HPLC (HT-HPLC) (de Boer et al., 2005a). A recently published review gives an overview about the application of mass spectrometry to investigate enzymological issues regarding complex mixtures (Appendix I). Main discussed topics are experiments for the identification of inhibitors and/or endogenous substrates and proteins which act as enzymes in complex mixtures and sample-handling strategies are presented (Figure 1 and 2 in Appendix I).

Table 2: Enzymological research experiments with mass spectrometric detection. The selective overview especially refers to investigations of reaction profiles and the respective applications.

enzymes	*focus of the method*	*reference*
real-time measurements - quenched partitioned assays		
RNase A and β-galactosidase	LC/MS for determination of kinetic parameters	(Hsieh et al., 1995)
β-1,4-galactosyltransferase	ESI-MS detection of product formation depending on inhibitors	(Wu et al., 1997)
α-glucosidase and lipoprotein lipase	ESI-MS for determination of kinetic parameters	(Bothner et al., 2000)
glutathione S-transferase	ESI-MS for determination of kinetic parameters	(Ge et al., 2001)
protein kinase A	development and optimisation of the assay for ESI-MS	(de Boer et al., 2005c)
5α-reductase	GC/MS for evaluation of the enzymatic activity	(Amaral et al., 2012)
real-time measurements – without quenching		
lactase, α-chymotrypsin and leucine aminopeptidase	ESI-MS for determination of enzymatic hydrolysis	(Lee et al., 1989)
xylanase	ESI-MS for determination of kinetic parameters	(Zechel et al., 1998)
chymotrypsin	ESI-MS for determination of kinetic parameters	(Wilson and Konermann, 2004)
hen egg white lysozyme, chitinases and chitosanases	ESI-MS for monitoring enzymatic hydrolysis and determination of kinetic parameters	(Dennhart and Letzel, 2006; Dennhart et al., 2008; Dennhart et al., 2009; Taira et al., 2010), results of this work, Appendix VI)
pepsin and trypsin	probe ESI-MS for monitoring enzymatic hydrolysis	(Yu et al., 2012)
hen egg white lysozyme, chitinase, chymotrypsin, elastase, acetylcholinesterase	ESI-MS for monitoring enzymatic hydrolysis in the presence of organic solvents and multiplexing	(results of this work, Appendix IV)
miniaturised and automated setups		
DNase	nanoESI-MS for monitoring of enzymatic DNA hydrolysis (partially with stopping of the reaction)	(van den Heuvel et al., 2005)
hen egg white lysozyme, chitinase, chymotrypsin, acetylcholinesterase	nanoESI-MS for monitoring of enzymatic reactions	(results of this work, Appendix III)
continuous-flow mixing setups		
phosphodiesterase	screening on inhibitors in bacteria, fungi and plant extracts	(Schenk et al., 2003b)
cathepsin B	screening of a red clover extract spiked with known inhibitors and a nonspiked fungi extract for enzyme active compounds	(de Boer et al., 2004)
acetylcholinesterase	screening on inhibitors in natural Narcissus extract	(de Jong et al., 2006)
glutathione-S-transferase	screening on substrates and inhibitors	(Kool et al., 2007)

2 Aims of the Study

The present study focused on sample handling and technological strategies for establishing enzymatic assays with mass spectrometric detection and their strategic utilization in further technological setups (Figure 3). The development and optimization of a wide range of mass spectrometry compatible enzymatic assays was based on classical photometric approaches. The choice of the enzymes was related on their relevance in pharmaceutical, environmental and food issues, respectively. The systematic implementation of the assays in new technical setups should be tested and evaluated, thereby revealing limits and possibilities. In regard to high throughput screening experiments the work aimed on the implementation of enzymatic assays in a miniaturised and automated nanoESI system. The study further focused on the utilization of the established mass spectrometry compatible assays in diverse technological setups for the investigation of enzymological issues. The knowledge about handling enzymes in mass spectrometric setups with the appropriate application in technological instruments should be combined.

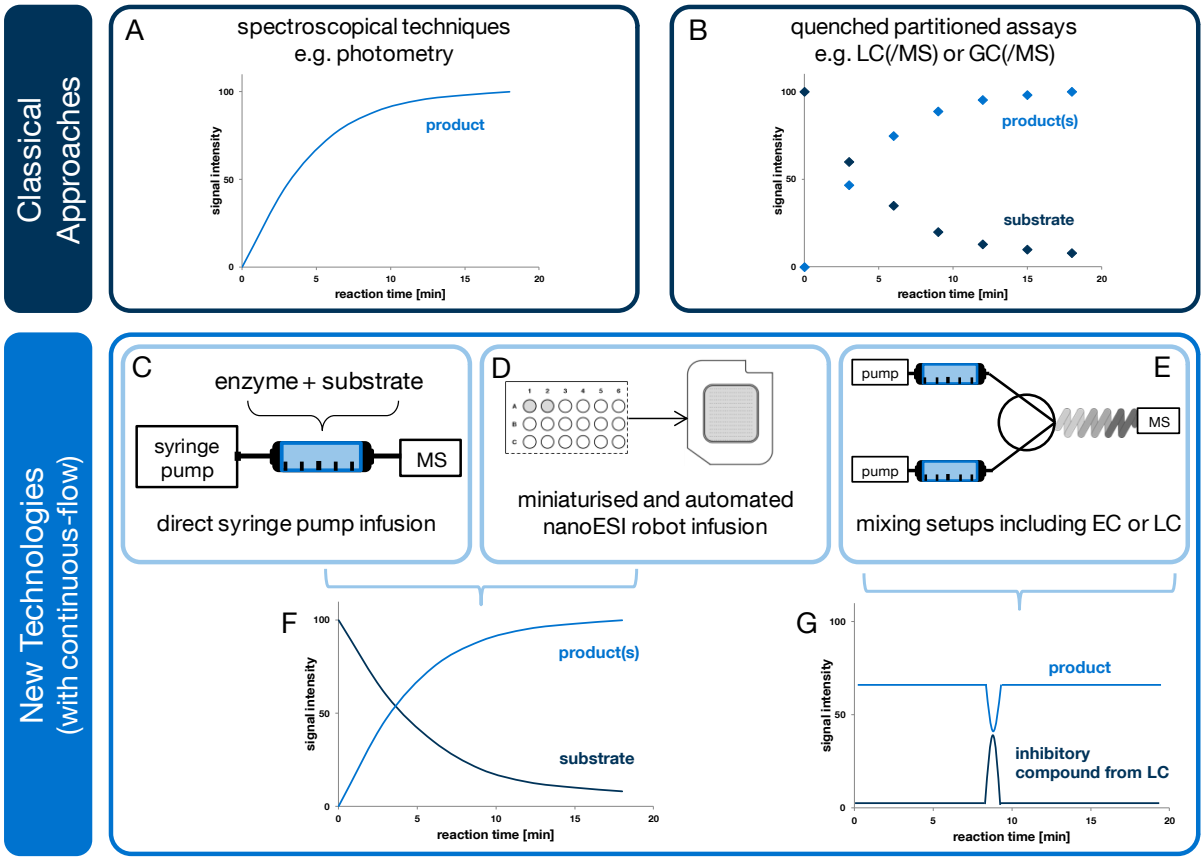

Figure 3: Overview of classical approaches and new technological setups for studying enzymatic assays by continuous-flow mass spectrometry. The figure schematically shows the setups of new technological combinations and the corresponding resulting data.

3 Material and Methods

3.1 Chemicals

Enzymes

Acetylcholinesterase from Electrophorus electricus type VI-S (AChE, Enzyme Commission (EC) number 3.1.1.7, relative molecular weight (M_w) ~280 kDa), adenosine 5'-triphosphatase from porcine cerebral cortex (ATPase, EC 3.6.1.3, M_w ~150 kDa), chitinase from Streptomyces griseus (ChiC, EC 3.2.1.14, M_w ~30 kDa), α-chymotrypsin from bovine pancreas (Chy, EC 3.4.21.1, M_w ~25 kDa), elastase from porcine pancreas (PE, EC 3.4.21.36, M_w ~25 kDa) and hen egg white lysozyme (HEWL, EC 3.2.1.17, M_w ~14 kDa) were obtained from Sigma-Aldrich (Steinheim, Germany). Elastase from human neutrophils (NE, EC 3.4.21.37, M_w ~30 kDa) was purchased from BioCentrum (Krakow, Poland). Myeloperoxidase from purulent human sputum (MPO, EC 1.11.2.2, M_w ~59 kDa) was obtained from Molecular Innovations Inc. (Peary Court, MI, USA). Chitosanase from *Paenibacillus* sp. 1794 (Csn1794, EC 3.2.1.132, M_w ~40 kDa) was obtained from Prof. Ryszard Brzezinski (Département de Biologie, Université de Sherbrooke, Canada). Diverse wild-type (WT) and mutated chitinases (Chi, EC 3.2.1.14) were obtained from Prof. Tamo Fukamizo (Department of Advanced Bioscience, Kinki University, Japan): chitinase from *Nicotiana tabacum* (NtChiV_WT and NTChiV_G74W), chitinase from *Arabidopsis thaliana* (AtChiC_WT and AtChiC_G75W), chitinase from palm, *Cycas revoluta* (CrChiA_WT and CrChiA_G77W), chitinase from rye seeds, *Secale cereal* (RSC-c_WT and RSC-c_E67Q (inactive)) and chitinase from moss, *Bryum coronatum* (BcChiA_WT and BcChiA_E61A (inactive)).

Substrates

Substrate for AChE, acetylcholine chloride (AChCl, M_w 181.7 Da), substrate for ATPase, adenosine 5'-triphosphate disodium salt hydrate (ATP, M_w 551.1 Da), substrate for NE with chromogenic group p-nitroaniline (N-Suc-Tyr-Leu-Val-pNA, M_w 181.7 Da), substrate for PE (N-Succinyl-Ala-Ala-Ala-pNA, M_w 451.4 Da), substrate for MPO, L-tyrosine (Tyr, M_w 181.2 Da) were obtained from Sigma-Aldrich (Steinheim, Germany). Substrate for Chy (Ala-Ala-Pro-Phe-pNA, M_w 520.4 Da) was obtained from LOXO (Dossenheim, Germany). Substrates for chitinases and chitosanase, chitosan oligosaccharides ($(GlcN)_n$, ß-1,4-linked D-glucosamine oligosaccharides with a polymerization degree of n = 1-6) and chitin

oligosaccharides ($(GlcNAc)_n$, ß-1,4-linked N-Acetyl-D-glucosamin with a polymerization degree of n = 1-6) were purchased from Seikagaku Kogyo Co. (Tokyo, Japan). Cello-oligosaccharides ($(Glc)_n$, ß-1,4-linked D-glucose oligosaccharides with a polymerization degree of n = 3, 4 or 6) were purchased from Coring System Diagnostix (Gernsheim, Germany). Isomers of di-*N*-acetylchitotetraoses (AADD, ADDA, ADAD, DADA, DAAD, and DDAA, with A = GlcNAc and D = GlcN) were obtained from Prof. Martin Peter (University Potsdam, Institute of Chemistry, Potsdam, Germany).

Inhibitors and extracts

The inhibitor for AChE, galanthamine hydrobromide from *Lycoris* sp. (M_w 368.3 Da) and the inhibitor for MPO, epigallocatechin gallate (EGCG, M_w 458.4 Da) were purchased from Sigma-Aldrich (Steinheim, Germany).

Diverse house dust samples were used for screening experiments. The samples were prepared and analyzed at the 'Institut für Energie- und Umwelttechnik e.V.' (IUTA, Duisburg, Germany) as follows: 0.5 g house dust was sifted and the fraction with particles ≤ 63 µm was extracted with 5 mL methanol/H_20 (84:16). 1 mL was evaporated and resolved in methanol/H_2O (20:80) to reduce the organic solvent part. The different types of samples with further information about the composition are presented in Table 3 (personal communication with IUTA).

Table 3: Overview of house dust extract samples with different composition. The samples were used for screening on regulatory compounds in a continuous-flow mixing setup with a HT-HPLC module.

sample	***origin of the extract and further information***
dust 1	mixed dust extract of samples from 171 households, no visible mould in households
dust 2	sample from mildewed wallpaper with infestation of *Aspergillus versicolor, Cladosporium cladosporoides* and *Penicillium chrysogenum,* detection of 485 ng/mL sterigmatocystin
dust 3	sample from mildewed dust with infestation of *Stachybotrys chartarum*

Additional Chemicals

Unless otherwise stated all chemicals were purchased from Sigma-Aldrich, VWR, AppliChem or Merck and of high purity grade. LC/MS grade water and ammonium acetate (NH_4Ac) were used for preparation of solutions. Ammonia or acetic acid was used for pH adjustment. Organic solvents acetone, acetonitrile, ethanol, methanol and 2-propanol were of LC/MS grade purity. Chemicals for ATPase assay were: ammonium heptamolybdate,

magnesium acetate ($MgAc_2$), magnesium chloride ($MgCl_2$), malachite green oxalate, polyvinyl alcohol, potassium acetate (KAc), potassium chloride (KCl), sodium acetate (NaAc), sodium chloride (NaCl), tris(hydroxymethyl)aminomethane (Tris). The following chemicals were used for MPO assay: ammonium chloride (NH_4Cl), hydrogen peroxide (H_2O_2) and sodium nitrite ($NaNO_2$). Acetylthiocholine iodide (ATCI) and 5,5'-dithiobis(2-nitrobenzoic acid) (DTNB) were used for photometrical AChE assay.

3.2 Measurement of Enzymatic Assays

Enzymatic assays were measured by photometry, in a direct infusion setup with syringe pump or in a new approach with a nanoESI setup. The methods are described in detail in the following section.

3.2.1 Photometric Setup

Photometrical measurements of enzymatic assays were carried out for first adjustments towards mass spectrometric requirements. Several parameters were tested systematically for the adaption of the enzymatic assays from the classical photometric assay to the mass spectrometer, e.g. concentrations, buffer, pH and additional compounds such as salts. The Spectra III instrument from SLT Labinstruments (Crailsheim, Germany) with XReadPlus evaluation software was used for measurement of enzymatic assays by photometry. Samples were prepared and measured in 96 well plates (Greiner Bio-One, Solingen, Germany). The reactions were monitored at laboratory temperature with 1 cycle/min for 30 min. The final concentrations for photometric experiments are shown in the results section in Table 7.

AChE

The photometric reaction of AChE was monitored by using the artificial thiol ester ATCI instead of AChCl, which was used for mass spectrometric measurements. AChE hydrolyses the ATCI to the substrate thiocholine which reduces DTNB to a coloured nitrobenzoate with absorption at 405 nm (Ellman et al., 1961; Ingkaninan et al., 2003). The final assay volume was 250 µL with the final concentrations of 200 µM DTNB, 200 µM ATCI and 2.4 nM AChE.

All solutions were prepared and diluted in 10 mM NH_4Ac (pH 7.4). Immediately after mixing all components the reaction solution was monitored at 405 nm.

ATPase

The activity of ATPase was investigated by means of a colorimetric detection of phosphate released through enzymatic activity (Itaya and Ui, 1966; Baykov et al., 1988; Singh and Shukla, 2003). A malachite green reagent consisting of H_2O/0.08% malachitgreen oxalate/2.3% polyvinyl alcohol/5.7% ammonium heptamolybdate (2:2:1:1) was used for the detection of free phosphate in solution. As a starting point a classical 'standard' assay, according to literature data was used: 0.2 mM ATP, 0.5 µM ATPase, 120 mM NaCl, 20 mM KCl and 4.5 mM $MgCl_2$ in 100 mM Tris buffer (pH 7.4) (Robinson et al., 1984; Henkel et al., 1988; Rowlands et al., 2004). For the adaption of the ATPase assay for mass spectrometry, several parameters were changed: replacement of Tris buffer by NH_4Ac buffer, replacement of the three relevant ions Na^+, K^+ and Mg^{2+} as chlorides by the respective acetates and reduction of buffer and salt concentrations. Further optimisation was carried out: pre-incubation of enzyme and salts for 0 min or 10 min and reaction at 20°C±2°C or 37°C±2°C. For all measurements the enzyme and additional salts were mixed and the reaction was started by adding substrate. 50 µL aliquot of the assay was taken at the time points 0, 5, 10, 15, 20, 25 and 30 min and mixed with 200 µL malachite green reagent provided in a well plate for stopping the reaction. The solution with 250 µL final volume of was incubated for 20 min at 20°C±2°C until the color reaction is finished and measured at 620 nm to detect the free phosphate released up to that point.

MPO

The enzymatic reaction of the substrate Tyr to the yellow coloured product nitroTyr with an absorbance at 405 nm was measured. An initial assay was chosen with the following concentrations: 500 µM Tyr, 500 µM H_2O_2, 500 µM $NaNO_2$ and 43 nM MPO with 250 µL final assay volume (Franck et al., 2008). All relevant compounds $NaNO_2$, H_2O_2 and Tyr were mixed with enzyme and the reaction was monitored at 405 nm immediately after mixing all components.

Proteases Chy, NE and PE

Peptides with the chromophore group pNA were used as substrates for proteases Chy, NE and PE. 250 µM Ala-Ala-Pro-Phe-pNA was mixed with 0.7 µM Chy, 250 µM N-Suc-Tyr-Leu-Val-pNA with 1.9 µM NE and 250 µM N-Suc-Ala-Ala-Ala-pNA with 0.2 µM PE. The

enzymatic cleavage at the respective amino acid releases the yellow coloured 4-nitroanilide which has its absorption maximum at 405 nm. Enzyme and substrate solutions were prepared in 10 mM NH_4Ac (pH 7.4). The enzyme and substrate solutions were mixed to 200 µL final assay volume of and immediately measured at 405 nm.

3.2.2 Direct Infusion Setup

Several enzymatic assays were established and optimized for mass spectrometry. All solutions were prepared in mass spectrometric compatible 10 mM NH_4Ac. The pH was set at 7.4, except for Csn1794 with pH 5.2. The concentrations for the substrates were chosen between 5 µM and 25 µM. According to the substrate concentration, the enzyme concentration was adjusted in order to obtain sufficient mass spectrometric signals for substrate and product(s). Batches for the assay optimisation, consisting solely of enzyme and substrate, were the following: AChE with AChCl, Chy with Ala-Ala-Pro-Phe-pNA, chitinases with $(GlcNAc)_n$ (n = 4 or 6) or (A_2D_2)-isomers, Csn1794 with $(GlcN)_n$ (n = 3, 4, 5 and 6) or $(Glc)_n$ (n = 3, 4 or 6), HEWL with $(GlcNAc)_6$, NE with N-Suc-Tyr-Leu-Val-pNA and PE with N-Suc-Ala-Ala-Ala-pNA. The experiments were started by adding substrate to the enzyme solution. In case of more complex assays with additional compounds such as salts, all assay compounds and enzyme were mixed and the reaction was started by substrate addition. ATPase was mixed with NaAc, KAc and $MgAc_2$ and reaction was started by ATP addition. MPO was mixed with H_2O_2, $NaNO_2$ and/or NH_4Cl and reaction was started by Tyr addition. The final optimized enzyme and substrate concentrations are summarized in the results section (Table 7).

The influence of several common organic solvents on enzymatic activity was tested by addition of 10% or 30% methanol, ethanol, acetonitrile, acetone and 2-propanol, respectively. Assays with organic solvents were prepared in the following order: enzyme solution, addition of organic solvent, addition of substrate solution. Control assays were prepared in a reaction tube by mixing enzyme solution with substrate solution. For multiplexing assays, mixtures of all enzymes and all substrates were prepared and subsequently mixed. Multiplexing assays with the addition of organic solvent were prepared in the following order: organic solvent was added to the mixture of enzymes and immediately mixed with the substrate mixture. All appropriate controls were conducted to prove that there are no interferences between the compounds of different assays.

All instruments and equipment were stored and experiments were carried out in the air-conditioned room at 20±2°C. A tempering of the syringe pump setup was not designated. After mixing all components, the samples were immediately infused into the mass spectrometric interface via a 100 µL or 250 µL-syringe (Hamilton-Bonaduz, Switzerland) located in a syringe pump (Model 11 Plus, Harvard Apparatus, Hugo Sachs Elektronik, Hugstetten, Germany). The solutions were continuously infused (Tubing: 1/16", 0.13 mm ID; 300 mm length) with a flow rate of 5 µL/min (TripleQuadrupole and Ion Trap) or 10 µL/min (Time-of-Flight).

3.2.3 NanoESI Robot Setup

The miniaturised and automated measurements were carried out with the nanoESI system TriVersa NanoMate (Advion BioSciences, Ithaca, NY) (Figure 4A). The system is installed in front of the mass spectrometer instead of the conventional ion source (Figure 4B). Special brackets for using the nanoESI robot with the Agilent systems TripleQuadrupole and Time-of-Flight and the Finnigan Ion Trap were used. The TriVersa NanoMate system includes a robot part and the ESI chip (HD_A_384, Advion BioSciences, Ithaca, NY) (Figure 4C).

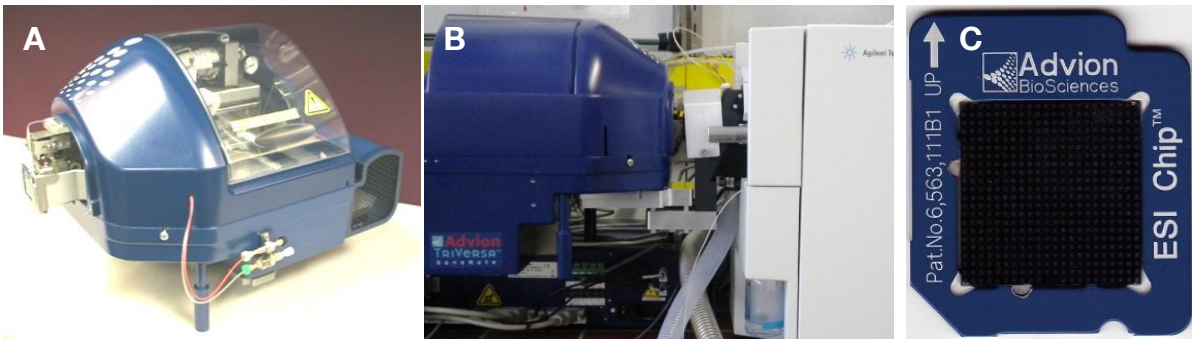

Figure 4: (A) TriVersa Nanomate nanoESI system overview, (B) TriVersa Nanomate connected to a mass spectrometer and (C) nanoESI chip.

The robot part is utilized for pipetting and mixing several solutions provided in a conventional microplate. The robot holds a 96 well plate and a tip rack with 384 disposable and conductive pipette tips (Advion BioSciences, Ithaca, NY) as well as the ESI chip. The chip comprises the nanoelectrospray device and consists of 20 x 20 channels (5 µm ID) to which the samples are delivered (Figure 5, step 5). A new channel and pipette tip are used

for every new sample, therefore cross contamination is excluded. The nanoelectrospray is generated by applying voltage and head pressure to each sample in the pipette tip, which is similar to an electrospray needle in nanoESI. The approximate flow rate in this 'infusion mode' is between 100 and 200 nL/min, depending on solvent composition, voltage and head pressure. The system is controlled by the Chip Soft software (version 8.3.1, Advion BioSciences, Ithaca, NY). The process of monitoring an enzymatic reaction was developed in this work and proceeds as shown in (Figure 5).

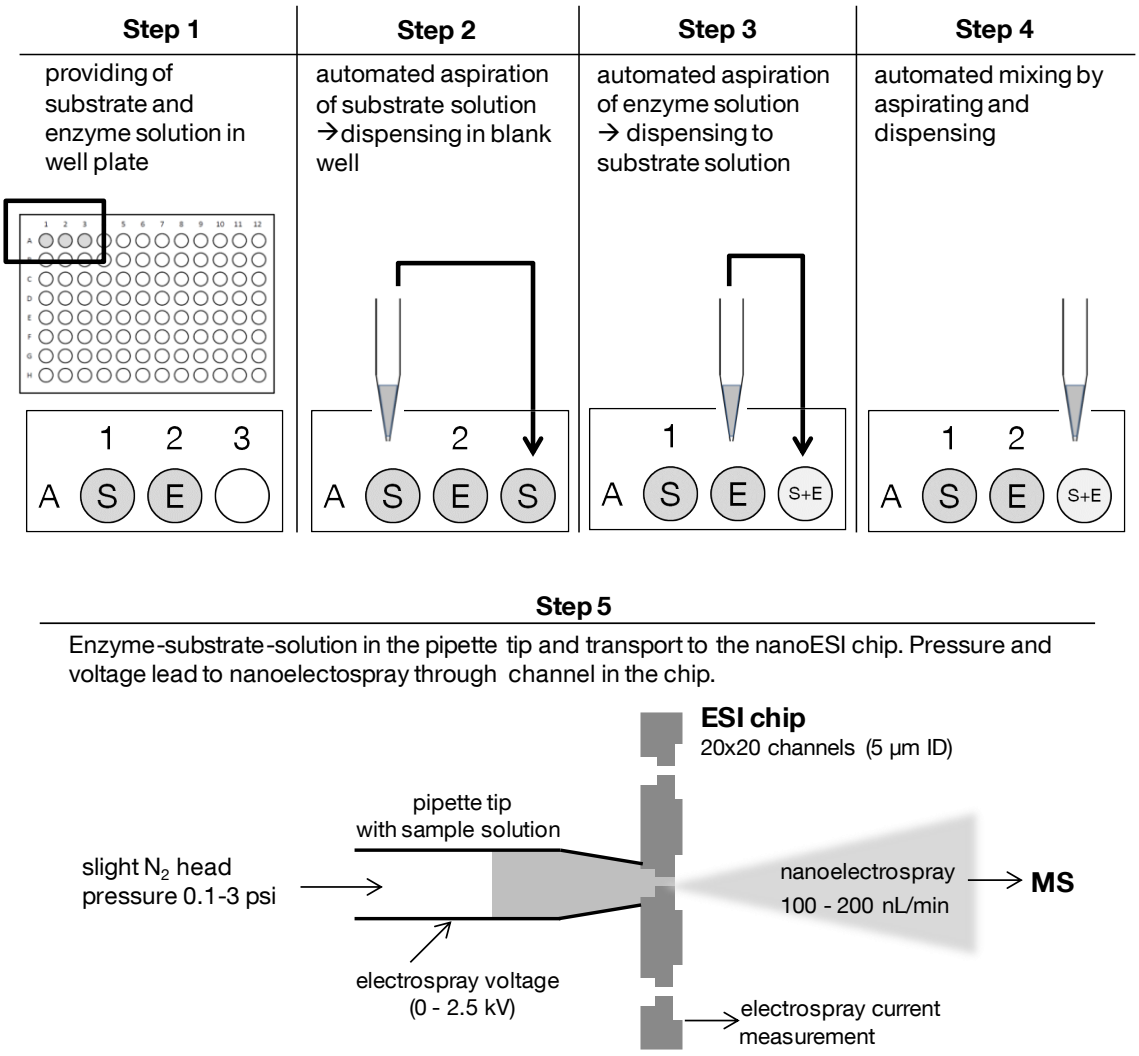

Figure 5: Procedure of measuring an enzymatic assay with the nanoESI robot TriVersa Nanomate (Advion Biosciences, Ithaca, NY) in the infusion setup (Figure adapted from Appendix III).

Two wells of the 96 well microplate are preloaded with solutions of enzyme and substrate. The robot part with the mandrel and a pipette tip aspirates a defined volume (e.g. 10 µL) of the substrate solution and then dispenses the solution in a blank 'reaction well' (Figure 5,

step 1 and 2). In the next step the enzyme solution is aspirated and added to the substrate solution in the reaction well (Figure 5, step 3). Enzyme and substrate solution are mixed automatically by aspirating and dispensing a defined volume (e.g. 10 µL) of the solution three times (Figure 5, step 4). Subsequently the robot delivers the reacting assay solution in a conductive pipette tip to the inlet side of the ESI chip and the nanoelectrospray process is initiated at the channel (Figure 5, step 5). Single substrate or enzyme solutions are measured by one aspirating and spraying step each. With 10 µL sample solution and a flow rate of 100 to 200 nL/min, the reactions can be monitored about 50 to 100 min (Appendix III). The two nanoESI spraying parameters, head pressure and electrospray voltage, have been varied between 0.6 and 1.0 psi and 1.65 and 1.9 kV, respectively. The optimisation procedure for enzymatic assay measurements and the developed modifications 'Flow control' and 'LC coupling' are explained in the results sections 4.2.2 and 4.2.3.

3.3 Measurements in Continuous-Flow Mixing Setups

3.3.1 Online Electrochemistry

Experiments with the online electrochemical conversion of a compound directly in front of the mass spectrometer were performed with the ROXY™ system (Antec, Zoeterwoude, The Netherlands). The target compounds are directly infused through an electrochemical cell and the reaction products are detected with the Time-of-Flight mass spectrometer via a direct hyphenation. The system was applied for reduction of $(GlcN)_5$. Different available working electrodes were tested on their suitability for reducing $(GlcN)_5$: a) ReactorCell™ composed of glassy carbon, diamond, platinum, gold or a reductive electrode with 10 µL/min sample flow rate and b) the µ-PrepCell™ composed of glassy carbon or diamond with 50 µL/min flow rate. The HyREF™ electrode (Pd/H_2) was used as reference electrode. The system was controlled by the software Dialogue (Antec, Zoeterwoude, The Netherlands).

Determination of the Optimal Conditions for the Electrochemical Conversion of $(GlcN)_5$

50 µM $(GlcN)_5$ in 10 mM NH_4Ac (pH 5.2) were filled in a 1 ml-syringe (Hamilton-Bonaduz, Switzerland) which then was located in a syringe pump (Model 11 Plus, Harvard Apparatus, Hugo Sachs Elektronik, Hugstetten, Germany). The solution was infused into the mass

spectrometer via the different electrochemical cells. The working electrode potential was applied in a scan mode, i.e. with a scan rate of 10 mV/sec and 0 V to -2 V for the reduction process. The mass spectrum was recorded in real-time during the whole acquisition process. The mass spectrometric detection parameters are given in Table 5.

Electrochemical Conversion Coupled with Enzymatic Reactions

50 µM $(GlcN)_5$ and 5 nM Csn1794 in 10 mM NH_4Ac (pH 5.2) were loaded in two separate syringe pumps and pumped with 20 µL/min flow rate. Both, enzyme and substrate were mixed in a mixing tee (PEEK with 10 µm UHMWPE frit, 2.2 µL volume, Upchurch Scientific, Oak Harbor, USA). A reaction coil (Teflon, 0.5 mm ID, 102 mm) with a reaction time of 5 min was implemented in front of the mass spectrometer, for appropriate mixing of enzyme and substrate. Prior to mixing of enzyme and substrate, the $(GlcN)_5$ solution passed the electrochemical µ-PrepCell™ with glassy carbon electrode for generation of reduction products. The complete setup with tubing lengths is presented in detail in Figure 6.

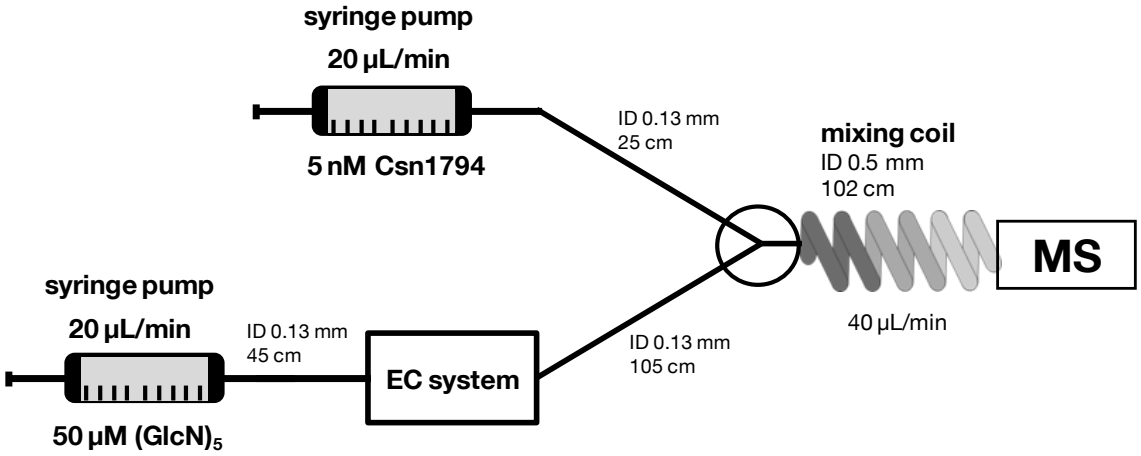

Figure 6: Experimental setup for continuous-flow mixing experiments with $(GlcN)_5$ and Csn1794 in combination with an electrochemical (EC) module and mass spectrometric detection.

3.3.2 High Temperature Liquid Chromatography

A continuous-flow mixing setup was used for detecting regulatory active substances in complex house dust mixtures. This method combines a chromatographic separation by HT-HPLC with a continuous-flow enzymatic assay and mass spectrometric detection (Figure 7) (de Boer et al., 2005a). The enzyme solution was provided in a syringe (2.5 mL, Hamilton-

Bonaduz, Switzerland) located in a syringe pump with a flow rate of 25 µL/min (Model 11 Plus, Harvard Apparatus, Hugo Sachs Elektronik, Hugstetten, Germany) and substrate solution was filled in a superloop (volume 10 mL, Amersham Biosciences, Uppsala, Sweden). Samples were injected into the continuous-flow system via injector (volume 2 µL, Rheodyne, California). A quaternary pump (1100 series, Agilent Technologies, Waldbronn, Germany) with a flow rate of 25 µL/min was used for the continuous-flow of the injected samples and the chromatographic separation. An isocratic pump (1260 series, Agilent Technologies, Waldbronn, Germany) with a flow rate of 50 µL/min was connected to the superloop for pumping the substrate solution. Pumps were controlled by the ChemStation software (version B.04.03, Agilent Technologies, Waldbronn, Germany). Mixing coils (Teflon, 0.25 mm ID) were used for sufficient mixing of enzyme with the injected sample (1 min, coil length 102 cm) and the enzymatic reaction (2 min, coil length 407 cm) and they were knitted as described in literature (Schebb et al., 2009). All connection tubings (PEEK, Upchurch Scientific, Oak Harbor, USA) between the single modules were as indicated in Figure 7.

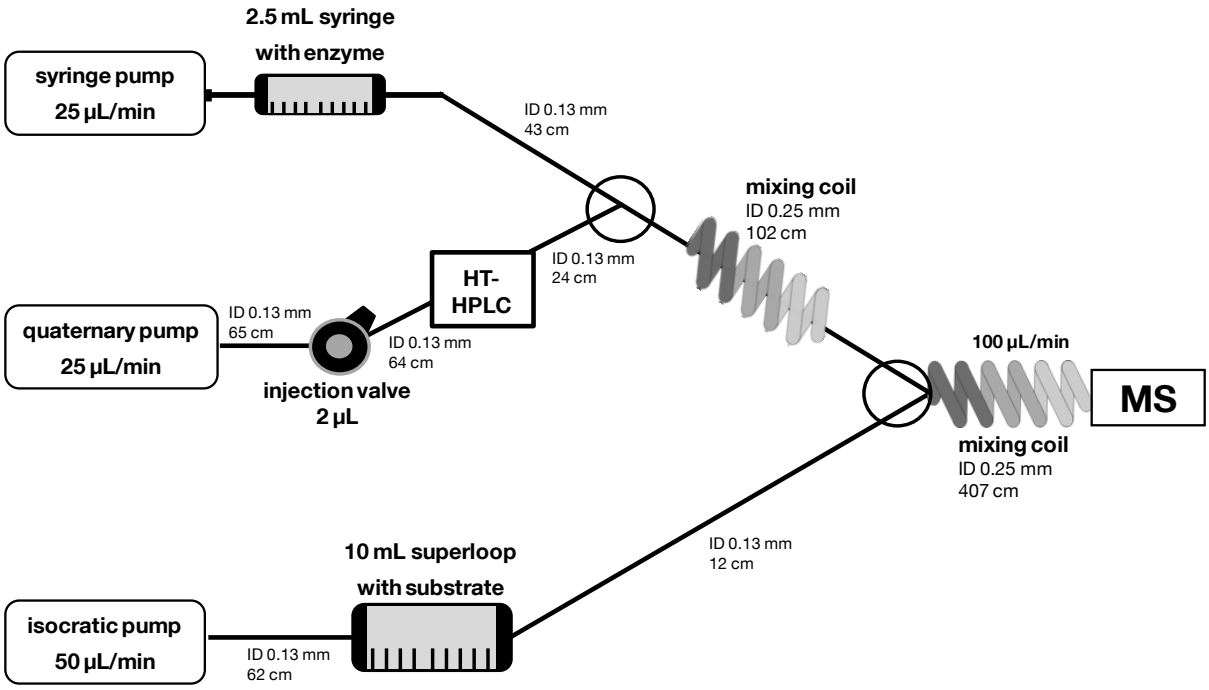

Figure 7: Experimental setup for continuous-flow mixing experiments in combination with a high temperature HPLC module and mass spectrometric detection. The setup was used for screening complex house dust mixtures for enzyme regulatory compounds.

The established enzymatic assays with AChE, Chi and Chy were applied in this setup, respectively. The respective enzyme and substrate concentrations are presented in Table 4.

The starting concentrations of the enzyme and substrate have to be adjusted according to the dilution effects in the system. The enzyme solution is reduced fourfold, i.e. the mixing step 1 with the HPLC eluent and the following mixing step 2 with the substrate solution (Figure 7). Accordingly, the substrate solution is reduced twofold, i.e. the mixture with the enzyme/HPLC solution (Figure 7). The chromatographic separation was carried out with HT-HPLC by using a temperature gradient. The amount of organic solvent for separation was set at 10% methanol, enabling the compatibility of the HPLC eluent with the enzymatic assay (de Boer et al., 2005a; Teutenberg, 2010). An isocratic eluent with 90% NH_4Ac (pH 7.4) and 10% methanol was used with the HT-compatible column Zirchrom-PBD (100 x 1 mm, 3 µm, ZirChrom Separations, Anoka, MN). The temperature gradient was controlled by using a column oven (Scientific Instruments Manufacturer GmbH, Oberhausen, Germany). Starting at 30°C, the temperature was increased up to 120°C within 20 min and 120°C were kept for 10 min. Inhibitors and house dust extracts (Table 3) were injected into the system via injection valve (2 µL). The temperature gradient was started immediately after injection of the samples. The respective controls and inhibitor experiments were carried out in solutions with 20% methanol, according to the extract composition. All samples were measured with a Quadrupole mass spectrometer (Table 5).

Table 4: Enzyme and substrate concentrations for enzymatic assay measurements in the continuous-flow mixing setup in combination with a high temperature HPLC module.

				AChE ***+ AChCl***	***ChiC*** ***+ $(GlcNAc)_6$***	***Chy*** ***+ Ala-Ala-Pro-Phe-pNA***
enzyme concentration	syringe		1:4	0.05 nM	40 nM	100 nM
	MS			0.0125 nM	10 nM	25 nM
substrate concentration	superloop		1:2	10 µM	10 µM	10 µM
	MS			5 µM	5 µM	5 µM

3.4 Mass Spectrometric Instrumentation

Experiments were carried out with different mass spectrometers. Depending on the application, the issue of the experiment and the required system requirements different mass spectrometers and parameters were chosen. For reasons of clarity and comprehensibility Table 5 presents the instruments with the respective parameters and corresponding application.

Table 5: Mass spectrometric equipment and the appropriate parameters for the different applications in this work.

Instrument	*Ion Source*	*Parameter*	*Application*
Triple Quadrupole Series 6410, Agilent Technologies, Waldbronn, Germany	ESI	fragmentor voltage 135 V, nebulizer 15 psi, drying gas flow 3 L/min, drying gas temperature 300°C, capillary voltage 2500 V, positive ionisation mode, full scan	establishment and optimization of enzymatic assays with AChE, ChiC, Chy, HEWL, NE, PE impact of organic solvent and multiplexing
	nanoESI robot	fragmentor voltage 135 V, drying gas flow 1.2 L min^{-1}, drying gas temperature 40°C to 170°C, capillary voltage 0 V, positive ionisation mode, full scan robot parameters: gas pressure 0.6-1 psi, voltage 1.65-1.9 kV	measurement of enzymatic assays by nanoESI ('infusion' and 'flow control' mode)
Ion Trap Finnigan LCQ Duo, Thermo Quest, San Jose, CA	ESI	sheath gas flow 0.3 L/min, capillary temperature 200°C, capillary voltage 50V, positive ionisation mode, full scan for MS/MS: fragmentation voltage at 20%	impact of organic solvent and multiplexing, MS/MS measurements with MPO
	nanoESI robot	capillary temperature 200°C, capillary voltage 10 V, positive ionisation mode, full scan robot parameters: gas pressure 0 psi, voltage 1.7 kV	measurement of enzymatic assays by nanoESI ('LC coupling' mode)
Quadrupole MSQ Plus, Wiss. Gerätebau Dr. Ing. Herbert Knauer GmbH, Berlin, Germany	ESI	probe temperature 300°C, needle voltage 3.5 kV, cone voltage 75 V, positive ionization mode, full scan	house dust extract measurements in the continuous-flow mixing setup
Time-of-Flight Series 6230, Agilent Technologies, Santa Clara, USA	ESI Jet Stream	drying gas temperature 200°C, drying gas flow rate 2 L min^{-1}, nebulizer gas pressure 20 psi, capillary voltage 1500 V, fragmentor voltage 175 V, skimmer voltage 65 V, octapole RF voltage 750 V, positive ionization mode, full scan	establishment and optimization of enzymatic assays with ATPase, MPO and characterization of Csn 1794

3.5 Data Analysis

The data of the Agilent systems Triple Quadrupole and Time-of-Flight were processed using the MassHunter Workstation software, Qualitative Analysis (version B02.00, Agilent Technologies, Waldbronn, Germany). The data from the Ion Trap and the Quadrupole were processed by using Xcalibur software, Qual Browser (version 2.1, Thermo Scientific, Waltham, USA). If not stated otherwise, all extracted ion chromatogram (EIC) time-courses were smoothed in Microsoft Excel 2007 with a moving average function (interval of 25). Depending on the assay, solvent composition, ionisation method and the type of mass spectrometer different adduct formations and protonation states were detected. The m/z signals for all detected substrate and product molecules of the enzymatic assays are presented in Table 6. The signals for the inhibitors were the following: galanthamine with m/z 288.3 for $[M+H]^+$ and EGCG with m/z 459.1 for $[M+H]^+$. In case of multiple detected m/z, all signals belonging to one molecule were summed and shown as single EIC.
The signal intensities were normalized for calculating the conversion rates (Appendix IV). The obtained time-courses were extrapolated using an exponential function in Microsoft Excel 2007, resulting in equation (1). The starting point was set at two minutes, since at this time point in all measurements a signal was detected after signal delay. The reactions were observed to reach a plateau at a remaining intensity of about 5; therefore, this value was set as the end point of the reaction. Using equation (1), conversion rates were calculated according to equation (2). The calculation of the conversion rate for Chy substrate Ala-Ala-Pro-Phe-pNA is presented in the Appendix IV in Figure 1. The conversion rate of control assays in pure aqueous solution is set at 100%; therefore the conversion rates for assays in the presence of organic solvent or for multiplexing assays are calculated accordingly.

$$y = a \cdot \exp(bx) \quad (1)$$

$$\text{conversion rate } [\text{min}^{-1}] = ([\text{substrate}]/[\text{enzyme}])/(\ln(5/a)/b) \quad (2)$$

The mass spectrometric data for house dust screening experiments in the continuous-flow mixing setup were calculated with software ‘Achroma’ (Hochschule Weihenstephan-Triesdorf, Freising, Germany). The Achroma software was especially developed for handling large amounts and unusual mass spectrometric data (Krappmann and Letzel, 2012). The software can be downloaded as freeware (http://openmasp.hswt.de/pages/project/achroma.php). The Achroma modules ‘signal recognition’ and ‘spectra comparison’ were used for data interpretation of the enzymatic assays measured in the online coupled setup

(chapter 4.3.3.2). The modules enable the detection of enzymatic regulation manifested as negative or positive peaks present in the signal traces. More detailed information about the software and examples for data handling are to be found in literature (Krappmann and Letzel, 2011; Krappmann and Letzel, 2012).

Table 6: Detected mass-to-charge (m/z) ratios for all mass spectrometric substrate and product signals of the enzymatic assays.

enzyme	*substrate and product(s)*	*monoisotopic mass [g/mol]*	*m/z for protonation states*			
			$[M + H]^+$	$[M + Na]^+$	$[M + 2H]^{2+}$	$[M]^+$
ATPase	ATP	507.0	508.0	530.0		
	ADP	427.0	428.0	450.0		
AChE	ACh	181.7				146.1
	choline	104.1				104.1
Chi HEWL	$(GlcNAc)_6$	1236.5	1237.5	1259.5	619.2	
	$(GlcNAc)_5$	1033.4	1034.4	1056.4		
	$(GlcNAc)_4$	830.3	831.3	853.3		
	$(GlcNAc)_3$	627.2	628.2	650.2		
	$(GlcNAc)_2$	424.2	425.2	447.2		
	(GlcNAc)	221.1	222.1	244.1		
Csn	$(GlcN)_6$	984.4	985.4	1007.4	493.2	
	$(GlcN)_5$	823.4	824.4	846.3	412.7	
	$(GlcN)_4$	662.3	663.3	685.3		
	$(GlcN)_3$	501.2	502.2	524.2		
	$(GlcN)_2$	340.1	341.1	363.1		
	(GlcN)	179.1	180.1	202.1		
	$(Glc)_6$	990.3	991.3	1013.3		
	$(Glc)_5$	828.2	829.2	851.2		
	$(Glc)_4$	666.2	667.2	689.2		
	$(Glc)_3$	504.2	505.2	527.2		
	$(Glc)_2$	342.1	343.1	365.1		
	(Glc)	180.1	181.1	203.1		
Chy	Ala-Ala-Pro-Phe-pNA	524.3	525.3	547.3		
	Ala-Ala-Pro-Phe	404.2	405.2	427.2		
MPO	Tyr	181.1	182.1	204.1		
	NitroTyr	226.2	227.1	249.1		
	DiTyr	360.1	361.1	383.1		
	TriTyr	539.2	540.2			
	Nitro-DiTyr	405.1	406.1			
	Nitro-TriTyr	584.2	585.2			
NE	N-Suc-Tyr-Leu-Val-pNA	613.3	614.4	636.3		
	N-Suc-Tyr-Leu-Val	493.4	494.3	516.3		
PE	N-Suc-Ala-Ala-Ala-pNA	451.4	452.4	474.2		
	N-Suc-Ala-Ala-Ala	331.2	332.2	354.2		

4 Results and Discussion

This work deals with the fundamental establishment of mass spectrometric experiments for measuring enzymatic reactions and their implementation in new technological setups. Chapter 4.1 gives basic approaches for the usage of enzymatic assays in mass spectrometric measurements and associated strategies for further optimisation. The additional progress with a miniaturised and automated setup and the specific modification of the new technology is topic of chapter 4.2. The knowledge about the handling of enzymatic assays in mass spectrometric experiments and the usage of new technological approaches was implemented in applications for studying various enzymological issues, e.g. reaction mechanisms, cleavage specifities and inhibition reactions. The diverse technological applications are presented in chapter 4.3.

4.1 Establishment of Mass Spectrometry Compatible Enzymatic Assays

The following chapter provides an overview on the establishment of diverse enzymatic assays for mass spectrometric measurements and their optimisation for applications in further technical setups.
Parts of this chapter were published in Scheerle et al., Analytical Sciences, 2012, 28 (6), 607-612 (Appendix IV).

4.1.1 Adaption from Classical Photometric Approaches to Continuous-Flow Mass Spectrometry

Classical methods for the measurement of enzymatic assays use spectroscopic, electrochemical or radioisotopic detection (Eisenthal and Danson, 2002; Bisswanger, 2007). The measurement of enzymatic assays by mass spectrometry requires the modification of various parameters from those classical experiments. Major conditions which have to be

adjusted from photometric to mass spectrometric measurements are shown in Table 1. The photometric enzymatic reactions were carried out according to well-established methods and were used for preliminary tests. Substrates with the chromophoric group pNA were used for proteases. The enzymatic cleavage of the peptide yields the photometric detectable product pNA (Liesener and Karst, 2005b; Bisswanger, 2007). The MPO assay with substrate Tyr leads to the yellow coloured product nitroTyr in the presence of nitrite (Sampson et al., 1998; Klebanoff, 2005; Franck et al., 2008). A well established assay with malachite green reagent for phosphate detection was used for ATPase (Henkel et al., 1988; Rowlands et al., 2004). The AChE activity was determined based on the Ellmans detection with DNTB (Ellman et al., 1961). No photometric measurements were conducted for the glycosidases, HEWL and ChiC. These enzyme assays were adapted for mass spectrometry according to the real-time monitoring of the HEWL-catalyzed hydrolysis of $(GlcNAc)_6$, described in literature (Dennhart and Letzel, 2006).

4.1.1.1 Exemplification with ATPase Assay

This chapter presents an exemplary procedure for the adaption of an enzymatic assay from photometric to mass spectrometric detection by means of the ATPase assay (Figure 8).
Several required parameters for mass spectrometric compatibility were adjusted with few simple and systematic preliminary photometric experiments.
The initial photometric (and non-mass spectrometric compatible) assay was the following: 0.2 mM ATP and 0.5 µM ATPase, 120 mM NaCl, 20 mM KCl and 4.5 mM $MgCl_2$ in 0.1 M Tris buffer (pH 7.4) (Robinson et al., 1984; Henkel et al., 1988; Schenk et al., 2003a) (Figure 8A). The exchange of 100 mM Tris buffer by 10 mM NH_4Ac, the exchange of NaCl, $MgCl_2$ and KCl by the acetates and the reduction of salt concentrations to 6 mM NaAc, 1 mM KAc and 0.3 mM $MgAc_2$ led to a mass spectrometry compatible assay composition (Figure 8D, dark blue signal).

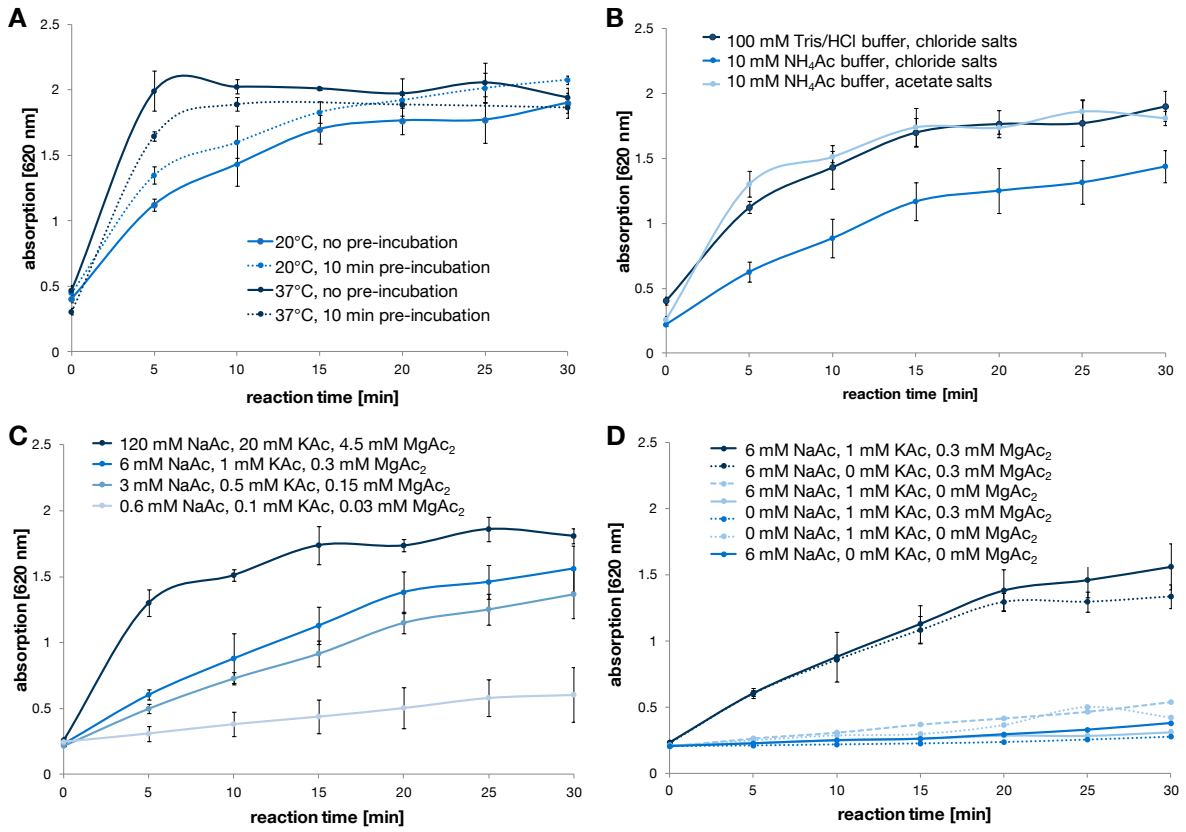

Figure 8: Photometric measurements of the enzymatic assay with ATPase and ATP. Measurements were used as preliminary tests for the adjustment of the assay for mass spectrometric requirements. Changes compared to the initial assay with 120 mM NaCl, 20 mM KCl, 4.5 mM $MgCl_2$, 0.2 mM ATP and 0.5 µM ATPase in 0.1 M Tris buffer are explained in the figures.

The following part gives a detailed insight in the adjustment procedure and data interpretation regarding a) optimisation of temperature and pre-incubation time, b) mass spectrometry compatible buffer and salt composition and c) optimisation of concentrations.

a) The enzymatic reaction depends on the temperature and pre-incubation (Nakao et al., 1965; Robinson et al., 1984; Robinson, 1988; Skou, 1989; Takahashi et al., 2006). The ATPase assay was carried out at 20±2°C or at 37±2°C and the enzyme was pre-incubated with all relevant salts for 10 min. Figure 8A illustrates the time-courses of phosphate release for the four modifications. The reaction at 37°C is finished after about 10 min and the reaction at 20°C reaches a plateau after about 30 min. The difference between preincubated and non-preincubated samples is negligible. As described in the materials and method section, a tempering of the mass spectrometric syringe pump setup is not designated. For these reasons the reaction at 20°C without pre-incubation was chosen for the further assay development. The enzymatic reaction was carried out at pH 7.4 and showed a

sufficient time-course. Regarding the pH optimum and multiplexing experiments at pH 7.4, no further pH values were tested (chapter 4.1.2.2) (Skou, 1957; Esmann, 1988).

b) Regarding mass spectrometric compatibility, the Tris buffer and chloride salts were replaced by 10 mM NH_4Ac and the respective acetate salts (Figure 8B). These changes remain a sufficient enzymatic activity and fulfill important requirements for a mass spectrometric compatible assay.
c) The enzymatic activity is sufficient after 20-fold decrease of all salts to 7.3 mM in comparison to the initial photometric assay with a total amount of 145 mM salts (Figure 8C). This is very important for the mass spectrometric compatibility, where the salt concentration should not exceed about 10 mM for prevention of contamination and signal suppression effects. The optimal ratio of the cations Na^+, K^+ and Mg^{2+} was set at 6:1:0.3 for Na:K:Mg (Skou, 1957; Robinson et al., 1984; Esmann, 1988). As indicated in Figure 8D Na^+ and Mg^{2+} are essential for the reaction whereas the omission of K^+ results in an identical phosphate release as in the assay with K^+. The similar product formation curve in the presence or absence of 1 mM KAc is in accordance with the earlier profound study on the influence of cations on ATPase (Skou, 1957).

According to the preliminary photometric experiments the adapted mass spectrometry compatible assay with acetate salts and reduced concentrations was measured by continuous-flow mass spectrometry with direct infusion. Figure 9 shows the real-time mass spectrometric measurement with the simultaneous detection of ATP degradation and ADP formation. The enzyme and substrate concentrations were readjusted leading to optimal signal intensities of substrate ATP and product ADP (data not shown). With 1.8 µM and in the presence of Na^+ and Mg^{2+}, the substrate time-course overlaps the product time-course after about 28 min. The doubling of the enzyme concentration to 3.8 µM leads to a more than twice as fast substrate and product overlap after about 12 min and the substrate ATP is almost depleted after the reaction time of 36 min. Similar to the photometric experiments the influence of assay compounds was tested, e.g. the substrate and product course crossing in the absence of K^+ occurs after about 27 min and in the presence of K^+ after about 33 min.

In this setup, attention should be paid on ATPase properties: The commercial available ATPase contains 90% sucrose for stabilisation. The high sucrose concentration causes mass spectrometric signal suppression of the substrate and product signals ATP and ADP.

The removal of sucrose, e.g. by filtration, leads to a loss of ATPase activity (data not shown). Preliminary tests indicated an adsorptive effect of this enzyme on different material such as the tubing material (PEEK). Thus, in comparison to the photometric measurements with 0.5 µM ATPase the enzyme concentration for mass spectrometry has to be increased four- to sevenfold.

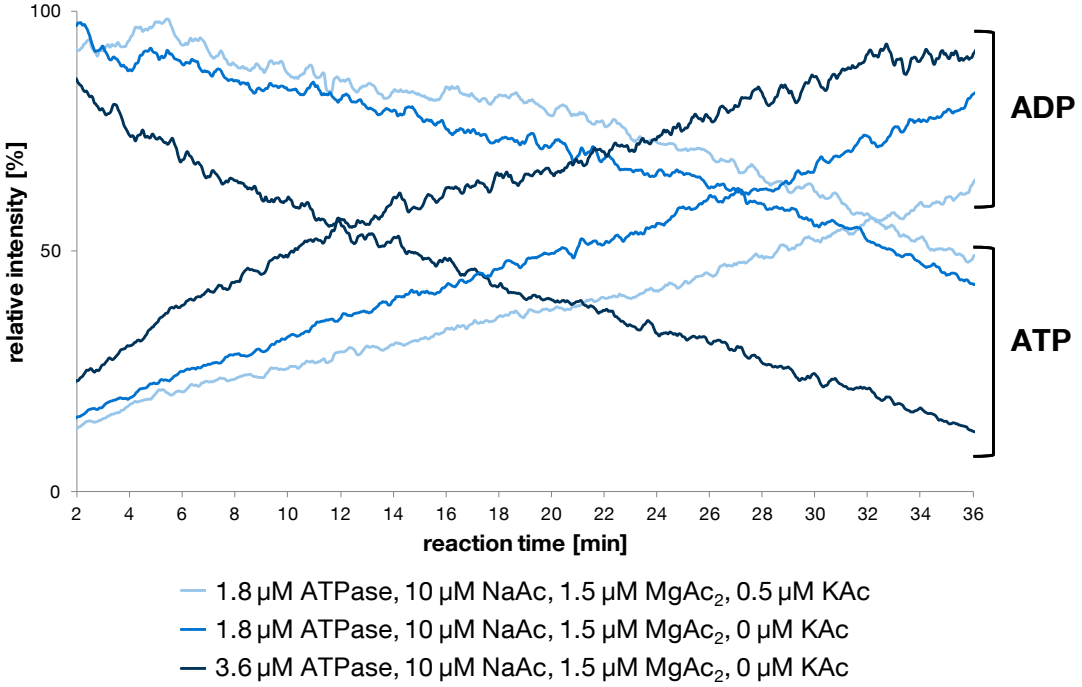

Figure 9: Continuous-flow mass spectrometric measurements of the ATPase assay by direct infusion. Measurements were carried out mixing 20 µM substrate ATP (100% = 3.4 x 10^4 counts) with 1.8 µM or 3.6 µM ATPase and different concentrations of NaAc, KAc and $MgAc_2$ as indicated.

4.1.1.2 Further Mass Spectrometry Compatible Enzymatic Assays

Figure 10 shows the enzymatic assays with HEWL and $(GlcNAc)_6$, ChiC and $(GlcNAc)_6$, NE and N-Suc-Tyr-Leu-Val-pNA, PE and N-Suc-Ala-Ala-Ala-pNA, Chy and Ala-Ala-Pro-Phe-pNA and AChE and acetylcholine measured by continuous-flow mass spectrometry with direct infusion. The figure shows the decreasing substrate time-courses and the increasing product time-courses as well as standard deviation of the measurements as shaded area. The enzymatic reactions were established and optimized according to the procedure described in chapter 4.1.1.1. The final photometric parameters and mass spectrometry compatible concentrations are summarized in Table 7. All enzymatic assays were adjusted

on common buffer and pH conditions, i.e. 10 mM NH_4Ac and pH 7.4, which are important requirements for the multiplexing experiments described below (chapter 4.1.2).

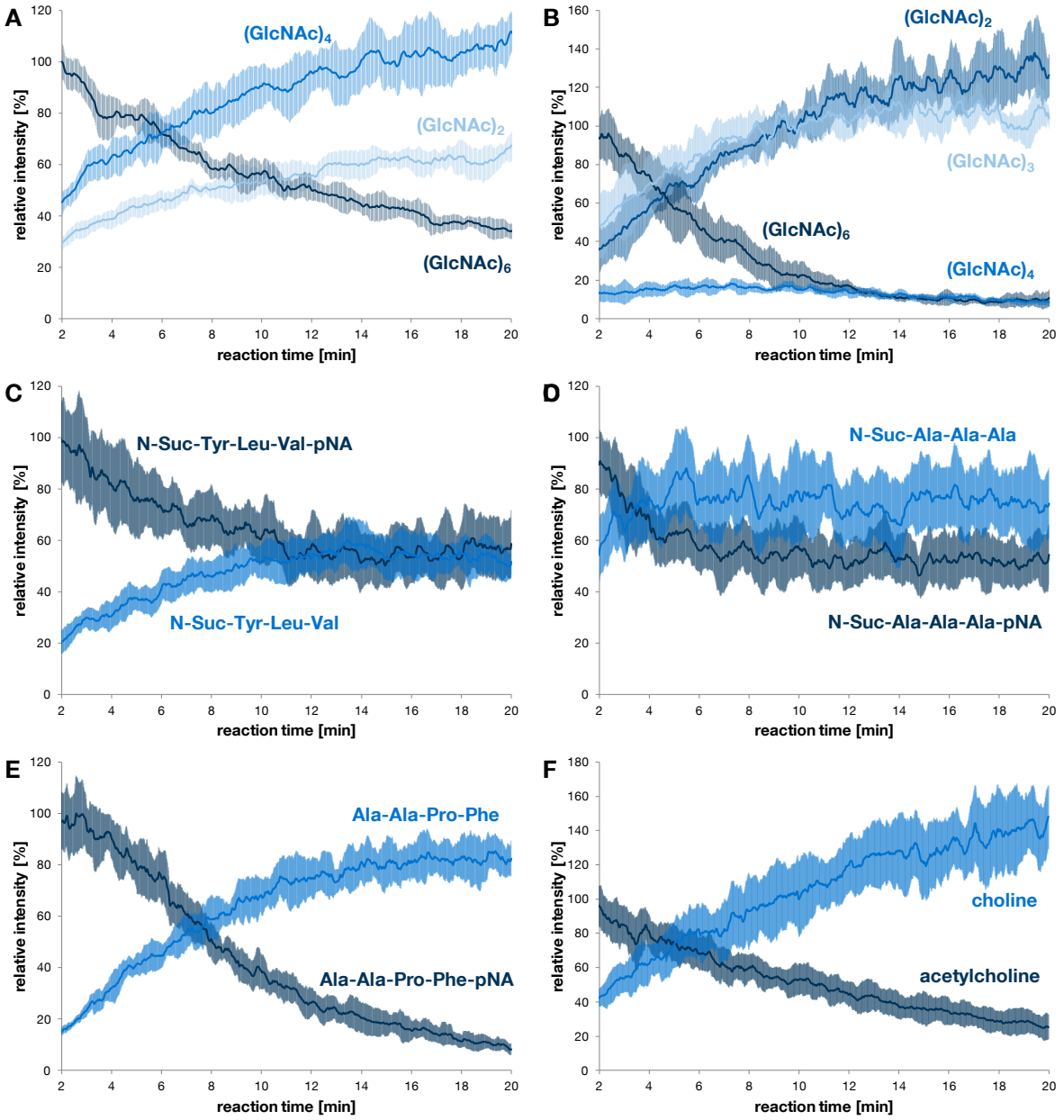

Figure 10: Continuous-flow direct infusion of enzymatic reactions with mass spectrometric detection. (A) HEWL and $(GlcNAc)_6$ (100% ≈ 1.1 x 10^5 counts), (B) ChiC and $(GlcNAc)_6$ (100% ≈ 6.8 x 10^4 counts), (C) NE and N-Suc-Tyr-Leu-Val-pNA (100% ≈ 3.4 x 10^4 counts), (D) PE and N-Suc-Ala-Ala-Ala-pNA (100% ≈ 4.4 x 10^4 counts), (E) Chy and Ala-Ala-Pro-Phe-pNA (100% ≈ 2.2 x 10^5 counts) and (F) AChE and acetylcholine (100% ≈ 6.4 x 10^5 counts). Measurements were carried out in triplicate and the standard deviation is shown as shaded area.

Table 7: Final concentrations of initial photometric and of the established and optimized enzymatic assays for continuous-flow mass spectrometric measurements conducted by direct syringe pump infusion setup. All solutions were prepared in 10 mM NH_4Ac (pH 7.4).

photometry			*mass spectrometry*		
enzyme	***substrate***	***additional compounds***	***enzyme***	***substrate***	***additional compounds***
AChE 2.4 nM	**AChI** 200 µM	200 µM DTNB	**AChE** 0.32 nM	**AChCl** 10 µM	-
ATPase 0.5 µM	**ATP** 200 mM	6 mM NaAc 0 µM KAc 0.3 mM $MgAc_2$	**ATPase** 3.6 µM	**ATP** 20 µM	10 µM NaAc 0 µM KAc 1.5 µM $MgAc_2$
no photometric measurement			**ChiC** 15 nM	**$(GlcNAc)_6$** 5 µM	-
Chy 0.7 µM	**Ala-Ala-Pro-Phe-pNA** 250 µM	-	**Chy** 0.2 µM	**Ala-Ala-Pro-Phe-pNA** 5 µM	-
no photometric measurement			**HEWL** 5 µM	**$(GlcNAc)_6$** 25 µM	-
MPO 40 nM	**Tyr** 500 µM	0.5 mM H_2O_2 0.5 mM $NaNO_2$	**MPO** 10 nM	**Tyr** 50 µM	200 µM H_2O_2 50 µM $NaNO_2$
NE 1.9 µM	**N-Suc-Tyr-Leu-Val-pNA** 250 µM	-	**NE** 1 µM	**N-Suc-Tyr-Leu-Val-pNA** 5 µM	-
PE 0.2 µM	**N-Suc-Ala-Ala-Ala-pNA** 250 µM	-	**PE** 1 µM	**N-Suc-Ala-Ala-Ala-pNA** 5 µM	-

4.1.2 Optimisation of Mass Spectrometry Compatible Enzymatic Assays

The enzymatic assays were characterized systematically in the presence of organic solvents as well as in multiplex approaches and in a combination of both. The use of organic solvents for enzymatic reactions is very useful for biotechnological issues, e.g. for specific industrial synthesis or in analytical chemistry, e.g. as modifier for mass spectrometric detection. Multiplexing experiments play an important role for high-throughput screening setups. The results, presented in this chapter, provide a fundamental basis for the technological applications described in chapter 4.3.

4.1.2.1 Impact of Organic Solvent on Enzymatic Conversion

The use of organic solvents in combination with enzymatic assays offers interesting possibilities and enables several new applications in chemical industry which have been discussed in detail in literature (Gupta, 1992; Klibanov, 2001). The addition of organic solvent as so called 'modifier' is a benefit for ESI-MS measurements (de Boer et al., 2005c; Kebarle and Verkerk, 2009), especially for miniaturised systems such as nanoESI-MS setups, which often pose problems with pure aqueous solutions (chapter 4.2, Appendix III). Furthermore, studies with continuous-flow microfluidic assay systems require the systematical research of impact of organic solvents (de Boer et al., 2005b).

For these reasons the influence of the common organic solvents methanol, ethanol, 2-propanol, acetone and acetonitrile on the enzymatic activity of HEWL, ChiC, NE, PE, Chy and AChE was investigated systematically by real-time ESI-MS with direct infusion (Appendix IV). Thereby the enzymatic activity was monitored in the absence and presence of organic solvents.

Figure 11A exemplifies the $(GlcNAc)_6$ hydrolysis by ChiC and Figure 11B the corresponding $(GlcNAc)_2$ formation in the presence of 30% methanol, ethanol, 2-propanol, acetonitrile and acetone, respectively.

Figure 12 shows the influence of 0%, 10% and 30% methanol on the activity of PE. The effect of the organic solvent on the enzymatic assay is already apparent comparing the positive control assay in 10 mM NH_4Ac and the assays in the presence of 10% and 30% organic solvent.

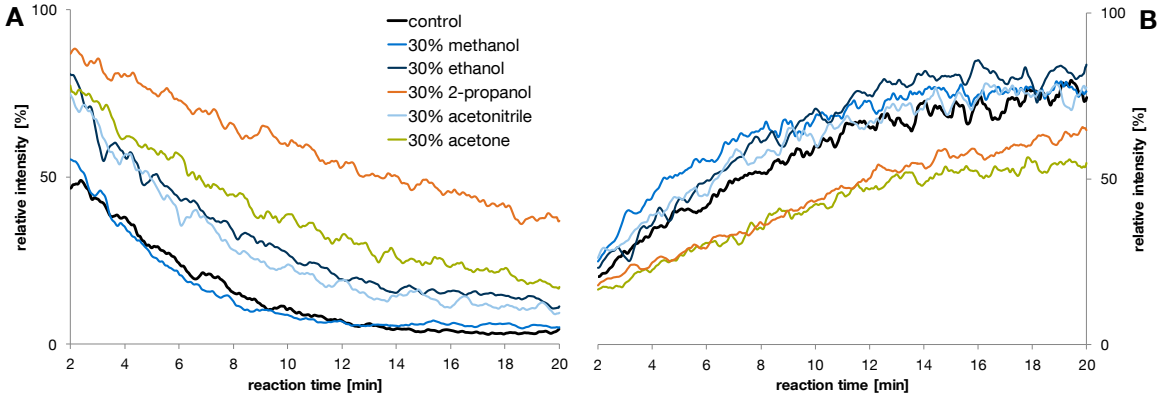

Figure 11: Continuous-flow measurements of the enzymatic reaction with 15 nM ChiC and 5 µM substrate $(GlcNAc)_6$ by direct infusion with mass spectrometric detection. Assays were carried out in pure aqueous solution and in the presence of 30% methanol, ethanol, 2-propanol, acetonitrile or acetone, respectively. (A) Substrate decrease of $(GlcNAc)_6$ (100% ≈ 6.7 x 10^4 counts) and (B) product increase of $(GlcNAc)_2$.

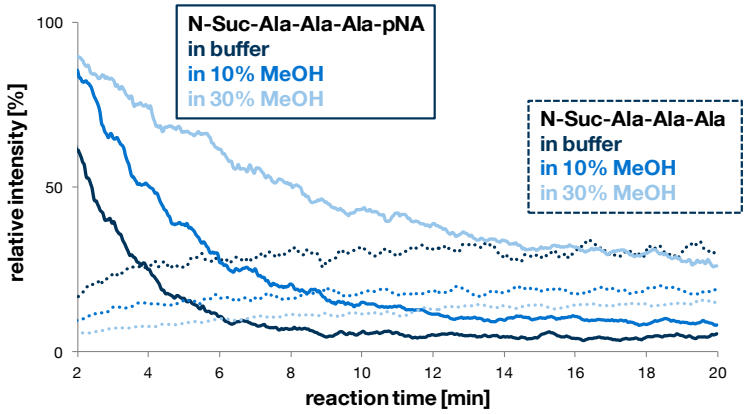

Figure 12: Continuous-flow measurements of the enzymatic reaction with 1 µM PE and 5 µM substrate N-Suc-Ala-Ala-Ala-pNA (100% ≈ 2.8 x 10^5 counts) by direct infusion with mass spectrometric detection. Assays were carried out in pure aqueous solution and in the presence of 10% and 30% methanol.

As indicated in Figure 11 and Figure 12 the addition of organic solvents influences the electrospray and the ionisation of the molecules and therewith causes differences in the intensities. The exact impact of an organic solvent was calculated by using the conversion rate (Figure 1 in Appendix IV).

Figure 13 reflects the conversion rates for all enzymatic assays in the presence of 10% and 30% organic solvents. Assays which showed markedly reduced activity in 10% organic solvent, were not further tested with higher solvent concentration (indicated by *). In all tested combinations enzymatic activity was measurable. Some combinations showed a decreased conversion rate in the presence of organic solvent. Typically, the activity of enzymes are lower in non-aqueous systems, which is primarily caused by denaturation effects (Klibanov, 2001; Ogino and Ishikawa, 2001; Krishna, 2002). In some enzyme-organic

solvent combinations the enzymatic activity remains unaffected, e.g. NE with 10% methanol. Further combinations even show conversion rates >100%, i.e. HEWL with methanol or ethanol and ChiC with acetonitrile, respectively. In general, an increase of the organic solvent content from 10% to 30% is associated with a decrease of enzymatic activity, except for ChiC with methanol and HEWL with 2-propanol, where the activity in 30% is distinctly higher than in 10% organic solvent. The stimulation of enzymatic activity at specific concentrations of solvent is a phenomenon which has already been reported (Butler, 1979; Batra and Gupta, 1994). The formation of a new enzyme conformation or the disruption of water in the vicinity of the active site may be explanations (Faller and Sturtevant, 1966; Khmelnitsky et al., 1991).

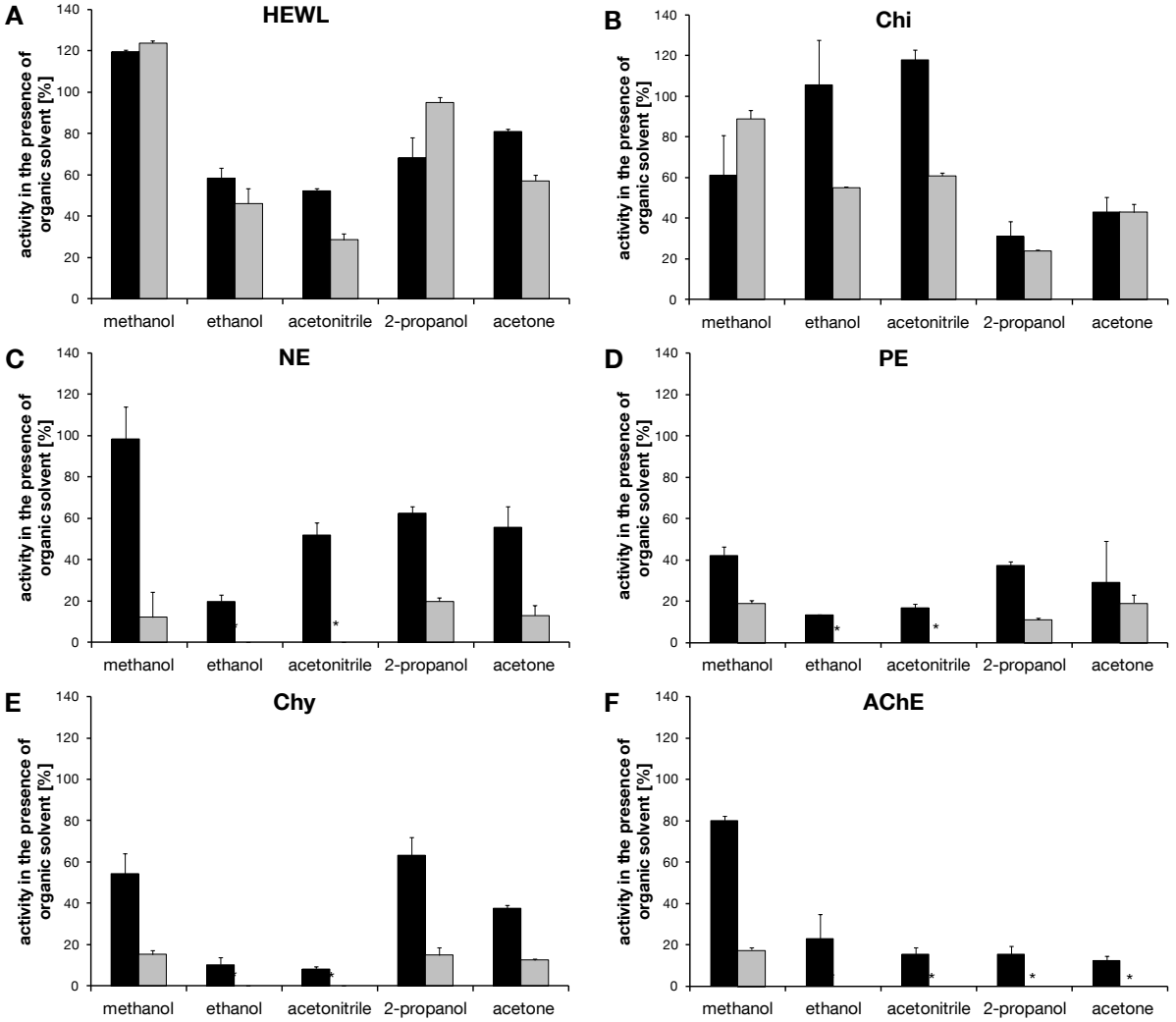

Figure 13: Enzymatic activity in % of enzymatic assays conducted with (A) hen egg white lysozyme (HEWL), (B) chitinase (ChiC), (C) elastase from human neutrophils (NE), (D) elastase from porcine pancreas (PE), (E) α-chymotrypsin (Chy) and (F) acetylcholinesterase (AChE) by addition of 10% (black) and 30% (shaded) organic solvents (methanol, ethanol, 2-propanol, acetone, acetonitrile). The activity was obtained by means of the conversion rate in comparison to the control assay in 10 mM NH_4Ac without addition of organic solvent (*, not determined). For exact numeric values refer to Table 1 in Appendix IV.

For the current combinations, no obvious trend can be stated; the influence of solvents on enzymatic activity differs from enzyme to enzyme, caused by diverse effects: Interaction of organic solvents with enzymes, competition with substrate binding, conformational changes of the enzyme and changes in charge state distribution due to denaturation effects (Butler, 1979; Samalikova and Grandori, 2005).

In general, 10% methanol is the best tolerated organic solvent for all tested enzymes in this work. Enzymes belonging to the same subclass and with same/similar active sites show a similar behavior in the presence of organic solvents e.g. the glycosidases (HEWL and ChiC) or the proteases Chy, NE and PE, respectively. This may be explained by their similar active site and a similar molecular weight. The glycosidases HEWL and ChiC are quite unsusceptible towards organic solvents. AChE is most susceptible towards organic solvents; but in case of 10% methanol there is a remaining activity of 80%, all other solvents decrease the activity below 25% even in a concentration of 10%.

In general, no obvious trend is observable regarding the polarity or the dielectric constant of solvents and the impact of organic solvents on enzymatic activity concerning the polarity and hydrophobicity was also discussed in literature quite contradictory (Butler, 1979; Laane et al., 1987; Khmelnitsky et al., 1991; Gupta et al., 1997). Thus, the influence of organic solvent on each enzyme has to be tested individually. The presented data are reference points for diverse applications in this work (chapter 4.3). Regarding the measurements in the miniaturised and automated nanoESI setup the addition of organic solvent improves droplet generation in the mass spectrometric electrospray interface and thus leads to a better droplet evaporation (de Boer et al., 2005c; Kebarle and Verkerk, 2009) (chapter 4.3.2). The knowledge about the susceptibility of enzymes towards diverse organic solvents is moreover very helpful for the optimisation of chromatographic separation by HT-HPLC, where a low amount of organic solvent is required (chapter 4.3.3.2).

4.1.2.2 Impact of Multiplexing on Enzymatic Conversion

The multiplexing of two or more enzymatic assays in one measurement is an essential approach for fast and cost-efficient screening methods, e.g. for the determination of inhibitors in complex mixtures or in the field of biomedical and pharmaceutical drug research. The enzymatic activity may be affected in the presence of other substrates and/or enzymes, but the expected advantages possibly will predominate. Multiplexing approaches were described for determination and characterization of protease activity in the presence

of different substrates or for the simultaneous determination of the activities of different cytochrome P450 isoforms (Gerber et al., 1999; Hempen et al., 2005; Liesener and Karst, 2005b; Liesener et al., 2005; Dixit et al., 2007).

In this work, multiple enzymatic assays were measured simultaneously and conversion rates, which reflect the enzymatic activity, were used for data interpretation. Multiplexing experiments were performed with two or more enzymatic assays in parallel. All enzymatic assays are active and measureable at room temperature in 10 mM NH_4Ac and at pH 7.4 as described in chapter 4.1. The common basis, i.e. pH, buffer, temperature and concentrations for the multiplexed enzymatic assays were chosen in such a way that each single enzymatic assay retains sufficient activity, even if the parameters are not in strict conformity with the enzyme optimum (Appendix IV).

Initially, combinations of two assays, consisting of both enzymes and both substrates were measured and the enzymatic activity in the presence of the second assay was determined. All control experiments were carried out, i.e. each substrate was measured with all available enzymes separately. Figure 14 presents the activity for ChiC, NE, PE, Chy and AChE in those duplex assays. In the presence of a second assay, the enzymes show activities between 50% and 100% in comparison to the control experiment. Even ChiC in the presence of NE shows an increased activity of 133% and NE in the presence of ChiC 106%. There are some combinations where the activity of an enzyme is reduced significantly to ≤ 50%, e.g. NE in the presence of Chy and PE, PE in the presence of NE or AChE in the presence of NE.

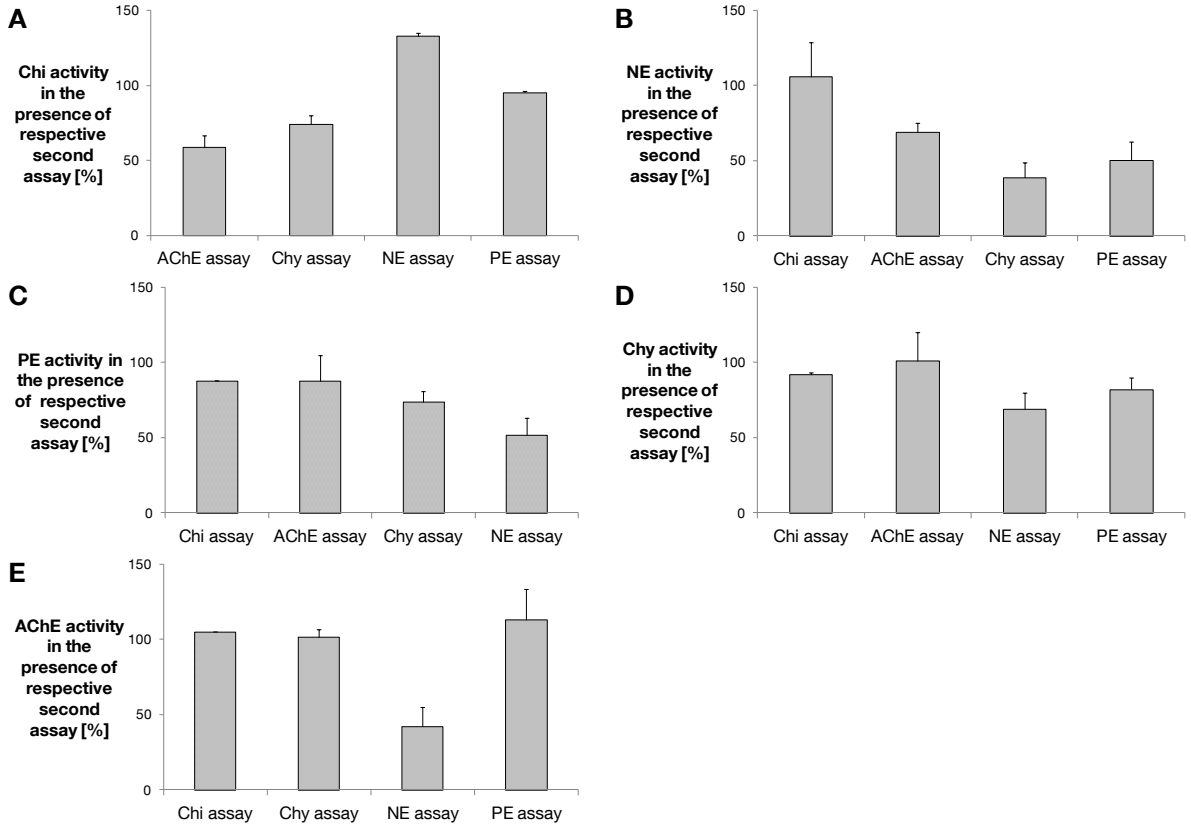

Figure 14: Enzymatic activity in % in duplex multiplexing experiments. The activity of the enzymes (A) chitinase (ChiC), (B) elastase from neutrophils (NE), (C) elastase from pancreas (PE), (D) chymotrypsin (Chy) and (E) acetylcholinesterase (AChE) was determined in the presence of a second assay (x-axis) (Fig. 13D adapted from Figure 2 in Appendix IV).

Obviously, the interacting influence of the proteases NE, PE and Chy may be referred to their same active site, the catalytic triad of His-Asp-Ser and the similarity of the substrates (Shirasu et al., 1986; Takahashi et al., 1988). The active site of AChE also contains a catalytic triad of three amino acids: Ser-His-Glu. This sequence is similar to the triad of the proteases, except of the Glu instead of Asp. The poor interaction between ChiC and the proteases/AChE may be explained by the completely different active site of ChiC, which consists of two amino acids Glu-Asp (Fukamizo, 2000). Further, the Chy, PE and NE assay were conducted with similar substrates, consisting of four amino acids and the chromogenic group pNA. The substrates for ChiC and for AChE, i.e the hexasaccharide $(GlcNAc)_6$ and the ester acetylcholine, obtain a completely different structure.

These observations are in accordance with literature data, that enzymatic assays, especially with resembling enzymes, cannot be multiplexed in any way. Assays need to be tested individually up to which amount assays can be multiplexed and which assays are combinable (Dixit et al., 2007).

In a next step, five enzymatic assays were performed in a multiplexed assay with Chy, ChiC, AChE, PE and NE. Even in this complex mixture, consisting of five different substrates and five enzymes, respectively, the enzymes show activities between 19% (AChE) and 108% (ChiC) (Figure 15). ChiC seems to be a quite 'rough' enzyme, which is much less susceptible towards multiplexing than the other enzymes. Based on the similar active sites, the proteases and AChE pose a stronger interaction on each other in the multiplexing solution and thus, do not or only marginal interact with ChiC.

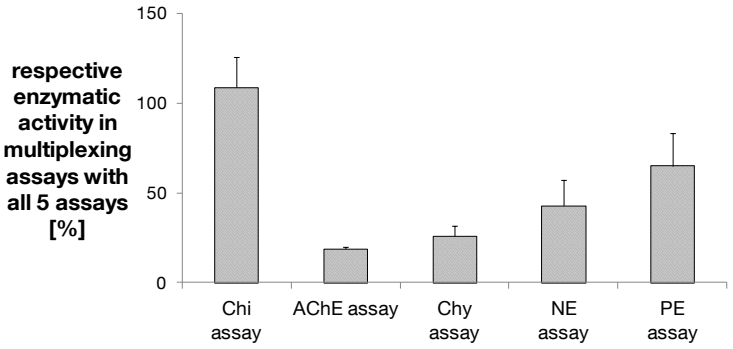

Figure 15: Activity in % of each enzyme in a multiplexing experiment with all five assays chitinase (ChiC), acetylcholinesterase (AChE), chymotrypsin (Chy), elastase from neutrophils (NE) and elastase from pancreas (PE) (adapted from Figure 3 in Appendix IV).

Finally, the enzymatic activity was determined in a multiplexing experiment and in the presence of organic solvent. The four enzymatic assays with Chy, ChiC, AChE and NE were conducted in parallel and in the presence of 10% methanol, ethanol, acetonitrile, acetone or 2-propanol, respectively (Figure 16). Even in this combination the enzymes show enzymatic activity. Compared to the single assays the conversion rate is reduced between four- and fivefold. In this setup, AChE again is the most susceptible enzyme with a conversion rate ≤6.5%. The two tested proteases, NE and Chy show a remaining enzymatic activity between 10% and 30% for all organic solvent combinations. And as already determined before, ChiC is most insensitive to organic solvent and multiplexing with 25% activity in the presence of acetone and even 68% with ethanol.

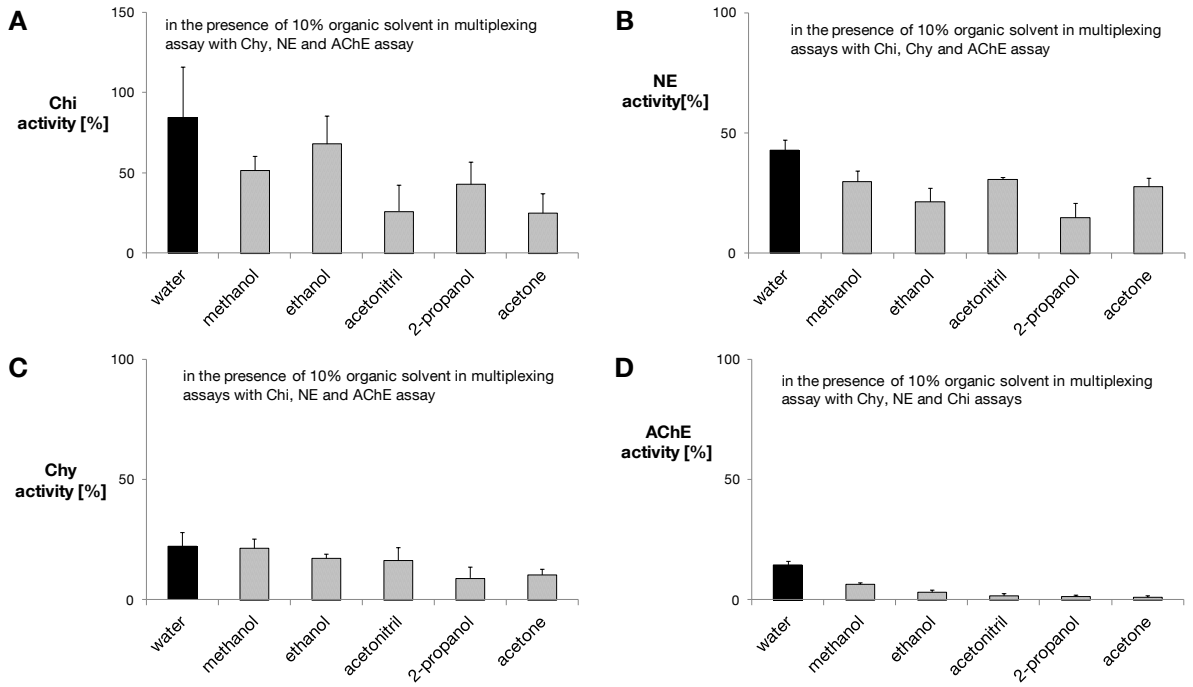

Figure 16: Enzymatic activity in % in multiplexing experiments with the four enzymatic assays with (A) chitinase (ChiC), (B) elastase from neutrophils (NE), (C) chymotrypsin (Chy) and for (D) acetylcholinesterase (AChE) in the presence of 10% organic solvent. (Fig. 15C adapted from Figure 3 in Appendix IV).

4.1.3 Summary

The real-time mass spectrometric monitoring of enzymatic reactions is a powerful tool in enzymological research and provides several key benefits in comparison to classical approaches. It is a promising technique which enables the simultaneous detection of substrate and product time-courses.

This chapter described the establishment of diverse enzymatic assays - ChiC, NE, PE, AChE, Chy and ATPase - from classical photometric assays to continuous-flow mass spectrometric detection. The enzymatic assays can be adapted for mass spectrometric experiments considering some general parameters which are important for the mass spectrometric compatibility: buffer, pH value, concentrations of substrates, enzymes and additional compounds. Assays with single substrate and single enzyme (HEWL, ChiC, NE, PE, Chy and AChE) are very easy to be handled whereas more complex assays, such as ATPase with additional assay compounds such as salts, need a more detailed optimisation procedure. But even more complex assays can be adapted for mass spectrometric direct infusion measurements.

The systematic tests with organic solvents and multiplexing provide an overview about the susceptibility of the enzymes towards diverse impact factors. In multiplexing experiments with two or even five assays and in the presence of organic solvent, the enzymes still possess activity. In all combinations the substrate consumption and a simultaneous product formation can be monitored. Thus, sensitive multiplexed assays are advantageous for analytical applications in pharmaceutical or biotechnological industry. The high throughput of a large number of enzymes and/or substrates can be used for studying reaction pathways or inhibitor screening. Detecting the activity of numerous enzymes in one sample is especially beneficial when only small quantities of analytes are available.

The data provide a fundamental and beneficial basis and can be used as a reference point for many other applications in analytical chemistry and biotechnology. The addition of organic solvent to the solution may be helpful in nanoESI systems for improved nanoelectrospray stability and was implemented in the automated and miniaturised setup as described in the following section 4.2 and 4.3.2. The obtained results moreover enabled the conduction of HT-HPLC measurements in a continuous-flow mixing setup, where the addition of organic solvent is required for an effective chromatographic separation (chapter 4.3.3.2).

4.2 Automation and Miniaturisation of Mass Spectrometry Compatible Enzymatic Assays

The automation and miniaturisation of mass spectrometry based analytical techniques gained increasing interest in recent years. High sample throughput, higher ionisation efficiency, timesaving and low sample volume are the main benefits of nanoESI-MS systems in contrast to conventional ESI-MS (Wilm and Mann, 1994; Wilm and Mann, 1996; Wilm et al., 1996).

In this work a miniaturised and automated system – the nanoESI robot TriVersa Nanomate (Advion BioSciences, Ithaca, NY) – was established in this study for the real-time monitoring of enzymatic assays. The usage of such an automated and miniaturised system provides an important step towards the fast and cost-efficient systematic development of enzymatic assays, especially for complex assays such as the above described ATPase assay (chapter 4.1.1.1) or the MPO assay described in the application section (chapter 4.3.1.3). Therewith a wide range of assay parameters such as buffer conditions, pH, concentrations of all assay compounds and influence of organic solvent or inhibitory substances can be tested automatically and quickly. Within this work, the utilization of the nanoESI setup for monitoring enzymatic reactions was evaluated for the first time systematically: Assay parameters were optimized regarding system requirements, instruments settings were evaluated and technical modifications of the system were carried out.

Parts of this chapter were published in Scheerle et al., Analytical Methods, 2011, 3, 822-830 (Appendix III) and Scheerle and Grassmann, Royal Society of Chemistry, 2011 (Appendix II).

4.2.1 Measurement of Enzymatic Assays in the nanoESI Setup 'Infusion'

The enzymatic assay consisting of HEWL and $(GlcNAc)_6$ was applied for the systematic establishment of the continuous-flow monitoring of enzymatic assays with a nanoESI-MS robot system. Samples were measured in the classical 'infusion mode', described in the material section 3.2.3. After mixing all compounds, the solution reacts in the pipette tip and the nanoelectrospray is initiated at the ESI chip with a flow rate of ~100-200 nL/min. The time range was set at 20 minutes to approve the spray stability and to monitor the substrate and product time-courses.

Concentrations were adjusted and various parameters regarding the nanoelectrospray and the mass spectrometer were tested and optimized to discover a stable nanoelectrospray during the total time period. Examples of measurements with HEWL and $(GlcNAc)_6$ in the nanoESI setup 'Infusion' are shown in Figure 17.

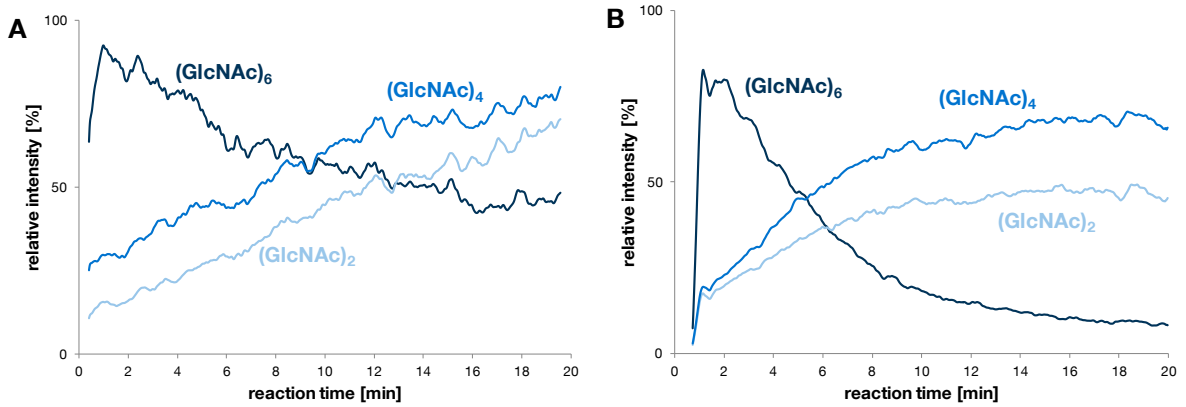

Figure 17: Continuous-flow measurement of enzymatic assays with the nanoESI-MS setup with (A) 0.5 µM HEWL and 5 µM $(GlcNAc)_6$ and (B) 1 µM HEWL and 10 µM $(GlcNAc)_6$. Extracted ion chromatograms for substrate $(GlcNAc)_6$ (with (A) 100% ≈ 6.8 x 10^4 counts and (B) 100% ≈ 9.5 x 10^4 counts) and products $(GlcNAc)_2$ and $(GlcNAc)_4$ are shown.

Comparable conversion rates for substrate $(GlcNAc)_6$ in the nanoESI and the direct infusion experiments by syringe pump emphasize the promising applicability of nanoESI setup. Numeric values for the calculated conversion rates in both setups are summarized in Table 1 in Appendix III.

However, when measuring the pure aqueous enzymatic solutions in combination with the nanoESI-MS two main complexities were observed: Spray instability and the impairment of enzymatic activity. They are explained in detail in the following section and possibilities to solve them are presented.

4.2.1.1 Spray Instability

Experiments with 25 µM $(GlcNAc)_6$ and 5 µM HEWL often showed spray instabilities. In some cases the spray discontinues after a certain stable spraying time and in some cases right from the start (Figure 4 in Appendix III). This is mainly based on the high surface tension of aqueous solutions compared to samples containing organic solvent and the aqueous solutions are difficult to spray through the small channels in the ESIchip (Schultz et al., 2000).

Several parameters were tested systematically to overcome spray instabilities: The nanoESI operating parameters spraying voltage and head pressure, the mass spectrometric parameters and sample composition and concentrations.

The nanoESI robot parameters voltage and pressure were optimized for the specific aqueous sample composition with $(GlcNAc)_6$ and HEWL. According to literature data and preliminary tests the combination of 1.8 kV and 0.8 psi showed the best results (Appendix III). Additionally to the spraying parameters mass spectrometric parameters were tested in a wide range between 40°C to 170°C drying gas temperature and 0.5 L/min to 3 L/min drying gas flow and were finally set to 170°C and to 1.2 L/min, respectively.

Furthermore, substrate and enzyme solutions were tested in single experiments. Measuring the substrate $(GlcNAc)_6$ and products $(GlcNAc)_2$ and $(GlcNAc)_4$ as well as further solutions with small molecules (AChCl and Ala-Ala-Pro-Phe-pNA) showed a stable spray (Figure 2 in Appendix III and unpublished data). The measurement with HEWL showed a rapid drop of the electrospray current and simultaneously the mass spectrometric signals, even after a channel change (Figure 3 in Appendix III). Further measurements with enzymes AChE and Chy showed similar spray instabilities (data not shown).

For measuring the complete enzymatic assay, concentrations with 25 µM $(GlcNAc)_6$ and 5 µM HEWL were chosen since these concentrations resulted in an effective performance over 20 minutes using the syringe pump setup as described in section 4.1 and in literature (Dennhart and Letzel, 2006). Unfortunately, the nanoESI-MS setup with the adjusted parameters seemed not to be applicable for these concentrations (Appendix III, Figure 4). The higher the enzyme concentration the more the spray stability was influenced by clogging the channels. The clogging of the channels or the pipette tip with protein solutions may be mainly caused by denaturation of the enzyme. A more constant mass spectrometric signal was obtained using lower absolute concentrations. Combinations between 0.5 to 2 µM HEWL and 5 to 15 µM $(GlcNAc)_6$ led to a more stable and reproducible nanoelectrospray. Signal intensities were unaffected, since nanoESI transfers ions more

efficient than microESI (Wilm and Mann, 1994; Wilm and Mann, 1996; Kebarle and Verkerk, 2009). Exemplary measurements with 0.5 µM HEWL and 5 µM $(GlcNAc)_6$ and 1 µM HEWL and 10 µM $(GlcNAc)_6$ are shown in Figure 17 A and B.
Concluding this set of experiments, low sample concentrations improve the nanoelectrospray signal in nanoESI measurements of enzymatic assays and lead to a stable and continuous signal. Further improvements for a complete elimination of this difficulty were carried out and explained in chapters 4.2.2 and 4.2.3.

4.2.1.2 Impairment of the Enzymatic Activity

According to the HEWL experiments, the hydrolysis profile of ChiC with substrate $(GlcNAc)_6$ was investigated in the nanoESI setup. In comparison to direct infusion experiments equal assay concentrations led to no enzymatic reaction in the nanoESI assay (Figure 18 A and B). The fivefold increase of the enzyme concentration resulted in a moderate substrate formation (Figure 18C). But still ChiC activity was lower compared to the syringe pump setup. This effect was also tested with the enzymatic assays with Chy and AChE, even with increased concentrations, but no enzymatic activity was observed (data not shown). The experiments lead to the assumption that obviously, the applied voltage at the pipette tip can impair the enzymatic activity (Appendix III). This is in agreement with an earlier study of Yang and coworkers who studied the effect of pulsed electric field on different enzymes. When studying HEWL, they did not observe a significant change in enzymatic activity, whereas Chy activity was reduced after treatment with a pulsed electric field (Yang et al., 2004a).
The principal applicability of the system for the fast and automated monitoring of enzymatic reactions is given for enzymes, which are insensitive towards electric field. As discussed, this ‘infusion’ setup is not the ultimate setup for measurements of enzymatic assays by nanoESI-MS. Thus, the chapters 4.2.2 and 4.2.3 present further modifications of the system to overcome the spray instability and the impairment of the enzymatic activity in the current ‘Infusion’ setup.

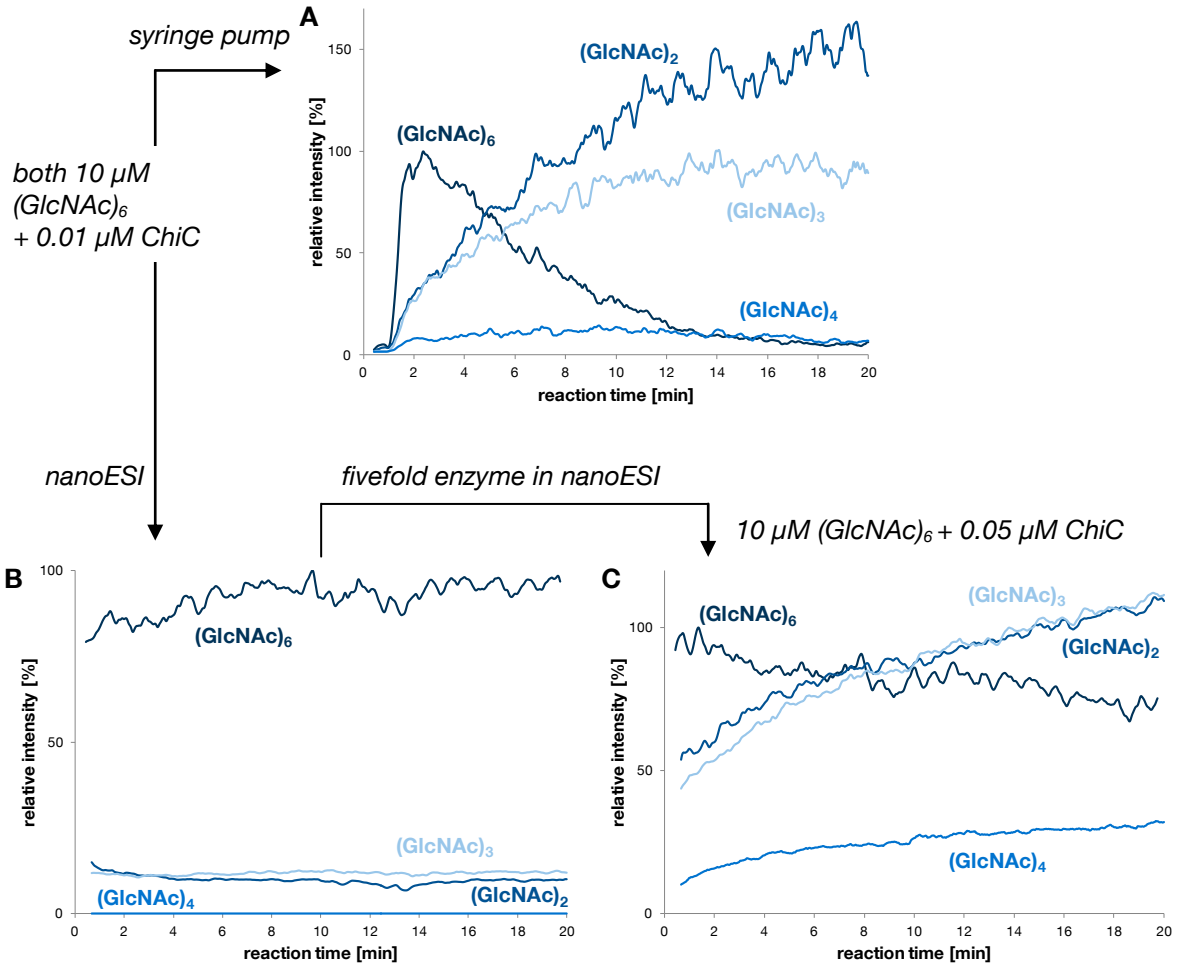

Figure 18: Comparison of the chitinase assay performed with 10 µM $(GlcNAc)_6$ and 0.01 µM ChiC in (A) the direct infusion syringe pump setup and (B) in the nanoESI setup. (C) The increase of the concentrations to 10 µM $(GlcNAc)_6$ and 0.05 µM ChiC results in product formation in the nanoESI setup ((A) 100% ≈ 3.9 x 10^4 counts $(GlcNAc)_6$, (B) 100% ≈ 2.7 x 10^5 counts $(GlcNAc)_6$, (C) 100% ≈ 1.3 x 10^5 counts $(GlcNAc)_6$), (Figure adapted from Figure 5 in Appendix III).

4.2.2 Measurement of Enzymatic Assays in the Modified nanoESI setup 'Flow-Control'

The nanoESI system was modified, regarding an improvement for the measurement of enzymatic assays. Two different setups were developed: the so called 'Flow control' setup and the 'LC coupling' setup.

The 'flow control' setup consists of a modified robotic arm (mandrel) for pipetting the solutions. This mandrel is connected via capillary with an HPLC flow instead of a connection to the integrated syringe in the 'infusion' setup. In comparison to the integrated syringe, the HPLC flow provides a higher head pressure on the solution in the pipette tip

and leads to a flow with ~400 to 500 nL/min. Therewith, a stable spray over the whole measurement time is generated and blocking effects of the channels in the ESIchip are eliminated. Figure 19 shows the measurement of the enzymatic assay with 25 µM $(GlcNAc)_6$ and 5 µM HEWL, i.e. the concentrations as used in the direct infusion experiments (Figure 10A). The measurements show a stable and reproducible signal (standard deviation as shaded time-courses). The increased sample flow leads to a mass spectrometric signal immediately after about 0.5 min which is an important benefit in comparison to the classical syringe pump setup with a mass spectrometric signal after ~2 min. The improved sample flow through the nanoESI chip with the LC flow offers the possibility for using the nanoESI robot system for monitoring enzymatic reactions in real-time. However, in this setup the solution in the pipette tip is still in contact with the applied voltage. Thus, the inactivation of the enzyme is still possible in this setup. For this reason, enzymes which are rather insensitive towards the application of voltage, e.g. HEWL, can be used in this setup.

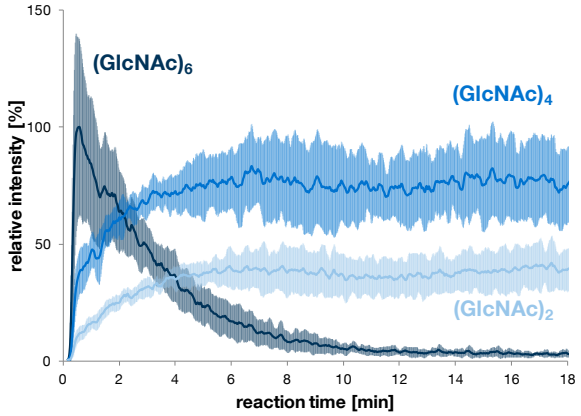

Figure 19: Continuous-flow measurement of the enzymatic assay with 5 µM HEWL and 25 µM $(GlcNAc)_6$ (100% ≈ 1.4 x 10^5 counts) in the 'flow control' setup with the nanoESI robot. Substrate and product traces show a constant signal (4 measurements, standard deviation shown as shaded area).

4.2.3 Measurement of Enzymatic Assays in the Modified nanoESI setup 'LC Coupling'

The 'LC coupling' setup was developed for elimination of the enzyme inactivation caused by voltage in the pipette tip, in order to develop a setup for more sensitive enzymes towards electric field. In this modification the mandrel is connected with a capillary located in the 'LC coupler' (Figure 20). The LC coupler is a small adapter which directly moves to the chip and sprays the solution through the ESI chip. The enzyme-substrate solution is no

longer in contact with the voltage on the pipette tip, preventing the enzyme inactivation. As already realized in the 'flow control' setup, here the sample flow is supported by an LC flow for generating a stable and constant nanoelectrospray. The automated measurement of the enzymatic assays is realized by switching between a mixing step and a spraying step. The switch occurs via an integrated 6-port-valve in the robot system and is controlled by the robot software (Chip soft, Version 7.2.0, Advion BioSciences, Ithaca, NY). All assay compounds are mixed in position 1 (Figure 20A) and in position 2 the enzyme assay solution is transported to chip with 500 nL/min (Figure 20B). The single compounds of the setup are connected via fused silica capillaries (inner diameter and lengths are shown in Figure 20A).

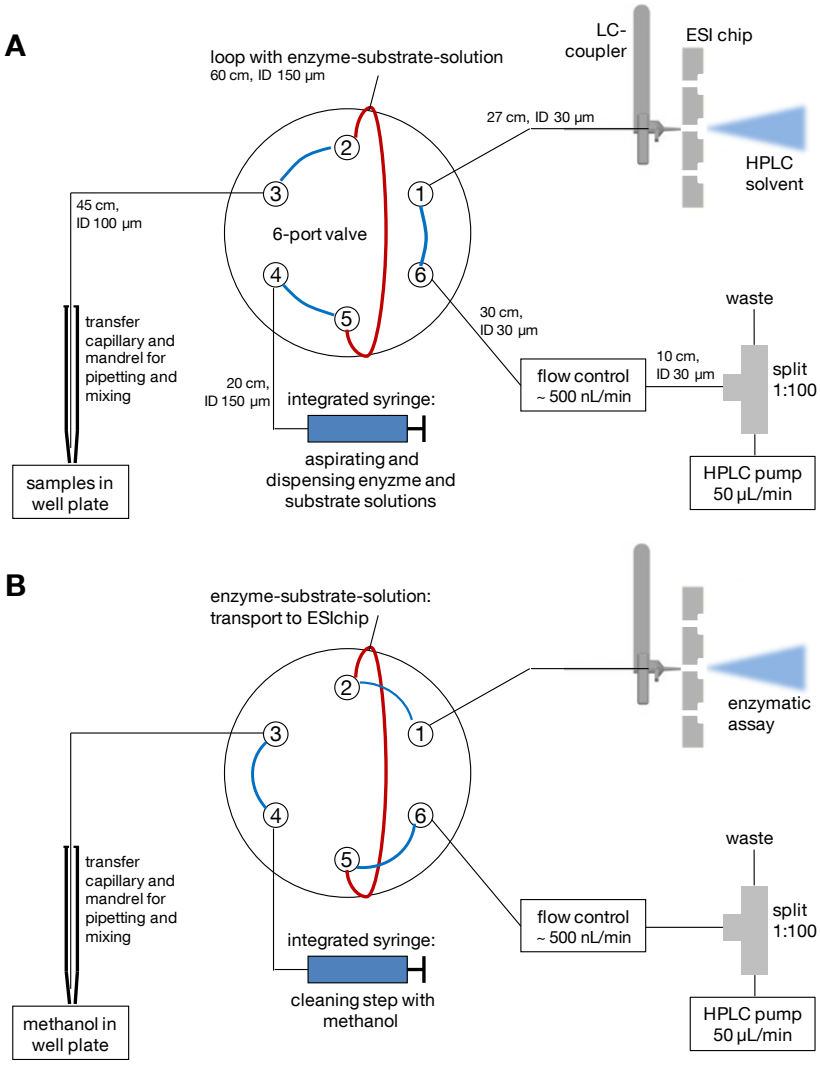

Figure 20: Setup for the measurement of enzymatic assays in the nanoESI 'LC coupling' setup with the nanoESI robot. (A) Position 1 for mixing enzyme and substrate and (B) position 2 for spraying the sample.

Figure 21 shows the measurement of 5 µM HEWL and 25 µM $(GlcNAc)_6$ in the 'LC coupling' setup. The sample flow of ~500 nL/min enables a constant nanoelectrospray flow through the chip without channel blocking. The time range between start of the enzymatic reaction and the mass spectrometric signal in this setup is two minutes and therewith longer than in the 'flow control' setup. This time has to be reduced by faster mixing and aspiration steps, which have to be implemented in the software. The aspirating and dispensing steps are controlled via the integrated syringe with 60 µL/min (unchangeable factory setting). Incorrect pipetting and air bubbles in the system are a consequence of the syringe velocity and the plenty of fused silica capillaries in the system (Figure 20). The velocity of the integrated syringe could be programmed in the software, which has to be carried out in cooperation with the company.

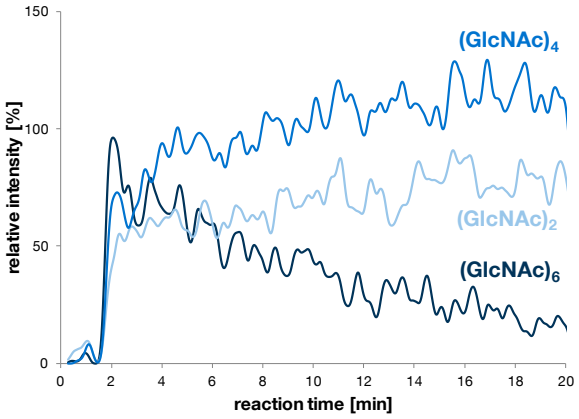

Figure 21: Continuous-flow measurement of an enzymatic assay with 5 µM HEWL and 25 µM $(GlcNAc)_6$ (100% ≈ 1.1 x 10^4 counts) in the 'LC coupling' setup with the nanoESI robot (1 exemplary measurement).

4.2.4 Summary

The nanoESI robot provides various key benefits for measuring enzymatic assays in real-time. Mass spectrometric enzymatic assay measurements by direct syringe pump infusion and in the nanoESI setup were compared and advantages are presented in Table 8. One key benefit is the automation of the complete process of measurement. Several compounds are automatically mixed, which is an enormous advantage for screening and monitoring complex enzymatic assays with several compounds. Mixing enzyme, substrate and further compounds can be automated as well, which is a critical step in the assay, since the enzymatic reaction immediately starts after mixing enzyme and substrate. Further,

the miniaturisation of the process offers a wide range of advantages. The sample volume and the concentrations can be decreased enormously, based on the very efficient ion transfer in nanoESI.

Table 8: Comparison of mass spectrometric measurements of enzymatic assays in the direct infusion syringe pump setup and with the nanoESI setup (adapted from Appendix II).

parameter	***direct infusion by syringe pump***	***nanoESI infusion mode***	***technical innovation***
process of mixing enzyme and substrate	manually	automated	automation
concentrations	~ 25 µM substrate ~ 5 µM enzyme	5-15 µM substrate 1-2 µM enzyme	miniaturisation
volume enzymatic assay	~ 1mL	~ 10-20 µL	miniaturisation
process of infusion	tubing-connected syringe and syringe pump	pipette tip, pump	automation
flow rate	5-10 µL/min	100-200 nL/min	miniaturisation
loss of time at the beginning of the assay	2 -3 min (manually mixing, filling the syringe, transfer capillary)	1 min (automated mixing, transfer to chip)	automation

Three setups of the miniaturised and automated system were evaluated in this work: ‘infusion’, ‘flow control’ and the ‘LC coupling’ setup. Concerning the key elements spray stability, inactivation of enzymes, cross contamination and the pipetting step they still do not meet all needs. Table 9 gives again an overview of the three different tested setups.

Table 9: Benefits and detriments of the three different setups ‘infusion’, ‘flow-control’ and ‘LC-coupling’ for measuring enzymatic assays in the nanoESI setup TriVersa Nanomate.

setup	***stable nanoelectrospray***	***enzymes insulated from voltage***	***correct pipetting***
infusion	no	no	yes
flow control	yes	no	yes
LC coupling	yes	yes	no

Concluding, a miniaturised and automated nanoESI system was developed for the first time, enabling the continuous monitoring of enzymatic reactions. A final technical setup combining the benefits of all three tested setups could not be realized finally in this work and has to be refined in a further project.

4.3 Technical Applications with Mass Spectrometry Compatible Enzymatic Assays

This chapter presents the usage of the mass spectrometry compatible enzymatic assays (chapter 4.1), the implementation of the obtained results and the knowledge about handling the assays in mass spectrometric experiments in further technological applications.
Diverse (bio)analytical issues of cooperative projects could be studied during this work based on the knowledge of handling and establishing mass spectrometry compatible enzymatic assays and the appropriate and targeted usage of the technological know-how. Different applications were investigated using one of the following technological setups: direct infusion, nanoESI or more complex mixing setups. Cleavage specifities of diverse chitinases, the hydrolysis profile of oligosaccharides by a chitosanase and the reaction profile of MPO were investigated by direct infusion experiments. The reaction mechanism of the chitosanase was further investigated by a continuous-flow mixing setup including an electrochemical reaction module. A continuous-flow mixing setup with a HT-HPLC module was used for screening complex house dust mixtures on enzyme regulatory compounds. The results concerning susceptibility of the enzymes towards organic solvents (chapter 4.1.2.1) served as basis for the HT-HPLC mixing setup and the investigation of the MPO in the nanoESI setup.
Parts of this chapter were published in Shinya et al., 2013, Nova Science Publishers, New York (Appendix V) and Zitouni et al., Applied Microbiology and Biotechnology, 2013, 97 (13), 5801-5813 (Appendix VI).

4.3.1 Continuous-Flow Assays with Direct Infusion

The direct infusion of an enzymatic assay into the mass spectrometer was for the investigation of several enzymological issues (Figure 22). Differences in the cleavage specifities of various chitinases and chitosanases towards diverse substrates and the reaction profile of the new isolated chitosanase Csn1794 were studied. Further, the reaction of MPO with the substrate Tyr was investigated for the first time by real-time mass spectrometry. The respective results are explained and discussed in the following.

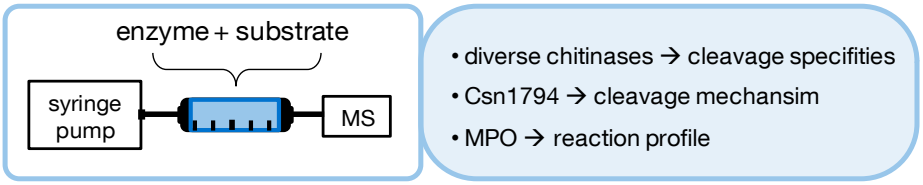

Figure 22: Schematic setup for measuring enzymatic assays in direct infusion experiments by mass spectrometry.

4.3.1.1 Determination of Cleavage Specifities of Chitinases

Glycoside hydrolases such as lysozyme and chitinases play a crucial role in hydrolysis of chitin. Chitin oligosaccharides consist of $(GlcNAc)_n$ and $(GlcN)_n$, with a degree of acetylation above 50%. They can be used as 'natural' substrate for glycoside hydrolases in mass spectrometry. The detailed investigation of chitinolytic enzymes is of multifaceted interest: They are used for biological control of plant disease and assist in the defense against fungal pathogens by destroying their cell walls. They also have been reported as possible targets in drug design of novel chemotherapeuticals against human pathogens such as fungi and protozoan parasites (Fukamizo, 2000; Vinetz et al., 2000; Fusetti et al., 2002).

In this work the mode of action and the cleavage specifities towards oligosaccharides of six chitinases were investigated in direct infusion experiments by real-time ESI-MS (Appendix IV and V). The close investigation by continuous-flow measurements gives information of preferable chain lengths of the substrates and the product chain length at specific time points. Thus, the role of the diverse enzymes in the oligosaccharide degradation can be specified, leading to efficient application of the enzymes.

The set of enzymes included the commercially available ChiC and especially for this work purified chitinase wild-types (WT) and mutants: RSC-c_WT and RSC-c_E67Q (inactive mutant), BcChiA_WT and BcChiA_E61A (inactive mutant), NtChiV_WT and NtChiV_G74W, AtChiC_WT and ATChiC_G75W and CrChiA_WT and CrChiA_G77W, respectively.

The composition and parameters of the mass spectrometric compatible ChiC assay was presented in chapter 4.1 and the other chitinases were measured according to this (ESI-MS reaction profiles not shown). The resulting conversion rates for the tested combinations of enzymes and oligosaccharides are summarized in Table 10.

Table 10: Overview of the measured chitinases by direct infusion and mass spectrometric detection for determination of the cleavage specifities towards diverse oligosaccharides (-, not determined).

enzyme	*substrate*	*enzyme concentration [µM]*	*conversion rate [min^{-1}]*
ChiC	$(GlcNAc)_6$	0.01	30
	$(GlcNAc)_4$	0.01	12
	DAAD, AADD, DDAA, DADA	0.01; 0.1; 1	no reaction
NtChiV_WT	$(GlcNAc)_6$	0.5	0.22
	$(GlcNAc)_4$	1	0.05
	DAAD, AADD, DDAA, DADA	1	no reaction
NtChiV_ G74W	$(GlcNAc)_6$	1	0.10
	$(GlcNAc)_4$	2	0.03
AtChiC_WT	$(GlcNAc)_6$	0.1	0.77
	$(GlcNAc)_4$	0.5	0.11
	DAAD	0.5	no reaction
AtChiC_G75W	$(GlcNAc)_6$	0.05	1.20
	$(GlcNAc)_4$	0.1	0.47
CrChiA_WT	$(GlcNAc)_6$	0.1	0.97
	$(GlcNAc)_4$	-	-
CrChiA_G77W	$(GlcNAc)_6$	0.03	3.97
	$(GlcNAc)_4$	0.5	0.12
	DAAD	0.5	no reaction
RSC-c_WT	$(GlcNAc)_6$	0.05	1.47
	$(GlcNAc)_4$	1	no reaction
RSC-c_E67Q	$(GlcNAc)_6$	0	no reaction
	$(GlcNAc)_4$	0	no reaction
BcChiA_WT	$(GlcNAc)_6$	0.02	1.80
	$(GlcNAc)_4$	0.1	1.15
	DAAD	0.5	no reaction
BcChiA_E61A	$(GlcNAc)_6$	0	no reaction
	$(GlcNAc)_4$	0	no reaction

For all enzymes the hydrolysis of the hexasaccharide $(GlcNAc)_6$ proceeds faster than of the tetrasaccharide $(GlcNAc)_4$. The $(GlcNAc)_6$ is hydrolyzed about two to sevenfold faster than the $(GlcNAc)_4$, except for CrChiA-G77W with a 33-fold faster $(GlcNAc)_6$ hydrolysis. These results confirm the fact, that the longer the chain length of oligosaccharide substrate, the higher the hydrolysis rate. This in agreement with earlier observations for HEWL (by mass spectrometry) and NtChiV (by HPLC) and is a typical property of most 'endo-splitting' glycoside hydrolases (Dennhart et al., 2009; Ohnuma et al., 2011). Different conversion rates were observed comparing wildtypes and mutants. Mutant NtChiV_G74W hydrolyzed both, $(GlcNAc)_6$ and $(GlcNAc)_4$ about two times slower than the corresponding wildtype. In contrast, the mutants AtChiC_G75W and CrChiA_G77W hydrolyzed the substrates faster than the respective wildtype. Both inactive mutants RSC-c_E67Q and BcChiA_E61A did not hydrolyze $(GlcNAc)_6$ and $(GlcNAc)_4$ as expected. Thus, targeted mutations, leading to faster and/or specific substrate hydrolysis provide a very useful tool in industrial processes, e.g. for the biotechnological production of special oligosaccharide chain lengths.

The enzyme-specific product distributions are shown in Figure 23. The figure includes the results of this work and earlier findings as described in literature for giving a complete overview (Dennhart et al., 2008; Dennhart et al., 2009; Taira et al., 2010). Differences in the mode of action are obvious, e.g. $(GlcNAc)_6$ is mainly split into $(GlcNAc)_3$+$(GlcNAc)_3$ by RSC-c, BcChiA and CrChiA whereas ChiC, NtChiV and AtChiC prefer the $(GlcNAc)_6$ hydrolysis into $(GlcNAc)_4$+$(GlcNAc)_2$. The different product distributions might be caused by the amino acid substitutions and the arrangement of loop structures at the substrate binding clefts.

The specially synthesized isomers of di-N-acetylchitotetraoses (AADD, ADDA, ADAD, DADA, DAAD, and DDAA, with D = GlcN and A = GlcNAc) (Vijayakrishnan et al., 2011) should give a more detailed insight in the mode of action of the chitinases. As already mentioned, chitinases preferably hydrolyze the ß-1,4-glycosidic linkage in chitin and experiments with $(GlcNAc)_4$ showed a symmetrical cleavage mechanism to products $(GlcNAc)_2$+$(GlcNAc)_2$ (Figure 23). Thus, the tetrasaccharide isomers DAAD, AADD, DDAA or DADA with the acetylated (GlcNAc) monomer in the middle position were chosen as a first selection for the enzymatic reaction. However, with none of these combinations an enzymatic cleavage could be observed. Even an increase of enzyme concentration for ChiC up to 100 fold in comparison to the measurement with $(GlcNAc)_4$, did not result in an enzymatic conversion. As shown in Table 10, the conversion rate for all chitinases is two- to 30-fold slower for $(GlcNAc)_4$ than for $(GlcNAc)_6$. The additional replacement of two (GlcNAc) molecules by (GlcN) seems to change the compound structure in such a way, that they can be no longer hydrolyzed by the chitinases.

Concluding, the real-time ESI-MS experiments provide a beneficial and appropriate method for the determination of enzyme-specific cleavage profiles and product distribution (Figure 23). The experiments give an excellent overview of a variety of chitinases and are an essential basis for biotechnological applications such as the industrial controlled hydrolysis, in secondary fuel generation and white biotechnology and makes new chemical procedures available.

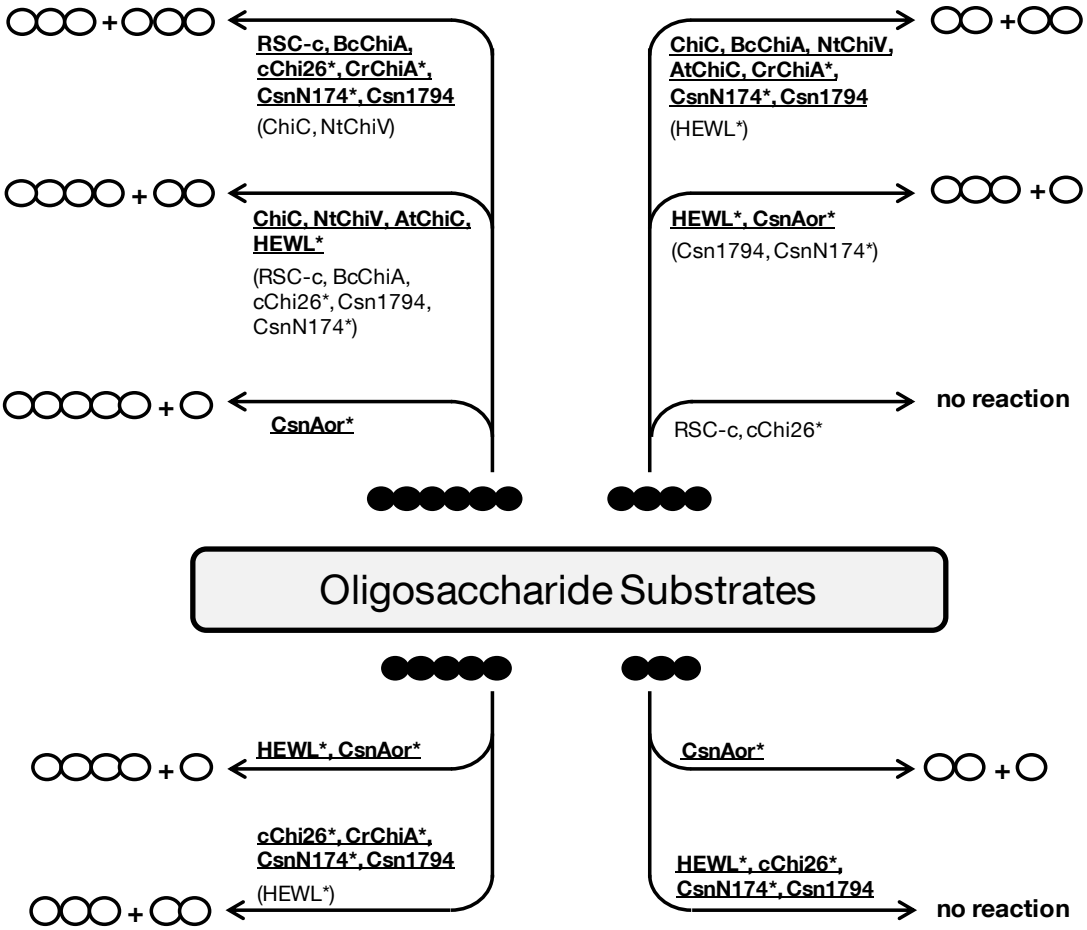

Figure 23: Overview of hydrolysis profiles of glycoside hydrolases HEWL, chitinases and chitosanases with different oligosaccharides determined by ESI-MS experiments. ● = substrate (GlcNAc) and ○ = products (GlcNAc). Major pathways are 'bold and underlined' and the minor pathways of the enzymes are presented in 'brackets'. For a complete overview of all ESI-MS results with glycoside hydrolases, enzymes described in literature (Dennhart et al., 2008; Dennhart et al., 2009; Taira et al., 2010) are also shown in this chart (marked with *) (Figure adapted from Figure 16 in Appendix V).

4.3.1.2 Determination of the Hydrolysis Profile of Csn1794

As well as chitin, chitosan is of great biotechnological interest due to its potential for biomedical or environmental fields. The enzymatic chitosan hydrolysis is a recognized method for the controlled optimization of its molecular size.

The thermostable chitosanase Csn1794, produced from *Paenibacillus* sp. 1974, was isolated in the group of Prof. Brzezinski for the first time. The usage of a thermostable enzyme is beneficial for the enzymatic hydrolysis at higher temperature, which enables a chitosan solution at higher concentrations.

The continuous-flow mass spectrometric monitoring of enzymatic reactions was applied for the characterisation of the new isolated chitosanase Csn1794 for the first time (Appendix VI). A wide range of oligosaccharide substrates was used: $(GlcN)_n$ (n = 3, 4, 5 and 6) and $(Glc)_n$ (n = 3, 4 and 6), respectively. Figure 24 shows the hydrolysis profile of Csn1794 of chitosan- and cellulose derived oligosaccharides of different chain lengths.

For these experiments a semi-quantitative estimation of the cleavage mode for $(GlcN)_6$ and $(Glc)_6$ was applied and both were compared (Appendix VI). The cleavage mode at 100% $(GlcN)_6$ consumption shows a clear preference to symmetrical cuts ($(GlcN)_3$+$(GlcN)_3$ and $(GlcN)_2$+$(GlcN)_2$) compared to the asymmetrical ones ($(GlcN)_4$+$(GlcN)_2$) in a 12:1 proportion. In contrast, the ratio of symmetrical/asymmetrical mode of cleavage of $(Glc)_6$ was only 2:1. These results point towards a substantial difference in the substrate binding mode among chitosan and cellulose-derived hexasaccharides. The Csn1794 activity towards the different substrates was determined by means of the conversion rates: 228 min^{-1} for $(GlcN)_6$, 722 min^{-1} for $(GlcN)_5$, 0.4 min^{-1} for $(GlcN)_4$, 8 min^{-1} for $(Glc)_6$ and 0.2 min^{-1} for $(Glc)_4$. The trimers $(GlcN)_3$ and $(Glc)_3$ were not hydrolyzed, even with 1 µM Csn1794. Thus, the enzyme needs at least five sugar units for an efficient hydrolysis, binding three units on one side of the catalytic center. Regarding the chain length, $(GlcN)_5$ shows the highest conversion rate, followed by $(GlcN)_6$ and $(GlcN)_4$. These results are in accordance with the enzyme CsnN174, which was studied earlier by Dennhart and coworkers (Dennhart et al., 2008). Both chitosanases do not hydrolyze $(GlcN)_3$ and do not show the '5+1' type of cleavage of hexasaccharides. This indicates that both enzymes are essentially endo-type chitosanases.

Regarding the substrate specifities of Csn1794, the conversion rates for the substrates with the glucosamine units are higher than the substrate with glucose units. The conversion of $(GlcN)_6$ is about 30 times faster than for $(Glc)_6$. The hydrolysis of $(Glc)_6$ could not be significantly increased, even with higher substrate and enzyme concentrations of 25 µM $(Glc)_6$ with 10 or 50 nM Csn1794, which led to conversion rates of 20 and 21 min^{-1}, respectively (data not shown). Thus, the presence of charged amino groups in the substrate may be important for substrate binding and enzyme activity.

The mode of action of Csn1974 was implemented in Figure 23 giving a complete overview of glycosidase hydrolysis profiles obtained by real-time ESI-MS measurements up to now. The chitosanases CsnN174 and CsnAor, which were investigated in earlier studies, are also presented in Figure 23 (Dennhart et al., 2008; Dennhart et al., 2009; Taira et al., 2010). The results from these literature data are marked with *.

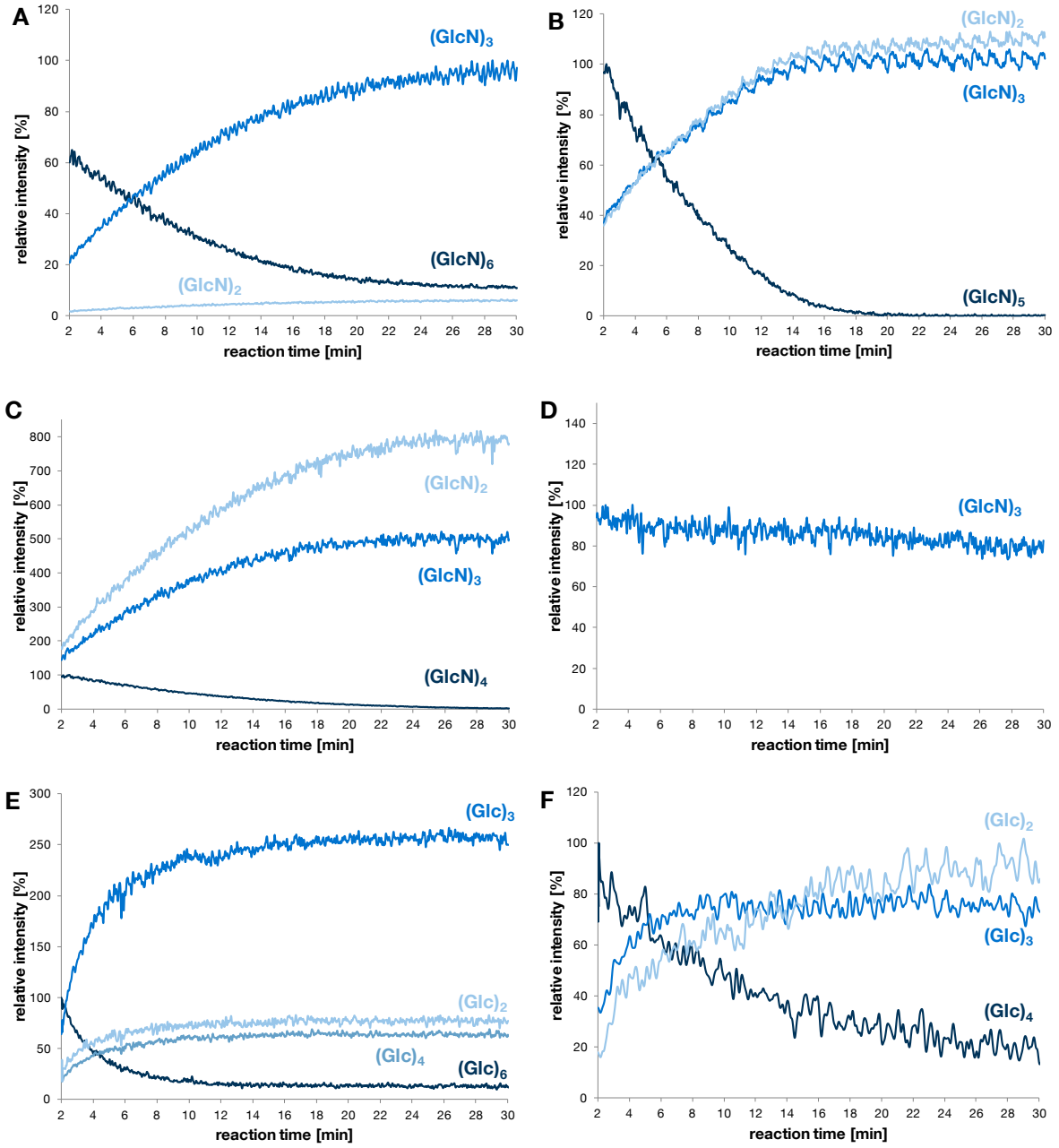

Figure 24: Continuous-flow direct infusion of enzymatic assays with enzyme Csn1794 and mass spectrometric detection. Reactions were performed with (A) 10 µM $(GlcN)_6$ and 1 nM Csn1794 (100% ≈ 2.9 x 10^4 counts), (B) 10 µM $(GlcN)_5$ and 1 nM Csn1794 (100% ≈ 1.6 x 10^4 counts), (C) 10 µM $(GlcN)_4$ and 1 µM Csn1794 (100% ≈ 2.3 x 10^4 counts), (D) 10 µM $(GlcN)_3$ and 1 µM Csn 1794 (100% ≈ 4.5 x 10^3 counts), (E) 10 µM $(Glc)_6$ and 50 nM Csn1794 (100% ≈ 1.3 x 10^4 counts) and (F) 10 µM $(Glc)_4$ and 500 nM Csn1794 (100% ≈ 2.3 x 10^3 counts) (Figure adapted from Figure 5 in Appendix VI).

4.3.1.3 Investigation of the Myeloperoxidase Assay

The reaction of MPO is an emerging topic in biomedical research, since MPO is involved inflammatory processes and in the pathogenesis ranging from cardiovascular diseases, tissue injury to lung cancer (Harrison and Schultz, 1976; Podrez et al., 2000; Klebanoff, 2005). Up to now, the enzymatic reaction of MPO was only studied in quenched assays with determination of products at defined time points, either photometrically, by NMR, HPLC or mass spectrometric detection (Heinecke et al., 1993; Domigan et al., 1995; Marquez and Dunford, 1995; Hazen et al., 1996; Jacob et al., 1996; Sampson et al., 1998; Gaut et al., 2001; Kato et al., 2003).

In the current work, the enzymatic reaction of MPO with substrate Tyr was investigated for the first time by continuous-flow mass spectrometric experiments. The study gives a complete overview of the reaction profile, i.e. substrate depletion and product and intermediate formation in real-time. The assay was studied regarding the impact of diverse assay compounds and the inhibitory impact of epigallocatechingallate (EGCG). The implementation of the assay in the nanoESI setup is described in chapter 4.3.2.

The reaction mechanism of MPO with substrate Tyr, which was determined by direct infusion mass spectrometric experiments and the determined products are shown in Figure 25. Based on the chlorinating and nitrating activity of MPO, the reaction was studied in the presence/absence of $NaNO_2$ and NH_4Cl and the product distribution is indicated in Figure 25.

Figure 26 shows the continuous-flow mass spectrometric time-courses for all detected compounds when measuring the MPO assay with Tyr as substrate. According to preliminary photometrical tests the assay with 50 µM Tyr and 0.03 µM MPO, 200 µM H_2O_2 and 50 µM $NaNO_2$ in the presence or absence of chloride was used as initial assay for determination of all decreasing and increasing compounds in the reaction. Accurate measurements with the ToF-MS and MS/MS experiments were used for identification of the compounds. In the presence of nitrite the formation of NitroTyr is the preferred product of the MPO assay (Figure 26B). The NitroTyr formation was also reported Sampson and coworkers who investigated the Tyr nitration in proteins by western blots and by Franck and coworkers by UV-vis spectroscopy (Sampson et al., 1998; Franck et al., 2008).

Besides the NitroTyr, the signal with m/z 194 is a main product of the MPO assay (Figure 26B). However, the exact structure of this compound could not be identified up to now. Several presumptions are possible by means of different information (data not shown): a) The m/z 194 cannot be detected in the pure solutions with Tyr, NitroTyr and ClTyr and even

in the corresponding MS/MS experiments. Thus, these compounds as well as a respective fragmentation product can be excluded. b) The m/z with 194 is obviously no chlorinated product since the lack of the isotope ratio of 75:25 of ^{35}Cl:^{37}Cl. c) The curve progression of the m/z 194 is independent of the presence or the absence of $NaNO_2$. Thus, the m/z 194 is probably no nitrated product and no sodium adduct.

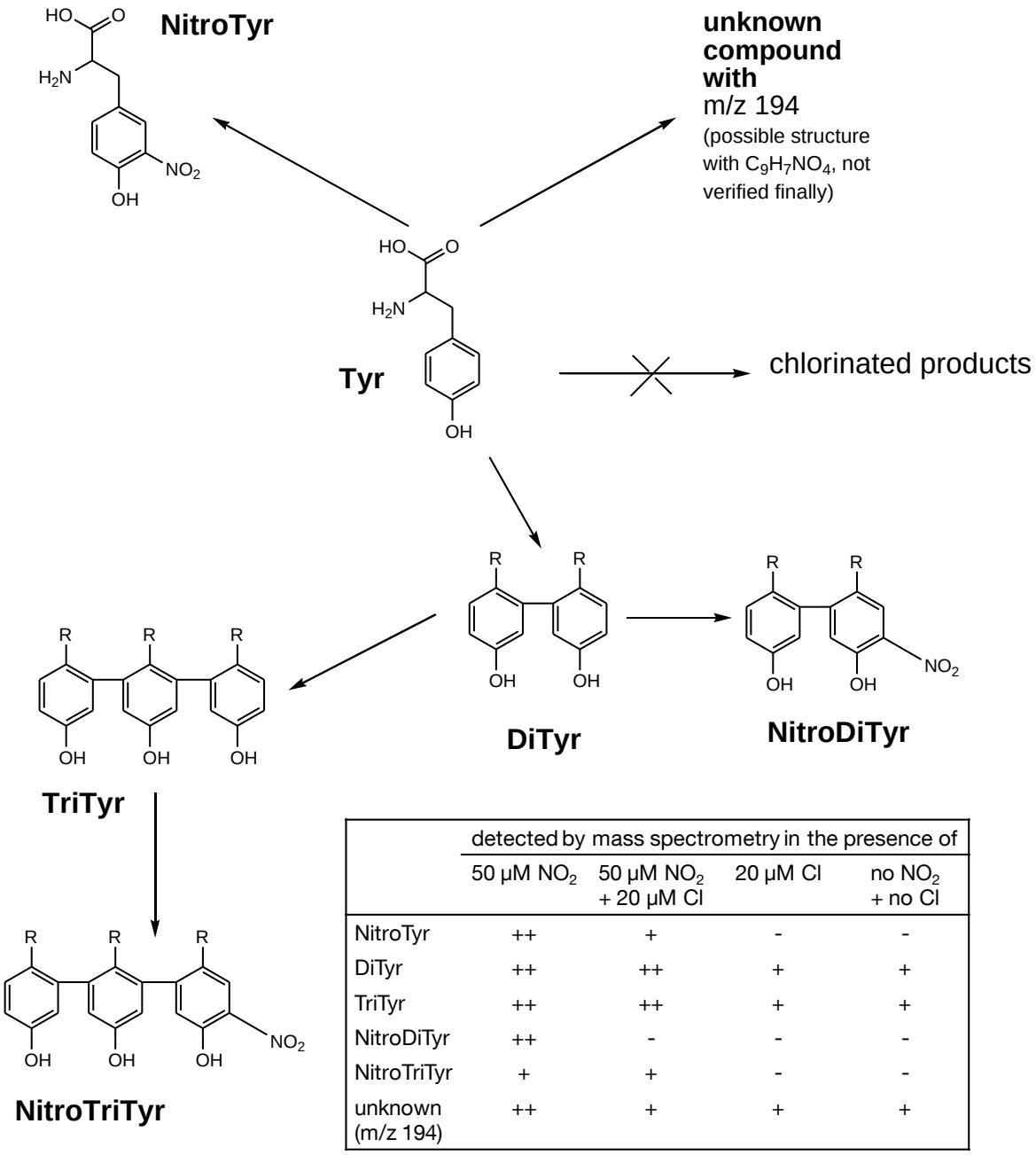

	detected by mass spectrometry in the presence of			
	50 µM NO_2	50 µM NO_2 + 20 µM Cl	20 µM Cl	no NO_2 + no Cl
NitroTyr	++	+	-	-
DiTyr	++	++	+	+
TriTyr	++	++	+	+
NitroDiTyr	++	-	-	-
NitroTriTyr	+	+	-	-
unknown (m/z 194)	++	+	+	+

Figure 25: Reaction mechanism of enzyme myeloperoxidase with substrate Tyrosine (Tyr) obtained by mass spectrometric direct infusion experiments. The measurements with 50 µM Tyr, 0.03 µM MPO and 200 µM H_2O_2 were carried out in the presence and/or absence of NO_2 and Cl. The spectrometric detected and identified compounds are shown. The NO_2 and Cl depending product formation is indicated in the inserted table.

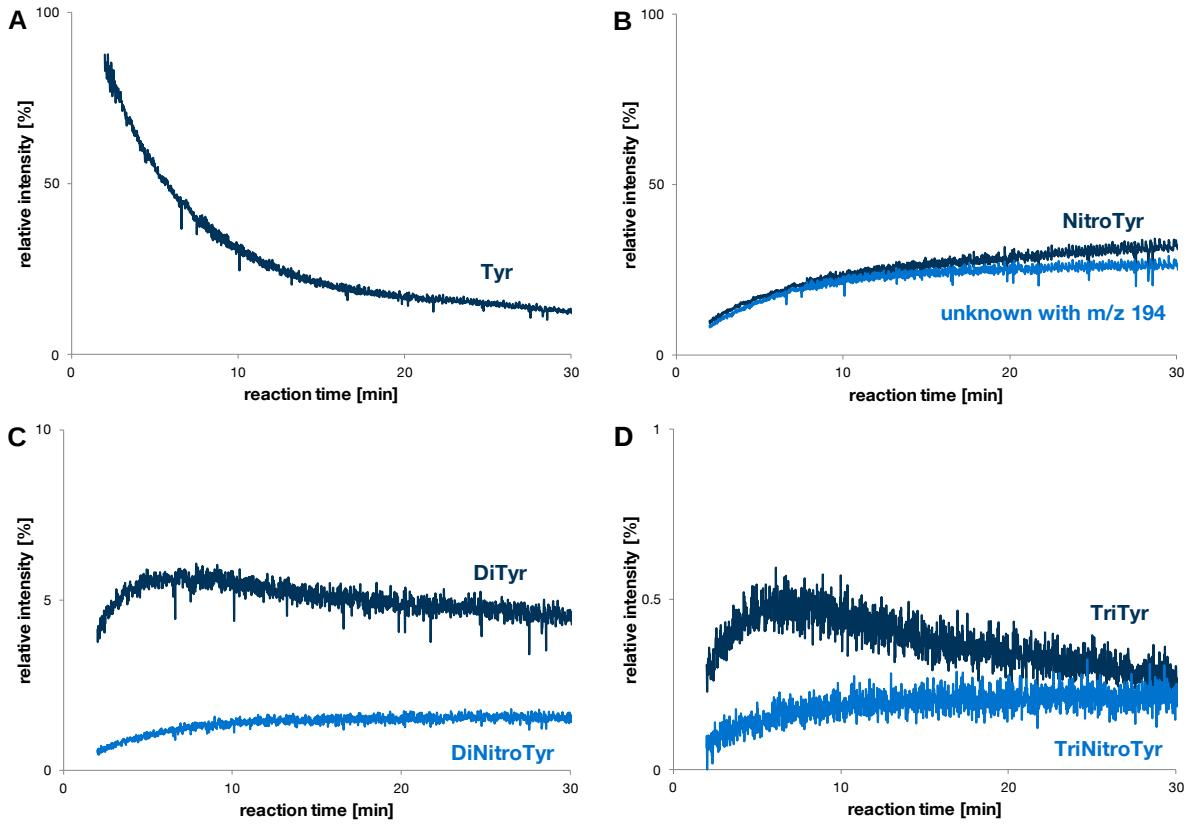

Figure 26: Real-time ESI-MS measurement of the MPO assay with 50 µM Tyr, 0.03 µM MPO, 200 µM H_2O_2 and 50 µM $NaNO_2$ with direct infusion and mass spectrometric detection (mean value of three measurements). (A) The decreasing substrate Tyr (100% ≈ 2.5 x 10^5 counts) and the main increasing product signals are shown with (B) NitroTyr and an unknown compound with m/z 194, (C) DiTyr and NitroDiTyr and (D) TriTyr and NitroTriTyr.

As shown in Figure 26C and 26D polymerized dimer and trimer products are detectable. The signal with m/z 361 corresponds to DiTyr or Isotyr and m/z 540 to TriTyr or pulcherosine, respectively (Heinecke, 2002). The MPO catalyzed reaction of tyrosine to tyrosine radical yields to the cross-linked polymer products (Heinecke et al., 1993). The signal development of DiTyr and TriTyr shows a sharp increase from the beginning up to the reaction time of about five minutes and then decrease slightly. Simultaneously, both nitrated forms, the NitroDiTyr and NitroTriTyr show a slight but continuous increase, indicating a further nitration step after polymerisation (Figure 26C and 26D).

Besides the nitration activity, MPO also offers chlorination activity (Domigan et al., 1995; Hazen et al., 1997; Gaut et al., 2001). In the current study, chlorination products were not identified, even in the presence of chloride, ranging from 20 µM to physiological concentration of 10 mM chloride. In the presence of nitrite and even in high concentrations of Cl the NitroTyr is the main product and no chlorination products can be detected. These observations are in accordance with the work of Sampson and coworkers. In their work,

physiological levels of chloride did not significantly inhibit the nitration by MPO and the nitration of BSA did not require chloride (Sampson et al., 1998). The lack of the chlorination activity of MPO in the current setup might depend on the pH value of 7.4. Literature is available, reporting an increased chlorinating activity of MPO with a decreasing pH (Bakkenist et al., 1980; Vlasova et al., 2006). Regarding further measurements in multiplexing experiments (chapter 4.1.2.2), the pH was not varied in this set of experiments.
According to the decreasing Tyr signal (Figure 26A) further decreasing signals with m/z 119, 136 and 165 were identified as ion source fragments (data not shown). The signal with m/z 165 corresponds to a loss of NH_3, the m/z 136 to a loss of $CO+H_2O$ (immonium ion) and m/z 119 is a loss of 63 Da, i.e. loss of NH_3 from the immonium ion (Piraud et al., 2003). These ion source fragments were neglected due to their low signal intensity.
The epigallocatechin-3-gallate (EGCG) is the major present polyphenolic compound in green tea (Cabrera et al., 2006). Literature is available, discussing the inhibitory effect of EGCG on MPO activity (Mazzon et al., 2005; Mochizuki and Hasegawa, 2005). Thus, the established measurement of the MPO assay was applied for investigation of the inhibitory effect of EGCG. The MPO assay was carried out in the presence of different EGCG concentrations ranging from 0.1 µM to 100 µM. By calculating the conversion rates of the Tyr degradation the relative MPO activity was determined (Figure 27). Therewith the IC_{50} of 6 µM value was calculated for EGCG by using an exponential function. Mochizuki and Hasegawa studied the MPO activity in mucosa in the presence of EGCG (Mochizuki and Hasegawa, 2005). They reported a reduced MPO activity after treatment with EGCG by 46%, but they did not give any information about the concentration.

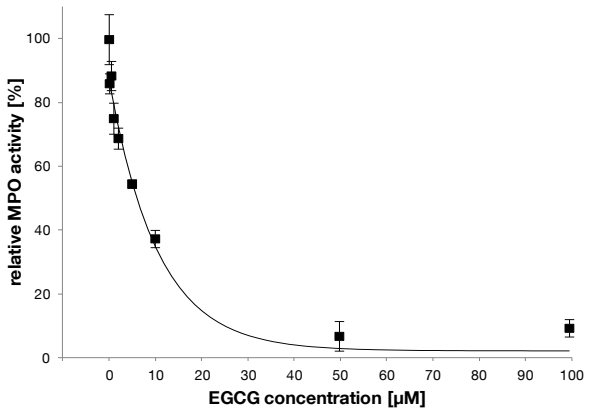

Figure 27: Inhibition plot of the inhibitory effect of epigallocatechingallate (EGCG) on the activity of MPO. The relative MPO activity [%] was determined by conversion rates calculated from real-time ESI-MS experiments (mean value of three measurements). The reaction of the MPO assay with substrate tyrosine was carried out in the presence of different EGCG concentrations from 0.1 µM to 100 µM. The IC_{50} value was calculated by an exponential function (y=84.95 e^(-x/10.55)).

The reaction time courses of the products strongly depend on the presence and concentration of EGCG. With increasing EGCG concentrations the product signals are detected with a delay after the beginning. Figure 28 exemplarily shows the NitroTyr formation in the presence of diverse EGCG concentrations and e.g. 10 µM EGCG leads to a NitroTyr formation after 10 minutes. The other polymer products and unknown product with m/z 194 show a similar product formation course such as NitroTyr (data not shown).

This set of experiments shows the beneficial applicability of mass spectrometric direct infusion for obtaining detailed insights in enzymological issues. Even more complex enzymatic reaction, such as the presented assay with MPO which requires diverse additional compounds (H_2O_2 and salts) are easy to handle in this setup. The continuous-flow setup with mass spectrometric detection leads to manifold information in few experiments, ranging from reaction mechanism, influence of assay compounds and inhibition studies.

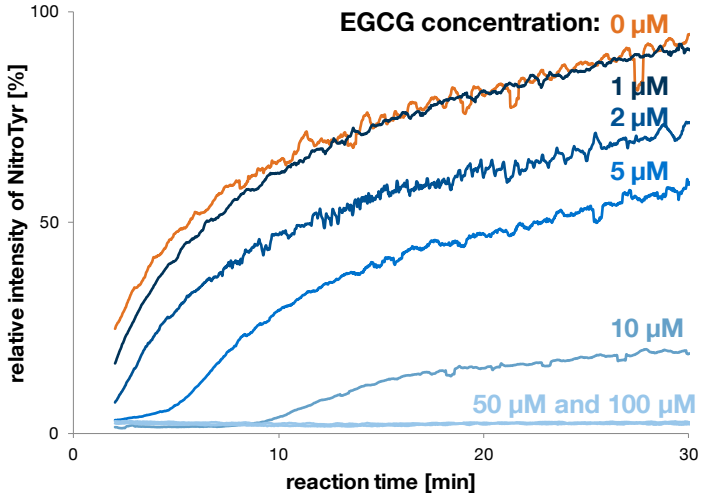

Figure 28: Reaction time course of nitrotyrosine (NitroTyr) in the MPO assays with the direct infusion setup and mass spectrometric detection. The measurement was carried out with 50 µM Tyr, 0.03 µM MPO, 200 µM H_2O_2 and 50 µM $NaNO_2$ in the presence of 0 µM, 1 µM, 2 µM, 5 µM, 10 µM, 50 µM and 100 µM epigallocatechingallate (EGCG) (100% NitroTriTyr ≈ 7 x 10^4 counts).

4.3.2 Continuous-Flow Assays with nanoESI Robot Infusion

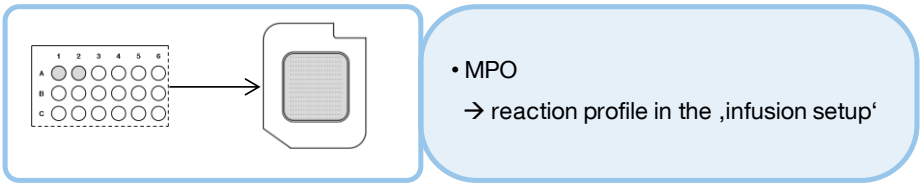

Figure 29: Schematic setup for measuring enzymatic assays in nanoESI experiments by mass spectrometry.

The measurement of enzymatic assays in the miniaturised and automated nanoESI setup was described in chapter 4.2. The high surface tension of aqueous solutions leads in the ‘infusion setup’ to a blocking of the channels in the ESI chip and thus to a termination of the nanoelectrospray. This difficulty was overcome for the following application with the enzyme MPO. The setup was used for real-time measurements by addition of organic solvent to the sample solution. The addition of 10% methanol or 2-propanol was sufficient for generating a stable nanoelectrospray over about 30 minutes. The compatibility of methanol and 2-propanol with MPO was confirmed in preliminary photometric experiments (data not shown). Figure 30 shows the measurement of the MPO assay with the substrate Tyr and $NaNO_2$ in the presence of 10% methanol in the nano ESI ‘infusion’ setup. The simultaneous Tyr depletion and NitroTyr product formation are monitored in this setup. In comparison to the ToF experiments (chapter 4.3.1.3) these measurements were carried out with a less sensitive ion trap mass spectrometer. Thus, further assay products (Figure 25) could not be detected. The addition of organic solvent facilitates a stable nanoelectrospray flow through the nanoESI chip over the 30 minutes reaction time. As determined in the direct infusion syringe pump experiments (chapter 4.3.1.3) NitroTyr is the main product.
Thus, when measuring enzymatic assays with enzymes, tolerating about 10% to 20% organic solvent, the ‘infusion’ nanoESI setup is a beneficial system for the miniaturised and automated measuring.

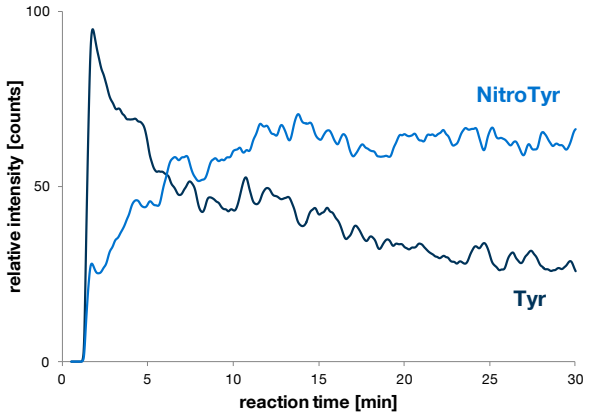

Figure 30: Measurement of the enzymatic assay in the nanoESI 'infusion' setup with 50 µM tyrosine (Tyr), 50 µM $NaNO_2$, 200 µM H_2O_2 and 0.05 µM myeloperoxidase. The extracted ion chromatograms for substrate Tyr (100% ≈ 1.7 x 10^4 counts) and product nitrotyrosine (NitroTyr) are shown.

4.3.3 Continuous-Flow Mixing Assays

The coupling of diverse instrumental modules in continuous-flow mixing setups in combination with enzymatic assays was a further part of the current work. The implementation of an electrochemical cell for substrate reduction upfront the mixing with the enzyme was used for the final investigation of the Csn1794 hydrolysis profile. In another setup a high-temperature HPLC module was integrated in the continuous-flow system for screening experiments with house dust extracts.

Both applications including the technological setups and their enzymological relevance are described in the following.

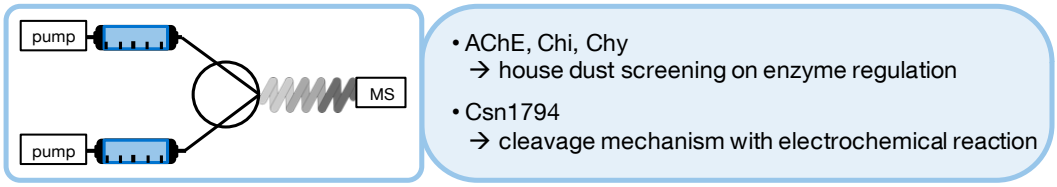

Figure 31: Schematic setup for measuring enzymatic assays in continuous-flow mixing experiments by mass spectrometry.

4.3.3.1 Cleavage Mechanism of Csn1794

Csn1794 hydrolyzes $(GlcN)_5$ into $(GlcN)_2$+$(GlcN)_3$ as determined in continuous-flow direct infusion experiments (chapter 4.3.1.2). The mass spectrometric data do not provide information about the hydrolysis pathway, i.e. if the enzyme hydrolyses into the molecules '2+3' or '3+2' from the reducing end.

A specific reduction of $(GlcN)_5$ is a way to distinguish if the reducing end is in the dimer product or the trimer product after enzymatic hydrolysis. In this work a new continuous-flow mixing technique, the online coupling of electrochemistry with mass spectrometric detection, was applied for this enzymological issue. The usage of an electrochemical system is beneficial for mass spectrometry, since chemical reduction proceedings, e.g. with $NaBH_4$, are not compatible for mass spectrometric experiments (Kongruang and Penner, 2004). The electrochemical preparation of sorbitol by electrolyzing glucose with a hydrogen-storage electrode has been reported (Tang et al., 2004).

Here, the electrochemical ROXY system (Antec, Zoeterwoude, The Netherlands) was used as a tool for the electrochemical reduction of the $(GlcN)_5$ solution. Within this system, the reduction of the $(GlcN)_5$ solution proceeds in front of the mass spectrometer. The specific reduction of $(GlcN)_5$ would lead to a change of the $[M+H]^+$ signal of 2 Da (Figure 32). The change in the reducing end is a way to distinguish if the reducing end after enzymatic hydrolysis is in the dimer product or the trimer product. The mass of $(GlcN)_2$–2 Da will point to a splitting mechanism of '3+2' and the mass of $(GlcN)_3$–2 Da to a splitting mode of '2+3'. Coupled with the enzymatic reaction with Csn1794, this experimental setup enables a more detailed insight into the enzymatic reaction (Figure 33).

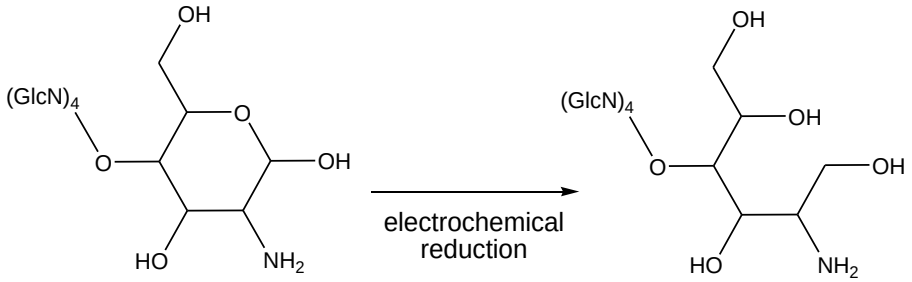

$(GlcN)_5$
$C_{30}H_{57}N_5O_{21}$
exact Mass: 823.35

reduced form of $(GlcN)_5$
$C_{30}H_{59}N_5O_{21}$
Exact Mass: 825.37

Figure 32: Specific reduction of $(GlcN)_5$ with 2 Da difference in the molecular weight for determination by mass spectrometry.

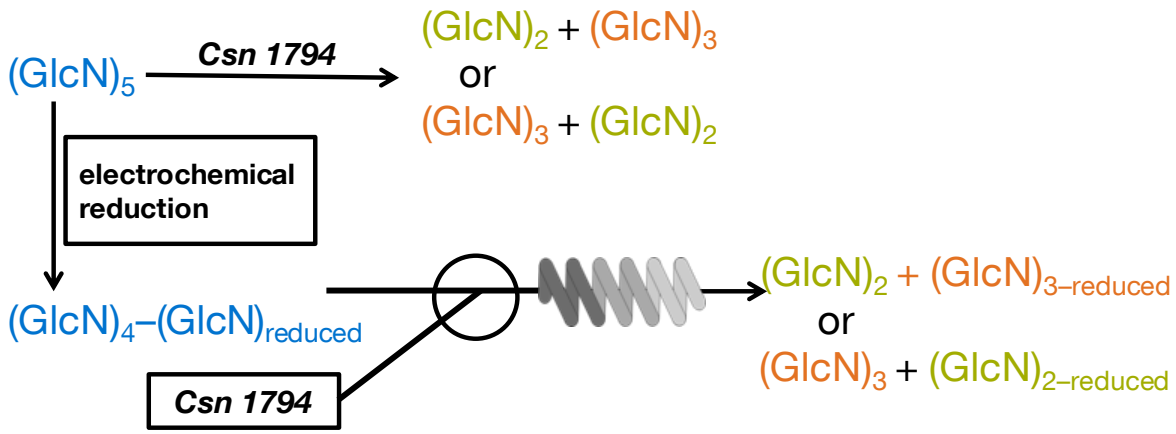

Figure 33: Instrumental setup of a continuous-flow mixing assay with the enzymatic reaction of $(GlcN)_5$ with Csn1794 in combination with an electrochemical reduction module. The targeted electrochemical reduction of $(GlcN)_5$ upfront the enzymatic reaction provides an experimental setup for the determination of the Csn1794 cleavage mechanism. The system is installed upfront a mass spectrometer and reaction products are determined by their different m/z.

The $(GlcN)_5$ reduction with the diamond electrode was combined with the enzymatic assay with Csn1794 and results are shown Figure 34. The target molecule $(GlcN)_5$ passes the electrochemical cell where 0-(-2) V for the reduction are applied. In the following reaction coil $(GlcN)_5$ or $(GlcN)_{5,reduced}$ reacts with Csn1794. Then the respective products, either $(GlcN)_2$ and $(GlcN)_{3,reduced}$ or $(GlcN)_3$ and $(GlcN)_{2,reduced}$, can be detected by mass spectrometry (Figure 33). Figure 34 shows the significant decreasing $(GlcN)_5$ signal during the application of voltage. According to this, the enzymatic assay products $(GlcN)_3$ and $(GlcN)_2$ decrease, due to less available substrate $(GlcN)_5$. In case of the targeted $(GlcN)_5$ reduction, the signal with m/z 825 should increase during voltage application (Figure 32). Such specific signals were not detected in this setup, rather nonspecific signals around m/z 800-808 were determined (Figure 34). Reduced forms of $(GlcN)_2$ or $(GlcN)_3$, respectively, were not observed. Several parameters have been tested systematically with the ROXY system to optimize the conditions for the $(GlcN)_5$ reduction. Both electrodes with 10 µL/min and 50 µL/min and all materials (glassy carbon, diamond, gold, platinum and reductive electrode) have been tested. The concentration for $(GlcN)_5$ was varied from 10 µM to 50 µM and even the oxidation mode was tested. In all combinations the substrate signal $(GlcN)_5$ decreased and a small increase of reaction products was observed in some experiments. However, these products were not characteristic and it was not possible to refer them to a special product (data not shown). Poor ionization or mass spectrometric fragmentation of the reaction products might be a possible explanation or an inefficient reduction in the electrochemical cell.

However, the principal potential for using this setup for enzymological issues is clearly shown with the current data. The technological combination of the continuous-flow electrochemical system with a continuous-flow of an enzymatic reaction is possible and may be used in future bioanalytical applications.

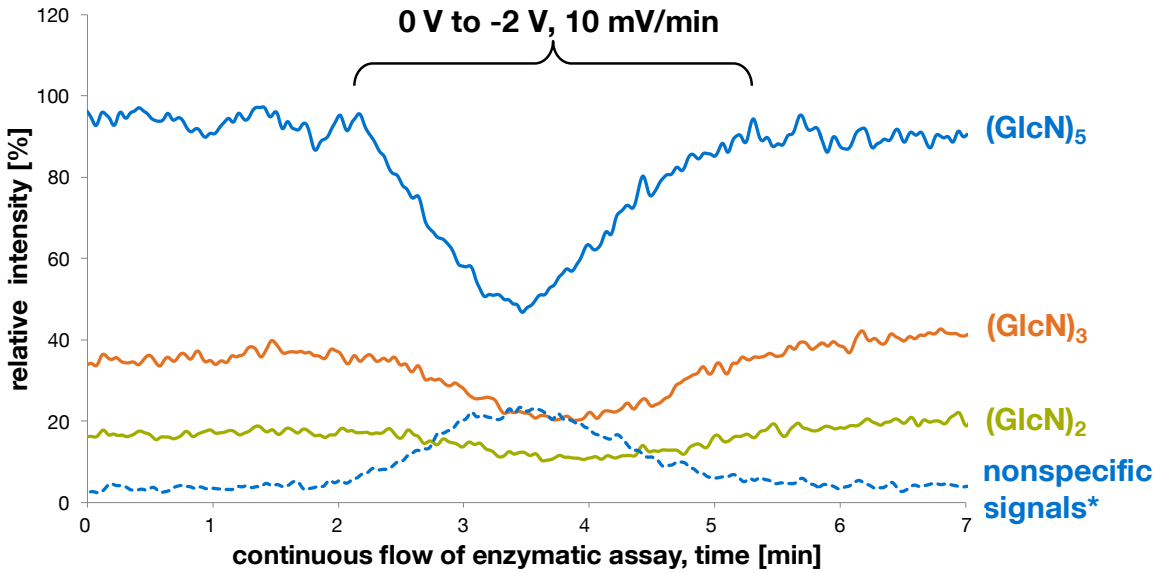

Figure 34: Continuous-flow experiment with the electrochemical reduction of $(GlcN)_5$ and the online coupling with the enzymatic reaction with Csn1794. During the applied voltage for reduction, the signal for $(GlcN)_5$ (100% ≈ 1.5 x 10^4 counts) significantly decreases and therewith the products $(GlcN)_3$ and $(GlcN)_2$. Simultaneously, some nonspecific signals in the mass range of m/z 800-808 Da increase (*).

4.3.3.2 Determination of Enzyme-Regulatory Compounds in House Dust Extracts

The fast and cost-efficient screening for functional components in complex mixtures is an emerging research area, e.g. in drug discovery. Major challenges of mass spectrometry-based applications are the inhibitor screening or identification of enzymatic activity (de Boer et al., 2007; Schluter et al., 2007). Mass spectrometry compatible enzymatic assays provide a widespread opportunity for the determination of regulatory compounds in complex mixtures (de Boer et al., 2004; de Boer et al., 2005a; de Jong et al., 2006).

Consequently, the established mass spectrometry compatible enzymatic assays, described in chapter 4.1, were implemented in a continuous-flow mixing setup which provides a basis to screen on regulatory compounds in complex mixtures (Figure 7). The system consists of the online coupling of a chromatographic separation to the enzymatic assays AChE, ChiC

or Chy with mass spectrometric detection. In the current work house dust samples from different households were used for the screening experiments, obtainable from an associating project which dealt on the composition of diverse house dust from different households. House dust is a complex matrix and may contain more than 100 critical compounds or compound groups. Thus, house dust extract samples provide a suspenseful mixture for screening experiments. Compound groups with influence on enzymatic activity are for example mycotoxins, pesticides or polycyclic aromatic hydrocarbons (Carrer et al., 2001; Salthammer and Bahadir, 2009). Moreover, the examination of house dust extracts indicated enzymatic activity including proteases, glycosidases or phosphatases (Thomas et al., 2002; Morgan and Arlian, 2006).

Table 11 gives an overview of enzymatic activity determined in house dust and enzymes, that are influenced by compounds found in house dust. The house dust extracts were used as a model system to determine regulatory substances within the continuous-flow mixing setup with a HT-HPLC module.

Table 11: Overview of relevant enzymes for screening experiments with house dust extract samples.

	contained in house dust?	***influenced by components from house dust?***	***examples***
proteases	+++	?	Chy, Elastases
glycosidases	+++	+	HEWL, Chi
cholinesterases	?	+++	AChE
phosphatases	++	+++	ATPase

The established enzymatic assays with ChiC, AChE and Chy (chapter 4.1.1.2, Figure 9) were applied in the continuous-flow mixing system to screen on substances in house dust interacting with the enzymes. Detailed information to the technological setup and the relevant concentrations of enzymes and substrate are given in the material and method section (Figure 7 and Table 4).

The chromatographic separation of the house dust extract was performed by a HT-HPLC module. In order to maintain the enzymatic activity, the organic solvent in the mobile phase for the chromatographic separation has to be reduced depending on the enzyme susceptibility towards organic solvent (chapter 4.1.2.1). In HT-HPLC, the amount of organic solvent can be decreased markedly and 10% organic solvent enables chromatographic separation (de Boer et al., 2005a; Teutenberg, 2010). This setup provides a beneficial tool for the continuous-flow mixing combination of chromatographic separation with enzymatic

assays. The susceptibility of the enzymes ChiC, Chy and AChE towards organic solvent was investigated (chapter 4.1.2.1). According to these preliminary tests a separation method with isocratic solvent composition containing 10% methanol and 10 mM NH_4Ac and a temperature gradient was chosen for the HT-HPLC separation of the house dust extracts (chapter 3.3.2). The isocratic solvent composition is beneficial in the current setup: Changes in the enzymatic activity due to different organic solvent content can be excluded and the electrospray shows the same composition and changes in signal intensities since inconsistent droplet evaporation and ionisation can be excluded. A Zirchrom-PBD column consisting of a suitable material for HT-HPLC was used for the chromatographic separation (Teutenberg, 2010).

Figure 35 shows the screening experiment of a house dust extract (dust 1, Table 3) on its influence on the AChE activity and the data evaluation with the Achroma software. The house dust extract was spiked with 100 µM of the known AChE inhibitor galanthamine for verification of the system. As presented in Figure 35A, the Achroma 'signal recognition' module automatically identified and tagged three negative peaks in the continuous product trace. Compared to 'classical' HPLC experiments the peak widths over about 3 min are unusual and mainly caused by the setup with the mixing tees, mixing coils and connection tubings (Figure 7) (Ingkaninan et al., 2000; de Boer et al., 2004; de Boer et al., 2005a; de Jong et al., 2006). The negative peaks at the time points 11 min, 13 min and 15 min indicate an AChE regulatory compound within the house dust sample. The negative peak areas in the product trace can be easily determined with the 'signal recognition' module of Achroma, thereby giving further information about the strength of the enzymatic regulation. The 'spectra comparison' module compares the spectra in the negative peak signal time ranges with those in a constant signal time range (baseline) and information about different spectra compositions are obtained (Figure 35B and C). The spectra comparison of the first (Figure 35B) and the second (data not shown) negative peak shows no significant characteristic differences of m/z signals. In contrast, the comparison of the third negative peak spectra with the baseline spectra shows a distinct and characteristic signal with m/z 288. To verify this finding, the extracted ion chromatogram of the identified m/z was visualized (Figure 35E), thereby revealing a retention time of m/z 288 which is highly comparable with the time point of the negative EIC peak signal within the choline product trace. As mentioned above, the house dust extract was spiked with the inhibitor galanthamine. The m/z 288 corresponds to the mass spectrometric signal $[M+H]^+$ of galanthamine and thus, the applicability of the system could be shown.

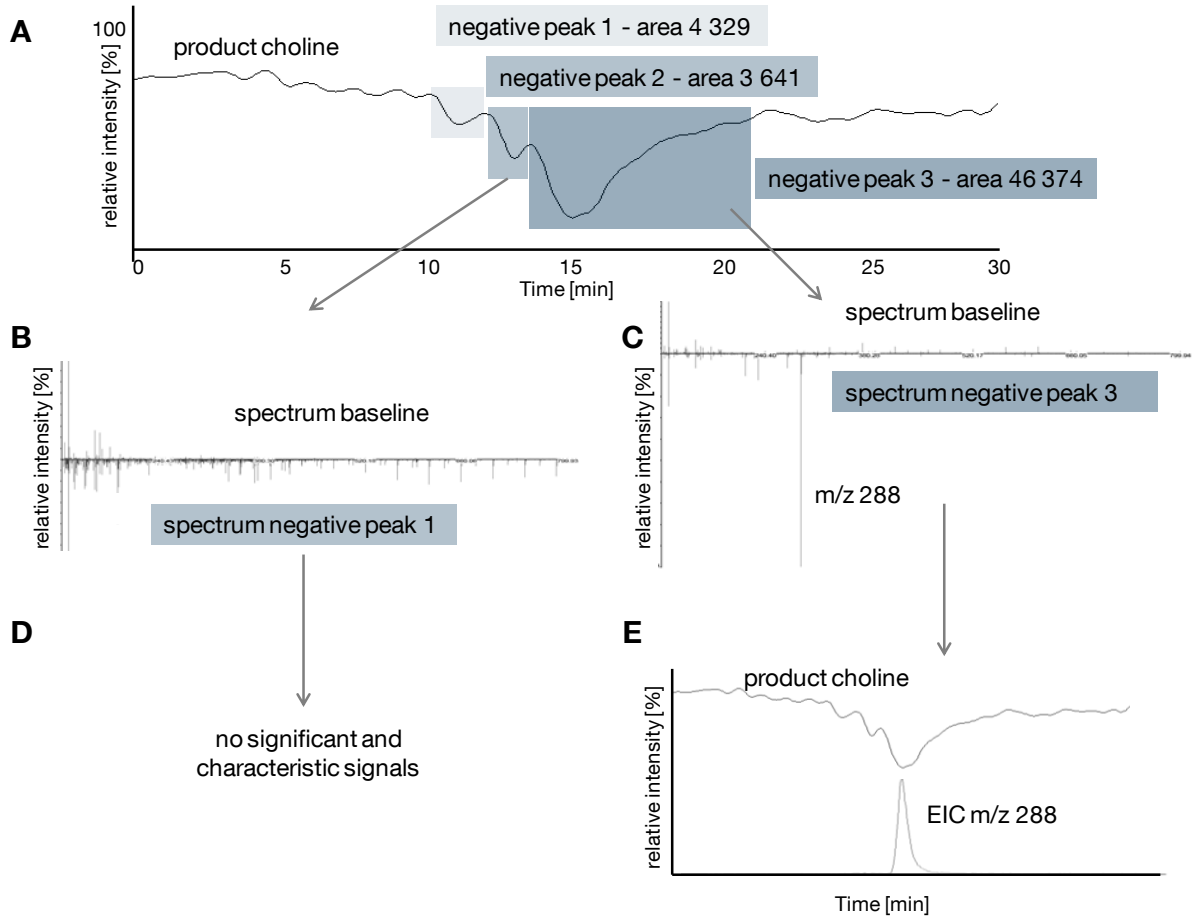

Figure 35: Screening experiment with a house dust extract (dust 1, spiked with 100 µM galanthamine) on its regulatory influence on AChE activity. Software 'Achroma' (grey-shaded box) was used for data interpretation. (A) Detection of negative signals and calculation of signal areas in the online monitored product trace with the 'signal recognition' software tool. (B) and (C) Comparison of the spectrum in the products EIC baseline and the spectra in the negative peak areas with 'spectra comparison' tool. (D) and (E) Identification of enzyme regulatory substances in the complex mixture.

Generally, the house dust extracts in the continuous-flow showed no significant regulatory effects on the enzymatic assays AChE, ChiC or Chy. Possibly the house dust extracts do not contain any enzyme-regulatory compounds or concentration and dilution effects in the system have to be readjusted. Figure 36 shows the measurement of house dust extract 2 (Table 3), which was injected into the continuous-flow of the AChE assay. The enzymatic assay substrate and product signals acetylcholine and choline are unaffected. Marginal changes in the substrate and product signal between 8 to 15 min can be explained by signal suppression effects due to the eluting compounds. Sucrose, sterigmatocystin, $(GlcNAc)_2$ and an unknown compound (m/z 388) were identified in this time range (MS/MS experiments and results from project at the 'IUTA', Table 3). In the current measuring setup and the injected concentration they do not show regulatory influence on AChE.

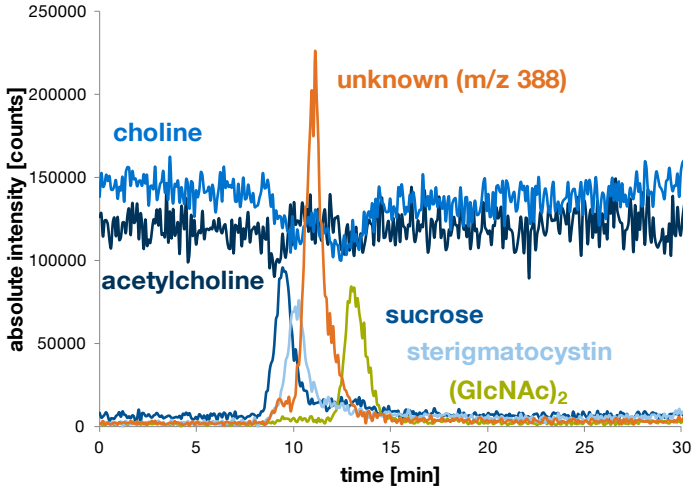

Figure 36: Measurement of the AChE assay in the online coupled setup with injection of the house dust extract 2. Several compounds were chromatographically separated by HT-HPLC and sucrose, sterigmatocystin and $(GlcNAc)_2$ could be identified. No regulatory influence on the AChE assay is observed.

For optimization of the system several technical parameters were adjusted: flow rates, tubing material, lengths and inner diameters of tubings and mixing coils. The connection tubings between the single modules were set as short as possible and small inner diameters, preventing adsorption effects on the material surface (Goebel-Stengel et al., 2011). With small inner diameters and short tubings the enzyme adsorption on the tubing material could not be prevented completely and intensive washing steps with organic solvent were carried out before each single measurement. The addition of albumin from bovine serum, polyethylene glycol or high salt concentrations can prevent these adsorption problems. Otherwise they may interact with the enzymes/substrates and cause mass spectrometric signal suppression effects. More appropriate than PEEK (polyetherether-ketone) and teflon tubings is glass material. The adaption of this setup on a glass chip in a future project will be a beneficial step to overcome adsorption effects and pose a promising setup towards miniaturisation.

4.3.4 Summary

The appropriate usage of diverse technological applications for enzymological issues was presented in this chapter. The versatile applications were based on the previously obtained experience and the results regarding realization and handling enzymatic assays in mass spectrometric experiments (chapter 4.1 and 4.2). The knowledge and the appropriate usage of diverse technical setups provide profound and detailed information for enzymological research.

Continuous-flow direct infusion was used and shows detailed insights in reaction profiles and substrate specifities of chitinases and chitosanases. The results give fundamental information for the industrial hydrolysis of chitin and chitosan. The enzyme MPO was investigated using both, direct infusion and nanoESI. The reaction profile, i.e. the simultaneous investigation of substrate, intermediates and products, was determined for the first time in a single experiment. Further, the direct infusion experiments are a beneficial technique for studying the enzyme-inhibitory strength of inhibitors, as shown for EGCG on the MPO activity.

Various instrumental modules can be implemented and combined with continuous-flow experiments and enzymatic reactions. In the current study, chromatographic and electrochemical instruments were used in continuous-flow mixing setups. They present the technological applicability for the innovative monitoring enzymatic reactions and inhibitor screening of complex mixtures. The continuous-flow mixing setups provide the opportunity to determine enzymatic regulation, e.g. in food extracts or pharmaceutics.

5 Conclusion

The combination of enzymatic reactions with mass spectrometric detection offers widespread opportunities in enzymological research.

The current work demonstrates a comprehensive analysis of handling enzymatic assays in mass spectrometric experiments. Diverse new technological setups were applied for enzymological issues, based on the wide experience of enzyme and technical requirements for their successful technological combination.

Several enzymatic assays were established for continuous-flow mass spectrometric experiments and investigated in further technological applications: hen egg white lysozyme, diverse chitinases, a chitosanase, acetylcholinesterase, α-chymotrypsin, elastase from pancreas, elastase from neutrophils, ATPase and myeloperoxidase. The variety of enzymes and substrates shows the powerful applicability of mass spectrometry for studying enzymatic reactions. The establishment for mass spectrometric detection was performed based on classical photometric approaches. When considering some parameters which are important for the mass spectrometric compatibility the adaption of the enzymatic assays from classical photometric approaches to mass spectrometry is easily to handle. The consequent implementation of the enzymatic assays in a nanoESI system enabled the miniaturised and automated monitoring of enzymatic reactions. In regard to a miniaturised, fast and cost-efficient setup the nanoESI is a promising system, especially if enzymes are used that are available only in small amounts or quite expensive. The system provides various key benefits in comparison to the classical syringe pump setup such as automatically mixing, spraying and very low sample consumption.

Diverse innovative applications were used with the established enzymatic assays giving detailed insights in reaction profiles, inhibitor screening and data handling strategies. The established and optimized enzymatic reactions were combined and implemented in further complex setups, e.g. in combination with electrochemical reaction module or the combination with a HT-HTPLC module.

The presented results provide a beneficial basis for widespread technological and enzymological opportunities in biotechnology or pharmaceutical and environmental applications.

6 References

Amaral, C., Cunha, S.C., Fernandes, J.O., Roleira, F., da Silva, E.T., Correia-da-Siva, G., Teixeira, N., 2012. A new gas chromatography - mass spectrometry (GC-MS) methodology to evaluate the 5 alpha-reductase activity. Febs Journal 279**,** 113-114.

Bakkenist, A.R.J., Deboer, J.E.G., Plat, H., Wever, R., 1980. The Halide-Complexes of Myeloperoxidase and the Mechanism of the Halogenation Reactions. Biochimica Et Biophysica Acta 613**,** 337-348.

Bantscheff, M., Schirle, M., Sweetman, G., Rick, J., Kuster, B., 2007. Quantitative mass spectrometry in proteomics: a critical review. Analytical and Bioanalytical Chemistry 389**,** 1017-1031.

Batra, R., Gupta, M.N., 1994. Enhancement of Enzyme-Activity in Aqueous-Organic Solvent Mixtures. Biotechnology Letters 16**,** 1059-1064.

Baykov, A.A., Evtushenko, O.A., Avaeva, S.M., 1988. A Malachite Green Procedure for Ortho-Phosphate Determination and its use in Alkaline Phosphatase-Based Enyzme-Immunoassay. Analytical Biochemistry 171**,** 266-270.

Belitz, H.D., Grosch, W., 1999. Food Chemistry. Springer Berlin.

Benesch, J.L., Robinson, C.V., 2006. Mass spectrometry of macromolecular assemblies: preservation and dissociation. Current Opinion in Structural Biology 16**,** 245-251.

Benetton, S., Kameoka, J., Tan, A.M., Wachs, T., Craighead, H., Henion, J.D., 2003. Chip-based P450 drug metabolism coupled to electrospray ionization-mass spectrometry detection. Analytical Chemistry 75**,** 6430-6436.

Bisswanger, H., 2007. Practical Enzymology. WILEY-VCH, Weinheim.

Bothner, B., Chavez, R., Wei, J., Strupp, C., Phung, Q., Schneemann, A., Siuzdak, G., 2000. Monitoring enzyme catalysis with mass spectrometry. Journal of Biological Chemistry 275**,** 13455-13459.

Butler, L.G., 1979. Enzymes in Non-Aqueous Solvents. Enzyme Microb. Tech. 1**,** 253-259.

Cabrera, C., Artacho, R., Gimenez, R., 2006. Beneficial effects of green tea - A review. Journal of the American College of Nutrition 25**,** 79-99.

Carrer, P., Maroni, M., Alcini, D., Cavallo, D., 2001. Allergens in indoor air: environmental assessment and health effects. Science of the Total Environment 270**,** 33-42.

Chaplin, M.F., Bucke, C., 1990. Enzyme Technology. Cambridge University Press, Cambridge, England.

Clark, S.M., Konermann, L., 2004a. Determination of ligand-protein dissociation constants by electrospray mass spectrometry-based diffusion measurements. Analytical Chemistry 76**,** 7077-7083.

Clark, S.M., Konermann, L., 2004b. Screening for noncovalent ligand-receptor interactions by electrospray ionization mass spectrometry-based diffusion measurements. Analytical Chemistry 76, 1257-1263.

de Boer, A.R., Letzel, T., van Elswijk, D.A., Lingeman, H., Niessen, W.M.A., Irth, H., 2004. On-line coupling of high-performance liquid chromatography to a continuous-flow enzyme assay based on electrospray ionization mass spectrometry. Analytical Chemistry 76, 3155-3161.

de Boer, A.R., Alcaide-Hidalgo, J.M., Krabbe, J.G., Kolkman, J., Boas, C.N.V., Niessen, W.M.A., Lingeman, H., Irth, H., 2005a. High-temperature liquid chromatography coupled on-line to a continuous-flow biochemical screening assay with electrospray ionization mass spectrometric detection. Analytical Chemistry 77, 7894-7900.

de Boer, A.R., Bruyneel, B., Krabbe, J.G., Lingeman, H., Niessen, W.M.A., Irth, H., 2005b. A microfluidic-based enzymatic assay for bioactivity screening combined with capillary liquid chromatography and mass spectrometry. Lab on a Chip 5, 1286-1292.

de Boer, A.R., Letzel, T., Lingeman, H., Irth, H., 2005c. Systematic development of an enzymatic phosphorylation assay compatible with mass spectrometric detection. Analytical and Bioanalytical Chemistry 381, 647-655.

de Boer, A.R., Lingeman, H., Niessen, W.M.A., Irth, H., 2007. Mass spectrometry-based biochemical assays for enzyme-inhibitor screening. Trac-Trends in Analytical Chemistry 26, 867-883.

de Jong, C.F., Derks, R.J.E., Bruyneel, B., Niessen, W., Irth, H., 2006. High-performance liquid chromatography-mass spectrometry-based acetylcholinesterase assay for the screening of inhibitors in natural extracts. Journal of Chromatography A 1112, 303-310.

Dennhart, N., Letzel, T., 2006. Mass spectrometric real-time monitoring of enzymatic glycosidic hydrolysis, enzymatic inhibition and enzyme complexes. Analytical and Bioanalytical Chemistry 386, 689-698.

Dennhart, N., Fukamizo, T., Brzezinski, R., Lacombe-Harvey, M.E., Letzel, T., 2008. Oligosaccharide hydrolysis by chitosanase enzymes monitored by real-time electrospray ionization-mass spectrometry. Journal of Biotechnology 134, 253-260.

Dennhart, N., Weigang, L.M.M., Fujiwara, M., Fukamizo, T., Skriver, K., Letzel, T., 2009. 26 kDa endochitinase from barley seeds: Real-time monitoring of the enzymatic reaction and substrate binding experiments using electrospray ionization mass spectrometry. Journal of Biotechnology 143, 274-283.

Dixit, V., Hariparsad, N., Desai, P., Unadkat, J.D., 2007. In vitro LC-MS cocktail assays to simultaneously determine human cytochrome p450 activities. Biopharmaceutics & Drug Disposition 28, 257-262.

Domigan, N.M., Charlton, T.S., Duncan, M.W., Winterbourn, C.C., Kettle, A.J., 1995. Chlorination of Tyrosyl Residues in Peptides by Myeloperoxidase and Human Neutrophils. Journal of Biological Chemistry 270, 16542-16548.

Eisenthal, R., Danson, M.J., 2002. Enzyme assays: A practical approach. Second Edition. In: Eisenthal, R., Danson, M.J., Eds.), Enzyme assays: A practical approach. Second Edition. Oxford University Press.

Ellman, G.L., Courtney, K.D., Andres, V., Featherstone, R.M., 1961. A New and Rapid Colorimetric Determination of Acetylcholinesterase Activity. Biochemical Pharmacology 7, 91-95.

Esmann, M., 1988. Atpase and Phosphatase-Activity of Na+,K+-Atpase - Molar and Specific Activity, Protein Determination. Methods in Enzymology 156, 105-115.

Faller, L., Sturtevant, J.M., 1966. Kinetics of Alpha-Chymotrypsin-Catalyzed Hydrolysis of p-Nitrophenyl Acetate in Organic Solvent-Water Mixtures. Journal of Biological Chemistry 241, 4825-4834.

Franck, T., Kohnen, S., Grulke, S., Neven, P., Goutman, Y., Peters, F., Pirotte, B., Deby-Dupont, G., Serteyn, D., 2008. Inhibitory effect of curcuminoids and tetrahydrocurcuminoids on equine activated neutrophils and myeloperoxidase activity. Physiological Research 57, 577-587.

Froesch, M., Bindila, L.M., Baykut, G., Allen, M., Peter-Katalinic, J., Zamfir, A.D., 2004. Coupling of fully automated chip electrospray to Fourier transform ion cyclotron resonance mass spectrometry for high-performance glycoscreening and sequencing. Rapid Communications in Mass Spectrometry 18, 3084-3092.

Fukamizo, T., Minematsu, T., Yanase, Y., Hayashi, K., Goto, S., 1986. Substrate Size Dependence of Lysozyme-Catalyzed Reaction. Archives of Biochemistry and Biophysics 250, 312-321.

Fukamizo, T., Honda, Y., Goto, S., Boucher, I., Brzezinski, R., 1995. Reaction Mechanism of Chitosanase from Streptomyces sp. N174. Biochemical Journal 311, 377-383.

Fukamizo, T., 2000. Chitinolytic enzymes: Catalysis, substrate binding, and their application. Current Protein and Peptide Science 1, 105-124.

Fukamizo, T., Fleury, A., Cote, N., Mitsutomi, M., Brzezinski, R., 2006. Exo-beta-D-glucosaminidase from Amycolatopsis orientalis: catalytic residues, sugar recognition specificity, kinetics, and synergism. Glycobiology 16, 1064-1072.

Fusetti, F., von Moeller, H., Houston, D., Rozeboom, H.J., Dijkstra, B.W., Boot, R.G., Aerts, J., van Aalten, D.M.F., 2002. Structure of human chitotriosidase - Implications for specific inhibitor design and function of mammalian chitinase-like lectins. Journal of Biological Chemistry 277, 25537-25544.

Ganem, B., Li, Y.T., Henion, J.D., 1991. Observation of Noncovalent Enzyme Substrate and Enzyme Product Complexes by Ion-Spray Mass-Spectrometry. Journal of the American Chemical Society 113, 7818-7819.

Gao, H., Chen, Y., Leary, J.A., 2005. Kinetic measurements of phosphoglucose isomerase and phosphomannose isomerase by direct analysis of phosphorylated aldose-ketose isomers using tandem mass spectrometry. International Journal of Mass Spectrometry 240, 291-299.

Gaut, J.P., Yeh, G.C., Byun, J., Tran, H., Belaaouaj, A., Heinecke, J.W., 2001. Neutrophils employ the myeloperoxidase system to generate antimicrobial brominating and chlorinating oxidants during sepsis. Free Radical Biology and Medicine 31, 11961-11966.

Ge, X., Sirich, T.L., Beyer, M.K., Desaire, H., Leary, J.A., 2001. A Strategy for the Determination of Enzyme Kinetics Using Electrospray Ionization with an Ion Trap Mass Spectrometer. Analytical Chemistry 73, 5078-5082.

Geoghegan, K.F., Kelly, M.A., 2005. Biochemical applications of mass spectrometry in pharmaceutical drug discovery. Mass Spectrometry Reviews 24, 347-366.

Gerber, S.A., Scott, C.R., Turecek, F., Gelb, M.H., 1999. Analysis of rates of multiple enzymes in cell lysates by electrospray ionization mass spectrometry. Journal of the American Chemical Society 121, 1102-1103.

Goebel-Stengel, M., Stengel, A., Tache, Y., Reeve, J.R., Jr., 2011. The importance of using the optimal plasticware and glassware in studies involving peptides. Analytical Biochemistry 414, 38-46.

Greis, K.D., 2007. Mass spectrometry for enzyme assays and inhibitor screening: An emerging application in pharmaceutical research. Mass Spectrometry Reviews 26, 324-339.

Gupta, M.N., 1992. Enzyme Function in Organic Solvents. Eur. J. Biochem. 203, 25-32.

Gupta, M.N., Batra, R., Tyagi, R., Sharma, A., 1997. Polarity index: The guiding solvent parameter for enzyme stability in aqueous-organic cosolvent mixtures. Biotechnol. Progr. 13, 284-288.

Harrison, J.E., Schultz, J., 1976. Studies on Chlorinating Activity of Myeloperoxidase. Journal of Biological Chemistry 251, 1371-1374.

Hazen, S.L., Hsu, F.F., Heinecke, J.W., 1996. p-hydroxyphenylacetaldehyde is the major product of L-tyrosine oxidation by activated human phagocytes - A chloride-dependent mechanism for the conversion of free amino acids into reactive aldehydes by myeloperoxidase. Journal of Biological Chemistry 271, 1861-1867.

Hazen, S.L., Crowley, J.R., Mueller, D.M., Heinecke, J.W., 1997. Mass spectrometric quantification of 3-chlorotyrosine in human tissues with attomole sensitivity: A sensitive and specific marker for myeloperoxidase-catalyzed chlorination at sites of inflammation. Free Radical Biology and Medicine 23, 909-916.

Heinecke, J.W., Li, W., Daehnke, H.L., Goldstein, J.A., 1993. Dityrosine, a Specific Marker of Oxidation, is Synthesized by the Myeloperoxidase-Hydrogen Peroxide System of Human Neutrophils and Macrophages. Journal of Biological Chemistry 268, 4069-4077.

Heinecke, J.W., 2002. Tyrosyl radical production by myeloperoxidase: a phagocyte pathway for lipid peroxidation and dityrosine cross-linking of proteins. Toxicology 177, 11-22.

Hempen, C., Liesener, A., Karst, U., 2005. Fluorescence and mass spectrometric detection schemes for simultaneous enzymatic conversions: Method development and comparison. Analytica Chimica Acta 543**,** 137-142.

Henkel, R.D., Vandeberg, J.L., Walsh, R.A., 1988. A Microassay for Atpase. Analytical Biochemistry 169**,** 312-318.

Hsieh, F.Y.L., Tong, X., Wachs, T., Ganem, B., Henion, J., 1995. Kinetic Monitoring of Enzymatic-Reactions in Real-Time by Quantitative High-Performance Liquid-Chromatography Mass Spectrometry. Analytical Biochemistry 229**,** 20-25.

Ingkaninan, K., de Best, C.M., van der Heijden, R., Hofte, A.J.P., Karabatak, B., Irth, H., Tjaden, U.R., van der Greef, J., Verpoorte, R., 2000. High-performance liquid chromatography with on-line coupled UV, mass spectrometric and biochemical detection for identification of acetylcholinesterase inhibitors from natural products. Journal of Chromatography A 872**,** 61-73.

Ingkaninan, K., Temkitthawon, P., Chuenchom, K., Yuyaem, T., Thongnoi, W., 2003. Screening for acetylcholinesterase inhibitory activity in plants used in Thai traditional rejuvenating and neurotonic remedies. Journal of Ethnopharmacology 89**,** 261-264.

Itaya, K., Ui, M., 1966. A new Micromethod for Colorimetric Determination of Inorganic Phosphate. Clinica Chimica Acta 14**,** 361-366.

Jacob, J.S., Cistola, D.P., Hsu, F.F., Muzaffar, S., Mueller, D.M., Hazen, S.L., Heinecke, J.W., 1996. Human phagocytes employ the myeloperoxidase-hydrogen peroxide system to synthesize dityrosine, trityrosine, pulcherosine, and isodityrosine by a tyrosyl radical-dependent pathway. Journal of Biological Chemistry 271**,** 19950-19956.

Jankowski, J., Stephan, N., Knobloch, M., Fischer, S., Schmaltz, D., Zidek, W., Schluter, H., 2001. Mass-spectrometry-linked screening of protein fractions for enzymatic activities - A tool for functional genomics. Analytical Biochemistry 290**,** 324-329.

Jecklin, M.C., Touboul, D., Bovet, C., Wortmann, A., Zenobi, R., 2008. Which electrospray-based ionization method best reflects protein-ligand interactions found in solution? A comparison of ESI, nanoESI, and ESSI for the determination of dissociation constants with mass spectrometry. Journal of the American Society for Mass Spectrometry 19**,** 1237-1237.

Jecklin, M.C., Touboul, D., Jain, R., Toole, E.N., Tallarico, J., Drueckes, P., Ramage, P., Zenobi, R., 2009. Affinity Classification of Kinase Inhibitors by Mass Spectrometric Methods and Validation Using Standard IC50 Measurements. Analytical Chemistry 81**,** 408-419.

Kato, Y., Nagao, A., Terao, J., Osawa, T., 2003. Inhibition of myeloperoxidase-catalyzed tyrosylation by phenolic antioxidants in vitro. Bioscience Biotechnology and Biochemistry 67**,** 1136-1139.

Kebarle, P., Verkerk, U.H., 2009. Electrospray: From Ions in Solution to Ions in the Gas Phase, What We Know Now. Mass Spectrometry Reviews 28**,** 898-917.

Keetch, C.A., Hernandez, H., Sterling, A., Baumert, M., Allen, M.H., Robinson, C.V., 2003. Use of a microchip device coupled with mass spectrometry for ligand screening of a multi-protein target. Analytical Chemistry 75, 4937-4941.

Khmelnitsky, Y.L., Mozhaev, V.V., Belova, A.B., Sergeeva, M.V., Martinek, K., 1991. Denaturation Capacity - A New Quantitative Criterion for Selection of Organic-Solvents as Reaction Media in Biocatalysis. Eur. J. Biochem. 198, 31-41.

Kirk, O., Borchert, T.V., Fuglsang, C.C., 2002. Industrial enzyme applications. Current Opinion in Biotechnology 13, 345-351.

Klebanoff, S.J., 2005. Myeloperoxidase: friend and foe. Journal of Leukocyte Biology 77, 598-625.

Klibanov, A.M., 2001. Improving enzymes by using them in organic solvents. Nature 409, 241-246.

Kongruang, S., Penner, M.H., 2004. Borohydride reactivity of cellulose reducing ends. Carbohydrate Polymers 58, 131-138.

Kool, J., Eggink, M., Van Rossum, H., van Liempd, S.M., van Elswijk, D.A., Irth, H., Commandeur, J.N.M., Meerman, J.H.N., Vermeulen, N.P.E., 2007. Online biochemical detection of glutathione-S-transferase P1-specific inhibitors in complex mixtures. Journal of Biomolecular Screening 12, 396-405.

Kool, J., Giera, M., Irth, H., Niessen, W.M.A., 2011. Advances in mass spectrometry-based post-column bioaffinity profiling of mixtures. Analytical and Bioanalytical Chemistry 399, 2655-2668.

Kouach, M., Belaiche, D., Jaquinod, M., Couppez, M., Kmiecik, D., Ricart, G., Vandorsselaer, A., Sautiere, P., Briand, G., 1994. Application of Electrospray and Fast-Atom-Bombardment Mass-Spectrometry to the Identification of Posttranslational and other Chemical Modifications of Proteins and Peptides. Biological Mass Spectrometry 23, 283-294.

Krappmann, M., Letzel, T., 2011. Functional Analysis of Proteins, Including LC-MS and Special Freeware. In: Letzel, T., (Ed.), Protein and Peptide Analysis by LC-MS. Royal Society of Chemistry, Cambridge.

Krappmann, M., Letzel, T., 2012. Achroma: a software strategy for analysing (a-)typical mass-spectrometric data. Analytical Methods 4, 1060-1071.

Krishna, S.H., 2002. Developments and trends in enzyme catalysis in nonconventional media. Biotechnol. Adv. 20, 239-267.

Laane, C., Boeren, S., Vos, K., Veeger, C., 1987. Rules for Optimization of Biocatalysis in Organic-Solvents. Biotechnol. Bioeng. 30, 81-87.

Lee, E.D., Muck, W., Henion, J.D., Covey, T.R., 1989. Real-Time Reaction Monitoring by Continuous-Introduction Ion-Spray Tandem Mass-Spectrometry. Journal of the American Chemical Society 111, 4600-4604.

Letzel, T., 2008. Real-time mass spectrometry in enzymology. Analytical and Bioanalytical Chemistry 390, 257-261.

Letzel, T., Sahmel-Schneider, E., Skriver, K., Ohnuma, T., Fukamizo, T., 2011. Chitinase-catalyzed hydrolysis of 4-nitrophenyl penta-N-acetyl-beta-chitopentaoside as determined by real-time ESIMS: The 4-nitrophenyl moiety of the substrate interacts with the enzyme binding site. Carbohyd. Res. 346, 863-866.

Li, Z.L., Song, F., Zhuang, Z.H., Dunaway-Mariano, D., Anderson, K.S., 2009. Monitoring enzyme catalysis in the multimeric state: Direct observation of Arthrobacter 4-hydroxybenzoyl-coenzyme A thioesterase catalytic complexes using time-resolved electrospray ionization mass spectrometry. Analytical Biochemistry 394, 209-216.

Liesener, A., Karst, U., 2005a. Monitoring enzymatic conversions by mass spectrometry: a critical review. Analytical and Bioanalytical Chemistry 382, 1451-1464.

Liesener, A., Karst, U., 2005b. Assessing protease activity pattern by means of multiple substrate ESI-MS assays. Analyst 130, 850-854.

Liesener, A., Perchuc, A.M., Schoni, R., Wilmer, M., Karst, U., 2005. Screening for proteolytic activities in snake venom by means of a multiplexing electrospray ionization mass spectrometry assay scheme. Rapid Communications in Mass Spectrometry 19, 2923-2928.

Liesener, A., Perchuc, A.M., Schoni, R., Schebb, N.H., Wilmer, M., Karst, U., 2007. Screening of acetylcholinesterase inhibitors in snake venom by electrospray mass spectrometry. Pure and Applied Chemistry 79, 2339-2349.

Marquez, L.A., Dunford, H.B., 1995. Kinetics of oxidation of tyrosine and dityrosine by myeloperoxidase compounds I and II - Implications for lipoprotein peroxidation studies. Journal of Biological Chemistry 270, 30434-30440.

Masaki, A., Fukamizo, T., Otakara, A., Torikata, T., Hayashi, K., Imoto, T., 1981. Lysozyme-Catalyzed Reaction of Chitooligosaccharides. Journal of Biochemistry 90, 527-533.

Mazzon, E., Muia, C., Di Paola, R., Genovese, T., Menegazzi, M., De Sarro, A., Suzuki, H., Cuzzocrea, S., 2005. Green tea polyphenol extract attenuates colon injury induced by experimental colitis. Free Radical Research 39, 1017-1025.

Mochizuki, M., Hasegawa, N., 2005. Protective effect of (-)-epigallocatechin gallate on acute experimental colitis. Journal of Health Science 51, 362-364.

Morgan, M.S., Arlian, L.G., 2006. Enzymatic activity in extracts of allergy-causing astigmatid mites. Journal of Medical Entomology 43, 1200-1207.

Nakao, T., Tashima, Y., Nagano, K., Nakao, M., 1965. Highly Specific Sodium-Potassium-Activated Adenosine Triphosphatase from Various Tissues of Rabbit. Biochemical and Biophysical Research Communications 19, 755-758.

Northrop, D.B., Simpson, F.B., 1997. Beyond enzyme kinetics: Direct determination of mechanisms by stopped-flow mass spectrometry. Bioorgan. Med. Chem. 5, 641-644.

Ogino, H., Ishikawa, H., 2001. Enzymes which are stable in the presence of organic solvents. J. Biosci. Bioeng. 91, 109-116.

Ohnuma, T., Numata, T., Osawa, T., Mizuhara, M., Varum, K.M., Fukamizo, T., 2011. Crystal structure and mode of action of a class V chitinase from Nicotiana tabacum. Plant Molecular Biology 75, 291-304.

Pi, N., Hoang, M.B., Gao, H., Mougous, J.D., Bertozzi, C.R., Leary, J.A., 2005. Kinetic measurements and mechanism determination of Stf0 sulfotransferase using mass spectrometry. Analytical Biochemistry 341, 94-104.

Pi, N.A., Yu, Y.H., Mougous, J.D., Leary, J.A., 2004. Observation of a hybrid random ping-pong mechanism of catalysis for NodST: A mass spectrometry approach. Protein Science 13, 903-912.

Piraud, M., Vianey-Saban, C., Petritis, K., Elfakir, C., Steghens, J.P., Morla, A., Bouchu, D., 2003. ESI-MS/MS analysis of underivatised amino acids: a new tool for the diagnosis of inherited disorders of amino acid metabolism. Fragmentation study of 79 molecules of biological interest in positive and negative ionisation mode. Rapid Communications in Mass Spectrometry 17, 1297-1311.

Podrez, E.A., Abu-Soud, H.M., Hazen, S.L., 2000. Myeloperoxidase-generated oxidants and atherosclerosis. Free Radical Biology and Medicine 28, 1717-1725.

Reinders, J., Sickmann, A., 2007. Modificomics: Posttranslational modifications beyond protein phosphorylation and glycosylation. Biomolecular Engineering 24, 169-177.

Robinson, J.D., Robinson, L.J., Martin, N.J., 1984. Effects of Oligomycin and Quercetin on the Hydrolytic Activities of the (Na^+ + K^+)-Dependent Atpase. Biochimica Et Biophysica Acta 772, 295-306.

Robinson, J.D., 1988. Estimating Affinities for Physiological Ligands and Inhibitors by Kinetic-Studies on Na+,K+-Atpase and Its Partial Activities. Methods in Enzymology 156, 236-251.

Rowlands, M.G., Newbatt, Y.M., Prodromou, C., Pearl, L.H., Workman, P., Aherne, W., 2004. High-throughput screening assay for inhibitors of heat-shock protein 90 ATPase activity. Analytical Biochemistry 327, 176-183.

Salthammer, T., Bahadir, M., 2009. Occurrence, Dynamics and Reactions of Organic Pollutants in the Indoor Environment. Clean-Soil Air Water 37, 417-435.

Samalikova, M., Grandori, R., 2005. Testing the role of solvent surface tension in protein ionization by electrospray. J. Mass Spectrom. 40, 503-510.

Sampson, J.B., Ye, Y.Z., Rosen, H., Beckman, J.S., 1998. Myeloperoxidase and horseradish peroxidase catalyze tyrosine nitration in proteins from nitrite and hydrogen peroxide. Archives of Biochemistry and Biophysics 356, 207-213.

Schebb, N.H., Vielhaber, T., Jousset, A., Karst, U., 2009. Development of a liquid chromatography-based screening methodology for proteolytic enzyme activity. Journal of Chromatography A 1216, 4407-4415.

Schenk, T., Appels, N.M.G.M., van Elswijk, D.A., Irth, H., Tjaden, U.R., van der Greef, J., 2003a. A generic assay for phosphate-consuming or -releasing enzymes coupled on-line to liquid chromatography for lead finding in natural products. Analytical Biochemistry 316, 118-126.

Schenk, T., Breel, J., Koevoets, P., van den Berg, S., Hogenboom, A.C., Irth, H., Tjaden, U.R., van der Greef, J., 2003b. Screening of natural products extracts for the presence of phosphodiesterase inhibitors using liquid chromatography coupled online to parallel biochemical detection and chemical characterization. Journal of Biomolecular Screening 8**,** 421-429.

Schluter, H., Jankowski, J., Rykl, J., Thiemann, J., Belgardt, S., Zidek, W., Wittmann, B., Pohl, T., 2003. Detection of protease activities with the mass-spectrometry-assisted enzyme-screening (MES) system. Analytical and Bioanalytical Chemistry 377**,** 1102-1107.

Schluter, H., Rykl, J., Thiemann, J., Kurzawski, S., Gobom, J., Tepel, M., Zidek, W., Linscheid, M., 2007. Mass spectrometry-assisted protease substrate screening. Analytical Chemistry 79**,** 1251-1255.

Schluter, H., Hildebrand, D., Gallin, C., Schulz, A., Thiemann, J., Trusch, M., 2008. Mass spectrometry for monitoring protease reactions. Analytical and Bioanalytical Chemistry 392**,** 783-792.

Schultz, G.A., Corso, T.N., Prosser, S.J., Zhang, S., 2000. A fully integrated monolithic microchip electrospray device for mass spectrometry. Analytical Chemistry 72**,** 4058-4063.

Sharon, M., Robinson, C.V., 2007. The role of mass Spectrometry in structure elucidation of dynamic protein complexes. Annual Review of Biochemistry 76**,** 167-193.

Shi, S.Y., Zhou, H.H., Zhang, Y.P., Jiang, X.Y., Chen, X.Q., Huang, K.L., 2009. Coupling HPLC to on-line, post-column (bio)chemical assays for high-resolution screening of bioactive compounds from complex mixtures. Trac-Trends in Analytical Chemistry 28**,** 865-877.

Shipovskov, S., Reimann, C.T., 2007. Electrospray ionization mass spectrometry in enzymology: uncovering the mechanisms of two- substrate reactions. Analyst 132**,** 397-402.

Shirasu, Y., Yoshida, H., Mikayama, T., Matsuki, S., Tanaka, J., Ikenaga, H., 1986. Isolation and Expression in Escherichia-Coli of a cDNA Clone Encoding Porcine Prancreatic Elastase. Journal of Biochemistry 99**,** 1707-1712.

Singh, K., Shukla, A.K., 2003. Poly-vinyl alcohol (PVA) and malachite green: a new reagent system for the microdetermination of phosphate in water and wastewater. Indian Journal Environ Health 45**,** 203-208.

Skou, J.C., 1957. The Influence of Some Cations on an Adenosine Triphosphatase from Peripheral Nerves. Biochimica Et Biophysica Acta 23**,** 394-401.

Skou, J.C., 1989. The Identification of the Sodium-Pump as the Membrane-Bound Na^+/K^+-ATPase - Commentary. Biochimica Et Biophysica Acta 1000**,** 435-446.

Svobodova, J., Mathur, S., Muck, A., Letzel, T., Svatos, A., 2010. Microchip-ESI-MS determination of dissociation constant of the lysozyme-NAG(3) complex. Electrophoresis 31**,** 2680-2685.

Taira, T., Fujiwara, M., Dennhart, N., Hayashi, H., Onaga, S., Ohnuma, T., Letzel, T., Sakuda, S., Fukamizo, T., 2010. Transglycosylation reaction catalyzed by a class V chitinase from cycad, Cycas revoluta: A study involving site-directed mutagenesis, HPLC, and real-time ESI-MS. Biochimica et Biophysica Acta (BBA) - Proteins & Proteomics 1804, 668-675.

Takahashi, H., Nukiwa, T., Yoshimura, K., Quick, C.D., States, D.J., Holmes, M.D., Whangpeng, J., Knutsen, T., Crystal, R.G., 1988. Structure of the Human Neutrophil Elastase Gene. Journal of Biological Chemistry 263, 14739-14747.

Takahashi, K., Kimura, Y., Kioka, N., Matsuo, M., Ueda, K., 2006. Purification and ATPase activity of human ABCA1. Journal of Biological Chemistry 281, 10760-10768.

Tang, Y., Chen, H., Jiang, J.Z., Tang, Z., Huang, B.Y., Roesky, H.W., 2004. Application of hydrogen-storage alloy electrode in electrochemical reduction of glucose. Journal of Power Sources 130, 56-60.

Teutenberg, T., 2010. High-Temperature Liquid Chromatography - A User's Guide for Method Development. Royal Society of Chemistry.

Thomas, W.R., Smith, W.A., Hales, B.J., Mills, K.L., O'Brien, R.M., 2002. Characterization and immunobiology of house dust mite allergens. International Archives of Allergy and Immunology 129, 1-18.

van den Heuvel, R.H.H., Gato, S., Versluis, C., Gerbaux, P., Kleanthous, C., Heck, A.J.R., 2005. Real-time monitoring of enzymatic DNA hydrolysis by electrospray ionization mass spectrometry. Nucleic Acids Research 33, online, e96.

Van Pelt, C., Zhang, S., Henion, J., 2002. Characterization of a fully automated nanoelectrospray system with mass spectrometric detection for proteomic analyses. J Biomol Tech 13, 72-84.

Vijayakrishnan, B., Issaree, A., Corilo, Y.E., Ferreira, C.R., Eberlin, M.N., Peter, M.G., 2011. MS(n) of the six isomers of (GlcN)(2)(GlcNAc)(2) aminoglucan tetrasaccharides (diacetylchitotetraoses): Rules of fragmentation for the sodiated molecules and application to sequence analysis of hetero-chitooligosaccharides. Carbohydrate Polymers 84, 713-726.

Vinetz, J.M., Valenzuela, J.G., Specht, C.A., Aravind, L., Langer, R.C., Ribeiro, J.M.C., Kaslow, D.C., 2000. Chitinases of the avian malaria parasite Plasmodium gallinaceum, a class of enzymes necessary for parasite invasion of the mosquito midgut. Journal of Biological Chemistry 275, 10331-10341.

Vlasova, II, Arnhold, J., Osipov, A.N., Panasenko, O.M., 2006. pH-dependent regulation of myeloperoxidase activity. Biochemistry-Moscow 71, 667-677.

Wallenfels, K., 1962. ß-Galactosidase (crystalline). Methods in Enzymology 5, 212-219.

Weigang, L.M.M., Langosch, D., Letzel, T., 2008. Gas-phase behavior of noncovalent transmembrane segment complexes. Rapid Communications in Mass Spectrometry 22, 4089-4097.

Wilm, M., Mann, M., 1996. Analytical properties of the nanoelectrospray ion source. Analytical Chemistry 68, 1-8.

Wilm, M., Shevchenko, A., Houthaeve, T., Breit, S., Schweigerer, L., Fotsis, T., Mann, M., 1996. Femtomole sequencing of proteins from polyacrylamide gels by nano-electrospray mass spectrometry. Nature 379**,** 466-469.

Wilm, M.S., Mann, M., 1994. Electrospray and Taylor-Cone Theory, Doles Beam of Macromolecules at Last. International Journal of Mass Spectrometry 136**,** 167-180.

Wilson, D.J., Konermann, L., 2004. Mechanistic studies on enzymatic reactions by electrospray ionization MS using a capillary mixer with adjustable reaction chamber volume for time-resolved measurements. Analytical Chemistry 76**,** 2537-2543.

Wu, J.Y., Takayama, S., Wong, C.H., Siuzdak, G., 1997. Quantitative electrospray mass spectrometry for the rapid assay of enzyme inhibitors. Chemistry & Biology 4**,** 653-657.

Yang, R.J., Li, S.Q., Zhang, Q.H., 2004a. Effects of pulsed electric fields on the activity of enzymes in aqueous solution. Journal of Food Science 69**,** C241-C248.

Yang, Y.N., Kameoka, J., Wachs, T., Henion, J.D., Craighead, H.G., 2004b. Quantitative mass spectrometric determination of methylphenidate concentration in urine using an electrospray ionization source integrated with a polymer microchip. Analytical Chemistry 76**,** 2568-2574.

Yu, Z., Chen, L.C., Mandal, M.K., Nonami, H., Erra-Balsells, R., Hiraoka, K., 2012. Online Electrospray Ionization Mass Spectrometric Monitoring of Protease-Catalyzed Reactions in Real Time. Journal of the American Society for Mass Spectrometry 23**,** 728-735.

Zechel, D.L., Konermann, L., Withers, S.G., Douglas, D.J., 1998. Pre-steady state kinetic analysis of an enzymatic reaction monitored by time-resolved electrospray ionization mass spectrometry. Biochemistry 37**,** 7664-7669.

Zhang, S., Van Pelt, C.K., Henion, J.D., 2003a. Automated chip-based nanoelectrospray-mass spectrometry for rapid identification of proteins separated by two-dimensional gel electrophoresis. Electrophoresis 24**,** 3620-3632.

Zhang, S., Van Pelt, C.K., Wilson, D.B., 2003b. Quantitative determination of noncovalent binding interactions using automated nanoelectrospray mass spectrometry. Analytical Chemistry 75**,** 3010-3018.

Acknowledgements

My first and greatest thanks go to PD Dr. Thomas Letzel for giving me the opportunity to work in his group and especially for his enthusiasm for mass spectrometry, his encouragement and for giving advice whenever I needed. I really appreciate the opportunities to join scientific meetings and present my results there.

I want to thank Prof. Dr. Michael Rychlik and Prof. Dr. Dieter Treutter for their participation in my rigorosum committee.

Special thanks go to PD Dr. Johanna Graßmann for always being ready to answer my questions and discuss my ideas. Many thanks for keeping me motivated and your suggestions for my first attempts in scientific writing.

I would like to thank Prof. Dr. Brzezinski und Prof. Dr. Fukamizo for the preparation and provision of the enzymes and the excellent collaboration for common publications. I thank Prof. Dr. Peter for the friendly provision of the tetrasaccharides. Many thanks to Dr. Reinaldo Almeida from Advion BioSciences for his dedicated technical and professional support. I also thank Dr. Daniel Vetter from ERC GmbH for the provision of the electrochemical system and his technical support.

I would like to acknowledge the German Federal Ministry of Economics and Technology and the Arbeitsgemeinschaft industrieller Forschungsvereinigungen for financial support and I thank the colleagues from the Institut für Energie- und Umwelttechnik e.V., Duisburg for the collaboration.

Many thanks to the TUM graduate school for providing a framework of courses to develop my academic skills. The Graduiertenzentrum Weihenstephan, part of the graduate school was of particular help in building contacts and friendships with other doctoral candidates.

Many thank to my colleagues Sylvia Große, Christine Kaufmann, Dr. Alper Aydin, Dr. Giorgia Greco and Dr. Christoforos Christoforidis and of course all other colleagues at the institute for general help and the enjoyable atmosphere. I also thank my students Matthias Graf, Stefan Tilp and Stefan Bieber for their excellent work.

Finally I want to thank my family for their support and always being there.

Scientific Communications

Original peer reviewed scientific publications

Scheerle, R.K., Grassmann, J., Letzel, T., 2011. Enzymatic conversion continuously monitored with a robotic nanoESI-MS tool: Experimental status. *Analytical Methods* 3**,** 822-830.

Scheerle, R.K., Grassmann, J., Letzel, T., 2012. Real-time ESI-MS of Enzymatic Conversion: Impact of Organic Solvents and Multiplexing. *Analytical Sciences* 28 (6)**,** 607-612.

Grassmann, J., **Scheerle, R.K.**, Letzel, T., 2012. Functional Proteomics: Mass Spectrometric Applications studying Enzymology in Complex Mixtures. *Analytical and Bioanalytical Chemistry* 402**,** 625-645.

Zitouni, M., Fortin, M., **Scheerle, R.K.**, Letzel, T., Matteau, D., Rodrigue, S. and Brzezinski, R., 2013. Biochemical and Molecular Characterization of a Thermostable Chitosanase Produced by the Strain Paenibacillus sp. 1794 Newly Isolated from Compost. *Applied Microbiology and Biotechnology*, 97(13), 5801-5813.

Krappmann, M., Kaufmann, C., **Scheerle, R.K.**, Letzel, T., 2013. Handling of mass spectrometric data: possibilities and application of the software Achroma, in preparation

Book chapters

Scheerle, R.K., Grassmann, J., 2011. LC-MS for the Determination of the Enzymatic Activity of Proteins. In: Letzel, T., (Ed.), Protein and Peptide Analysis by LC-MS. *Royal Society of Chemistry*, Cambridge, 133-141.

Shinya, S., Ohnuma, T., Brzezinski, R., **Scheerle, R.K**., Grassmann, J., Letzel, T. and Fukamizo, T., 2013. Lysozyme Superfamily: Progress in Functional Analysis using ESI-MS and NMR Spectroscopy. In: Maang, X.G. and Cheung, W.F. (Ed.), Lysozymes: Sources, Functions and Role in Disease, *Nova Science Publishers*, New York, 127-154.

Oral scientific presentations

Scheerle, R.K.: Kopplung von Enzymassays mit Hochtemperatur-HPLC zur massenspektrometrischen Identifizierung von enzymregulatorischen Substanzen in komplexen Gemischen.
21. Doktorandenseminar des AK Separation Science, GDCh, 09. - 11. 01. 2011, Hohenroda, Germany

Scheerle, R.K.: How to handle huge amount of mass spectrometric data? A new strategy with the Achroma software.
Joint Conference of Polish Mass Spectrometry Society and German Mass Spectrometry Society 2012, 04. - 07. 03. 2012, Poznań, Poland

Abstracts and posters presented at scientific meetings

Scheerle, R.K., Oeste, K., Portner, C., Teutenberg, T., Graßmann, J., Letzel, T.: Development of a direct coupled mass spectrometric method for the fast determination of biological activity in house dust using an enzymatic assay.
Analytica Conference, 23. - 25. 03. 2010, Munich, Germany

Scheerle, R.K., Graßmann, J., Letzel, T.: Miniaturisierung und Automatisierung massenspektrometrischer Verfahren zur Untersuchung von Enzymassays.
39. Deutscher Lebensmittelchemikertag, 20. - 22. 09. 2010, Stuttgart, Germany

Scheerle, R.K., Graßmann, J., Letzel, T.: Poster 1: Optimization of a miniaturised and automated setup for real-time monitoring of enzymatic assays by mass spectrometry. Poster 2: Adaptation of enzymatic reactions for use with a nanoESI-MS robotic setup.
ANAKON 2011, 22. - 25. 03. 2011, Zürich, Switzerland

Scheerle, R.K., Teutenberg, T., Grassmann, J., Letzel, T.: Coupling of high temperature - HPLC with Enzymatic Assays – The Issue of Organic Solvent.
HPLC 2011, 19. - 23. 06. 2011, Budapest, Hungary

Scheerle, R.K., Graßmann, J., Letzel, T.: Online-coupling of Liquid Chromatography with Enzymatic Assays.
18th International Symposium on Electro- and Liquid Phase-separation Techniques, 28. - 31. 08. 2011, Tbilisi, Georgia

Scheerle, R.K., Ureña de Vivanco, M., Letzel, T.: Studying Oxidative and Reductive Reactions Using a Potentiostat Coupled To MS: Applications in Water Research and Enzymology.
Joint Conference of Polish Mass Spectrometry Society and German Mass Spectrometry Society 2012, 04.-07. 3. 2012, Poznań, Poland and *Langenauer Wasserforum*, 12. – 13. 11. 2012, Langenau, Germany

Scheerle, R.K., Graßmann, J., Letzel, T.: Investigation of enzymatic reactions using a miniaturised and automated nanoESI-MS system.
ANAKON 2013, 04. - 07. 03. 2013, Essen, Germany

Curriculum Vitae

Name	Romy Katharina Scheerle
Date of birth	December, 3th 1983
Place of birth	Tuttlingen, Germany

11/2009 – 03/2013	Doctoral candidate at Analytische Forschungsgruppe am Wissenschaftszentrum Weihenstephan, Fachgebiet für Obstbau, TU München
11/2008 - 10/2009	State examination in Food Chemistry, Chemisches und Veterinäruntersuchungsamt Karlsruhe
03/2008 - 08/2008	Diploma thesis, Institut für Angewandte Biowissenschaften, Karlsruhe Institute of Technology
10/2003 - 08/2008	Studies in Food Chemistry, Karlsruhe Institute of Technology
08/1994 - 07/2003	Graduation, Allgemeine Hochschulreife, Immanuel-Kant-Gymnasium, Tuttlingen

Appendix

Appendix I

Functional Proteomics: Application of Mass Spectrometry to the Study of Enzymology in Complex Mixtures

Grassmann, J., Scheerle, R.K. and Letzel, T.

Analytical and Bioanalytical Chemistry, 2012, 402, 625-645

This review gives an overview of mass spectrometric applications in the field of functional proteomics in combination with enzymatic assays. The enormous increase of enzymological studies by mass spectrometry in recent years is summarized in this review. I was involved in the literature research and the preparation of the manuscript.

Anal Bioanal Chem (2012) 402:625–645
DOI 10.1007/s00216-011-5236-4

REVIEW

Functional proteomics: application of mass spectrometry to the study of enzymology in complex mixtures

Johanna Graßmann · Romy K. Scheerle · Thomas Letzel

Received: 19 May 2011 / Revised: 30 June 2011 / Accepted: 4 July 2011 / Published online: 16 July 2011

Abstract This review covers recent developments in mass spectrometry-based applications dealing with functional proteomics with special emphasis on enzymology. The introduction of mass spectrometry into this research field has led to an enormous increase in knowledge in recent years. A major challenge is the identification of "biologically active substances" in complex mixtures. These biologically active substances are, on the one hand, potential regulators of enzymes. Elucidation of function and identity of those regulators may be accomplished by different strategies, which are discussed in this review. The most promising approach thereby seems to be the one-step procedure, because it enables identification of the functionality and identity of biologically active substances in parallel and thus avoids misinterpretation. On the other hand, besides the detection of regulators, the identification of endogenous substrates for known enzymes is an emerging research field, but in this case studies are quite rare. Moreover, the term biologically active substances may also encompass proteins with diverse biological functions. Elucidation of the functionality of those—so far unknown—proteins in complex mixtures is another branch of functional proteomics and those investigations will also be discussed in this review.

J. Graßmann (✉) · R. K. Scheerle
Analytical Research Group, Chair of Chemical-Technical Analysis and Chemical Food Technology, Technische Universität München, Weihenstephaner Steig 23,
85354 Freising-Weihenstephan, Germany
e-mail: johanna.grassmann@wzw.tum.de

T. Letzel (✉)
Competence Pool Weihenstephan,
Technische Universität München,
Weihenstephaner Steig 23,
85354 Freising-Weihenstephan, Germany
e-mail: T.Letzel@wzw.tum.de

Keywords Protein function · mass spectrometry · inhibitor screening · continuous-flow assays

Introduction

Research fields ending on the suffix "omics" are neoterisms for the study of biological or related systems as global entities. So far, approximately 200 counted "omics"-containing terms have been included in publicly available scientific glossaries [1, 2].

One of the most popular areas of research is, obviously, the analytical determination of molecules with their effects and regulation in biological systems, as reflected by their corresponding names genomics [3–5], transcriptomics [6, 7], proteomics [8, 9], and metabolomics [10–12].

In addition to general biological research fields [13], whole application areas can be described by use of the "omics" ending, for example babelomics [14], metallomics [15, 16], nutrigenomics [17, 18], or oncogenomics [19, 20].

Subclasses are generated by differentiating the overall "omics" topics into more detailed classifications. Proteomics for instance has previously been split into "differential" proteomics [21, 22], "structural" proteomics [23, 24], and "functional" proteomics [25–32]. However, these subclasses are diffusely and broadly defined rather than having clear structured scopes. Functional proteomics, for example, has several definitions with overlapping and independent topics. Godovac-Zimmermann and Brown defined functional proteomics in their extensive and impressive "mass spectrometric" review from 2001 [26] as "the use of proteomics methods to monitor and analyse the spatial and temporal properties of the molecular networks and fluxes involved in living cells. Conversely, functional proteomics is also the use of proteomics methods

to identify the molecular species that participate in such networks via functional simulation, perturbation, or isolation of these networks". On the other hand, the review of mass spectrometry by Naylor and Kumar in 2003 [25] describes functional proteomics as the "identification of all protein-protein interactions within a specified cell system as well as protein-DNA and protein-RNA interactions occurring in an organism or cells and the modulation effects of ligands, toxins, drugs, and metal ions on all those protein interactions that affect function".

Other authors classify the topic by use of such terminology as "interaction proteomics, posttranslational modification, and quantitative proteomics" [27] or "yeast genomics, affinity purified protein complexes, and mouse knockouts" [28]. Thus a clear direction can hardly be recognized in the definition "functional proteomics". Furthermore, terms with a focus on functional proteomics, for example chemistry-based proteomics [33, 34], activity-based proteomics [35–37], kinomics [38, 39], interactomics [40, 41] and other fields of application are broadening the definition even more.

The problematic impreciseness described above has to be overcome. One approach is to classify proteomics not solely biologically but also on the basis of its analytical applications. Thus proteomics work can be merged into groups of similar analytical techniques.

In this scientific review we specifically classify the field of proteomics according to its mass spectrometric aspects and exclusively review in-vitro analytical techniques, with the main emphasis on enzymology, mass spectrometry, and enzymatic conversion monitored by use of this technique.

The enzymatic functionality of proteins, and their regulation, are usually discovered by application of enzymatic in-vitro assays. Such in-vitro assays are conducted either by analysing aliquots of the enzymatic reaction after defined time points or by continuous monitoring of the enzymatic conversion.

Different detection methods are possible for both assay types; currently, however, most assays use photometric or fluorescence detection, because of their easy application and the long-term established spectroscopic techniques. In these methods chromophores and fluorophores are attached to or detached from the substrate during the enzymatic reaction. Numerous applications with spectroscopic detection methods have been described in detail by Bisswanger [42]. The major disadvantage of such assays is the need for artificial substrates, which can affect the enzymatic reaction [43]. Radioisotopic labelling in in-vitro enzymology is on the decease, because of health risks during handling.

As mentioned above, mass spectrometric detection is an essential analytical tool in (functional) proteomics [44], e.g. in early proteomics [45, 46], current proteomics [47, 48], protein quantification [49], location of posttranslational modifications [50], and elucidation of protein structure [51]. Furthermore, research on protein function by means of non-covalent complexes nowadays needs mass spectrometry [52] just as enzymology does [53]. Compared with spectroscopic or radioisotopic methods mass spectrometric detection not only has the advantages of safe handling and applicability to natural substrates but also enables the simultaneous detection of substrate, intermediates, products, and, in some cases, also the enzyme and its complexes. For this reason, the development of mass spectrometry-based enzymatic assays has increased rapidly in recent years, and the reader is referred to some interesting review articles [54–57].

Proteomic approaches multiplied the number of known enzymes and significantly extended knowledge about the involvement of enzymes in diverse pathological disorders. This led to new key aspects of enzymology. First, it is desirable to screen large compound libraries or complex mixtures (e.g. plant extracts) for potential enzyme regulators thereby exploring new drug candidates. Moreover, it is necessary to gain knowledge about natural (endogenous) substrates of newly discovered enzymes in order to assign those enzymes to a known functionality. Furthermore, identification of enzyme activity in mixtures (e.g. human plasma) is of interest in order to discover potential enzyme dysfunction and its relationship with diseases. This may enable diagnosis of diseases at an early stage and thus improve therapeutic treatment.

The forthcoming sections give an overview of mass spectrometric enzymatic assays and their versatile areas of application. Further, deeper insight is provided into several mass spectrometric strategies used, on the one hand, for identification of enzyme regulators or endogenous substrates in complex mixtures and, on the other hand, with the purpose of identification of (unknown) enzyme activity in crude samples.

Mass spectrometry-based enzymatic assays with single enzyme solutions

As mentioned above, mass spectrometric detection has several advantages for investigation of enzymatic reactions. For that reason MS-based enzymatic assays have become a widespread application ranging from determination of inhibition constants and kinetic values to the detection of non-covalent complexes and much more.

Most of those assays use the classical approach, i.e. the partitioned enzymatic assay. A typical partitioned enzymatic in-vitro assay consists of:

1. starting the reaction by mixing the reacting compounds;
2. taking aliquots after different reaction times;

3. interrupting the reaction in each aliquot;
4. separating the reaction products; and
5. detecting the compounds for quantification [53].

For instance, for determination of kinetic values a single enzyme is incubated with the respective substrate. The same basic approach is used for the investigation of inhibition constants, but in these cases the reactions are mostly performed in microtitre plates thus enabling high-throughput screening. Such classical assays have been conducted for numerous single enzyme–single substrate–single inhibitor combinations; for information about these the reader is referred to recently published reviews [54–58]. Screening for inhibitors has also been reviewed recently [54–56, 59, 60]. In most of these screening setups a single enzyme was incubated with different potential inhibitors in microtitre plates and the reaction mixture was analysed after quenching of the reaction (i.e. the partitioned assay). As none of these approaches dealt with complex mixtures they will not be discussed any further herein [54–56, 60].

Simultaneously with classical "quenched reaction" setups continuous-flow assays have also been developed in recent years; these enable real-time monitoring of enzymatic reactions [61–63]. In these assays a constant stream of enzyme and substrate solution is subjected to the mass spectrometer. This kind of measurement is less time-consuming than the conventional approach and enables the determination of enzyme kinetics, substrate(s), products, and (in an extended setup) the effect and fate of inhibitors in a single run. By means of this assay scheme different sugar-hydrolysing enzymes have been studied, both earlier [64, 65] and nowadays [66–70]. For instance the hydrolysis of hexa-*N*-acetylchitohexaose by lysozyme was monitored by real-time ESI–MS and the effect of inhibitors was also investigated [66]. The observed dissociation constants are comparable with results obtained previously [65] and in conventional experiments [71]. Furthermore, the activity of the glycosidases chitosanase, chitinase, and several mutants were investigated by use of a similar setup. In a chitosanase project it was proved that the specific loss of activity was caused by a point mutation and not by partial unfolding of the mutated enzyme used [68]. In another project a chitinase type with transglycosylation activity was investigated and the authors verified that the transglycosylation reaction takes place solely at the higher substrate concentrations used for HPLC–UV analysis [69] . By use of two mutants of the enzyme, the side chains responsible for the transglycosylation activity could be identified [69].

Other real-time ESI approaches were presented earlier by different groups [61, 62, 72, 73], and recently by Li et al. [74]. In the latter work, two syringe pumps delivered the enzyme 4-hydroxybenzoyl-coenzyme A (4-HBA) thioesterase and its substrate via a mixing unit to ESI–MS detection. Monitoring of substrate and product complexes enabled suggestion of a mechanism for the catalytic process, in particular that the product 4-HBA is released from the active site before release of CoA.

These and other examples illustrate the widespread opportunities offered by real-time ESI–MS. In further studies this principle was also used to screen for inhibitors in complex mixtures; this work will be discussed in the next section.

Mass spectrometry-based enzymatic assays in complex mixtures

Generally, research on enzymatic conversion dealing with complex mixtures can be split into two complementary strategies. Figure 1 illustrates the two different approaches used to investigate known enzymes (left panel) and to identify enzymatic activity for unknown enzymes in complex mixtures (right panel). An overview of sample-handling strategies used to screen for inhibitors in complex mixtures is given in Fig. 2.

Reaction with known enzymes—inhibitor screening

Although several approaches are used for identification of inhibitors of enzyme systems, few data are available for the identification of endogenous substrates of the enzymes. An overview is given in Table 1.

Identification of binding affinity

Some methodological approaches are not capable of quantification of the inhibitory strength of compounds but reveal the binding affinity of components from a mixture for a protein. This screening for protein–ligand interactions has been reviewed recently [98]. As can be seen from Fig. 1 and Table 1, diverse methods exist for this purpose; these are discussed in the following sections.

Use of an immobilized enzyme Tagore et al. [75] presented a general setup for screening for protein–metabolite interactions. In this setup an immobilized enzyme (a retinoic acid binding protein) was incubated with a mixture of small molecules (a lipid extract from mouse brain). Subsequently the protein–metabolite complex was separated from unbound compounds and analysed by means of global metabolite profiling (i.e. comparison of the isolated protein–metabolite complex with the appropriate controls). The specific identification of protein-bound metabolites was performed by means of LC–MS. This experimental setup may also be applicable to other enzymes and mixtures of small molecules, for example plant extracts. For the latter the

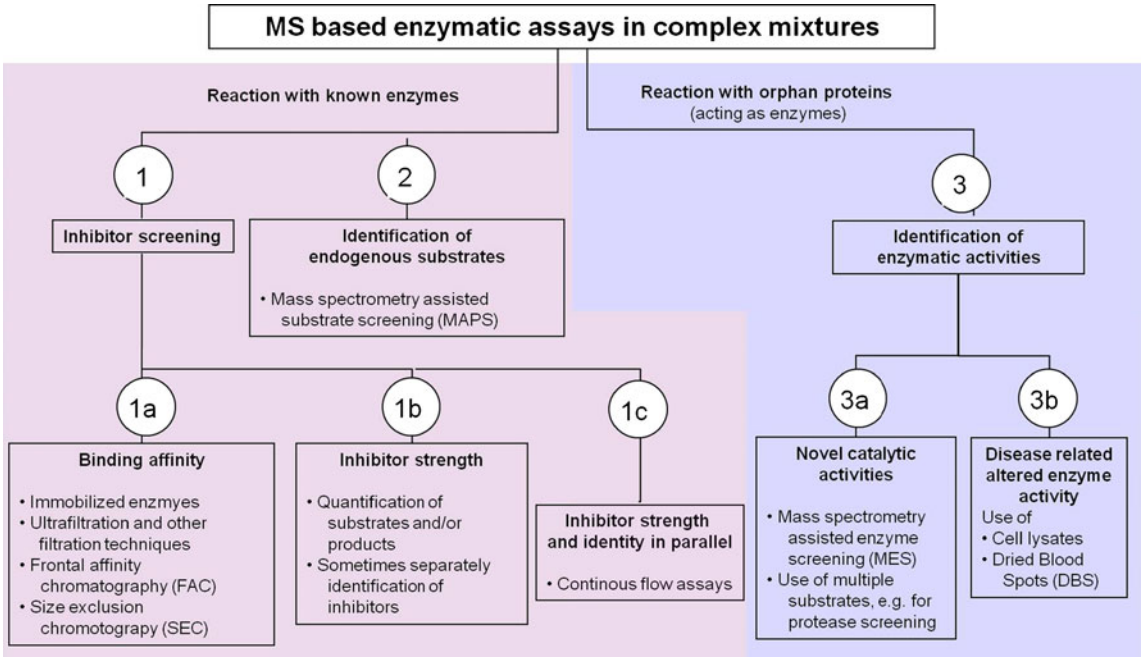

Fig. 1 Identification of inhibitors (*left trace, i.e. 1*) and/or endogenous substrates (*middle trace, i.e. 2*) and orphan proteins (*right trace, i.e. 3*) in complex mixtures

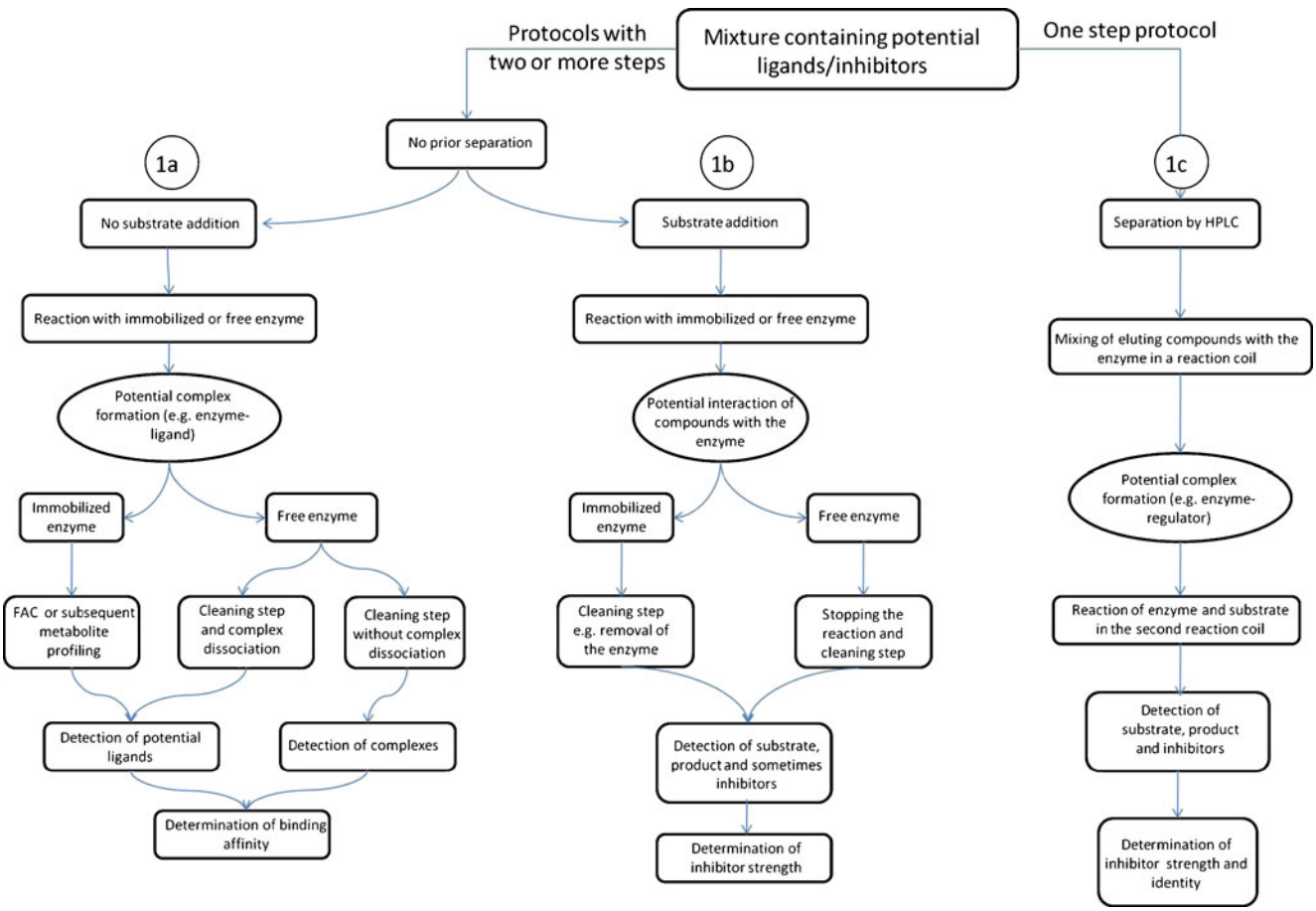

Fig. 2 Sample-handling strategies to screen for inhibitors in complex mixtures

Table 1 Reaction with known enzymes—screening for inhibitors and endogenous substrates

Identification of		Enzyme	Mixture	Key features of the method	Main results	Ref.
(1a) Binding affinity	Use of an immobilized enzyme	Retinoic acid binding protein	Lipid extract from mouse brain	Immobilized enzyme Global metabolite profiling LC–MS	Specific binding partners were identified	[75]
	Use of different filtration techniques	Dihydrofolate reductase (DHFR)	Green tea extract	Filtration to remove small (unbound) molecules Dissociation of the complex MALDI–TOF	Epigallocatechin gallate was identified as compound with binding affinity to DHFR	[76]
		Carbonic anhydrase	Methanolic fermentation broth	Micro volume pulsed ultrafiltration ESI–MS	Non-covalent binding was detected	[77]
		COX-2	Samples enriched with one or more inhibitors	Ultrafiltration to remove small (unbound) molecules Dissociation of the complex LC–MS	Ligands were identified in the samples	[78]
	Use of SEC	Bovine carbonic anhydrase	Several plant extracts	SEC, no dissociation of the complex ESI–FTICR–MS	Non-covalent complexes and the ligand mass were detected	[79]
	Use of FAC	Diverse	Diverse	FAC		[80]
(1b) Inhibitor strength	S/P	Cytochrome P450	Eight herbal remedies	LC–LC–MS to quantify reaction products from six CYP isoforms	Inhibitory strength of several plant extracts was detected	[81]
	S/P/I		Boswellia extracts	LC–LC–MS to quantify reaction products from six CYP isoforms	Boswellic acids were identified as inhibitors	[82]
			Woohwangcheongsimwon extract	LC–LC–MS to quantify reaction products from nine CYP isoforms Sequential extraction to identify inhibitors	Borneol and isoborneol were identified as inhibitors	[83]
		α-Glucosidase	Hawthorn leaf extract (flavonoids)	Photometric quantification of inhibition Isolation of enzyme–ligand complexes by ultrafiltration and analysis by LC–MS	Four flavonoids were identified as potential active principles	[84]
		Acetylcholinesterase	Rhizoma coptidis extract	Quantifying substrate and product by MALDI–FTMS Different extraction solvents for preparing the extracts	The most active inhibitor was contained in the DMSO extract and assigned to berberine	[85]
	S/P		*Huperiza serrata* extract	Immobilized enzyme Analysis of the reaction mixture by LC–MS Detection of substrate, product and extract compounds	Inhibitory strength of compounds of the extract were detected	[86]
		Trypsin	Extracts from Solanum species	Immobilized substrate on a MALDI chip	Extracts had inhibitory activity	[87]

Table 1 (continued)

Identification of	Enzyme	Mixture	Key features of the method	Main results	Ref.
			Analysis of reaction products by MALDI–TOF		
	Carboxypeptidase B	Extracts from Solanum species	Immobilized enzyme Analysis of reaction products by MALDI–TOF	Tomato and potato extracts had inhibitory activity	[88]
(1c) Inhibitor strength and identity	Cathepsin B	Red clover extract	Online coupling of HPLC to a continuous-flow enzymatic assay Detection by ESI–MS	Several compounds had inhibitory activity	[89]
		Tea extract	Online coupling of HT–HPLC to a continuous-flow enzymatic assay Detection by ESI–MS	Three known inhibitors were identified	[90]
		Tea extract	Microfluidic chip coupled to a continuous-flow enzymatic assays Detection by ESI–MS	Two catechins were identified as inhibitors	[91]
	Acetylcholinesterase	Narcissus extract	Online coupling of HPLC to a continuous-flow enzymatic assay Detection by ESI–MS	Galanthamine was identified as inhibitor	[92]
	Adenosine deaminase	Mixture of seven inhibitors	Enzyme immobilized on a column Detection of substrate and product by ESI–MS	Different inhibitory strength was observed	[93]
	Glycogen synthase kinase 3b	Ten mixtures containing ten compounds each	Enzyme immobilized on a column Detection of substrate and product by ESI–MS	Different inhibitory strength was observed	[94]
(2) Endogenous substrates	Thrombin	Human plasma	Immobilized human plasma Detection of peptides by MALDI-TOF	Fibrinopeptides were detected	[95]
	Fatty acid amide hydrolase (FAAH)		Untargeted LC–MS of tissue metabolomes	Several lipids were detected which seem to be regulated by FAAH in vivo	[96]
	Cytochrome P450	Human liver extract	Isotopic labelling of the products Detection of products by LC–MS	Seven fatty acids were identified as substrates	[97]

S/P, quantification of substrates and products; S/P/I, quantification of substrates and products and separate identification of inhibitors

identification of putative binding partners for proteins is possible.

Use of different filtration techniques The binding capability of compounds from such plant extracts has been investigated with dihydrofolate reductase (DHFR) as the target enzyme [76]. The enzyme was incubated with green tea extract and after a defined reaction time the small molecules (<10,000 $gmol^{-1}$) were removed from the incubation mixture using a specific filter. By washing the filter the DHFR–ligand complex was released and analysed by MALDI–TOF. By applying this procedure, epigallocatechin gallate could be identified as the active compound. A related approach is the use of pulsed ultrafiltration to identify binding partners for carbonic anhydrase contained in a methanolic fermentation broth [77]. In a similar setup, samples enriched with known inhibitors of cyclooxygenase 2 (COX-2) were incubated with this enzyme. Subsequent to ultrafiltration and a cleaning step, the disrupted complexes were analysed by LC–MS. By this means interacting compounds could be identified [78]. The application of (pulsed) ultrafiltration thus seems to be an useful methodology for detection of ligand–receptor interactions [99–101]. Another setup using complexes and the separation of free ligands was performed with the GABA receptor and a mixture of small compounds. The separation was conducted using vacuum filtration, subsequent ligand dissociation, and mass spectrometric analysis [101].

Use of size-exclusion chromatography In early 1998 Heck and co-workers reported an affinity experiment with direct mass spectrometry of non-covalent complexes for several peptide ligands which were simultaneously incubated with glycopeptide antibiotics. Investigation of their specific interaction shows clearly the applicability of direct mass spectrometric detection, at least for complexes stable in gas phase [102]. Another approach without dissociation of the protein–ligand complex was developed by Vu et al. [79]. They used bovine carbonic anhydrase as a model enzyme and screened several plant extracts on potential binding partners. Subsequent to enzyme incubation with the respective extract, an aliquot of the mixture was subjected to size-exclusion chromatography directly coupled with mass spectrometry (SEC–ESI–FTICR–MS). The application of MS-compatible buffers is indispensable for this type of bioaffinity measurement and, therefore, the authors tested two volatile buffers. They observed significantly higher signal intensities using ammonium bicarbonate buffer compared with ammonium acetate buffer. Several non covalent complexes could be observed using this online coupling. The ligand mass was calculated from the difference between the average molecular weight of the enzyme–ligand complex and the average molecular weight of the enzyme. By means of mass directed purification the binding partners could be identified using UV spectroscopy, IR, and NMR.

Use of frontal affinity chromatography Another technique used to screen for protein–ligand interaction is frontal affinity chromatography (FAC) coupled with MS, which was developed by Schriemer et al. [103, 104]. In this case a receptor or enzyme is immobilized on a column and a mixture which may contain potential binding partners is infused through the column. The binding partners of the immobilized receptor or enzyme will be retained in the column and thus elute later than non-binding compounds [105]. The basic principle of FAC is shown in Fig. 3. As examples, the detection of binding partners in complex mixtures by FAC has been used to identify kinase inhibitors, to determine K_d values of trisaccharides towards *N*-acetylglucosaminyltransferase and to screen extracts from Chinese herbal medicines [80, 104].

Thus FAC enables online high-throughput screening for detection of interactions between proteins and small molecules. However, this method, and the techniques described above, provide information about binding affinity but not about biological functionality, because the ligand binding might occur at a non-functional side of the protein.

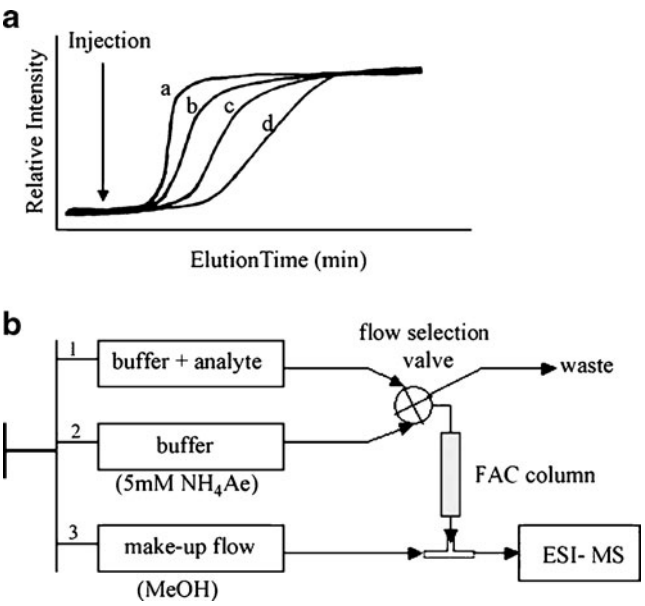

Fig. 3 Schematic diagram of EIC of compounds with different binding affinities monitored by FAC–MS (**a**) and instrument configuration (**b**). Reprinted from Ref. [105], Journal of Pharmaceutical and Biomedical Analysis, 2006, 40(3):528–538, with permission from Elsevier

Identification of inhibitor strength

An effective approach used to obtain data about ligand–enzyme interaction and to acquire knowledge about enzyme inhibition is a two-step procedure used by Li et al. to identify α-glucosidase inhibitors from a hawthorn leaf extract [84]. In a first step the α-glucosidase inhibition caused by a raw extract was quantified photometrically. In a second step the enzyme was again incubated with extract. The enzyme–ligand complexes were isolated by ultrafiltration and inhibitor identification was performed by analysing the released ligands by LC–MS. This analysis revealed four flavonoids as potential participants in the α-glucosidase inhibition. However, this interpretation equates binding affinity with inhibitory activity, which is not entirely correct, because there is still a possibility that compounds with low binding affinity are not identified as inhibitors although they may contribute to the observed enzyme inhibition.

Thus unambiguous detection of inhibitory activity should be the method of choice. In such an approach the enzyme is simultaneously incubated with substrate and potential inhibitors. The reaction mixture is then analysed either after defined incubation times (i.e. the partitioned assay) or continuously. Reduced product formation indicates enzyme inhibition.

Several inhibitory studies using this approach have been conducted with cytochrome P450 (CYP) isoforms. This enzyme is of crucial importance in the phase I metabolism of xenobiotics; induction or inhibition of CYP may therefore lead to severe side effects of pharmaceuticals or cause other toxic drug effects [106]. In recent years adverse reactions of herbal medicines have been reported which may be a result of the effect of those remedies on CYP. For this reason investigation of plant extracts for possible inducers or inhibitors of CYP is of growing interest. Various mass spectrometry-based assays have been described for assessing CYP activity in vitro, ranging from single enzyme–single substrate assays to cocktail approaches with multiple substrates [107–109]. However, most of these experiments were conducted with known inhibitors of CYP and only few deal with the effect of crude mixtures, for example natural extracts, on CYP activity. The group of Unger and co-workers tested eight popular herbal remedies for their effects on CYP [81]. The incubation mixture contained a commercially available mixture of six CYP isoforms, the respective substrate mixture, and different herbal extracts. After quenching the reaction, the resulting metabolites were analysed by LC–MS–MS. Several extracts had more or less pronounced inhibitory action towards all isoforms. Kava-kava and peppermint oil resulted in high inhibitor strength (IC_{50} <100 μg mL^{-1}) whereas all other extracts had lower inhibitor strength (IC_{50} >100 μg mL^{-1}). The inhibitory strength of each extract differed towards the six isoforms. In a similar setup the group tested Boswellia extracts and proved much stronger inhibitory strength towards four CYP isoforms (IC_{50} between 1 and 10 μg mL^{-1}) and a low activity towards other isoforms (20% inhibition at 10 μg mL^{-1}) [82]. The subject of both studies, however, was restricted to quantification of the inhibitory strength of the raw extract; no identification of the inhibitors was performed.

Identification of CYP-inhibitory compounds was indeed achieved by Kim et al. for the traditional Chinese Medicine Woohwangcheongsimwon [83]. Pooled human liver microsomes (which contain nine different CYP of different activity) were incubated with specific substrates and different concentrations of a Woohwangcheongsimwon suspension. After quenching the reaction, the supernatant was analysed by LC–MS–MS. It was found that the CYP isoforms were inhibited to different degrees by the suspension. In a subsequent step the Woohwangcheongiomwon suspension was sequentially extracted and the different fractions were again tested for their inhibitory strength towards CYP. The fraction with the highest inhibitory strength was analysed by GC–MS and two major signals were identified as borneol and isoborneol. Testing those revealed strong inhibition of CYP; thus the inhibitory strength of the suspension could be assigned to these two monoterpenes. So these results provided data about the total inhibitory strength and about the identity of the inhibitor. Again, as mentioned above, a two-step experimental procedure was necessary leaving the possibility of misinterpretation, especially regarding potential synergistic effects.

Another enzyme of interest in drug discovery is acetylcholinesterase (AChE), because it is of crucial importance in the nervous system. Inhibitors of AChE are putative candidates for treating neurological disorders, for example Alzheimer's disease, senile dementia, and ataxia [110–112]. Many synthetic drugs are used in this context but, however, suffer from side effects and/or are low in terms of efficiency. Therefore screening for new AChE inhibitors, preferably from natural sources, becomes important and can be regarded as a major objective in drug research. Despite this, few mass spectrometry-based investigations have been performed for screening of natural extracts for AChE-inhibitory potency. Xu and co-workers identified the inhibitor strength of *Rhizoma coptidis* extracts against AChE by applying classical 384-well plate incubation (i.e. each well contains the enzymatic assay without or with different inhibitors or a plant extract) [85]. Figure 4 shows typical mass spectra of known inhibitors and a *Rhizoma coptidis* extract in which, in addition to the substrate and the product, some compounds in the extract were also detected.

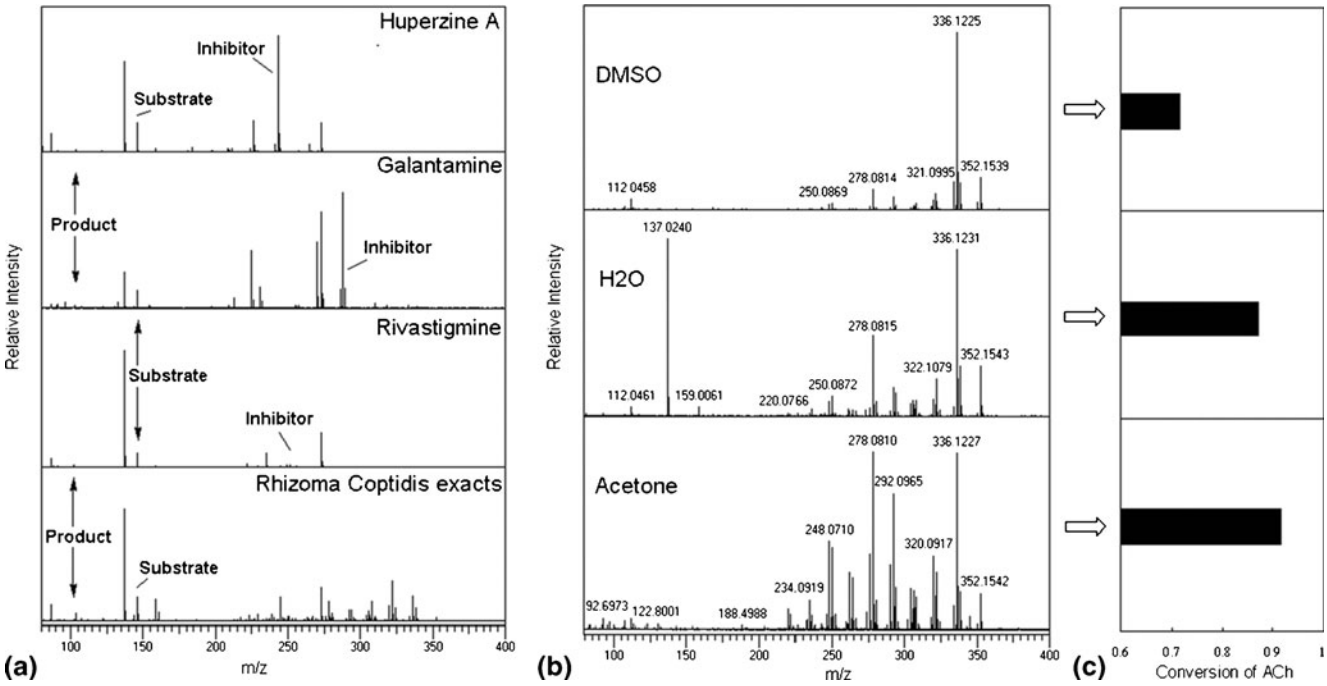

Fig. 4 (**a**) The mass spectra used for screening of inhibitors, including three commercially available drugs and Rhizoma Coptidis extracts. (**b**) The mass spectra obtained from crude Rhizoma Coptidis extracts using different solvents (*top*, DMSO; *middle*, H_2O; *bottom*, acetone). (**c**) Conversion of ACh in the presence of three Rhizoma Coptidis extracts (*top*, DMSO; *middle*, H_2O; *bottom*, acetone). Reprinted from Ref. [85], Journal of the American Society for Mass Spectrometry, 2008, 19(12):1849–1855, with permission from Elsevier

After testing different extraction solvents (water, acetone, or DMSO), the authors proved the most active inhibitor to be contained in the DMSO extract. Furthermore, they concluded that berberine, an AChE-inhibitor known from *Rhizoma coptidis* [113], was the active principle. Such an assignment, however, requires prior knowledge regarding the composition of the investigated extract. In a similar manner AChE inhibitors contained in *Huperiza serrata* [86] could be identified. The extract was incubated with the enzyme (immobilized on magnetic silica microspheres), subsequently the immobilized enzyme was removed with a magnet and the supernatant was analysed by ESI–MS. Besides the extract compounds, substrate and product of the AChE-reaction were also characterized. A control spectrum containing extract and substrate without enzyme was compared with that of the incubation mixture. By doing so it was concluded that the observed enzyme inhibition is caused by well known inhibitors, for example huperizine A and B, and by other, so far unknown, compounds from *Huperiza serrata*. Thus mass spectrometric detection of extract components enables detailed information about inhibitor identity to be obtained (although this was not done in the study presented) [86]. Extremely detailed characterization of AChE inhibitors was reported by Irth and co-workers. They identified them from a crude extract of *Narcissus* c.v. "Bridal Crown" [92] using a continuous-flow mixing system in combination with mass spectrometric detection. This investigation will be discussed in more detail in the section "Parallel determination of inhibitor activity and identity".

Most analytical inhibitory studies based on mass spectrometry have been conducted using different proteases. This may be because of the versatile biological functions of diverse proteases and because of the possibility of using protease inhibitors as therapeutic agents (e.g. HIV-protease inhibitors) [114–116]. Because a variety of mass spectrometry-based protease assays have recently been reviewed by Schlüter et al. [58], in the next section the main focus is again placed on identification of protease inhibitors from crude mixtures.

Such a study was conducted, for example, by Halim et al. [87] using a MALDI chip to differentiate the inhibitory strength of extracts from wild type and transgenic *Solanum* species towards trypsin. Initially, modified BSA serving as substrate was immobilized on a MALDI chip. Subsequently, the immobilized protein was incubated with trypsin in presence of plant extracts and finally, the reaction products (i.e. tryptic peptides) were analysed by MALDI–TOF. Extracts from those plants, the protease inhibitor expression of which had been silenced, led to distinctly more tryptic peptides than in extracts from wild type plants. Profiling the protease inhibitor proteins in the plant extracts indicated a relationship between the degree of inhibition and some small proteins, but obviously no final identification of these proteins was conducted.

Further, a setup has been used with immobilized enzyme instead of substrate. This strategy was chosen to investigate binding affinity and inhibitors from *Solanaceae* extracts towards carboxypeptidase B (CPB) [88]. In a first step the binding affinity to CPB was quantified by surface plasmon resonance. Subsequently, extracts with high binding affinity (i.e. from tomato and potato) were incubated with immobilized enzyme and a model peptide. The cleaved product peptides were recovered and analysed by MALDI-TOF. The tomato and potato extracts substantially inhibited CPB, as was proved by analysis of substrate and product ions. In a further step the enzyme–inhibitor complex was released from the immobilized enzyme and analysed by MALDI–TOF, whereupon a small peptide was identified as active principle.

As becomes apparent from a closer look at the methodological strategies described above, they all suffer from some deficits. Either they reveal binding affinity only, or inhibitors were perceived without identification or several separate steps are necessary to obtain information about both issues. This can be overcome by use of online assays, as described in the next section. These online assays enable real-time monitoring of enzymatic reactions and at the same time provide information about possible inhibitor candidates.

Parallel determination of inhibitor activity and identity

Several online detection techniques, or so called biochemical detection systems, have been described in the literature and recently reviewed by Shi et al. [59]. Their review covers several studies, most of them using colorimetric or fluorescence detection. Some of these approaches used mass spectrometry in combination with fluorescence or UV-detection by splitting the chromatographic separation flow for a mass spectrometric identification and simultaneous bioassay (detected via spectroscopy). One part is directed towards the bioassay, while the other part is analysed by MS for simultaneous identification of compounds causing signals in the bioassay. However, because UV–visible or fluorescence detection was applied, substrates had to be labelled with chromophores or fluorophores. An alternative to this "parallel detection" is the "one-step detection" by mass spectrometry [117]. The reaction compounds, their change in intensity, and the regulating compounds can be monitored directly by mass spectrometry. Thus biological activity monitoring and compound identification can be performed with one detection technique (if compounds are stable and ionic). However, inhibitor screening assays completely based on MS are rare and require experience with liquid flow systems. Despite this, several proofs-of-concept published by the group of Irth and co-workers reflect the power of this technique [89–92]. In their first publication in 2004 they introduced the direct online coupling of reversed-phase HPLC separation with a continuous-flow enzymatic assay and mass spectrometry. A complex mixture, e.g. a natural extract is separated on an HPLC column and the eluting compounds are mixed with the enzyme in a continuous flow reaction coil. After potential complex formation (e.g. enzyme–regulator) the substrate is added and the mixture is continuously pumped through a second reaction coil. The volume of the coils and the flow rates determine the reaction times. Subsequently to the second reaction coil the mixture is analysed by ESI–MS. Thereby, as stated above, the inhibitor effect is detected by changes in the substrate and product intensity. Additionally, the mass of the inhibitor can be identified in the mass spectrum, so this detection issue provides information about both the regulation activity and the molecular mass of inhibitory compounds.

By use of this method, inhibitor-containing standard mixtures (Fig. 5), inhibitor-spiked red clover extract, and non-spiked fungi extracts were screened for an inhibition of cathepsin B [89]. The detection limits for the known inhibitors are typically below the values obtained from common high-throughput screenings. On the other hand, the IC_{50} values for known inhibitors correspond to those from common microtitre plate assays. In a similar approach a crude *Narcissus* extract was screened for regulation of AChE. In this study galanthamine was detected as an inhibitor [92]. In subsequent studies the technique was modified and enhanced by Irth and co-workers. In a proof-of-concept study they used high-temperature liquid chromatography to reduce the amount of organic solvent necessary for separation, and in this way increased the compatibility with the enzymatic assay [90]. Again cathepsin B was used as model enzyme and a tea extract spiked with known inhibitors was investigated. The three known inhibitors could clearly be identified, however no further compound contained in the tea extract had inhibitor activity. A similar investigation by the same authors indeed resulted in the identification of new inhibitors in an extract from green tea [91]. In this second proof-of-concept study the system was miniaturized by use of a microfluidic chip with two reactors in which enzyme regulation and substrate conversion took place. In contrast with the investigation described above, in this miniaturized setup two catechins could be identified in the tea extract which were assumed to have inhibitory activity. Because the detection limits and IC_{50} values were even higher using the microchip method than with the conventional method, the inconsistent results may be because of the use of tea extracts of different composition. Unfortunately, no further specification was given for the different tea extracts.

In the procedures used for the continuous-flow online assays described so far, several reaction partners (enzyme, eluting compounds from HPLC, and substrate) were delivered continuously to the mass spectrometer. In con-

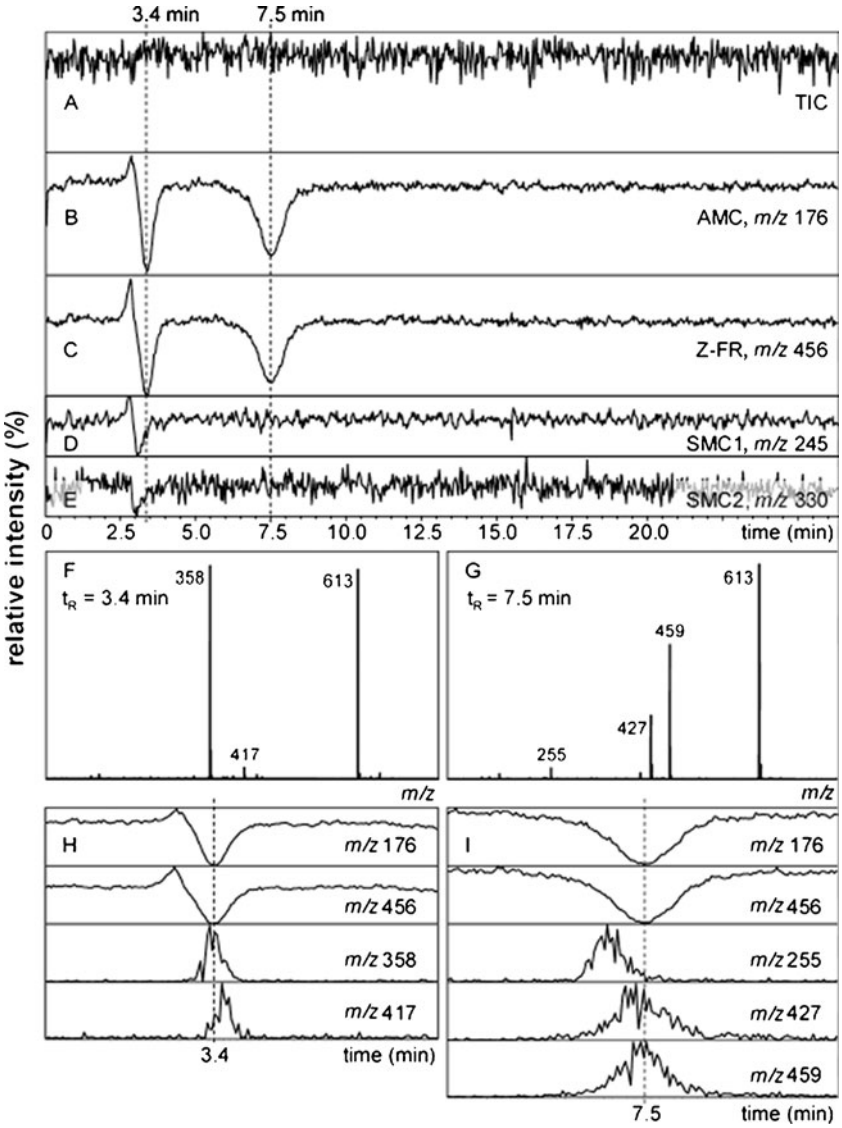

Fig. 5 On-line HPLC continuous-flow experiment of a mixture of five flavonoids spiked with two cathepsin B inhibitors, E-64 and leupeptin. (**A**) TIC chromatogram of the mixture, scan range *m*/*z* 75–750; (**B**) mass chromatogram of AMC, product 1 (*m*/*z* 176); (**C**) mass chromatogram of Z-FR, product 2 (*m*/*z* 456); (**D**) mass chromatogram of SMC1, internal standards 1 (*m*/*z* 245); (**E**) mass chromatogram of SMC2, internal standard 2 (*m*/*z* 330); (**F**) mass spectrum recorded at t_R 3.4 min; (**G**) mass spectrum recorded at t_R 7.5 min; (**H**) Extracted ion chromatograms of the most abundant peaks shown in the mass spectrum recorded at t_R 3.4 min; (**I**) RIC of the most abundant peaks shown in the mass spectrum recorded at t_R 7.5 min. Reprinted with permission from Ref. [89], Analytical Chemistry 76(11):3155–3161, Copyright 2004, American Chemical Society

trast, an assay using immobilized enzymes has been developed by the group of Brennan and co-workers [118, 119] and used to investigate inhibitors of adenosine deaminase (ADA) and glycogen synthase kinase-3β (GSK-3β) [93, 94]. Substrate and inhibitor (mixture) were continuously pumped through the column on which the respective enzyme had been immobilized. The use of two separate pumps for substrate and inhibitors enabled variation of inhibitor concentration by changing the respective pump flow. Product, substrate, and inhibitor were detected by MS and by so doing IC_{50} and K_I values could be determined. However, compared with the assays described above, with chromatographic separation before the enzymatic assay, the procedure from Brennan and co-workers does not result in a separation of inhibitors. Thus the presence of an inhibitor in a mixture could be verified but no direct identification was possible. On the other hand the enzymes can be regenerated and applied several times for further experiments.

The investigations reported clearly show versatile and flexible applications in the field of inhibitor screening using mass spectrometry. The most promising strategy with great potential for the future seems to be the one-step procedure furnishing information about affinity values and regulator identity. Use of MS seems to be very advantageous when dealing with diverse complex mixtures, although only few applications are yet routine. Most applications must still be validated by application under real conditions (pharmaceutical industry, white biotechnology and others).

Detection of endogenous substrates

Compared with the inhibition studies presented in the sections above, a reciprocal approach is the detection of

endogenous substrates for a given enzyme in a complex mixture (Table 1) but studies and results are rare. However, Schlüter and co-workers presented a mass spectrometry-assisted protease substrate screening (MAPS) procedure enabling screening for unknown substrates [95]. Figure 6 shows the basic principle of the MAPS system.

In this MAPS procedure, initially a protein mixture which possibly contains natural protease substrates was immobilized. After incubating this mixture with a protease of interest, the released peptides were analysed by MALDI–TOF–TOF and identified by database matching. The proof of principle could be demonstrated by incubating immobilized human plasma (i.e. a crude protein mixture serving as source of potential substrates) with thrombin. Fibrinogen was proved to serve as a substrate for thrombin by detecting correlated fibrinopeptides.

Another strategy used to assign endogenous substrates to enzymes is comparison of wild type enzyme activity with that from enzyme-inactivated organisms, as described by Saghatelian et al. [96]. They discovered several brain lipids which seemed to be regulated by fatty acid amide hydrolase (FAAH) in vivo by analysing the metabolomes of wild type and FAAH knocked out mice. A drawback of this method is the use of genetically modified animals which may prevent this from becoming a routine method in laboratory analysis.

Very recently, a possibly more applicable approach was described by Tang and co-workers [97]. The authors screened human liver extracts on endogenous substrates for different CYP isoforms and identified seven fatty acids as substrates. The basic feature of the experimental procedure was incubation of the tissue extract in presence of an $^{18}O_2/^{16}O_2$ mixture resulting in isotope-labelled products and thus in monoisotopic–mixed-isotopic doublets. Those doublets were then analysed by use of a special software tool enabling detection of peaks with a particular isotope ratio. The general procedure is a promising strategy for detection of so far unknown substrates of CYP enzymes. The application of isotope labelling is also of increasing importance in classical proteomic approaches for quantification strategies [49]. Thus, the more published applications and free software tools are available, the more scientists will apply this technique. New developments in mass spectrometric detection will accelerate progress even more.

In conclusion the area of mass spectrometric screening for endogenous substrates is still a rather unexploited field, but will gain significantly more interest and importance in the future.

Identification of enzyme activity in complex mixtures

So far, several approaches have been described for detection of enzyme activity in different crude samples,

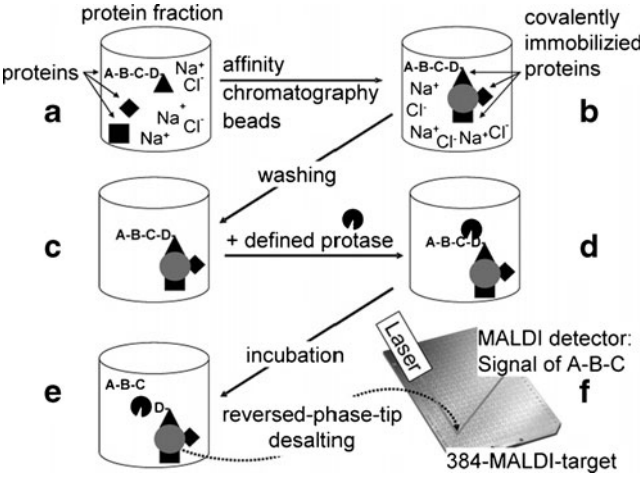

Fig. 6 Principle of the MAPS system. Proteins from any protein fraction (**a**) are covalently immobilized to cyanogen bromide-activated Sepharose beads (**a→b**). The immobilized proteins (**b**) are washed several times with pure water to remove any molecules (**b→c**), which are not immobilized (**f**). A defined protease is added to the mixture of the immobilized proteins and pure water (**c→d**). After defined incubation times (**d→e**), an aliquot of the reaction mixture is desalted by use of reversed-phase material packed in tips and eluted on to a MALDI target (**e→f**). The reaction products are analysed by MALDI mass spectrometry (**f**). The target substrate is present, if a signal of the cleaved protein fragment (here A-B-C) appears in the mass spectrum. Reprinted with permission from Ref. [95], Analytical Chemistry 79 (3):1251–1255, Copyright 2007, American Chemical Society

for example cell lysates, tissue homogenates and others (an overview is given in Table 2).

These approaches may be divided on the basis of their main objectives. One objective is determination of novel catalytic activity or substrate specificity in crude matrices. In screening of new born babies the main objective is to distinguish enzyme activity in healthy individuals from that in those affected by enzyme dysfunction. These two objectives will be discussed in the following sections.

Determination of novel catalytic activity or substrate specificity

Screening for novel enzymes is a challenging task in the scientific area of functional proteomics. Efforts in genome sequencing revealed a wealth of genes which encode for proteins of unknown function. Unravelling the catalytic activity of those proteins will contribute to improved understanding of metabolic pathways and establish further possibilities for the development of new drugs.

Mass spectrometry-assisted enzyme screening (MES)

Schlüter and co-workers identified the enzyme activity of orphan proteins contained in complex protein fractions

Table 2 Reaction with orphan proteins—identification of enzymatic activity

Identification of		Source of putative enzymes	Target enzymatic activity	Key features of the method	Main results	Ref.
(3a) Catalytic activity	MES	Porcine kidney extract	Phosphatase, glutathione reductase, kinase	Immobilized protein mixture Identification of reaction products by MALDI–MS	Activity of six different enzymes was detected	[120]
			Protease	Immobilized protein mixture Identification of reaction products by MALDI–MS	Diverse proteolytic activity was detected	[121]
	MuSub	Bacteria	Aminopeptidase	Immobilized bacteria incubated with substrate mixture	Bacteria species were differentiated by means of their aminopeptidase profile	[122]
			Glycosidases	Bacteria incubated with substrate mixture	Different glycosidase activity was detected in different bacteria strains	[123]
		Cell homogenates	β-Secretase	Immobilized substrates Analysis of released peptide fragments by MALDI–TOFMS	β-Secretase like activity was detected in two cell lines	[124]
		Snake venom	Proteases	Incubation of five different substrates with snake venom Analysis of the reaction mixture by FIA–ESI–MS	Different proteolytic patterns were detected in fractions of snake venom	[125]
		Snake venom and amoeba supernatant	Proteases	Incubation of up to eight different substrates with mixtures Analysis of the reaction mixture by FIA–ESI–MS	Both mixtures had activity toward one substrate	[126]
		Snake venom	Phospholipase A2 (PLA2)	Incubation of snake venom with glycerophosphatidycholine vesicles Analysis of the reaction mixture by ESI–MS	PLA2 activity was detected	[127]
		E. coli proteins	Uncharacterized	Incubation of yeast extract with proteins from *E. coli* Analysis of the reaction mixture by CE–ESI–MS	Phosphotransferase and phosphatase activity was detected	[128]
(3b) Disease-related altered enzyme activity	CL	Skin fibroblast homogenates	β-Galactosidase and *N*-acetyl-α-D-glucosaminidase	Biotin-conjugated substrates AC–ESI–MS	β-Galactosidase and *N*-acetyl-α-D-glucosaminidase-specific activity was detected; differences between healthy and enzyme deficiency-affected individuals were revealed	[129]
			Heparin-modifying enzymes	Biotin-conjugated substrates AC–ESI–MS	Enzymatic activity was detected for four heparin-modifying enzymes; differences between healthy and sanfilippo affected individuals were revealed	[130]
			Acid sphingomyelinase (ASM) and galactocerebroside β-galactosidase (GALC)	Biotin-conjugated substrates AC-ESI–MS	ASM and GALC were detected in cell homogenates; differences between healthy and enzyme deficiency-affected individuals could be revealed	[131]
			β-Galactosidase	Biotin-conjugated substrates Lab on valve/AC-ESI–MS	β-Galactosidase activity was detected in cell lysates	[132]

Table 2 (continued)

Identification of		Source of putative enzymes	Target enzymatic activity	Key features of the method	Main results	Ref.
			Phosphomannomutase (PMM) and phosphomannose isomerase (PMI)	Reaction was coupled to a transketolase reaction Biotin-conjugated substrates AC–ESI–MS	Differences in PMM and PMI activity between healthy individuals and CDG-affected persons was detected	[133]
	DBS	Dried blood spots	Galactocerebroside β-galactosidase (GALC)	Incubation of rehydrated dried blood spots with GALC substrate Analysis of reaction mixture by ESI–MS–MS	Differences between healthy individuals and Krabbe patients were detected	[134]
			N-acetylgalactosamine-6-sulfate sulfatase (GALNS)	Incubation of rehydrated dried blood spots with a novel \GALNS substrate Analysis of reaction mixture by ESI–MS–MS	The assay has the potential to be adopted for early diagnosis of Morquio A syndrome	[135]
			N-acetylgalactosamine-4-sulfatase	Incubation of rehydrated dried blood spots with *N*-acetylgalactosamine-4-sulfatase substrate Analysis of reaction mixture by ESI–MS–MS	The assay unambiguously distinguishes healthy individuals from mucopolysaccharidosis VI affected ones	[136]
			α-L-Iduronidase (IDUA)	Incubation of rehydrated dried blood spots with IDUA substrate Analysis of reaction mixture by ESI–MS–MS	Different IDUA activity among patients, carriers and unaffected newborns was detected	[137]
			Five lysosomal enzymes	Incubation of rehydrated dried blood spots with a cassette of substrates Analysis of reaction mixture by ESI–MS–MS	For five diseases the affected individuals and carriers were detected	[138]
			Diverse			[139]
		Serum samples	Exopeptidase	Incubation of serum samples with peptide substrates Semi automated MALDI–TOF analysis	Differences between cancer patients and healthy individuals were detected	[140]
			Proteases	Use of exogenous reporter peptides Analysis of fragments by MALDI–TOF	Disease-related proteases generated a characteristic pattern of fragments	[141, 142]

MES, mass spectrometry-assisted enzyme screening; MuSub, use of multiple substrates; CL, use of cell lysates; DBS, use of dried blood spots

[120]. They developed the so called mass spectrometry-assisted enzyme-screening (MES) system, enabling the detection of enzymes with defined substrate specificity in crude mixtures. In a first study, a protein extract from porcine kidneys was prepared and immobilized on sepharose beads. The crude extract contained several thousand proteins (as had been demonstrated by gel electrophoresis). These immobilized proteins were then incubated with different probes correlated with different enzyme activity (e.g. CoASSG for detection of phosphatase and glutathione reductase activity or the peptide kemptide for detection of kinase activity). Subsequent analysis of the reaction products by MALDI–MS revealed the activity of 5′-nucleotidase, phosphatase, kinase, glutathione reductase, renin, and angiotensin converting enzyme.

In a similar approach an immobilized extract from renal tissue was incubated with a mixture of protease substrates, whereupon diverse proteolytic activity was detected [121]. In the same work, the effects of inhibitors were also identified. This methodology thus seems to be applicable to the determination of unidentified enzyme activity and the effect of inhibitors in crude extracts.

Use of multiple substrates Another topic was pursued by Basile et al. [122] whose objective was to differentiate species of bacteria by means of their aminopeptidase profile. The different bacteria were immobilized on a filter and incubated with a mixture of substrates each producing a tag of unique molecular weight. Analysis of the four tags after incubation resulted in a specific aminopeptidase profile for each bacterium as a distinguishing feature. In a related approach Yu et al. [123] analysed the glycosidase profile of different strains of bacteria and detected distinct differences. The method seems to be expandable to other enzyme–substrate combinations but is not suitable for screening complex mixtures of bacteria.

In a reverse setup, not the enzyme mixture but the substrate (e.g. proteins) was immobilized on ceramic beads. The assay was used to screen for site-specific protease activity. The immobilized proteins were initially incubated with different cell homogenates. Subsequent to incubation, the beads were washed to remove the matrix from the protein. Additional digestion with endoproteinase Lys-C liberates a defined set of peptides. The released peptide hydrolysates were analysed by MALDI-TOF and β-secretase-like activity could be proved in the cell lines [124]. Moreover cathepsin D could be identified as the enzyme responsible for the site specific action in the two cell lines.

Also, in case of screening for enzyme activity, proteolytic enzymes have been most intensively studied, as has been described above for inhibitor screening. Besides the experiments already mentioned, different multiplexing approaches have been described. Based on an ESI–MS multi-substrate assay, the group of Karst and co-workers identified proteolytic activity in two complex samples, i.e. snake venom and amoeba supernatant [125, 126]. The methodology made use of different commercially available protease substrates which originally had been developed for spectrophotometric protease activity assays. These substrates have the advantageous feature that the m/z ratios of the substrates and the respective products do not overlap, fulfilling a prerequisite for mass spectrometric detection of multiplexing assays. The principle setup encompasses incubation of up to eight different substrates with the mixture of interest (which possibly has proteolytic activity), sampling of aliquots and—after quenching the reaction—analysing the samples by FIA–ESI–MS. The different mass spectra which were obtained with known proteases, snake venom, and amoeba supernatant are shown in Fig. 7.

Investigation of different fractions of snake venom revealed distinct differences in the proteolytic patterns of the fractions. When comparing snake venom with amoeba supernatant, the results indicated that both mixtures had high activity towards one specific substrate but differed in terms of their residual proteolytic pattern. So the activity fingerprints obtained enabled assignment of distinct proteolytic activity to a crude mixture.

The same group applied a modified setup in which snake venom was screened for phospholipase A2 (PLA2) activity [127]. The venom was incubated with glycerophosphatidylcholine vesicles and the resulting products again revealed distinct differences between the fractions. So this approach seems to be applicable to screen for multiple enzyme activity in complex biological samples and should be adaptable to a wide range of substrates and enzymes.

Detection of disease-related altered enzyme activity

The objective of several experiments described so far was detection of unknown enzyme activity in complex biological samples. The following section will discuss some widespread methods related to practice. They were designed to monitor and quantify enzyme activity in cell lysates or dried blood spots (DBS). Such screening methods are used in different biomedical applications to detect enzyme dysfunction in diverse pathological disorders.

Use of cell lysates In 1999 the group of Gelb and Turecek described a new method for the investigation of enzyme activity in cell homogenates [129]. This technique, called AC–ESI–MS, is based on two key features, i.e. use of affinity capture (AC) for purification and ESI–MS for detection. First, a substrate for the enzyme of interest is attached via a linker to a molecular handle. The reaction of the enzyme with this modified substrate leads to a change

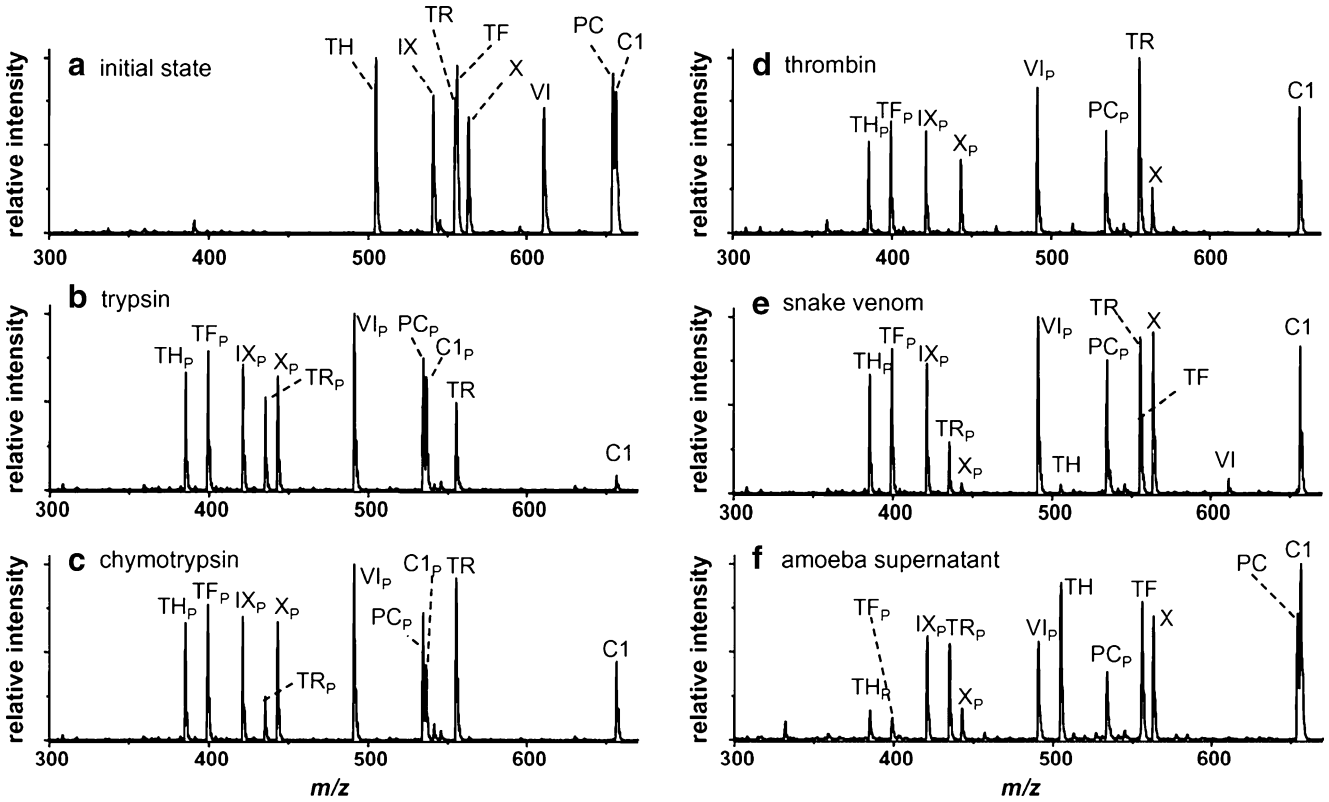

Fig. 7 Full-scan spectra obtained from FIA–ESI–MS multi-substrate assays. The conversion of a mixture of eight peptides (TH, IX, TR, TF, X, VI, PC, and C1) to their products (indicated by *p*) is monitored by ESI–MS. Spectra of the initial state (**a**) and after a 200 min conversion by trypsin (**b**, 100 UmL^{-1}), chymotrypsin (**c**, 100 UmL^{-1}), thrombin (**d**, 100 UmL^{-1}), snake venom (**e**, 0.2 mg protein mL^{-1}) and amoeba supernatant >3 kDa (**f**) fractions are shown. Reprinted from Ref. [126], Journal of Chromatography A 1216(20):4407–4415, 2009 with permission from Elsevier

in molecular mass and thus can be detected by ESI–MS. Linker and handle are designed to:

1. facilitate ionization;
2. prevent reaction with enzymes other than the one of interest; and
3. to ease product purification from the complex matrix.

By means of AC–ESI–MS in the years that followed several examples of enzyme dysfunction were analysed, e.g. regarding heparin-modifying enzymes [130] or lysosomal enzymes, for example acid sphingomyelinase [131]. Later, the method was enhanced by use of a lab-on valve apparatus to enable automated sample handling [132]. The options of this method were also expanded using a coupled assay. In such a coupled setup it was even possible to differentiate between isomeric (i.e. of equal mass) substrates and products by utilizing a second enzymatic reaction that cleaved the primary reaction products so that distinguishable products were obtained [133]. The authors could detect differences in phoshomannomutase and phosphomannose isomerase activity between healthy individuals and CGD (congenital disorder of glycosylation)-affected persons using this procedure. As is shown in Fig. 8, the different types of CGD result

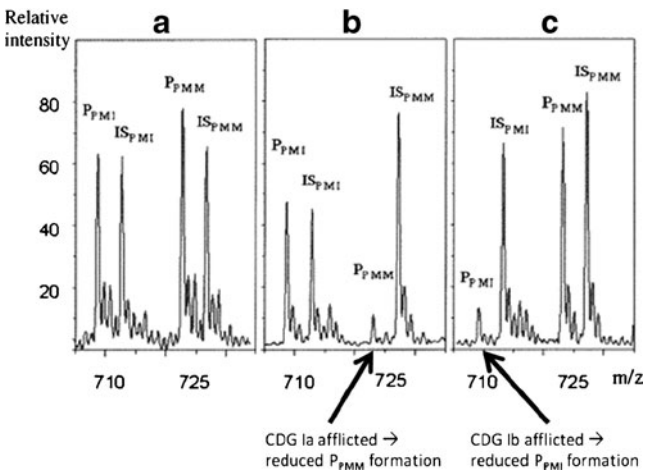

Fig. 8 ESI mass spectra of the PMI and PMM2 product conjugates and internal standards from assays of skin fibroblasts: **a**, healthy control; **b**, a CDG-Ia-afflicted patient; **c**, a CDG-Ib-afflicted patient. Adapted and reprinted with permission from Ref. [133], Analytical Chemistry 75(1):42–48, Copyright 2003, American Chemical Society

in different profiles of the respective products of PMM and PMI. A drawback of the methods described so far is the application of homogenates of cultured human fibroblasts which requires skin biopsies and cell-culture equipment.

Use of dried blood spots (DBS) A less invasive and complex approach is the application of dried blood spots (DBS), which has already become routine clinical practice. DBS are used in diverse medicinal assays, as has been reviewed by Edelbroek et al. [139]. Different assays have been described that enable screening of DBS for enzyme dysfunction; most of the assays have been reported by the group of Gelb and Turecek. The method is based on incubation of rehydrated DBS with substrates of the targeted enzyme and subsequent analysis of the products by ESI–MS. In this way DBS were investigated for several disorders, for example Krabbe disease, mucopolysaccharidose, and others. For all disorders, differences between healthy individuals and affected persons (and in some cases carriers) were detected [134, 137, 138]. In recent years the method has been expanded to enable multiplexing assay schemes and has thus become a versatile application for screening for disease-related enzyme dysfunction [138]. Instead of DBS, serum samples also may be used for investigation of disease-related enzymes. Most of these investigations have been conducted on disease-related proteases. Those proteases lead to a characteristic pattern of fragments of endogenous proteins and thus the analysis of such proteolytic fragments may serve as diagnostic tool, e.g. for cardiovascular risk, nutritional status, or detection of cancer. In cancer patients, for instance, exoprotease activity in serum has been identified and compared with that of healthy controls. Distinct differences could be detected and this information may serve for diagnostic or prognostic purposes [140]. However, the applicability of this method in most cases is limited to proteins or protein fragments of high molar abundance [143]. The group of Findeisen and colleagues recently described the use of exogenous reporter peptides for MS-based protease profiling to overcome this disadvantage [141, 142]. The authors spiked serum with defined exogenous peptides and monitored the modification of these peptides by endogenous proteases by means of MALDI–TOF. This so called reporter peptide spiking led to a distinct improvement in classification accuracy, i.e. the disease specific classification could be increased from 78% (unspiked samples) to 87% (spiked samples).

Further approaches However, all the methods described so far require knowledge about the enzyme of interest to enable choice of suitable substrates. A real unbiased attempt without previous knowledge, either about the enzymes or about possible substrates was carried out by Saito and co-workers [128]. They incubated a complex mixture of metabolites (i.e. yeast extract) with uncharacterized proteins from *E. coli*, separated the resulting reaction mixture by capillary electrophoresis, and analysed the products by ESI–MS. The observed changes in substrate and product levels in the reaction mixture were compared with an appropriate control. In this manner two proteins were proved to have phosphotransferase and phosphatase activity. By this innovative methodological approach the discovery of novel enzymatic activity should be possible.

We conclude that there has been a significant increase in research strategies for investigation of enzymatic behaviour and regulation. However, most applications to date deal with proteases and therefore the development of further enzymatic systems is still to be exploited. Additionally, most systems must be validated to enable their routine application. Nevertheless, the concepts presented are very challenging and innovative and furnish comprehensive information when used with MS detection.

Finally, this type of analysis depends on the data processing with bioinformatic and statistical tools. Both are in use by the community and several software development projects have already been started. Thus in forthcoming years it seems as if it might be possible to apply this technique routinely.

References

1. http://www.genomicglossaries.com/content/omes.asp (01.04.2009)
2. http://omics.org/index.php/Alphabetically_ordered_list_of_omes_and_omics (01.05.2010)
3. Lockhart DJ, Winzeler EA (2000) Genomics, gene expression and DNA arrays. Nature 405(6788):827–836
4. Albertson DG, Pinkel D (2003) Genomic microarrays in human genetic disease and cancer. Hum Mol Genet 12:R145–R152
5. Bartel DP (2004) MicroRNAs: Genomics, biogenesis, mechanism, and function. Cell 116(2):281–297
6. Storck T, von Brevern MC, Behrens CK, Scheel J, Bach A (2002) Transcriptomics in predictive toxicology. Curr Opin Drug Di De 5(1):90–97
7. Hegde PS, White IR, Debouck C (2003) Interplay of transcriptomics and proteomics. Curr Opin Biotech 14(6):647–651
8. Mann M, Hendrickson RC, Pandey A (2001) Analysis of proteins and proteomes by mass spectrometry. Annu Rev Biochem 70:437–473
9. Zhu H, Bilgin M, Snyder M (2003) Proteomics. Annu Rev Biochem 72:783–812
10. Fiehn O (2001) Combining genomics, metabolome analysis, and biochemical modelling to understand metabolic networks. Comp Funct Genom 2(3):155–168
11. Papin JA, Price ND, Wiback SJ, Fell DA, Palsson BO (2003) Metabolic pathways in the post-genome era. Trends Biochem Sci 28(5):250–258
12. Oldiges M, Lutz S, Pflug S, Schroer K, Stein N, Wiendahl C (2007) Metabolomics: current state and evolving methodologies and tools. Appl Microbiol Biot 76(3):495–511

13. Tyers M, Mann M (2003) From genomics to proteomics. Nature 422(6928):193–197
14. Al-Shahrour F, Minguez P, Vaquerizas JM, Conde L, Dopazo J (2005) BABELOMICS: a suite of web tools for functional annotation and analysis of groups of genes in high-throughput experiments. Nucleic Acids Res 33:W460–W464
15. Jimenez MS, Gomez MT, Rodriguez L, Martinez L, Castillo JR (2009) Some pitfalls in PAGE–LA–ICP–MS for quantitative elemental speciation of dissolved organic matter and metalomics. Anal Bioanal Chem 393(2):699–707
16. Shi W, Chance MR (2008) Metallomics and metalloproteomics. Cell Mol Life Sci 65(19):3040–3048
17. Muller M, Kersten S (2003) Nutrigenomics: goals and strategies. Nat Rev Genet 4(4):315–322
18. Corthesy-Theulaz I, den Dunnen JT, Ferre P, Geurts JMW, Muller M, van Belzen N, van Ommen B (2005) Nutrigenomics: The impact of biomics technology on nutrition research. Ann Nutr Metab 49(6):355–365
19. Rosell R, Monzo M, O'Brate A, Taron M (2002) Translational oncogenomics: toward rational therapeutic decision-making. Curr Opin Oncol 14(2):171–179
20. Strausberg RL, Simpson AJG, Old LJ, Riggins GJ (2004) Oncogenomics and the development of new cancer therapies. Nature 429(6990):469–474
21. Monteoliva L, Albar JP (2004) Differential proteomics: an overview of gel and non-gel based approaches. Brief Funct Genomic Proteomic 3(3):220–239
22. Mavroudi S, Papadimitriou S, Kossida S, Likothanassis SD, Vlahou A (2007) Computational methods and algorithms for mass-spectrometry based differential proteomics. Curr Proteomics 4(4):223–234
23. Sali A, Glaeser R, Earnest T, Baumeister W (2003) From words to literature in structural proteomics. Nature 422(6928):216–225
24. Yokoyama S (2003) Protein expression systems for structural genomics and proteomics. Curr Opin Chem Biol 7(1):39–43
25. Naylor S, Kumar R (2003) Emerging role of mass spectrometry in structural and functional proteomics. Adv Protein Chem 65:217–248
26. Godovac-Zimmermann J, Brown LR (2001) Perspectives for mass spectrometry and functional proteomics. Mass Spectrom Rev 20(1):1–57
27. Yanagida M (2002) Functional proteomics; current achievements. J Chromatogr B 771(1–2):89–106
28. Graves PR, Haystead TAJ (2002) Molecular biologist's guide to proteomics. Microbiol Mol Biol Rev 66(1):39–63
29. Hunter TC, Andon NL, Koller A, Yates JR, Haynes PA (2002) The functional proteomics toolbox: methods and applications. J Chromatogr B 782(1–2):165–181
30. Hubbard MJ (2002) Functional proteomics: The goalposts are moving. Proteomics 2(9):1069–1078
31. Monti M, Orru S, Pagnozzi D, Pucci P (2005) Functional proteomics. Clin Chim Acta 357(2):140–150
32. Kocher T, Superti-Furga G (2007) Mass spectrometry-based functional proteomics: from molecular machines to protein networks. Nat Methods 4(10):807–815
33. Adam GC, Sorensen EJ, Cravatt BF (2002) Chemical strategies for functional proteomics. Mol Cell Proteomics 1(10):781–790
34. Hemelaar J, Galardy PJ, Borodovsky A, Kessler BA, Ploegh HL, Ovaa H (2004) Chemistry-based functional proteomics: Mechanism-based activity-profiling tools for ubiquitin and ubiquitin-like specific proteases. J Proteome Res 3(2):268–276
35. Speers AE, Cravatt BF (2004) Chemical strategies for activity-based proteomics. ChemBioChem 5(1):41–47
36. Schmidinger H, Hermetter A, Birner-Gruenberger R (2006) Activity-based proteomics: enzymatic activity profiling in complex proteomes. Amino Acids 30(4):333–350
37. Sadaghiani AM, Verhelst SHL, Bogyo M (2007) Tagging and detection strategies for activity-based proteomics. Curr Opin Chem Biol 11(1):20–28
38. Johnson SA, Hunter T (2005) Kinomics: methods for deciphering the kinome. Nat Methods 2(1):17–25
39. Lawrence DS (2001) Functional proteomics: large-scale analysis of protein kinase activity. Genome Biol 2 (2):reviews1007
40. Collura V, Boissy G (2007) From protein–protein complexes to interactomics. Subcell Biochem 43:135–183
41. Kiemer L, Cesareni G (2007) Comparative interactomics: comparing apples and pears? Trends Biotechnol 25(10):448–454
42. Bisswanger H (2007) Practical Enzymology. WILEY–VCH, Weinheim
43. Letzel T, Sahmel-Schneider E, Skriver K, Ohnuma T, Fukamizo T (2011) Chitinase-catalyzed hydrolysis of 4-nitrophenyl penta-N-acetyl-[beta]-chitopentaoside as determined by real-time ESIMS: The 4-nitrophenyl moiety of the substrate interacts with the enzyme binding site. Carbohyd Res 346(6):863–866
44. Letzel T (ed) (2011) Protein and Peptide Analysis by LC–MS: Experimental Strategies. Royal Society of Chemistry, Cambridge, UK. doi:10.1039/9781849733144
45. Anderson NL, Anderson NG (1998) Proteome and proteomics: new technologies, new concepts, and new words. Electrophoresis 19(11):1853–1861
46. Celis JE, Ostergaard M, Jensen NA, Gromova I, Rasmussen HH, Gromov P (1998) Human and mouse proteomic databases: novel resources in the protein universe. FEBS Lett 430 (1–2):64–72
47. Aebersold R, Mann M (2003) Mass spectrometry-based proteomics. Nature 422(6928):198–207
48. Cravatt BF, Simon GM, Yates Iii JR (2007) The biological impact of mass-spectrometry-based proteomics. Nature 450 (7172):991–1000
49. Bantscheff M, Schirle M, Sweetman G, Rick J, Kuster B (2007) Quantitative mass spectrometry in proteomics: a critical review. Anal Bioanal Chem 389(4):1017–1031
50. Reinders J, Sickmann A (2007) Modificomics: Posttranslational modifications beyond protein phosphorylation and glycosylation. Biomol Eng 24(2):169–177
51. Sharon M, Robinson CV (2007) The role of mass Spectrometry in structure elucidation of dynamic protein complexes. Annu Rev Biochem 76:167–193
52. Benesch JL, Robinson CV (2006) Mass spectrometry of macromolecular assemblies: preservation and dissociation. Curr Opin Struc Biol 16(2):245–251
53. Letzel T (2008) Real-time mass spectrometry in enzymology. Anal Bioanal Chem 390(1):257–261
54. Greis KD (2007) Mass spectrometry for enzyme assays and inhibitor screening: An emerging application in pharmaceutical research. Mass Spectrom Rev 26(3):324–339
55. de Boer AR, Lingeman H, Niessen WMA, Irth H (2007) Mass spectrometry-based biochemical assays for enzyme inhibitor screening. Trends Anal Chem 26(9):867–883
56. Geoghegan KF, Kelly MA (2005) Biochemical applications of mass spectrometry in pharmaceutical drug discovery. Mass Spectrom Rev 24(3):347–366
57. Liesener A, Karst U (2005) Monitoring enzymatic conversions by mass spectrometry: a critical review. Anal Bioanal Chem 382 (7):1451–1464
58. Schluter H, Hildebrand D, Gallin C, Schulz A, Thiemann J, Trusch M (2008) Mass spectrometry for monitoring protease reactions. Anal Bioanal Chem 392(5):783–792
59. Shi SY, Zhou HH, Zhang YP, Jiang XY, Chen XQ, Huang KL (2009) Coupling HPLC to on-line, post-column (bio)chemical assays for high-resolution screening of bioactive compounds from complex mixtures. Trends Anal Chem 28(7):865–877

60. van Beek TA, Tetala KKR, Koleva II, Dapkevicius A, Exarchou V, Jeurissen SMF, Claassen FW, van der Klift EJC (2009) Recent developments in the rapid analysis of plants and tracking their bioactive constituents. Phytochem Rev 8(2):387–399
61. Zechel DL, Konermann L, Withers SG, Douglas DJ (1998) Pre-steady state kinetic analysis of an enzymatic reaction monitored by time-resolved electrospray ionization mass spectrometry. Biochemistry 37(21):7664–7669
62. Ge X, Sirich TL, Beyer MK, Desaire H, Leary JA (2001) A strategy for the determination of enzyme kinetics using electrospray ionization with an ion trap mass spectrometer. Anal Chem 73(21):5078–5082
63. Wilson DJ, Konermann L (2004) Mechanistic studies on enzymatic reactions by electrospray ionization MS using a capillary mixer with adjustable reaction chamber volume for time-resolved measurements. Anal Chem 76(9):2537–2543
64. Ganem B, Li YT, Henion JD (1991) Observation of Noncovalent Enzyme Substrate and Enzyme Product Complexes by Ion-Spray Mass-Spectrometry. J Am Chem Soc 113(20):7818–7819
65. Clark SM, Konermann L (2004) Screening for noncovalent ligand–receptor interactions by electrospray ionization mass spectrometry-based diffusion measurements. Anal Chem 76 (5):1257–1263
66. Dennhart N, Letzel T (2006) Mass spectrometric real-time monitoring of enzymatic glycosidic hydrolysis, enzymatic inhibition and enzyme complexes. Anal Bioanal Chem 386 (3):689–698
67. Dennhart N, Fukamizo T, Brzezinski R, Lacombe-Harvey ME, Letzel T (2008) Oligosaccharide hydrolysis by chitosanase enzymes monitored by real-time electrospray ionization-mass spectrometry. J Biotechnol 134(3–4):253–260
68. Dennhart N, Weigang LMM, Fujiwara M, Fukamizo T, Skriver K, Letzel T (2009) 26 kDa endochitinase from barley seeds: Real-time monitoring of the enzymatic reaction and substrate binding experiments using electrospray ionization mass spectrometry. J Biotechnol 143(4):274–283
69. Taira T, Fujiwara M, Dennhart N, Hayashi H, Onaga S, Ohnuma T, Letzel T, Sakuda S, Fukamizo T (2010) Transglycosylation reaction catalyzed by a class V chitinase from cycad, Cycas revoluta: A study involving site-directed mutagenesis, HPLC, and real-time ESI–MS. Biochim Biophys Acta 1804(4):668–675
70. Scheerle RK, Graßmann J, Letzel T (2011) Enzymatic conversion continuously monitored with a robotic nanoESI–MS tool: experimental status. Anal Meth 3(4):822–830
71. Imoto T, Johnson L, North A, Phillips D, Rupley J (eds) (1972) Vertebrate Lysozymes, vol 7. The Enzymes. Academic Press, NY
72. Lee ED, Muck W, Henion JD, Covey TR (1989) Real-Time Reaction Monitoring by Continuous-Introduction Ion-Spray Tandem Mass-Spectrometry. J Am Chem Soc 111(13):4600–4604
73. Northrop DB, Simpson FB (1997) Beyond enzyme kinetics: direct determination of mechanisms by stopped-flow mass spectrometry. Bioorg Med Chem 5(4):641–644
74. Li ZL, Song F, Zhuang ZH, Dunaway-Mariano D, Anderson KS (2009) Monitoring enzyme catalysis in the multimeric state: Direct observation of Arthrobacter 4-hydroxybenzoyl-coenzyme A thioesterase catalytic complexes using time-resolved electrospray ionization mass spectrometry. Anal Biochem 394(2):209–216
75. Tagore R, Thomas HR, Homan EA, Munawar A, Saghatelian A (2008) A Global Metabolite Profiling Approach to Identify Protein–Metabolite Interactions. J Am Chem Soc 130 (43):14111–+
76. Hannewald P, Maunit B, Muller JF (2008) Screening of DHFR-binding drugs by MALDI–TOFMS. Anal Bioanal Chem 392(7–8):1335–1344
77. Beverly MB, West P, Julian RK (2002) Evaluation of a micro volume pulsed ultrafiltration cell for screening ligands in non-covalent complexes. Comb Chem High Throughput Screen 5 (1):65–73
78. Nikolic D, Habibi-Goudarzi S, Corley DG, Gafner S, Pezzuto JM, van Breemen RB (2000) Evaluation of cyclooxygenase-2 inhibitors using pulsed ultrafiltration mass spectrometry. Anal Chem 72(16):3853–3859
79. Vu H, Quinn RJ (2008) Direct screening of natural product extracts using mass spectrometry. J Biomol Screen 13(4):265–275
80. Calleri E, Temporini C, Caccialanza G, Massolini G (2009) Target-Based Drug Discovery: the Emerging Success of Frontal Affinity Chromatography Coupled to Mass Spectrometry. ChemMedChem 4(6):905–916
81. Unger M, Frank A (2004) Simultaneous determination of the inhibitory potency of herbal extracts on the activity of six major cytochrome P450 enzymes using liquid chromatography mass spectrometry and automated online extraction. Rapid Commun Mass Spectrom 18(19):2273–2281
82. Frank A, Unger M (2006) Analysis of frankincense from various Boswellia species with inhibitory activity on human drug metabolising cytochrome P450 enzymes using liquid chromatography mass spectrometry after automated on-line extraction. J Chromatogr A 1112(1–2):255–262
83. Kim H, Kim KB, Ku HY, Park SJ, Choi H, Moon JK, Park BS, Kim JH, Yea SS, Lee CH, Lee HS, Shin JG, Liu KH (2008) Identification and characterization of potent CYP2B6 inhibitors in woohwangcheongsimwon suspension, an herbal preparation used in the treatment and prevention of apoplexy in Korea and China. Drug Metab Dispos 36(6):1010–1015
84. Li HL, Song FR, Xing JP, Tsao R, Liu ZQ, Liu SY (2009) Screening and Structural Characterization of alpha-Glucosidase Inhibitors from Hawthorn Leaf Flavonoids Extract by Ultrafiltration LC–DAD–MSn and SORI–CID FTICR MS. J Am Soc Mass Spectrom 20(8):1496–1503
85. Xu Z, Yao SJ, Wei YL, Zhou J, Zhang L, Wang CH, Guo YL (2008) Monitoring Enzyme Reaction and Screening of Inhibitors of Acetylcholinesterase by Quantitative Matrix-Assisted Laser Desorption/Ionization Fourier Transform Mass Spectrometry. J Am Soc Mass Spectrom 19(12):1849–1855
86. Hu FL, Zhang HY, Lin HQ, Deng CH, Zhang XM (2008) Enzyme inhibitor screening by electrospray mass spectrometry with immobilized enzyme on magnetic silica microspheres. J Am Soc Mass Spectrom 19(6):865–873
87. Halim VA, Muck A, Hartl M, Ibanez AJ, Giri A, Erfurth F, Baldwin IT, Svatos A (2009) A dual fluorescent/MALDI chip platform for analyzing enzymatic activity and for protein profiling. Proteomics 9(1):171–181
88. Borch J, Roepstorff P (2004) Screening for enzyme inhibitors by surface plasmon resonance combined with mass spectrometry. Anal Chem 76(18):5243–5248
89. de Boer AR, Letzel T, van Elswijk DA, Lingeman H, Niessen WMA, Irth H (2004) On-line coupling of high-performance liquid chromatography to a continuous-flow enzyme assay based on electrospray ionization mass spectrometry. Anal Chem 76 (11):3155–3161
90. de Boer AR, Alcaide-Hidalgo JM, Krabbe JG, Kolkman J, Boas CNV, Niessen WMA, Lingeman H, Irth H (2005) High-temperature liquid chromatography coupled on-line to a continuous-flow biochemical screening assay with electrospray ionization mass spectrometric detection. Anal Chem 77(24):7894–7900
91. de Boer AR, Bruyneel B, Krabbe JG, Lingeman H, Niessen WMA, Irth H (2005) A microfluidic-based enzymatic assay for bioactivity screening combined with capillary liquid chromatography and mass spectrometry. Lab Chip 5(11):1286–1292
92. de Jong CF, Derks RJE, Bruyneel B, Niessen W, Irth H (2006) High-performance liquid chromatography–mass spectrometry-

based acetylcholinesterase assay for the screening of inhibitors in natural extracts. J Chromatogr A 1112(1–2):303–310
93. Hodgson RJ, Besanger TR, Brook MA, Brennan JD (2005) Inhibitor screening using immobilized enzyme reactor chromatography/mass spectrometry. Anal Chem 77(23):7512–7519
94. Partserniak I, Werstuck G, Capretta A, Brennan JD (2008) An ESI–MS/MS method for screening of small-molecule mixtures against glycogen synthase kinase-3 beta (GSK-3 beta). ChemBioChem 9(7):1065–1073
95. Schluter H, Rykl J, Thiemann J, Kurzawski S, Gobom J, Tepel M, Zidek W, Linscheid M (2007) Mass spectrometry-assisted protease substrate screening. Anal Chem 79(3):1251–1255
96. Saghatelian A, Trauger SA, Want EJ, Hawkins EG, Siuzdak G, Cravatt BF (2004) Assignment of endogenous substrates to enzymes by global metabolite profiling. Biochemistry 43 (45):14332–14339
97. Tang ZM, Martin MV, Guengerich FP (2009) Elucidation of Functions of Human Cytochrome P450 Enzymes: Identification of Endogenous Substrates in Tissue Extracts Using Metabolomic and Isotopic Labeling Approaches. Anal Chem 81(8):3071–3078
98. Jonker N, Kool J, Irth H, Niessen WM (2010) Recent developments in protein–ligand affinity mass spectrometry. Anal Bioanal Chem. doi:10.1007/s00216-010-4350-z
99. Johnson BM, Nikolic D, van Breemen RB (2002) Applications of pulsed ultrafiltration-mass spectrometry. Mass Spectrom Rev 21(2):76–86
100. Shin YG, van Breemen RB (2001) Analysis and screening of combinatorial libraries using mass spectrometry. Biopharm Drug Dispos 22(7–8):353–372
101. Wanner K, Hoefner G (2007) Mass spectrometry in medicinal chemistry. Wiley–VCH, Weinheim
102. Jorgensen TJD, Roepstorff P, Heck AJR (1998) Direct determination of solution binding constants for noncovalent complexes between bacterial cell wall peptide analogues and vancomycin group antibiotics by electrospray ionization mass spectrometry. Anal Chem 70(20):4427–4432
103. Schriemer DC, Bundle DR, Li L, Hindsgaul O (1998) Microscale frontal affinity chromatography with mass spectrometric detection: A new method for the screening of compound libraries. Angew Chem-Int Edit 37(24):3383–3387
104. Zhang B, Palcic MM, Schriemer DC, Alvarez-Manilla G, Pierce M, Hindsgaul O (2001) Frontal affinity chromatography coupled to mass spectrometry for screening mixtures of enzyme inhibitors. Anal Biochem 299(2):173–182
105. Deng GJ, Sanyal G (2006) Applications of mass spectrometry in early stages of target based drug discovery. J Pharm Biomed Anal 40(3):528–538
106. Rabe KS, Gandubert VJ, Spengler M, Erkelenz M, Niemeyer CM (2008) Engineering and assaying of cytochrome P450 biocatalysts. Anal Bioanal Chem 392(6):1059–1073
107. Lahoz A, Donato MT, Castell JV, Gomez-Lechon MJ (2008) Strategies to in vitro assessment of major human CYP enzyme activities by using liquid chromatography tandem mass spectrometry. Curr Drug Metab 9(1):12–19
108. Walsky RL, Boldt SE (2008) In Vitro Cytochrome P450 Inhibition and Induction. Curr Drug Metab 9(9):928–939
109. Foti RS, Wienkers LC, Wahlstrom JL (2010) Application of Cytochrome P450 Drug Interaction Screening in Drug Discovery. Comb Chem High T Scr 13(2):145–158
110. Bassil N, Grossberg GT (2009) Novel Regimens and Delivery Systems in the Pharmacological Treatment of Alzheimer's Disease. CNS Drugs 23(4):293–307
111. Munoz-Torrero D (2008) Acetylcholinesterase Inhibitors as Disease-Modifying Therapies for Alzheimer's Disease. Curr Med Chem 15(24):2433–2455
112. Scatena R, Martorana GE, Bottoni P, Botta G, Pastore P, Giardina B (2007) An update on pharmacological approaches to neurodegenerative diseases. Expert Opin Investig Drugs 16(1):59–72
113. Houghton PJ, Howes MJ (2005) Natural products and derivatives affecting neurotransmission relevant to Alzheimer's and Parkinson's disease. Neurosignals 14(1–2):6–22. doi:10.1159/000085382
114. Dickinson L, Khoo S, Back D (2010) Pharmacokinetics and drug–drug interactions of antiretrovirals: An update. Antiviral Res 85(1):176–189
115. Steuber H, Hilgenfeld R (2010) Recent Advances in Targeting Viral Proteases for the Discovery of Novel Antivirals. Curr Top Med Chem 10(3):323–345
116. Wensing AMJ, van Maarseveen NM, Nijhuis M (2010) Fifteen years of HIV Protease Inhibitors: raising the barrier to resistance. Antiviral Res 85(1):59–74
117. Kool J, Giera M, Irth H, Niessen WM (2011) Advances in mass spectrometry-based post-column bioaffinity profiling of mixtures. Anal Bioanal Chem 399(8):2655–2668. doi:10.1007/s00216-010-4406-0
118. Besanger TR, Hodgson RJ, Green JRA, Brennan JD (2006) Immobilized enzyme reactor chromatography: Optimization of protein retention and enzyme activity in monolithic silica stationary phases. Anal Chim Acta 564(1):106–115. doi:10.1016/j.aca.2005.12.066
119. Lebert JM, Forsberg EM, Brennan JD (2008) Solid-phase assays for small molecule screening using sol–gel entrapped proteins. Biochem Cell Biol 86(2):100–110. doi:10.1139/o08-010
120. Jankowski J, Stephan N, Knobloch M, Fischer S, Schmaltz D, Zidek W, Schluter H (2001) Mass-spectrometry-linked screening of protein fractions for enzymatic activities - A tool for functional genomics. Anal Biochem 290(2):324–329
121. Schluter H, Jankowski J, Rykl J, Thiemann J, Belgardt S, Zidek W, Wittmann B, Pohl T (2003) Detection of protease activities with the mass-spectrometry-assisted enzyme-screening (MES) system. Anal Bioanal Chem 377(7–8):1102–1107
122. Basile F, Ferrer I, Furlong ET, Voorhees KJ (2002) Simultaneous multiple substrate tag detection with ESI–ion trap MS for in vivo bacterial enzyme activity profiling. Anal Chem 74(16):4290–4293
123. Yu Y, Mizanur RM, Pohl NL (2008) Glycosidase activity profiling for bacterial identification by a chemical proteomics approach. Biocatal Biotransfor 26(1–2):25–31. doi:10.1080/10242420701791151
124. Gruninger-Leitch F, Berndt P, Langen H, Nelboeck P, Dobeli H (2000) Identification of beta-secretase-like activity using a mass spectrometry-based assay system. Nat Biotechnol 18(1):66–70
125. Liesener A, Perchuc AM, Schoni R, Wilmer M, Karst U (2005) Screening for proteolytic activities in snake venom by means of a multiplexing electrospray ionization mass spectrometry assay scheme. Rapid Commun Mass Spectrom 19(20):2923–2928
126. Schebb NH, Vielhaber T, Jousset A, Karst U (2009) Development of a liquid chromatography-based screening methodology for proteolytic enzyme activity. J Chromatogr A 1216(20):4407–4415
127. Schebb NH, Falck D, Faber H, Hein EM, Karst U, Hayen H (2009) Fast method for monitoring phospholipase A(2) activity by liquid chromatography–electrospray ionization mass spectrometry. J Chromatogr A 1216(27):5249–5255
128. Saito N, Robert M, Kitamura S, Baran R, Soga T, Mori H, Nishioka T, Tomita M (2006) Metabolomics approach for enzyme discovery. J Proteome Res 5(8):1979–1987
129. Gerber SA, Scott CR, Turecek F, Gelb MH (1999) Analysis of rates of multiple enzymes in cell lysates by electrospray ionization mass spectrometry. J Am Chem Soc 121(5):1102–1103

130. Gerber SA, Scott CR, Turecek F, Gelb MH (2001) Direct profiling of multiple enzyme activities in human cell lysates by affinity chromatography/electrospray ionization mass spectrometry: Application to clinical enzymology. Anal Chem 73 (8):1651–1657
131. Zhou XF, Turecek F, Scott CR, Gelb MH (2001) Quantification of cellular acid sphingomyelinase and galactocerebroside beta-galactosidase activities by electrospray ionization mass spectrometry. Clin Chem 47(5):874–881
132. Ogata Y, Scampavia L, Ruzicka J, Scott CR, Gelb MH, Turecek F (2002) Automated affinity capture-release of biotin-containing conjugates using a lab-on-valve apparatus coupled to UV/visible and electrospray ionization mass Spectrometry. Anal Chem 74 (18):4702–4708
133. Li YJ, Ogata Y, Freeze HH, Scott CR, Turecek FE, Gelb MH (2003) Affinity capture and elution/electrospray ionization mass spectrometry assay of phosphomannomutase and phosphomannose isomerase for the multiplex analysis of congenital disorders of glycosylation types Ia and Ib. Anal Chem 75(1):42–48
134. Li YJ, Brockmann K, Turecek F, Scott CR, Gelb MH (2004) Tandem mass spectrometry for the direct assay of enzymes in dried blood spots: Application to newborn screening for Krabbe disease. Clin Chem 50(3):638–640
135. Khaliq T, Sadilek M, Scott CR, Turecek F, Gelb MH (2011) Tandem Mass Spectrometry for the Direct Assay of Lysosomal Enzymes in Dried Blood Spots: Application to Screening Newborns for Mucopolysaccharidosis IVA. Clin Chem 57(1):128–131
136. Duffey TA, Sadilek M, Scott CR, Turecek F, Gelb MH (2010) Tandem Mass Spectrometry for the Direct Assay of Lysosomal Enzymes in Dried Blood Spots: Application to Screening Newborns for Mucopolysaccharidosis VI (Maroteaux–Lamy Syndrome). Anal Chem 82(22):9587–9591
137. Wang D, Eadala L, Sadilek M, Chamoles NA, Turecek F, Scott CR, Gelb MH (2005) Tandem mass spectrometric analysis of dried blood spots for screening of mucopolysaccharidosis I in newborns. Clin Chem 51(5):898–900
138. Li YJ, Scott CR, Chamoles NA, Ghavami A, Pinto BM, Turecek F, Gelb MH (2004) Direct multiplex assay of lysosomal enzymes in dried blood spots for newborn screening. Clin Chem 50 (10):1785–1796
139. Edelbroek PM, van der Heijden J, Stolk LML (2009) Dried Blood Spot Methods in Therapeutic Drug Monitoring: Methods, Assays, and Pitfalls. Ther Drug Monit 31(3):327–336
140. Villanueva J, Nazarian A, Lawlor K, Yi SS, Robbins RJ, Temps P (2008) A sequence-specific exopeptidase activity test (SSEAT) for "Functional" biomarker discovery. Mol Cell Proteomics 7 (3):509–518
141. Findeisen P, Peccerella T, Post S, Wenz F, Neumaier M (2008) Spiking of serum specimens with exogenous reporter peptides for mass spectrometry based protease profiling as diagnostic tool. Rapid Commun Mass Spectrom 22(8):1223–1229
142. Findeisen P, Post S, Wenz F, Neumaier M (2007) Addition of exogenous reporter peptides to serum samples before mass spectrometry-based protease profiling provides advantages over profiling of endogenous peptides. Clin Chem 53:1864–1866
143. Hortin GL (2006) The MALDI–TOF mass spectrometric view of the plasma proteome and peptidome. Clin Chem 52(7):1223–1237

Appendix II

LC-MS for the Determination of the Enzymatic Activity of Proteins

Scheerle, R.K. and Grassmann, J.

In: Letzel, T., (Ed.), Protein and Peptide Analysis by LC-MS. 2011, Royal Society of Chemistry, Cambridge, 133-141

This book chapter presents an overview of LC-MS, real-time and nanoESI techniques for studying enzymatic reactions. Experimental guidelines are given for easy handling and working with enzymes. The manuscript was a collaborative work of both authors.

CHAPTER 10

LC-MS for the Determination of the Enzymatic Activity of Proteins

ROMY K. SCHEERLE AND JOHANNA GRAßMANN

Institute for Chemical-Technical Analysis and Chemical Food Technology, Center of Life and Food Sciences Weihenstephan, Technische Universität München, Weihenstephaner Steig 23, 85350 Freising, Germany

10.1 Introduction

Methods for studying enzymatic reactions are manifold, such as spectroscopic, electrochemical or radiometric assays. Spectroscopic and mainly photometric measurements are the most frequent employed methods in enzymatic analysis. This is due to the easy handling, moderate costs and the accuracy of the methods. However, these methods require labelling of the substrates, *e.g.* chromogenic or fluorogenic substrates or radioisotope labelled substances.[1] These labelled substrates may, however, affect the reaction rate and/or kinetics of the enzymatic reaction.[2] The use of natural substrates is therefore desirable and can be achieved by utilizing mass spectrometric (MS)-based enzymatic assays. Besides the advantage of the applicability of natural substrates, MS-based assays offer the possibility to observe not only the product of an enzymatic reaction but also the substrates and in some cases also the enzyme and enzyme complexes (for latter see also Chapter 11). Many applications have been described in recent years to follow enzymatic reactions by LC-MS. In most of these applications the enzymatic reaction is conducted in either a single reaction tube or a well plate.

RSC Chromatography Monographs No. 15
Protein and Peptide Analysis by LC-MS: Experimental Strategies
Edited by Thomas Letzel

Published by the Royal Society of Chemistry, www.rsc.org

After defined time points the reactions are quenched and the resulting aliquots are subjected to (LC-)MS analysis. This setup allows obtaining information about the concentration of substrate and product(s) at defined time points. A different approach is the real-time monitoring of enzymatic reactions with direct infusion of the assay mixture into the mass spectrometer using either a syringe pump or a robot system. Using this continuous flow measurement, a real-time kinetic of the enzymatic reaction can be obtained.[3]

The differences of these three setups as well as their advantages and disadvantages will be discussed in the present chapter. The enzymatic reaction of lysozyme with a hexasaccharide will serve as an example to illustrate several aspects of the various approaches.

10.2 Materials

10.2.1 The Example Assay

Hen egg white lysozyme (HEWL, muramidase) is a well-known protein that catalyses the hydrolysis of β-1,4-glycosidic linkages in certain Gram-positive bacterial cell walls and chitin.[4–6] Therefore the hexasaccharide hexa-*N*-acetylchitohexaose ($(GlcNAc)_6$) can be used as substrate. Lysozyme cleaves $(GlcNAc)_6$ into $(GlcNAc)_2$ and $(GlcNAc)_4$ as major products.[7] The assay conditions were adopted from Dennhart and Letzel.[8]

10.2.2 Chemicals

Ammonium acetate (NH_4Ac, M_r 77.08, $>98\%$) and acetic acid were purchased from Merck (Darmstadt, Germany); acetonitrile (M_r 41.05, $>99.9\%$) and hen egg white lysozyme (HEWL, 95%; M_r 14.3 kDa, 50 000 units/mg protein) were purchased from Sigma-Aldrich (Steinheim, Germany). Hexa-*N*-acetylchitohexaose ($(GlcNAc)_6$, M_r 1237.17, $\geq 95\%$) was obtained from Seikagaku Biobusiness (Tokyo, Japan). All buffers and solutions were prepared in LC-MS reagent water from J.T.Baker (Deveter, Holland).

10.2.3 Mass Spectrometer

- TripleQuadrupole LC/MS 6410 instrument, Agilent Technologies, Waldbronn, Germany
- MassHunter Workstation software, Qualitative Analysis, Agilent Technologies, Waldbronn, Germany

10.2.4 LC-MS Method

- Assay buffer: 10 mM NH_4Ac pH 5.2
- Substrate solution: 50 μM $(GlcNAc)_6$ in 10 mM NH_4Ac pH 5.2
- Enzyme solution: 10 μM lysozyme in 10 mM NH_4Ac pH 5.2
- Stopping reagent: 90% acetonitrile

- HPLC: 1200 Series, Agilent Technologies, Waldbronn, Germany
- HPLC solvents: 90% acetonitrile
- Column: LichroCART, 100 Diol, 5 μm, Merck, Darmstadt, Germany

10.2.5 Direct Infusion

- Assay buffer: 10 mM NH_4Ac pH 5.2
- Substrate solution: 50 μM $(GlcNAc)_6$ in 10 mM NH_4Ac pH 5.2
- Enzyme solution: 10 μM lysozyme in 10 mM NH_4Ac pH 5.2
- Syringe: 100 μL, Hamilton-Bonaduz, Switzerland
- Syringe pump: Model 11 Plus, Harvard Apparatus, Hugo Sachs Elektronik, Hugstetten, Germany

10.2.6 Robot Infusion

The TriVersa NanoMate® system is an automated nano-electrospray ion source for mass spectrometers that enables the direct infusion of samples from well plates to the MS. The system consists of a robot part and an ESI chip, consisting of 20×20 nozzles, through which the samples are delivered. The nano-electrospray is generated by applying a voltage and head pressure to the sample in the pipette tip.

- Assay buffer: 10 mM NH_4Ac pH 5.2
- Substrate solution: 20 μM $(GlcNAc)_6$ in 10 mM NH_4Ac pH 5.2
- Enzyme solution: 4 μM lysozyme in 10 mM NH_4Ac pH 5.2
- Robot device: Instrument Advion TriVersa NanoMate©, Advion BioSciences, Ithaca, NY
- Conductive pipette tips: Sample tip rack, 384, Advion BioSciences, Ithaca, NY
- ESI chip with 400 nozzles: HD_A_384, Advion BioSciences, Ithaca, NY
- Well plates: Thermo-Fast® 96 skirted, low profile, Thermo Scientific, Surrey, UK

10.3 Methods

10.3.1 LC-MS

10.3.1.1 Enzymatic Assay

- Mix appropriate volumes of enzyme and substrate solutions in a reaction tube to achieve the desired final concentrations
  - ➢ Example assay: Mix equal volumes of enzyme and substrate solutions to achieve final assay concentrations of 25 μM $(GlcNAc)_6$ and 5 μM lysozyme
  - ⓘ In general the mixing order is irrelevant, but keep the same order of mixing in all experiments

- Incubate the mixture, if possible at the temperature optimum of the enzyme
  - ⓘ When conducting repeated assays, be aware that the incubation takes place at the same, defined temperature for each of the assays
- At defined time points (*e.g.* 2, 4, 6, 8 min and so on) add the stopping reagent
  - ➢ Example assay: Stop the reaction with 90% acetonitrile
  - ⓘ Depending on your enzyme and your HPLC separation method you may stop the enzyme reaction with acid, alkali or some kind of organic solvent (methanol, acetonitrile)
- Centrifuge or filter the solution

10.3.1.2 LC-MS Measurement

- Separate the mixture on HPLC. Typical flow rates for MS detection are 0.1–0.2 mL min^{-1}; if you have to apply higher flow rates you should split the flow before subjecting it to the mass spectrometer
  - ➢ Example assay: Inject 10 μL of the mixture and perform the separation on a LichroCART, 100 Diol, 5 μm column with 90% acetonitrile (0.1% formic acid)/10% H_2O. In our case, however, we observed hydrolysis of the substances on the column
  - ⓘ If you do not use a 'make up' flow after the column, you have to use a suitable additive (*e.g.* formic acid for the positive ionization mode or ammonium hydroxide for the negative ionization mode) to achieve sufficient ionization of your molecules

10.3.1.3 Mass Spectrometric Detection

- Select the appropriate mass range to detect your substrate and product. The parameters of the ion source and the mass spectrometer depend on the device used. Typical values are: capillary voltage 4–4.5 kV; nebulizer pressure 15–30 psi; drying gas flow rate 5–10 L min^{-1}; drying gas temperature 250–350 °C
  - ➢ Example assay: Set the m/z range at 400–900; this allows the detection of the substrate $(GlcNAc)_6$ ($m/z = 619.3$) and the two products $(GlcNAc)_4$ ($m/z = 831.3$) and $(GlcNAc)_2$ ($m/z = 425.2$). The MS parameters are as follows: drying gas temperature 300 °C; drying gas flow rate 6 L min^{-1}; nebulizer pressure 30 psi; capillary voltage 2.5 kV; positive ionization mode
  - ⓘ In general for LC-MS measurements with flow rates of up to 0.2 mL min^{-1} you may need higher drying gas parameters than for the direct infusion measurements with flow rates of about 5 mL min^{-1}

10.3.2 Direct Infusion or Robot Infusion Measurement

10.3.2.1 Direct Infusion Enzymatic Assay

- Mix appropriate volumes of enzyme and substrate solutions in a reaction tube to achieve the desired final concentrations

- ➢ Example assay: Mix equal volumes of enzyme and substrate solutions to achieve final assay concentrations of 25 μM $(GlcNAc)_6$ and 5 μM lysozyme
- ⓘ In general the mixing order is irrelevant, but keep the same order of mixing in all experiments

- Transfer the mixture into a syringe, put the syringe into the syringe pump and connect it *via* needle port and PEEK tubing with the inlet of the mass spectrometer source
  - ⓘ Try to conduct these steps quickly, since the enzymatic reaction starts once the enzyme and substrate are mixed

10.3.2.2 Robot Infusion Enzymatic Assay

- Preload two wells of the microplate with the enzyme and substrate solutions
- Program the robot to conduct the following steps:
  1. Aspirating a defined volume of the substrate solution, followed by 1 μL of air and then dispensing the substrate solution in an unused well (in the following referred to as the 'reaction well')
  2. Aspirating a defined volume of the enzyme solution, followed by 1 μL of air and then dispensing the enzyme solution in the reaction well
  3. Mixing the substrate and enzyme solutions in the reaction well
  - ➢ Example assay: 10 μL of substrate solution are mixed with 10 μL of enzyme solution (final concentration of 10 μM $(GlcNAc)_6$ and 2 μM lysozyme), the mixing step with a mixing volume of 20 μL is repeated three times
  - ⓘ Compared to the syringe pump in case of the ESI chip device lower concentrations of enzyme and substrate are used in order to avoid clogging of the nozzles
  4. Transport of the mixed solutions (*i.e.* the enzymatic assay) to the ESI chip and initiation of the nano-electrospray with the appropriate values of voltage and gas pressure
  - ➢ Example assay: the applied values are 1.8 kV voltage and 0.8 psi head pressure
  - ⓘ In general, due to their higher surface tension aqueous solutions require higher values of voltage and gas pressure than organic solutions.[9] For each single assay you have to find the optimal combination of voltage and pressure in preliminary experiments

10.3.2.3 Mass Spectrometric Detection

- Select an appropriate time range to follow the enzymatic reaction
  - ➢ Example assay: Follow the reaction for 20 min; after this time the reaction is completed
- Select the appropriate mass range to detect your substrate and product. The parameters of the ion source and the mass spectrometer depend on the

device used. Typical values for direct infusion are: capillary voltage 4–4.5 kV; nebulizer pressure 15–30 psi; drying gas flow rate 5–10 L min^{-1}; drying gas temperature 250–350 °C. Values for the robot infusion are given in the example assay

- ➢ Example assay: Set the m/z range at 400–900; this allows the detection of the substrate $(GlcNAc)_6$ ($m/z = 619.3$) and the two products $(GlcNAc)_4$ ($m/z = 831.3$) and $(GlcNAc)_2$ ($m/z = 425.2$). The measurements are performed in the positive ionization mode. The parameters for the direct infusion are as follows: 250 °C drying gas temperature; 6 L min^{-1} drying gas flow; 15 psi nebulizer pressure and 4 kV capillary voltage. The MS parameters for the robot infusion are 170 °C drying gas temperature and 1.2 L min^{-1} drying gas flow. No nebulizer is used and capillary voltage must be set to 0 V
- ⓘ In general, for LC-MS measurements with flow rates of up to 0.2 mL min you may need higher drying gas parameters than for the direct infusion measurements (flow rates of about 5 µL min^{-1}) and for the robot infusion measurements (flow rates of 100–200 nL min^{-1})

10.3.3 Data Analysis

Extract the ion chromatograms of substrate and product(s). For LC-MS, integrate the respective peaks for each time point and plot the areas obtained against the time points. For the direct infusion measurements you will obtain a continuous ion chromatogram. Figure 10.1 schematically illustrates the resulting graphs from a LC-MS and a direct infusion measurement.

In case of sodium and/or potassium adducts you have to sum the respective areas or traces.

- ➢ Example assay: The extracted ion chromatogram signals were summed for the following compounds: for the products $(GlcNAc)_2$ and $(GlcNAc)_4$ the signals of $[(GlcNAc)_n + H^+]$ and $[(GlcNAc)_n + Na^+]$ were summed and for the substrate $(GlcNAc)_6$ only the signal $[GlcNAc)_6 + 2H^+]$ was considered

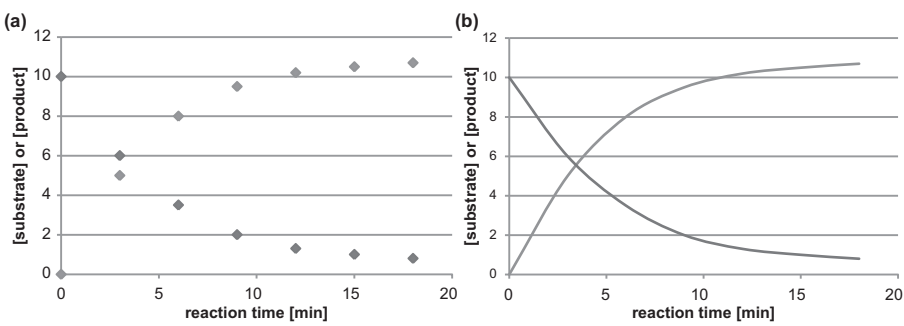

Figure 10.1 Change in substrate and product intensities of an enzymatic assay: (a) graph of LC/MS results; (b) graph of a direct infusion measurement.

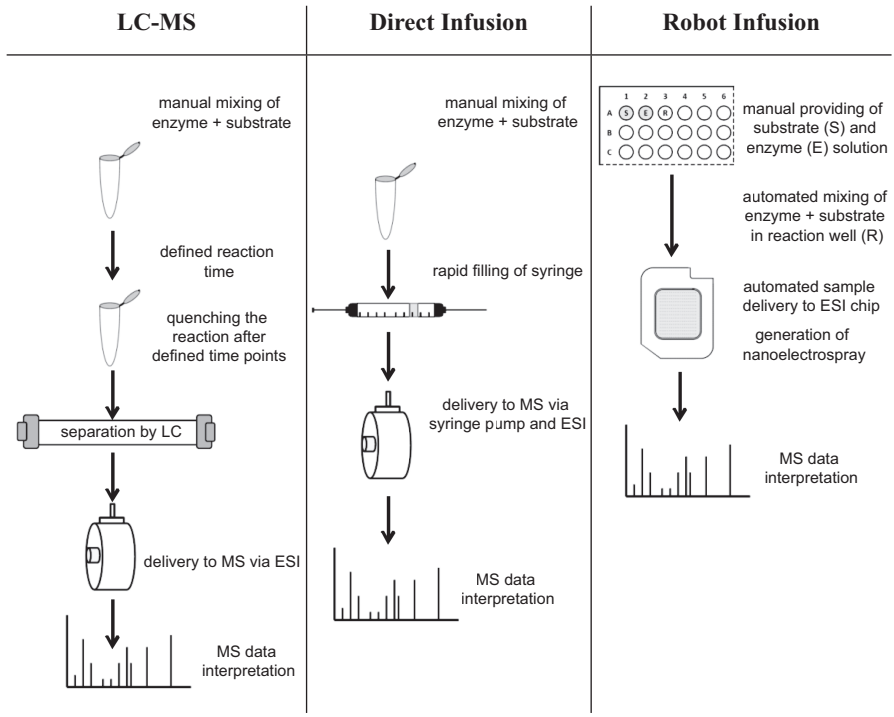

Figure 10.2 Procedural method of the different setups for studying enzymatic reactions.

10.3.4 Comparison of LC-MS, Direct Infusion and Robot Infusion

The LC-MS, direct infusion and robot infusion methods feature several differences. The procedure for each method is shown schematically in Figure 10.2. Additionally, Table 10.1 illustrates the advantages and disadvantages of the methods.

10.4 Notes

10.4.1 General Remarks for Working with Enzymes

10.4.1.1 Enzyme Stability

- Most enzymes are sensitive to temperature, but freezing enzymes may sometimes cause enzyme inactivation and/or denaturation. In this case, freezing should be avoided and enzyme should be kept on ice or at +4 °C
- pH may also affect the stability of enzymes
- Many enzymes are inhibited by heavy metals, so you should take care to exclude them from the assay

Table 10.1 Overview of advantages and disadvantages of setups for the study of enzymatic reactions

LC-MS	*Direct infusion*	*Robot infusion*
Advantages		
Buffer must not be MS-compatible	Real time measurement of the enzymatic reaction	Real-time measurement of the enzymatic reaction
Due to separation of the reaction mixture interferences between the metabolites are reduced	Smaller sample volumes are sufficient	Even smaller sample volumes than for the syringe pump are sufficient
Complex matrices can be used, *e.g.* plasma samples; interfering substances may be separated from the reaction mixture prior to the LC-MS step	No sample preparation necessary	Less delay between mixing and first data acquisition due to automation
		No sample preparation necessary
		No cross contamination since for each measurement a single pipette tip and nozzle are used
		No purging necessary after the measurements
Disadvantages		
Method development for LC separation may be time consuming	Delay between mixing and first data acquisition due to mixing and filling of the syringe	MS-compatible buffer must be used
Sample preparation is time consuming	MS-compatible buffer must be used	Metabolites of the reaction mixture may interfere
Substances may stick in the tubing	Metabolites of the reaction mixture may interfere	Metabolites may interact with the pipette tip or the chip
Only single time points can be measured	Syringe and tubing must be purged exhaustively after each measurement to avoid cross contamination	
The reaction mixture may undergo undesirable reactions on the column, *e.g.* hydrolysis	Substances may stick in the tubing	

- Some enzymes are sensitive to vigorous mixing, thus too strong mixing should be avoided
- Ultrasonics may also affect enzymatic activity (enhance or decrease it)

10.4.2 General Remarks for Mass Spectrometric Applications

- It is strongly recommended to utilize solvents of the highest purity grade (LC/MS grade) and to filter all solutions prior to measurement
- For filtering, make sure that the filter is compatible with your solvent and does not bind proteins
- Avoid high sodium or potassium concentrations to prevent sodium and/or potassium adducts. For this reason when adjusting the pH of buffers use ammoniac or ammonium hydroxide and formic or acetic acid solutions, respectively

10.4.3 Remarks Regarding MS-Based Enzymatic Assays

10.4.3.1 Selection of a Suitable Substrate

- Substrate has a characteristic m/z and is detectable *via* MS
- Enzyme changes the substrate in a characteristically way that is detectable *via* MS (not too small fragments; they should have $m/z \geq 100$)
- Substrate and product m/z values do not overlap
- Choose the appropriate enzyme and substrate concentrations
- In case of more complex assays which may require several cofactors, salts and other additives, mix all required solutions and start the reaction by adding the enzyme

10.4.3.2 Selection of a Suitable Buffer

- Buffer and pH must be in accordance with the requirements of the chosen enzyme (pH range, salt concentration)
- In case of direct infusion measurement, the MS-compatibility of your buffer is an additional criterion: utilize volatile salts like acetate and dependent on your detection method (positive or negative mode), a suitable pH that leads to sufficient ionization of your molecules. However, also take care about the optimum pH for your enzyme (see above)
- Before starting the measurements, make a complete digest of your substrate to check the activity of the enzyme and to check that you have chosen the right substrate

Another continuous-flow technique for the study of protein functions (*e.g.* enzymatic activity) can be found in Chapter 11.

References

1. A. Liesener and U. Karst, *Anal. Bioanal. Chem.*, 2005, **382**, 1451.
2. T. Letzel, E. Sahmel-Schneider, K. Skriver, T. Ohnuma, and T. Fukamizo, *Carbohydr. Res.* 2011, **346**, 863.
3. R. Scheerle, J. Graßmann and T. Letzel, *Anal. Meth.*, 2011, doi:10.1039/C0AY00727G.
4. R. A. John, in *Enzyme Assays: A Practical Approach*, 2nd edn, eds. R. Eisenthal and M. J. Danson, Oxford University Press, Oxford, UK, 2002.
5. B. W. Matthews, *FASEB J.*, 1996, **10**, 35.
6. A. Rau, T. Hogg, R. Marquardt and R. Hilgenfeld, *J. Biol. Chem.*, 2001, **276**, 31994.
7. T. Fukamizo, *Curr. Protein Pept. Sci.*, 2000, **1**, 105.
8. N. Dennhart and T. Letzel, *Anal. Bioanal. Chem.*, 2006, **386**, 689.
9. C. Van Pelt, S. Zhang and J. Henion, *J. Biomol. Tech.*, 2002, **13**, 72.

Appendix III

Enzymatic conversion continuously monitored with a robotic nanoESI-MS tool: Experimental status

Scheerle, R.K., Grassmann, J. and Letzel, T.

Analytical Methods, 2011, 3, 822-830

This publication presents a real-time strategy to research enzymatic assays with a miniaturised and automated setup in combination with mass spectrometric detection for the first time.
All the experiments were planned, conducted and analyzed on my part. The manuscript was mainly prepared on my part.

Analytical Methods

Cite this: DOI: 10.1039/c0ay00727g

www.rsc.org/methods

PAPER

Enzymatic conversion continuously monitored with a robotic nanoESI-MS tool: experimental status

Romy K. Scheerle,[a] Johanna Graßmann[a] and Thomas Letzel*[b]

Received 2nd December 2010, Accepted 7th February 2011
DOI: 10.1039/c0ay00727g

The presented study describes an adaptation of enzymatic assays to miniaturized and automated nanoelectrospray ionization (nanoESI)-mass spectrometry (MS). The system consists of a liquid handling robot including an ESI chip source and offers several advantages for the investigation of enzymatic reactions. Therewith different parameters can be tested rapidly and automatically. Thus the technique provides a basis for the efficient development of enzymatic assays using MS detection. In the present project the miniaturized setup was applied to become appropriate for the investigation of various enzymatic assays since real-time measurements using automated nanospray robots are not reported in detail so far. The reaction of hen egg white lysozyme (HEWL) and the saccharide hexa-*N*-acetylchitohexaose $(GlcNAc)_6$ was used as an exemplary model system. The generation of a stable nanoelectrospray using aqueous solution with enzymes/proteins was typically the main difficulty. Thus various parameters were systematically tested and adjusted to overcome these instabilities. This resulted in moderate, but improved, spray stability. Moreover, the new adjustments were applied to further enzymatic assays (chitinase, chymotrypsin and acetylcholinesterase). In doing so, they were tested whether they are applicable in universal manner. These assays reveal additional findings like a partial reduction of enzymatic activity in the nanoESI setup. The observed complicacies in spraying pure aqueous solutions and the partial enzyme inactivation will be discussed in detail as well as possible approaches to overcome them.

Introduction

Studying enzymatic reactions is of large interest since enzymes are involved in a wealth of biochemical processes, such as metabolic pathways or pathological dysfunctions. Furthermore, proteins with enzymatic function have gained great interest for the chemical industry *via* the so-called 'green chemistry' in which the enzymes act as catalysts for chemical synthesis. With the industrialization of biochemical processes the investigation of functionality, activity or regulation of enzymes is a resurgent research area. Classical methods apply spectroscopic, electrochemical or radioisotopic detection to study enzymatic reactions.[1] A major drawback of these detection techniques is the necessity of labeled substances, *e.g.* the use of chromogenic and fluorogenic labeled substrates. These hydrophobic labels may cause changes in specificity and interaction strength of the substrate regarding the enzyme as known for chitinase with chromogenic labeled and unlabelled substrate.[2] Nevertheless photometric assays are the most frequently used applications for the investigation of enzymatic reactions.[3]

The development of mass spectrometry in enzymology became a powerful tool in recent years. ESI-MS became very popular and widespread and is used in almost every analytical lab due to several advantages.[4–7] In enzymology for example, labeling becomes redundant if mass-depending techniques are used. This enables the examination of *in vitro* enzymatic reactions even with unlabeled substrates. Substrate, intermediates and products of enzymatic reactions can be identified simultaneously by their ionic mass-to-charge ratio. Furthermore this technique mostly is as efficient as fluorescence and radio assays and often quantitative data interpretation is possible by now. Over the past few years several enzymatic assays have been studied and monitored by mass spectrometry. Mostly, such enzymatic reactions are researched by quenching aliquots of the reaction mixture at defined time points. Subsequently, the aliquots are analyzed either directly by mass spectrometry[5,8] or after a high-performance liquid chromatographic separation (LC-MS).[4,9]

Additionally, in recent years the application of so-called continuous-flow assays has increased significantly.[4,10–18] In most cases the assay setup consists of a syringe pump or nanospray tips delivering a constant stream of the reaction mixture to an ESI source connected to the mass spectrometer. Continuous-flow assays were used to study several different enzymatic

[a]*Analytical Research Group, Chair of Chemical–Technical Analysis and Chemical Food Technology, Technische Universität München, Weihenstephaner Steig 23, 85354 Freising—Weihenstephan, Germany*
[b]*Competence Pool Weihenstephan, associated with Technische Universität München, Weihenstephaner Steig 23, 85354 Freising—Weihenstephan, Germany. E-mail: T.Letzel@wzw.tum.de; Fax: +49-(0)8161-715362; Tel: +49-(0)8161-713780*

mechanisms in real-time, to investigate kinetic parameters, noncovalent binding complexes and to elucidate the influence of inhibitory substances on enzymatic activity.

Moreover, the automation and miniaturization of MS-based analytical techniques gained more and more interest due to most notably key benefits like high sample throughput and low sample volume.[19] Miniaturization of the ESI source and the development of nanoESI were first described by Wilm and Mann who proved these two advancements to be applicable in various investigations.[20–22] Compared to conventional ESI with typical flow rates of 1 to 20 μL min^{-1} and capillaries with 100 μm inner diameter (ID) the nanoESI setup achieves flow rates from 20 to 100 nL min^{-1} using very small capillaries (1 to 5 μm ID).[21–23] However, the application of a syringe pump in both cases requires time-consuming manual syringe loading which is a limiting factor for higher sample throughput and for monitoring the reaction starting from the initial period. Thus in recent years robotic and chip-based ESI-MS systems have been established in mass spectrometry.[24–26]

In the present study a commercial chip-based nanoESI setup was used for the real-time monitoring of aqueous enzymatic assays due to its high and fast sample throughput as well as low sample consumption.[27] Earlier studies with this nanoESI interface type illustrate the successful implementation in protein identification,[26,28] carbohydrate analysis,[29] inhibition studies,[30] detection of noncovalent complexes[27,31–33] or the fundamental applicability for real-time monitoring of enzymatic reactions.[33,34]

In the current study the optimization of the nanoESI setup for the monitoring of enzymatic reactions is presented for the first time systematically regarding automation and miniaturization. Furthermore, advantages and disadvantages of the chosen strategy are discussed as well.

Experimental

Chemicals

Hen egg white lysozyme (HEWL, Enzyme Commission (EC) number 3.2.1.17, relative molecular weight (M_r) 14 kDa, 50 000 units mg^{-1} protein), chitinase from *Streptomyces griseus* (EC number 3.2.1.14, M_r 30 kDa, 2.4 units mg^{-1} protein), α-chymotrypsin from bovine pancreas (EC number 3.4.21.1, M_r 25 kDa, 55 units mg^{-1} protein), acetylcholinesterase from *Electrophorus electricus* type VI-S (AChE, EC number 3.1.1.7, M_r 280 kDa, 687 units mg^{-1} protein) and acetylcholine chloride (M_r 181.7 Da, ≥99%) were obtained from Sigma-Aldrich (Steinheim, Germany). Hexa-*N*-acetylchitohexaose ($(GlcNAc)_6$, M_r 1237.2 Da, ≥95%) was obtained from Seikagaku Biobusiness (Tokyo, Japan) and spectrozyme CTY (M_r 520.4 Da, substrate for chymotrypsin with chromogenic group *p*-nitroaniline (pNA)) was obtained from LOXO (Dossenheim, Germany). Ammonium acetate (NH_4Ac, M_r 77.1 Da, >98%) and acetic acid were purchased from Merck (Darmstadt, Germany). All buffers and solutions were prepared in LC-MS reagent water from J. T. Baker (Deventer, Holland).

Instrumentation

All samples were analyzed by a TripleQuadrupole instrument (Series 6410, Agilent Technologies, Waldbronn, Germany) combined with the nanoESI system TriVersa NanoMate (Advion BioSciences, Ithaca, NY).

The TriVersa NanoMate system includes a robot part and an ESI chip. The robot part is utilized for pipetting and mixing several solutions provided in a conventional microplate. In the presented project it holds a 96 well plate and a tip rack with 384 disposable and conductive pipette tips (Advion BioSciences, Ithaca, NY) as well as the ESI chip (HD_A_384, Advion BioSciences, Ithaca, NY). The ESI chip comprises the nanoelectrospray device and consists of 20 × 20 nozzles (5 μM ID) to which the samples are delivered (Fig. 1). To prevent cross-contamination a new nozzle and pipette tip are used for every new sample. Nanoelectrospray is generated by applying voltage and head pressure to each sample in the pipette tip, which is similar to an electrospray needle in nanoESI. The approximate flow rate is between 100 and 200 nL min^{-1}, depending on the solvent composition, voltage and head pressure (Fig. 1).

Mass spectrometric conditions

The samples were detected in positive ionization mode and with the Agilent-system specific parameter 'fragmentor voltage' of 135 V. Drying gas flow was set at 1.2 L min^{-1}, drying gas temperature between 40 °C and 170 °C and capillary voltage at 0 V.

The two nanoESI spraying parameters, head pressure and electrospray voltage, have been optimized between 0.6 and 1.0 psi and 1.65 and 1.9 kV, respectively.

Data evaluation

All samples for the HEWL and chitinase assay were detected in four scan segments (*m/z* 400–470; 600–660; 820–880; 1230–1270) monitoring the ionic $(GlcNAc)_2$, $(GlcNAc)_3$, $(GlcNAc)_4$, and $(GlcNAc)_6$, respectively. In the case of studying the spray stability of pure HEWL solutions, polysiloxane $(C_2H_6SiO)_6$ was monitored due to the lack of protein signals. Polysiloxane is a ubiquitous background signal in nanoelectrospray which can be found within the laboratory.[35,36] Data acquisition was performed with 1 cycle s^{-1}. The chymotrypsin and the acetylcholinesterase assays were detected in full scan mode from *m/z* 200 to *m/z* 600 and from *m/z* 80 to *m/z* 200 at 1 cycle s^{-1}, respectively.

The data were processed using the MassHunter Workstation software, Qualitative Analysis version B02.00 from Agilent Technologies.

The extracted ion chromatogram (EIC) signals for a typical HEWL reaction assay were summed for the following compounds: product signals $(GlcNAc)_2$ and $(GlcNAc)_4$ $[(GlcNAc)_n + H^+]$ and $[(GlcNAc)_n + Na^+]$ for each, $(GlcNAc)_6$ signal (substrate) $[(GlcNAc)_6 + 2H^+]$ as described by Dennhart

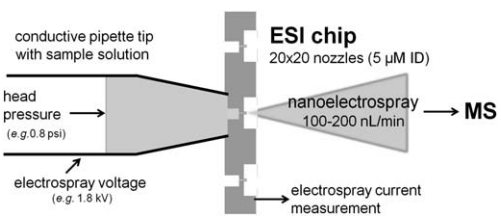

Fig. 1 Nanoelectrospray generated with the nanoESI-MS setup TriVersa NanoMate for the monitoring of aqueous enzymatic reactions.

and Letzel.[12] The EIC signals of the chitinase assay were summed for: $(GlcNAc)_2$, $(GlcNAc)_3$ and $(GlcNAc)_4$ signal (products) $[(GlcNAc)_n + H^+]$ and $[(GlcNAc)_n + Na^+]$ for each, $(GlcNAc)_6$ signal (substrate) $[(GlcNAc)_6 + 2H^+]$. The signals for the α-chymotrypsin assay were summed for: signals for substrate spectrozyme with *m/z* 525 $[M + H]^+$ and *m/z* 547 $[M + Na]^+$ and product signals with *m/z* 405 $[M - pNA + H]^+$ and *m/z* 427 $[M - pNA + Na]^+$. For the AChE assay with substrate acetylcholine the following signals were analyzed: substrate signal *m/z* 146 $[M]^+$ and product signal *m/z* 104 $[M - CH_3COOH]^+$. The signals *m/z* 445 $[M + H]^+$ and *m/z* 462 $[M + NH_4]^+$ were summed for the background signal polysiloxane.[35]

The time-courses were smoothed with a Gaussian function with 15 points function width and 5.000 points Gaussian width. They show a short delay of less than one minute because of the mixing step and delivering of the sample to the ESI chip.

For most of the measurements a calculation of mean values was not reasonable since contradictory results were obtained, such as complete signal break due to clogging of the nozzle (this is described in more detail in the Results and discussion section). Thus one representative experiment is shown for each measurement. Furthermore, the mass spectrometric signals in this manuscript are absolute values to prove the concept and not corrected with the 'fragmentation correction', *i.e.* the percentage of oligosaccharides in solution due to fragmentation and rearrangements as described by Dennhart *et al.*[13]

All settings concerning the robot parts such as pipetting volumes, mixing, analysis time and spraying parameters were set in the software ChipSoft (version 8.1.0.928, Advion BioSciences) by which the TriVersa NanoMate is controlled.

Calculation of conversion rate and collision number

Signal intensities were normalized for calculating conversion rates. The obtained time course was extrapolated using an exponential function in Microsoft Excel 2007 resulting in eqn (1). The starting point was set at one minute since at this time point in all measurements a signal was detected after a signal delay of less than one minute. The reactions were observed to reach a plateau at a remaining intensity of about 0.05; therefore this value was set as the end point of the reaction. Using eqn (1) conversion rates were calculated according to eqn (2), which includes enzyme and substrate concentrations.

$$y = a \times e^{bx} \tag{1}$$

$$\text{Conversion rate } \left[\text{min}^{-1}\right] = \frac{[\text{substrate}]/[\text{enzyme}]}{(\ln 0.05/a)/(b)} \tag{2}$$

The collision number Z_{ES} was calculated in approximation based on the kinetic theory of gases to discuss the conversion rates for the different enzyme-to-substrate concentrations. The collision number for the bimolecular reaction of substrate (S) and enzyme (E) to product was calculated according to eqn (3).

$$Z_{ES} = \sigma\sqrt{\frac{8kT}{\pi\mu}} \times \left(\frac{N_E N_S}{V^2}\right) \tag{3}$$

In eqn (3) the collision cross-section σ is given by $\sigma = \pi d_{ES}^2$, where d_{ES} with $d_{ES} = 1/2(d_E + d_S)$ is the collision diameter between enzyme and substrate diameter. d_E (HEWL) was set at 4.3×10^{-9} m according to Blake *et al.*[37] and d_E (Chitinase) at 16×10^{-9} m according to Kezuka *et al.*[38] The diameter for the small molecule d_S $(GlcNAc)_6$ with 3.4×10^{-9} m was calculated with the graphical software ACD/Labs (Version 12.01). The reduced mass μ is given by $\mu = \frac{m_E m_S}{m_E + m_S}$ where m_E and m_S are the masses of enzyme and substrate. T is the room temperature of 20 °C, k the Boltzmann's constant, N_E and N_S the number of molecules and V the assay volume (10 μL in the nanoESI setup and 100 μL in the syringe pump setup).

Sample preparation and measurement

All measurements were performed at 20 °C ± 2 °C. The samples were prepared in 10 mM NH_4Ac (pH 7.4). HEWL and chitinase assay were prepared with final assay concentrations of 5, 10, 15, 25 μM $(GlcNAc)_6$; 1, 2, 5 μM HEWL or 0.01, 0.05 μM chitinase, respectively. AChE assays were prepared with final concentrations of 0.3; 10 nM AChE and 10 μM acetylcholine chloride and chymotrypsin assay was prepared with 0.15 μM α-chymotrypsin and 5 μM spectrozyme CTY. All samples were prepared at least in duplicate.

The process of monitoring the enzymatic reaction proceeds as follows: two wells of the 96 well microplate are preloaded with solutions of enzyme and substrate. The robot part of the nanoESI system aspirates the defined volume (*e.g.* 10 μL) of the substrate solution, followed by 1 μL of air into the pipette tip and then dispenses the substrate solution in a 'reaction well'. In the next step the enzyme solution is aspirated and added to the substrate solution in the reaction well. Enzyme and substrate solution are mixed automatically by aspirating and dispensing 10 μL of the solution three times. Subsequently the robot delivers the reaction assay solution in a conductive pipette tip to the inlet side of the ESI chip and the nanoelectrospray process is initiated at the nozzle (Fig. 1). Single substrate or enzyme solutions are measured by one aspirating and spraying step each. All measurements are carried out in a 20 minute time period.

The experiments for a comparison of the robot system with direct infusion *via* syringe pump were conducted with the here described mass spectrometer according to Dennhart and Letzel.[12]

Results and discussion

The application of pure aqueous enzymatic solutions in combination with nanoelectrospray ionization poses general problems. On the one hand they are based on the high surface tension of aqueous solutions compared to samples containing organic solvent.[24] On the other hand the enzymes are labile molecules whose tertiary structure and activity might easily be affected by parameters such as temperature, voltage or pressure. These parameters might cause inactivation by unfolding and/or sedimenting proteins which can result in spray instabilities. The current nanoESI setup aims for monitoring enzymatic reactions in real-time; *i.e.* the enzymatic reaction occurs in the pipette tip delivering the sample solution directly to the MS. Thereby the reaction is not interrupted by taking new aliquots. This setup requires stable measurements over a certain time range, which depends on the issue of research. The time period was chosen for

about 20 minutes to approve the spray stability and to monitor substrate decrease and product increase depending on concentrations and enzymatic activity. Various parameters regarding the nanoelectrospray and the mass spectrometer needed to be tested and optimized to discover a stable nanoelectrospray during the total time period.

Controlling the nanoelectrospray stability

The stability of the nanoelectrospray can be monitored by means of the 'electrospray current' (Fig. 2–5, grey-shaded trace). This electrospray current results from an electric field around the nozzle and is detected during each measurement. The electrospray current graph provides a plot of the electrospray current by time for a particular sample. The curve progression of the electrospray current should not have large fluctuations; according to the user manual where constant values between 1 nA and 466 nA indicate a well performed nanoelectrospray. A decline of the electrospray current may point to a spray stop and may be a consequence of high surface tension of aqueous solutions and/or the continuous clogging of the nozzle by salts and proteins. The grey-marked electrospray current traces in Fig. 2–5 reflect typical results in the presented study using the nanospray robot. The system registered electrospray instabilities and the nozzle was changed several times due to a drop below or an increase above arbitrary limits. Fig. 2a exemplarily indicates a nozzle change by the inset 'next nozzle'. After a nozzle change was performed a stable nanoelectrospray could be generated. Changes in the electrospray current are simultaneously reflected in the mass spectrometric signal *via* changing total ion chromatogram (TIC) and EIC. Consequently, the stability of the TIC and EIC depends closely on the electrospray current. Thus, in the forthcoming figures the representative EIC will be shown always in combination with the electrospray current. That results in a deeper and specific insight and consequently in a higher information content.

Optimization of the nanoelectrospray ionization and spray stability using small molecules in aqueous solutions

Various parameters influence the stability of the nanoelectrospray (Fig. 1). One of these is the electrospray voltage. This voltage is applied to the analyte solution in the pipette tip. Furthermore, the head pressure at the tip inlet influences the spray. The pressure keeps the solution in the pipette tip and supports the sample flow through the nozzle to the mass spectrometric connected gas region. Voltage and pressure need to be optimized depending on the specific sample composition. The comparison of several literature data indicates a large range of both parameters. In comparison to organic solutions, aqueous solutions tend to require higher voltage and head pressure due to a higher surface tension. Typical nanoelectrospray voltage values are 1.4–1.8 kV for organic solutions whereas aqueous solutions were reported to be measured at 1.5–2.1 kV.[26,27,32,33,39,40] Organic solutions were reported to be typically measured at head pressures of about 0.1–1.0 psi and aqueous solutions were usually measured in a range between 0.2 and 1.5 psi.[26–30,32,33,39–41] Obviously general values cannot be stated and for each sample composition both spraying parameters need to be adjusted.

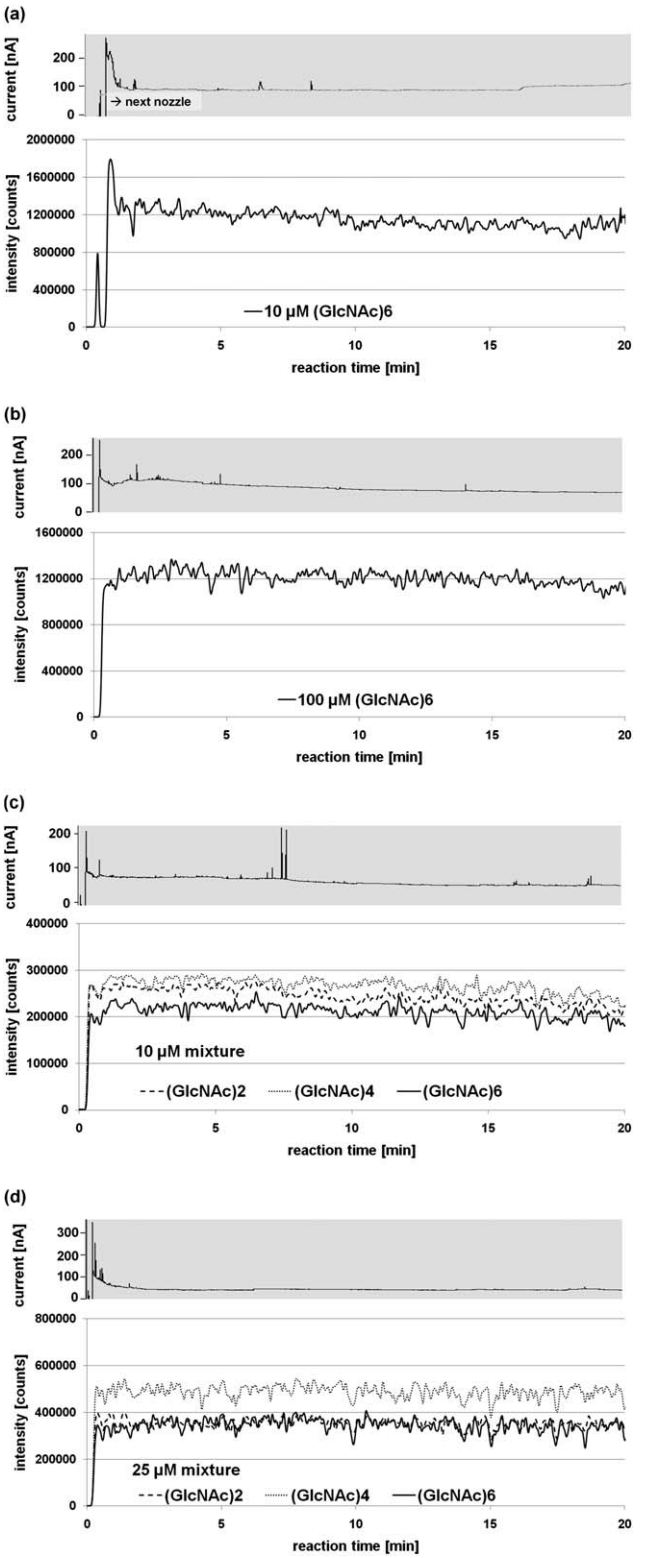

Fig. 2 Electrospray current (grey-shaded) and extracted ion chromatograms of different $(GlcNAc)_6$ (*i.e. m/z* 619) concentrations (a and b) and $(GlcNAc)_2$ (*i.e. m/z* 425 + 447), $(GlcNAc)_4$ (*i.e. m/z* 831 + 853) and $(GlcNAc)_6$ mixtures each 10 µM (c) and 25 µM (d).

Initial spray experiments were carried out with aqueous solutions containing substrate. Therewith optimal values and combinations of voltage and pressure should be determined.

According to literature data and preliminary tests in this study (data not shown) a combination of 1.8 kV and 0.8 psi was chosen for starting experiments. Thereby, drying gas temperature and flow were set to 170 °C and to 1.2 L min^{-1}, respectively.

Firstly, different concentrations of $(GlcNAc)_6$ were tested in 10 mM NH_4Ac-buffer (Fig. 2). The results in Fig. 2a and b show a stable nanoelectrospray for both concentrations in the spraying period up to 20 minutes. Since the aim was to monitor enzymatic conversion, mixtures of the substrate $(GlcNAc)_6$ and the two main HEWL assay products $(GlcNAc)_2$ and $(GlcNAc)_4$, each 10 μM or 25 μM, were prepared. Fig. 2c and d present the spray stabilities for these mixtures. All compounds give stable and reproducible EICs in the total time. Concluding, a stable spray can be obtained using aqueous solutions with small molecules such as oligosaccharides. This is even true in mixtures and in higher concentrations such as 100 μM.

Influence of functional proteins in aqueous solutions on spray stability

In a next step the enzyme HEWL was measured in two concentrations on the way to test a complete enzymatic assay solution (Fig. 3). In these cases the EIC of the ubiquitous background signal polysiloxane is shown in comparison to the electrospray current because HEWL was not detectable in the applied *m*/*z* range. The measurements show a rapid drop of the electrospray current and simultaneously the mass spectrometric signals even after a nozzle change. Obviously the chosen parameters are not suitable to obtain a stable spray for aqueous solutions containing molecules like proteins. This might be explained by a clogging of the nozzles or the tip due to denaturation of the enzyme and will be discussed in more detail below.

Furthermore, in spite of the observed instabilities the system was tested for its applicability with solutions representing the total enzymatic assay, *i.e.* containing substrate and enzyme. Initially, the same parameters were used as described in the previous chapter, namely 1.8 kV spray voltage, 0.8 psi head pressure, 170 °C drying gas temperature and a gas flow of 1.2 L min^{-1}. The enzymatic assay solution contained 25 μM $(GlcNAc)_6$ and 5 μM HEWL. In Fig. 4 several exemplary data from enzymatic assays are shown. Only one of multiple nanospray experiments resulted in an efficient performance of the nanoelectrospray over the total spraying time of 20 minutes (Fig. 4a). However, most measurements showed spray instabilities: in some cases the spray discontinued after a certain stable spraying time (Fig. 4b after 15 min and Fig. 4c after 6 min) and in some cases right from the start (Fig. 4d).

In the case of a stable experiment the fast mixing step of substrate with enzyme and short delivering time to the ESI chip leads to a MS signal already one minute after mixing. It is important to monitor the reaction directly after mixing all reaction components to calculate kinetic data of enzymatic reactions. Therefore the applied mixing steps provide a time saving of about 1–2 minutes in comparison to the recently described setup by syringe pump with a delay of 2–3 minutes.[42] Nevertheless often instabilities were observed in the spray process (Fig. 4b–d). Literature is available discussing that only small changes in spraying parameters may cause large differences in the electrospray stability. As an example De Vriendt and co-workers studied zinc affinity of several metallo-β-lactamases.[40] The native enzyme measurements were carried out in 10 mM NH_4Ac for four minutes at spraying voltages varying from 1.5 kV to 1.9 kV keeping the pressure at 0.2–0.3 psi. They already observed variations of the TIC by changing the voltage in 0.1 steps in between 1.5 and 1.9 kV and detected the best spray stability at 1.8 kV. Another experiment was carried out by van den Heuvel and co-workers detecting hydrolysis of ssDNA with DNAse in aqueous 50 mM NH_4Ac.[33] The spraying parameters with 1.85 kV and 0.2 psi were similar to those of De Vriendt and co-workers. Although they reported to have conducted real-time measurements, they show split MS data at 2, 15 and 45 min. In detailed information is given about the spray stability within these 45 minutes. For aqueous protein solutions, it seems that the optimal voltage is between 1.5 and 1.9 kV. The optimal head gas pressure is reported in a range between 0.2 and 0.3 psi.

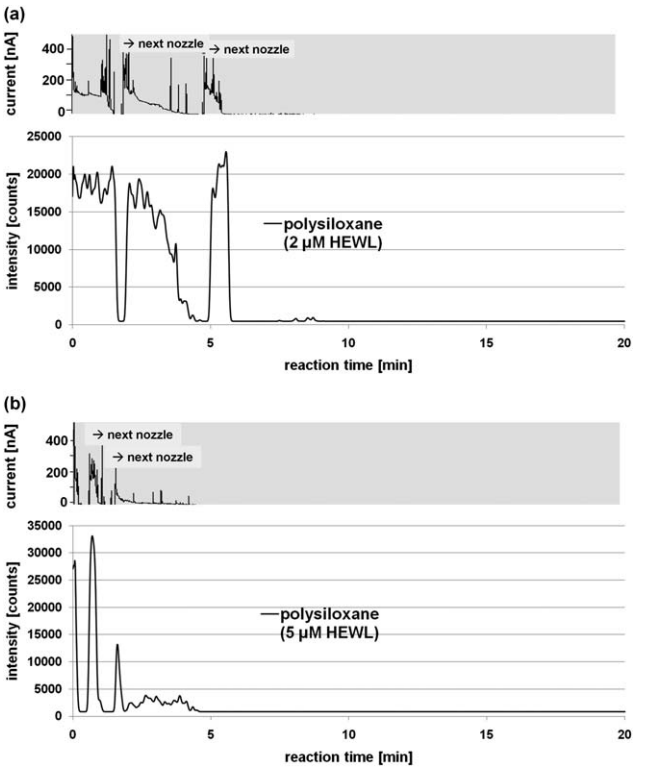

Fig. 3 Electrospray current (grey-shaded) and extracted ion chromatograms of ubiquitous background signal polysiloxane (*i.e.* *m*/*z* 445 + 462) at measuring aqueous enzyme solutions with 2 μM (a) and 5 μM (b) HEWL.

Further experiments were performed based on these literature data to enhance the stability and reproducibility by varying the voltage and head pressure to overcome the variations in spray stability. The MS parameters, drying gas temperature and gas flow, were kept constant at 170 °C and 1.2 L min^{-1}, whereas the nanoESI parameters electrospray voltage and the head pressure were tested systematically in several combinations between 0.2 and 1.0 psi and 1.6 and 2.0 kV. None of the modifications, however, led to an improved electrospray (data not shown). No obvious trend could be observed and all applied changes just worsened the spray stability. In the next section explanations for these difficulties are discussed and possible approaches to resolve them.

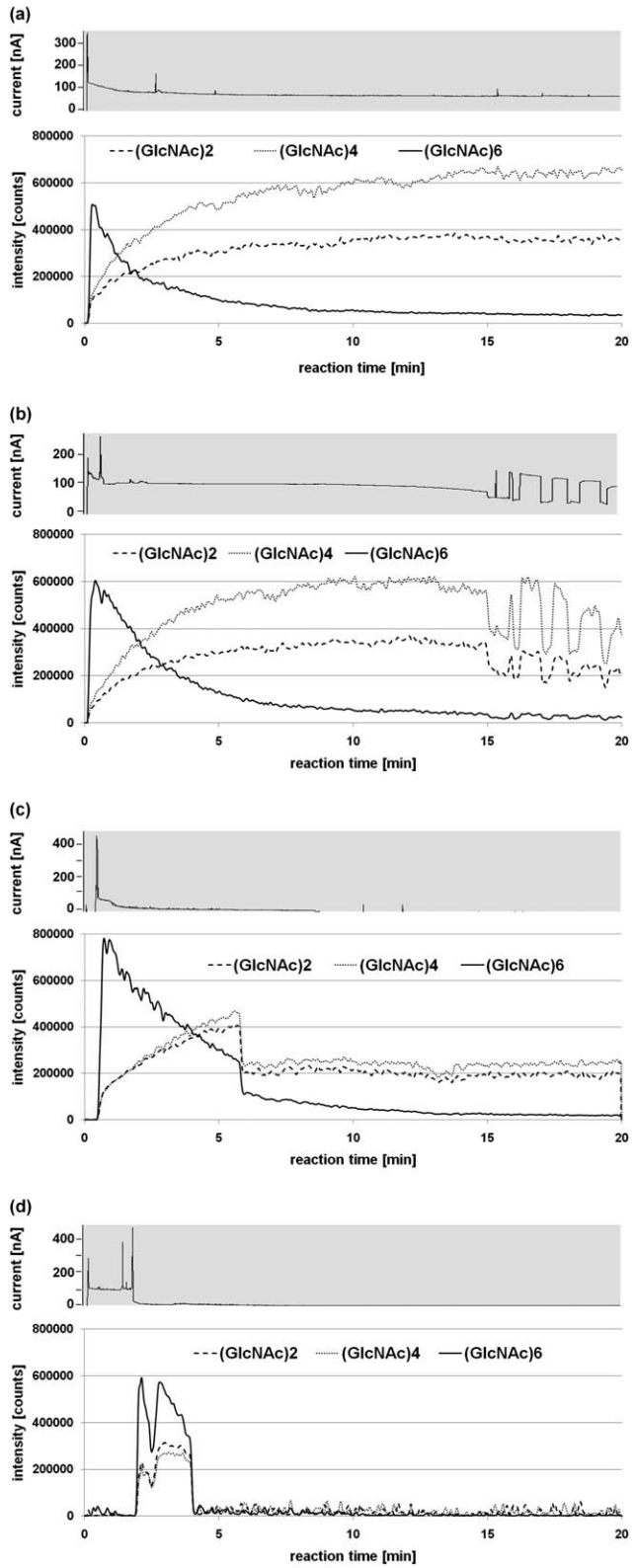

Fig. 4 (a–d) Differences in electrospray current (grey-shaded) and extracted ion chromatograms when measuring repeatedly an enzymatic assay consisting of 25 μM $(GlcNAc)_6$ and 5 μM HEWL. Instabilities in the EICs of substrate $(GlcNAc)_6$ (*i.e.* *m*/*z* 619) and products $(GlcNAc)_2$ (*i.e.* *m*/*z* 425 + 447) and $(GlcNAc)_4$ (*i.e.* *m*/*z* 831 + 853) are also reflected in the electrospray current.

Nozzle inner diameter as critical topic. Applications which use proteins in combination with nanoESI-MS are discussed in literature. These data suggest that indeed a stable spray can be achieved with pure water samples; however these setups differ from the current one. Van Pelt and co-workers achieved a stable spray with 0.5 μM cytochrome c in 100% water at 2.1 kV and 0.1 psi as well as in 99.9% water with 0.1% acetic acid at 1.9 kV and 1.0 psi. They did not observe any clogging of the nozzle during the infusion period of 15 minutes.[26] In those experiments the protein content was lower by factor 10 and different microchips were applied. They used chips with 10 × 10 nozzles, each having an ID of 10 μm.[24] In the current study 20 × 20 nozzle-chips were used with an ID of about 5 μm.

Keetch *et al.* discussed the stability of the spray using an ESI chip applying 1.9 kV and 0.6 psi.[32] They investigated noncovalent protein–protein and protein–ligand interactions and sprayed aqueous solutions containing the noncovalent tetramer transthyretin but they did not give details about a stable spray period. They observed a better stability of the nanoelectrospray chip compared to a nanospray capillary. Such a capillary had in their studies an internal diameter of 1–10 μm and the nozzles had an internal diameter of 8 μm.

Unfortunately, in several experiments described above, the inner diameter of the nozzles was higher than in the current setup. However, instabilities and lower reproducibility of the spray observed in the current experiments may partially be caused by the low inner diameter of the nozzles and have to be overcome in the case of robust and reproducible experiments. These properties might be set by applying a higher continuous head pressure in the pipette tip or using earlier ESI chips. The actual applied pressure keeps the sample in the tip and prevents sample backflow. A higher head pressure could support the nanospray in pushing or pumping the aqueous sample gently through the nozzle. The higher surface tension of water might be no problem anymore and clogging effects should be prevented by a continuous flow through the nozzle. This modification of the setup is currently under investigation and will be a promising improvement for the nanoelectrospray stability.

Protein denaturation as critical topic. The clogging process of the nozzles may also be provoked by a denaturation process of the enzyme. Possible reasons might be the high temperature of the drying gas or the direct voltage on the pipette tip. The next tests were performed with reduced gas temperature trying to prevent denaturation processes caused by high temperature. Gas temperature should be kept as low as possible to keep the enzymes active. On the other hand the drying gas temperature should be adjusted in a range which allows effective vaporization and desolvation of the aqueous droplets. Similar experiments by De Vriendt *et al.* and Jecklin *et al.* were conducted at 45 °C to 50 °C source temperature using other MS systems.[30,31,40,43] In the current study experiments were chosen with drying gas temperatures of 170 °C, 100 °C, 50 °C and 40 °C, respectively. The best results with a stable nanoelectrospray were achieved at 170 °C drying gas temperature. Decreasing the temperature to 100 °C already worsened the spray stability and when reducing the gas temperature further to 40 °C no reproducible measurements could be obtained and the low temperature even may cause contamination of the mass spectrometer (data not shown). Thus

the ion source of the applied mass spectrometer did not influence the enzymatic activity caused by high temperature.

Further the applied voltage on the pipette tip might cause denaturation of proteins in the sample solution. The effect of pulsed electric fields (PEFs) on enzymatic activity was studied by several research groups.[44–46] The studies demonstrated that PEF has an influence on activities and conformations of enzymes. Several enzymes were reduced in their enzymatic activity but some enzymatic activities were increased after treatment with PEF. Whereas PEF uses high pulses (20–40 kV cm^{-1}) for only few μs, in the presented nanoESI setup the electric field is applied during the measurement with lower intensities (1–2 kV). The potential influence of the electric field on several enzymes in the current study and a new approach to hopefully eliminate this fact are discussed in the last chapter.

Influence of sample concentration on spray stability

The concentrations of 25 μM substrate $(GlcNAc)_6$ and 5 μM enzyme HEWL were initially chosen since it has been shown that they will result in a good performance over a period of 20 minutes using a μL-flow system as described by Dennhart and Letzel.[12] However, the nanoESI-MS setup with the adjusted parameters seems not to be applicable for the described enzyme concentration. High concentrations of enzyme might influence the spray stability by clogging the nozzles as described above. On the other hand it is known that nanoESI transfers ions more efficiently than microESI.[20,21,47] Thus lower absolute concentrations should be applicable to obtain observable signals. In a next set of experiments the concentrations of enzyme and substrate therefore were reduced fivefold. The main aim thereby was to find a combination of enzyme and substrate concentrations that yields detectable intensities for the mass spectrometer. The tested combinations and the results are shown in Table 1. They were compared by calculating the real conversion rate of substrate and the theoretical collision number of all molecules in the sample solution.

The reactant concentrations for the nanoelectrospray measurements can be decreased considerably. In comparison to the above described results using 5 μM enzyme and 25 μM substrate, in the nanoESI setup combinations between 1 and 2 μM enzyme and 5 and 15 μM substrate led to a more stable and reproducible nanoelectrospray current and therefore to a more constant TIC and EIC as well. Regarding the assays with an equal substrate/enzyme ratio of 5, the calculated conversion rates of 0.30 min^{-1} (2 μM enzyme, 10 μM substrate) and 0.23 min^{-1} (1 μM enzyme, 5 μM substrate) are in agreement with the decreasing collision numbers of 2.1×10^{28} s^{-1} and 0.5×10^{28} s^{-1}.

For combinations with the same enzyme concentration, *e.g.* 2 μM enzyme, the conversion rate decreases from 0.37 min^{-1} to 0.13 min^{-1} in accordance to the decreasing collision number from 3.1×10^{28} to 1.0×10^{28}. In experiments with 1 μM HEWL and different substrate concentrations the conversion rate decreases from 0.49 min^{-1} to 0.23 min^{-1}, again in agreement with a decline of the collision numbers from 1.5×10^{28} to 0.5×10^{28}. In conclusion for the nanoESI setup reduction of enzyme and substrate concentrations resulted in an improved spray stability and enabled the continuous monitoring of the enzymatic reaction. In regard to a miniaturized, fast and cost-efficient setup the nanoESI is a promising system, especially if enzymes are used that are available in small amounts or quite expensive.

Method adaptation to further enzymatic assays

The method was applied to other enzymatic reactions to improve the optimized MS and spraying parameters in the following.

Chitinase. The first assay resembled the HEWL/$(GlcNAc)_6$ assay and consisted of chitinase and $(GlcNAc)_6$ (Fig.5). The assay for comparison with the original syringe pump setup contained 10 μM $(GlcNAc)_6$ and 0.01 μM chitinase (Fig. 5a) and led to a conversion rate of 13.6 min^{-1}. A stable nanoelectrospray was achieved when applying these concentrations in the nanoESI setup but neither substrate decrease nor product increase were observed and no conversion rate could be determined (Fig. 5b), even though in both experiments the collision number with 7.8×10^{19} is the same. Increasing the enzyme concentration to 0.05 μM led to substrate decrease and product increase along with a stable nanoelectrospray. In this experiment the conversion rate was 0.9 min^{-1}. Thus, compared to the shown syringe pump experiment the enzyme concentration had to be increased fivefold. But even then the conversion rate was considerably lower in the nanospray system (0.9 min^{-1}) than that from the microspray system (13.6 min^{-1}).

α-Chymotrypsin and acetylcholinesterase. In a further assay the same phenomena were observed. 0.15 μM α-chymotrypsin together with 5 μM spectrozyme CTY as substrate worked well with the syringe pump but led to an instable spray in the nanoESI setup without enzymatic conversion (data not shown).

Table 1 Conducted HEWL assays with various substrate $(GlcNAc)_6$ and enzyme (HEWL) concentrations and ratios as well as their respective conversion rates and theoretical collision numbers

Enzyme concentration/μM	Substrate concentration/μM	Ratio substrate/enzyme	Experimental conversion rate/min^{-1}	Theoretical collision number in 10 μL sample solution/$\times 10^{20}$ s^{-1}
5[a]	25[a]	5[a]	0.31[a]	15
2	15	7.5	0.37	3.6
2	10	5	0.30	2.4
2	5	2.5	0.13	1.2
1	15	15	0.49	1.9
1	10	10	0.47	1.2
1	5	5	0.23	0.6

[a] Assay conducted with syringe pump setup.

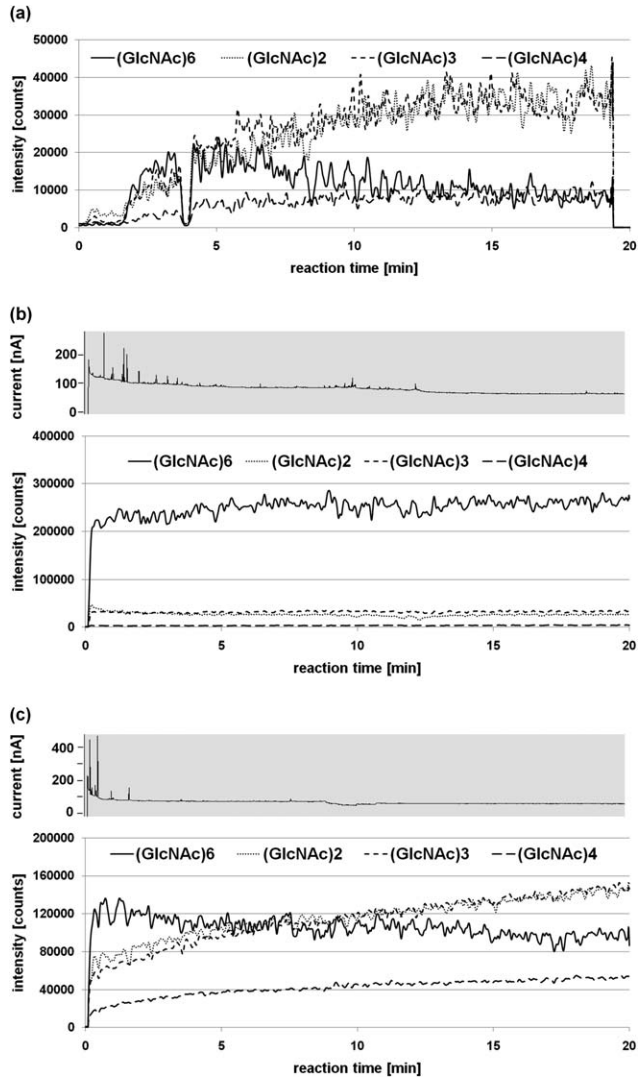

Fig. 5 Comparison of the chitinase assay performed in syringe pump experiments (a) with 10 μM $(GlcNAc)_6$ and 0.01 μM chitinase and in nanoESI experiments (b) with 10 μM $(GlcNAc)_6$ and 0.01 μM chitinase and (c) with 10 μM $(GlcNAc)_6$ and 0.05 μM chitinase. The EICs of substrate $(GlcNAc)_6$ (*i.e.* *m*/*z* 619) and products $(GlcNAc)_2$ (*i.e.* *m*/*z* 425 + 447), $(GlcNAc)_3$ (*i.e.* 628 + 650) and $(GlcNAc)_4$ (*i.e.* *m*/*z* 831 + 853) are shown.

In another assay conducted with AChE and acetylcholine as substrate the first measurements were carried out with 0.3 nM AChE and 10 μM acetylcholine. The concentrations are applied as in the positive syringe pump assay, but again no reaction could be observed in the nanospray setup (data not shown). Increasing the enzyme concentration to 10 nM (which corresponds to a 30 fold increase) led to product formation in the short term but this time no stable electrospray was achieved. This instability may be due to the considerably higher molecular weight of acetylcholinesterase (M_r 280 kDa) compared to HEWL, chitinase and α-chymotrypsin with molecular weights ≤30 kDa, which may provoke an even more pronounced clogging of the nozzles.

Obviously the enzymes chitinase, AChE and α-chymotrypsin are reduced markedly in their activity, which is likely caused by the apparatus conception. This assumption was proved by conducting a direct comparison with a syringe pump experiment applying exactly the same samples within one hour. In these experiments the enzymatic activity in the syringe pump assays was originally higher, but with the nanoESI setup for chitinase no or markedly decreased activities were observed. Additionally, for α-chymotrypsin and acetylcholinesterase regularly no stable nanoelectrospray could be achieved. Thus only marginal product formation could be detected. Concluding, there is a narrow concentration range in which the enzymes show activity but no nozzle clogging.

To elucidate the reason for this enzyme inactivation several materials such as microplate material and conductive pipette tips used in the nanoESI setup were tested. Microplates and pipette tips were preincubated with enzyme and substrate solutions prior to the procedure of the enzymatic assay with the syringe pump. The results clearly excluded adsorption or inhibition effects or that these materials had any impact on the enzymatic activity.

Apparently the enzymes lose their activity by applying voltage at the pipette tip where the enzymatic reaction occurs. The effect of PEF on the enzymatic activity was studied as described in the previous section by Yang and co-workers.[45] They observed a decreased activity of chymotrypsin after the treatment with PEF. These results are in accordance with the observations with the robot setup. The influence of the applied voltage on several enzymes is under further investigation with a modified setup. In the current setup the voltage is distributed over the whole pipette tip, thus the total enzymatic assay solution is exposed to voltage. In the modified setup the sample solution is very shortly in contact with the tip before it is sprayed and hence with the applied voltage. With this setup the deactivation and denaturation of enzymes by voltage might be weakened or eliminated.

Conclusion

A miniaturized method and its systematic development were described to analyze pure aqueous enzymatic assays *via* a robot nanoESI-MS. The current setup shows a promising method to generally study enzymatic reactions. However, as it is known from further studies the measurement of aqueous solutions by nanoESI-MS is difficult so far and requires the optimization of all variables such as spraying and MS parameters. Recapitulating the described experiments, it is obvious that the miniaturized setup for investigating enzymatic reactions cannot directly be adopted from conventional setups. Systematic test series are required and can be performed easily with such a robotic system. Each assay can be adjusted in particular, keeping in mind the most notable problems which are clogging of the nozzles and impaired enzymatic activity due to the applied voltage.

In the presented study the parameters for the nanoESI-MS were optimized for an enzymatic assay consisting of a hexasaccharide as substrate and HEWL as enzyme in order to allow an observation of the reaction over a time range of 20 minutes. In comparison to conventional setups with a syringe pump the reaction can be monitored in a miniaturized and automated way. The MS-signal can be detected already one minute after mixing the enzyme and substrate. In contrast to conventional ESI, due to the higher efficiency of nanoESI, the concentrations of enzyme and substrate can be decreased. This does not only prevent clogging effects of the nozzle and increases spray stability but

also represents a positive effect with the objective of a miniaturized setup. Less enzyme consumption is needed when working with enzymes that are expensive or only available in small amounts. Therefore the nanoESI setup principally provides a system for the fast and miniaturized monitoring of enzymatic assays.

The optimized spraying parameters were applied to other enzymatic assays. The parameters are indeed partially suitable for the chitinase assay, although a decrease in enzymatic activity was observed. Other chosen enzymes such as acetylcholinesterase and α-chymotrypsin seem to be impaired actually stronger in their activity, since even with increased enzyme concentrations no or marginal reaction could be detected.

Thus, the stability of the nanoelectrospray has to be optimized furthermore to achieve more reproducible results. A first approach is the application of a higher head pressure on the sample in the pipette tip to overcome the clogging of the nozzle. First experiments with an advanced setup connecting the pipette tip to a HPLC-flow have already been conducted and showed promising results. On the other hand the influence of the voltage applied on the pipette tip on enzymes and their activity have to be studied in more detail to elucidate possible mechanisms of deactivation and/or denaturation. A modified setup with minimized contact time between enzyme and the charged pipette tip will be tested in near future.

Concluding, the nanoESI robot shows high potential becoming a routine system in mass spectrometric monitoring enzymatic reactions in low concentrations. However, several modifications and studies are needed until a universal system can be handled in routine. We are looking forward.

Acknowledgements

The authors would like to thank for financial support from the German Federal Ministry of Economics and Technology within the agenda for the promotion of industrial cooperative research and development (IGF) based on a decision of the German Bundestag. The access was organised by the AiF, Arbeitsgemeinschaft industrieller Forschungsvereinigungen, Köln. We also thank Advion BioSciences (Ithaca, NY), especially Reinaldo Almeida, for the technical and professional support and Agilent Technologies (Waldbronn, Germany) for the TripleQuadrupole mass spectrometer as a loan.

References

1 H. Bisswanger, *Practical Enzymology*, Wiley-VCH, 2004.
2 T. Letzel, E. Sahmel-Schneider, K. Skriver, T. Ohnuma and T. Fukamizo, *Carbohydr. Res.*, 2011, DOI: 10.1016/j.carres.2011.01.012.
3 R. A. John, in *Enzyme Assays: a Practical Approach*, ed. R. Eisenthal and M. J. Danson, Oxford University Press, 2nd edn, 2002, pp. 1–282.
4 K. D. Greis, *Mass Spectrom. Rev.*, 2007, **26**, 324–339.
5 A. Liesener and U. Karst, *Anal. Bioanal. Chem.*, 2005, **382**, 1451–1464.
6 T. Letzel, *Anal. Bioanal. Chem.*, 2008, **390**, 257–261.
7 S. Shipovskov and C. T. Reimann, *Analyst*, 2007, **132**, 397–402.
8 N. A. Pi, Y. H. Yu, J. D. Mougous and J. A. Leary, *Protein Sci.*, 2004, **13**, 903–912.
9 T. Fukamizo, A. Fleury, N. Cote, M. Mitsutomi and R. Brzezinski, *Glycobiology*, 2006, **16**, 1064–1072.
10 N. Pi, M. B. Hoang, H. Gao, J. D. Mougous, C. R. Bertozzi and J. A. Leary, *Anal. Biochem.*, 2005, **341**, 94–104.
11 X. Ge, T. L. Sirich, M. K. Beyer, H. Desaire and J. A. Leary, *Anal. Chem.*, 2001, **73**, 5078–5082.
12 N. Dennhart and T. Letzel, *Anal. Bioanal. Chem.*, 2006, **386**, 689–698.
13 N. Dennhart, T. Fukamizo, R. Brzezinski, M. E. Lacombe-Harvey and T. Letzel, *J. Biotechnol.*, 2008, **134**, 253–260.
14 A. R. de Boer, B. Bruyneel, J. G. Krabbe, H. Lingeman, W. M. A. Niessen and H. Irth, *Lab Chip*, 2005, **5**, 1286–1292.
15 A. R. de Boer, H. Lingeman, W. M. A. Niessen and H. Irth, *TrAC, Trends Anal. Chem.*, 2007, **26**, 867–883.
16 D. J. Wilson and L. Konermann, *Anal. Chem.*, 2004, **76**, 2537–2543.
17 H. Gao, Y. Chen and J. A. Leary, *Int. J. Mass Spectrom. Ion Processes*, 2005, **240**, 291–299.
18 J. M. Daniel, S. D. Friess, S. Rajagopalan, S. Wendt and R. Zenobi, *Int. J. Mass Spectrom. Ion Processes*, 2002, **216**, 1–27.
19 Y. N. Yang, J. Kameoka, T. Wachs, J. D. Henion and H. G. Craighead, *Anal. Chem.*, 2004, **76**, 2568–2574.
20 M. Wilm and M. Mann, *Anal. Chem.*, 1996, **68**, 1–8.
21 M. S. Wilm and M. Mann, *Int. J. Mass Spectrom. Ion Processes*, 1994, **136**, 167–180.
22 M. Wilm, A. Shevchenko, T. Houthaeve, S. Breit, L. Schweigerer, T. Fotsis and M. Mann, *Nature*, 1996, **379**, 466–469.
23 P. Kebarle and L. Tang, *Anal. Chem.*, 1993, **65**, 972A–986A.
24 G. A. Schultz, T. N. Corso, S. J. Prosser and S. Zhang, *Anal. Chem.*, 2000, **72**, 4058–4063.
25 S. Benetton, J. Kameoka, A. M. Tan, T. Wachs, H. Craighead and J. D. Henion, *Anal. Chem.*, 2003, **75**, 6430–6436.
26 C. Van Pelt, S. Zhang and J. Henion, *J. Biomol. Tech.*, 2002, **13**, 72–84.
27 S. Zhang, C. K. Van Pelt and D. B. Wilson, *Anal. Chem.*, 2003, **75**, 3010–3018.
28 S. Zhang, C. K. Van Pelt and J. D. Henion, *Electrophoresis*, 2003, **24**, 3620–3632.
29 M. Froesch, L. M. Bindila, G. Baykut, M. Allen, J. Peter-Katalinic and A. D. Zamfir, *Rapid Commun. Mass Spectrom.*, 2004, **18**, 3084–3092.
30 M. C. Jecklin, D. Touboul, R. Jain, E. N. Toole, J. Tallarico, P. Drueckes, P. Ramage and R. Zenobi, *Anal. Chem.*, 2009, **81**, 408–419.
31 M. C. Jecklin, D. Touboul, C. Bovet, A. Wortmann and R. Zenobi, *J. Am. Soc. Mass Spectrom.*, 2008, **19**, 1237–1237.
32 C. A. Keetch, H. Hernandez, A. Sterling, M. Baumert, M. H. Allen and C. V. Robinson, *Anal. Chem.*, 2003, **75**, 4937–4941.
33 R. H. H. van den Heuvel, , S. Gato, , C. Versluis, , P. Gerbaux, , C. Kleanthous and and A. J. R. Heck, Nucleic Acids Res., , 2005, , **33**, published online 2005 June 13 , DOI: 10.1093/nar/gni099.
34 T. N. Corso, R. Almeida, N. Dennhart, J. Henion, M. Lees and T. Letzel, *Proceeding for a Poster Presentation at the 55th ASMS Conference 2007*, Indianapolis, USA, 2007.
35 B. O. Keller, J. Suj, A. B. Young and R. M. Whittal, *Anal. Chim. Acta*, 2008, **627**, 71–81.
36 A. Schlosser and R. Volkmer-Engert, *J. Mass Spectrom.*, 2003, **38**, 523–525.
37 C. C. F. Blake, D. F. Koenig, G. A. Mair, A. C. T. North, D. C. Phillips and V. R. Sarma, *Nature*, 1965, **206**, 757–761.
38 Y. Kezuka, M. Ohishi, Y. Itoh, J. Watanabe, M. Mitsutomi, T. Watarabe and T. Nonaka, *J. Mol. Biol.*, 2006, **358**, 472–484.
39 C. K. Van Pelt, S. Zhang, E. Fung, I. H. Chu, T. T. Liu, C. Li, W. A. Korfmacher and J. Henion, *Rapid Commun. Mass Spectrom.*, 2003, **17**, 1573–1578.
40 K. De Vriendt, G. Van Driessche, B. Devreese, C. Bebrone, C. Anne, J. M. Frere, M. Galleni and J. Van Beeumen, *J. Am. Soc. Mass Spectrom.*, 2006, **17**, 180–188.
41 M. C. Jecklin, 2010 personal communication.
42 N. Dennhart, L. M. M. Weigang, M. Fujiwara, T. Fukamizo, K. Skriver and T. Letzel, *J. Biotechnol.*, 2009, **143**, 274–283.
43 K. De Vriendt, K. Sandra, T. Desmet, W. Nerinckx, J. Van Beeumen and B. Devreese, *Rapid Commun. Mass Spectrom.*, 2004, **18**, 3061–3067.
44 S. Y. Ho, G. S. Mittal and J. D. Cross, *J. Food Eng.*, 1997, **31**, 69–84.
45 R. J. Yang, S. Q. Li and Q. H. Zhang, *J. Food Sci.*, 2004, **69**, C241–C248.
46 W. Zhao, R. J. Yang, R. R. Lu, Y. L. Tang and W. B. Zhang, *J. Agric. Food Chem.*, 2007, **55**, 9850–9858.
47 P. Kebarle and U. H. Verkerk, *Mass Spectrom. Rev.*, 2009, **28**, 898–917.

Appendix IV

Real-time ESI-MS of Enzymatic Conversion: Impact of Organic Solvents and Multiplexing

Scheerle, R.K., Grassmann, J. and Letzel, T.

Analytical Sciences 2012, 28, 607-612

The publication reports a detailed and systematic work in performing enzymatic assays in the presence of organic solvent contents and in multiplexing approaches using mass spectrometric detection.
All the experiments were planned, conducted and the data were evaluated on my part. The manuscript was mainly prepared on my part.

ANALYTICAL SCIENCES JUNE 2012, VOL. 28

Real-time ESI-MS of Enzymatic Conversion: Impact of Organic Solvents and Multiplexing

Romy K. SCHEERLE,* Johanna GRASSMANN,* and Thomas LETZEL†**

**Analytical Research Group, Wissenschaftszentrum Weihenstephan, Technische Universität München, Weihenstephaner Steig 23, 85354 Freising-Weihenstephan, Germany*
***Competence Pool Weihenstephan, associated with Technische Universität München, Weihenstephaner Steig 23, 85354 Freising-Weihenstephan, Germany*

Different enzymatic assays were characterized systematically by real-time electrospray ionization mass spectrometry (ESI-MS) in the presence of organic solvents as well as in multiplex approaches and in a combination of both. Typically, biological enzymatic reactions are studied in aqueous solutions, since most enzymes show their full activity solely in aqueous solutions. However, in recent years, the use of organic solvents in combination with enzymatic reactions has gained increasing interest due to biotechnological advantages in chemical synthesis, development of online coupled setups screening for enzyme regulatory compounds, advantages regarding mass spectrometric detection and others. In the current study, the influence of several common organic solvents (methanol, ethanol, isopropanol, acetone, acetonitrile) on enzymatic activity (hen egg white lysozyme, chitinase, α-chymotrypsin, elastase from human neutrophils and porcine pancreas, acetylcholinesterase) was tested. Moreover, multiplexing is a promising approach enabling fast and cost-efficient screening methods, *e.g.* for determination of inhibitors in complex mixtures or in the field of biomedical research. Although in multiplexed setups the enzymatic activity may be affected by the presence of other substrates and/or enzymes, the expected advantages possibly will predominate. To investigate those effects, we measured multiple enzymatic assays simultaneously. For all conducted measurements, the conversion rate of the substrate(s) was calculated, which reflects the enzymatic activity. The results provide an overview about the susceptibility of the selected enzymes towards diverse factors and a reference point for many applications in analytical chemistry and biotechnology.

(Received February 20, 2012; Accepted April 17, 2012; Published June 10, 2012)

Introduction

Studying enzymatic reactions is of interest since enzymes are involved in several research areas such as pharmaceutics, biotechnology or food industry. Recent studies have established electrospray ionization mass spectrometry (ESI-MS) as an appropriate tool for studying enzymatic reactions since it offers several advantages. The increasing interest in studying enzymatic reactions by MS and the MS-compatibility of enzymatic assays was described in recently published reviews.[1-5] In contrast to UV/Vis- or fluorescence-based detection, mass spectrometric detection is independent of chromogenic and fluorogenic labeled substrates but only depends on the mass-to-charge (m/z) ratio of the ionized analytes. As shown in a recent study, chromogenic labeled substrates may cause altered enzyme specificity compared to unlabeled substrates.[6] Studying enzymatic reactions by MS resulted in the determination of kinetic parameters, reaction pathways or regulator identification.[7-10] Since biological enzymes usually show their full activity only in aqueous media, enzymatic reactions are mostly studied in aqueous solutions. In classical biology, the activities of enzymes are typically lower in non-aqueous systems, this difference is primarily caused by denaturation effects.[11-13] However, the use of organic solvents may be useful in ESI-MS studies due to improved droplet generation in the electrospray interface and better droplet evaporation.[14,15] Recent studies with miniaturized systems showed that addition of organic modifier can be advantageous. In case of nanoESI-MS, aqueous enzyme solutions may pose problems, which can easily be avoided by the addition of an organic solvent as a so-called modifier.[16] Studies with continuous-flow microfluidic assay systems require the systematical research of the impact of organic solvents.[17] Additionally, for several applications in biotechnology and analytical chemistry, the use of organic solvents offers advantages and enables several new applications in industry, these have been discussed in detail in the literature.[12,18] Another promising approach to studying enzymatic reactions is the development of multiplexed assays with two or more different enzymes and their substrates in one single experiment. This can easily be handled by ESI-MS, as long as the compounds have different m/z ratios. UV/Vis-based assays require chromogenic substrates and therefore offer no possibility for simultaneous detection, whereas fluorescence-based assays can be multiplexed as long as the fluorescent substrates or products have different emission bands.[19] A first group working with multiplexed assays was Gerber and coworkers. By means of MS detection, they developed a new method for biomedical applications, in which the activites of two lysosomal enzymes in cell homogenates are simultaneously monitored using specific substrates.[20] Several other multiplexing

† To whom correspondence should be addressed.
E-mail: t.letzel@wzw.tum.de

approaches were described, *e.g.* for determination and characterization of protease activity in the presence of different substrates or for simultaneous determination of the activities of different cytochrome P450 isoforms.[21-23]

A promising application for the use of multiplexed enzymatic assays in combination with organic solvents are online coupled setups, consisting of high performance liquid chromatography (HPLC) combined with a biochemical (enzymatic) detection system. Such setups are applied for screening complex mixtures on potential regulatory compounds. In those analytical systems organic solvents are required for effective chromatographic separation and elution. However, the amount of organic solvents is limited in order to maintain the enzymatic activity. Thus, each single enzyme has to be tested in advance for its compatibility with organic solvent. As reviewed in Kool *et al.*, advances in separation techniques and mass spectrometric detection technology lead to increasing importance of online coupled setups and have already been studied with acetylcholinesterase, phosphodiesterase, cytochrome P450, glutathione-*S*-transferase and cathepsin B.[24-27] An innovative tool for the effective coupling of chromatographic separation with enzymatic screening methods was described by Irth and coworkers who used high-temperature HPLC (HT-HPLC).[28] Compared to conventional HPLC, the amount of organic solvent needed for the separation can be decreased markedly and 10% organic phase is often sufficient for chromatographic separation.[29] Multiplexing enzymatic assays in such online coupled setups would be an attractive possibility for screening of complex mixtures on regulatory substances by means of biochemical detection. Thus, for many applications one must conduct enzymatic assays in the presence of certain amounts of organic solvents. However, to our knowledge no systematic examination about the tolerance of enzymes towards organic solvents or multiplexing assays is available in the literature so far. Therefore, various enzymes were tested systematically on their tolerance to different common organic solvents. Additionally, the compatibility of enzymes towards other enzymatic assays was investigated. Finally a combination of both parameters, organic solvent and multiplexing, was studied regarding their joint influence on enzyme reactivity.

Experimental

Reagents and chemicals

Elastase from human neutrophils (NE, Enzyme Commission (EC) number 3.4.21.37, relative molecular weight (M_w) 30 kDa) was purchased from BioCentrum (Krakow, Poland). Hexa-*N*-acetylchitohexaose ((GlcNAc)$_6$, M_w 1237.2 Da) was obtained from Seikagaku Biobusiness (Tokyo, Japan) and substrate for α-chymotrypsin Ala-Ala-Pro-Phe-pNA (M_w 520.4 Da, with chromogenic group *p*-nitroaniline (pNA)) was obtained from LOXO (Dossenheim, Germany). The following compounds were obtained from Sigma-Aldrich (Steinheim, Germany): Hen egg white lysozyme (HEWL, EC 3.2.1.17, M_w 14 kDa), chitinase from *Streptomyces griseus* (Chi, EC 3.2.1.14, M_w 30 kDa), α-chymotrypsin from bovine pancreas (Chy, EC 3.4.21.1, M_w 25 kDa), acetylcholinesterase from Electrophorus electricus Type VI-S (AChE, EC 3.1.1.7, M_w 280 kDa), elastase from porcine pancreas (PE, EC 3.4.21.36, M_w 25 kDa), substrate for PE *N*-succinyl-Ala-Ala-Ala-pNA (M_w 451.4 Da), substrate for NE *N*-succinyl-Tyr-Leu-Val-pNA (M_w 181.7 Da), acetylcholine chloride (AChCl, M_w 181.7 Da), ammonium acetate (NH_4Ac, M_w 77.1 Da, >98%) and LC-MS reagent water, methanol (MeOH), ethanol (EtOH), isopropanol, acetone and acetonitrile (ACN).

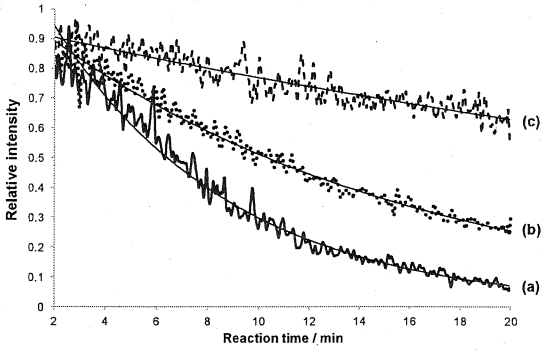

Fig. 1 Determination of Chy activity in 0% (a), 10% (b) and 30% (c) MeOH. Substrate (Ala-Ala-Pro-Phe-pNA) time-courses obtained from the reactions of 5 µM substrate and 1 µM enzyme lead to calculation of the conversion rates. Conversion rate for 0% MeOH is set at 100%, which results in a conversion rate of 52% in the presence of 10% MeOH and a conversion rate of 15% in the presence of 30% MeOH. Relative intensity 1.0 corresponds to absolute intensity of 1.5×10^5 counts for 0% MeOH, 2.9×10^5 counts for 10% MeOH and 5.3×10^5 counts for 30% MeOH, respectively.

Instrumentation

Samples were analyzed by a Triple Quadrupole (Series 6410, Agilent Technologies, Waldbronn, Germany) or an Ion Trap (Finnigan LCQ Duo, Thermo Quest, San Jose, CA), each equipped with an ESI source. The samples were detected in positive ionization mode. Triple Quadrupole samples were analyzed with the Agilent-system specific parameter "fragmentor voltage" of 135 V. Nebulizer was set at 15 psi, drying gas flow at 3 L/min, drying gas temperature at 300°C and capillary voltage at 2500 V. For Ion Trap samples sheath gas flow was set at 0.3 L/min, capillary temperature at 200°C and capillary voltage at 50 V. All samples were detected in full scan mode with a mass range of 80 - 1300 *m/z*.

Sample preparation

Enzyme and substrate solutions were prepared in 10 mM NH_4Ac buffer (pH 7.4). Enzymatic assays were prepared in the following concentrations: 5 µM HEWL with 25 µM (GlcNAc)$_6$, 0.015 µM Chi with 5 µM (GlcNAc)$_6$, 0.15 µM Chy with 5 µM Ala-Ala-Pro-Phe-pNA, 1 µM PE with 5 µM *N*-Suc-Ala-Ala-Ala-pNA, 1 µM NE with 5 µM *N*-Suc-Tyr-Leu-Val-pNA and 0.45 nM AChE with 5 µM AChCl. The influence of several common organic solvents on enzymatic activity was tested by addition of 10 or 30% MeOH, EtOH, ACN, acetone and isopropanol, respectively. Positive control assays were prepared in a reaction tube by mixing enzyme solution with substrate solution. Assays with organic solvents were prepared in the following order: enzyme solution, adding organic solvent, adding substrate solution. For multiplex assays, mixtures of all enzymes and all substrates were prepared and subsequently mixed. Multiplexing assays with the addition of organic solvent were prepared in the following order: organic solvent was added to the mixture of enzymes and immediately mixed with the substrate mixture. All appropriate controls were conducted to prove that there are no interferences between the compounds of different assays. All experiments were performed at least in duplicate and at 20 ± 2°C. After all components were mixed, the samples were immediately infused into the mass spectrometric interface *via* a 100-µL syringe (Hamilton-Bonaduz,

Table 1 Remaining activity in % of enzymatic assays conducted with chitinase, hen egg white lysozyme, elastase from human neutrophils, elastase from porcine pancreas, α-chymotrypsin and acetylcholinesterase by addition of 10 and 30% organic solvents

	Remaining enzymatic activity in % in the presence of									
	MeOH		EtOH		Isopropanol		Acetone		ACN	
	10%	30%	10%	30%	10%	30%	10%	30%	10%	30%
Chitinase (Chi)	57	101	106	55	31	6	42	43	119	62
Hen egg white lysozyme (HEWL)	120	124	58	45	66	94	81	57	52	29
Elastase from neutrophils (NE)	60	12	14	—	32	20	34	13	16	—
Elastase from pancreas (PE)	53	24	18	—	48	14	23	24	22	—
α-Chymotrypsin (Chy)	52	15	11	—	65	16	38	13	8	—
Acetylcholinesterase (AChE)	80	18	23	—	11	—	12	—	16	—

Remaining activity was obtained by calculation of the conversion rate in comparison to the control assay in 10 mM NH_4Ac without addition of organic solvent (—, not determined).

Switzerland) located in a syringe pump (Model 11 Plus, Harvard Apparatus, Hugo Sachs Elektronik, Hugstetten, Germany). The solutions were continuously infused for 20 min with a flow rate of 5 μL/min (Tubing: 1/16" × i.d., 0.13 mm; length, 300 mm).

Data evaluation

The Triple Quadrupole data were processed using the MassHunter Workstation software, Qualitative Analysis (Ver. B02.00 from Agilent Technologies) and the Ion Trap data were processed by using Xcalibur software (Ver. 1.3, Thermo Finnigan). The extracted ion chromatogram (EIC) signals for the HEWL reaction assay were summed for the following compounds: product signals $(GlcNAc)_2$ with *m/z* 425 and 447 and $(GlcNAc)_4$ with *m/z* 831 and 853, *i.e.* $[(GlcNAc)_n+H^+]$ and $[(GlcNAc)_n+Na^+]$. Substrate signal $(GlcNAc)_6$ was summed for $[(GlcNAc)_6+H^+]$ with *m/z* 1237, $[(GlcNAc)_6+2H^+]$ with *m/z* 619 and $[(GlcNAc)_6+Na^+]$ with *m/z* 1259 as described in the literature.[30] The EIC signals of the Chi assay were summed for $[(GlcNAc)_n+H^+]$ and $[(GlcNAc)_n+Na^+]$ for each: $(GlcNAc)_2$ with *m/z* 425 and 447 and $(GlcNAc)_4$ with *m/z* 831 and 853 signal (products), $(GlcNAc)_6$ signal (substrate) $[(GlcNAc)_6+H^+]$ with *m/z* 1237, $[(GlcNAc)_6+2H^+]$ with *m/z* 619 and $[(GlcNAc)_6+Na^+]$ with *m/z* 1259. The signals for the Chy assay were summed for: signals for substrate Ala-Ala-Pro-Phe-pNA with *m/z* 525 $[M+H]^+$ and *m/z* 547 $[M+Na]^+$ and product signals with *m/z* 405 $[M–pNA+H]^+$ and *m/z* 427 $[M–pNA+Na]^+$. The signals for an assay with NE were summed for: substrate signals (*N*-Suc-Tyr-Leu-Val-pNA) with *m/z* 614 $[M+H]^+$ as well as *m/z* 636 $[M+Na]^+$ and product signals with *m/z* 494 $[M–pNA+H]^+$ and *m/z* 516 $[M–pNA+Na]^+$. The signals for an assay with PE were summed for: substrate signals (*N*-Suc-Ala-Ala-Ala-pNA) with *m/z* 452 $[M+H]^+$ as well as *m/z* 474 $[M+Na]^+$ and product signals with *m/z* 332 $[M–pNA+H]^+$ and *m/z* 354 $[M–pNA+Na]^+$. The following signals were analyzed for the AChE assay with the substrate acetylcholine: substrate signal *m/z* 146 $[M]^+$ and product signal *m/z* 104 $[M–CH_3COOH]^+$.

The time-courses were smoothed with a Gaussian function using a 15 points function width and 5.000 points Gaussian width. The time courses show a short delay of about 2 min due to the attended time of manually mixing all compounds, filling and connecting the syringe and the transfer of the sample *via* ESI source to the mass spectrometer.

Calculation of conversion rate

Signal intensities were normalized for calculating conversion rates. The obtained time-courses were extrapolated using an exponential function in Microsoft Excel 2007, resulting in Eq. (1). The starting point was set at 2 min, since at this time point in all measurements a signal was detected after signal delay. The reactions were observed to reach a plateau at a remaining intensity of about 0.05; therefore, this value was set as the end point of the reaction. Using Eq. (1), we calculated conversion rates according to Eq. (2). The calculation of the conversion rate for Chy is shown in Fig. 1.

$$y = a \times \exp(bx) \quad (1)$$

$$\text{Conversion rate } (\text{min}^{-1}) = ([\text{substrate}]/[\text{enzyme}])/(\ln(0.05/a)/b) \quad (2)$$

Results and Discussion

Impact of organic solvent on enzymatic conversion

The effect of organic solvents on enzymatic activity was investigated systematically. Enzymatic assays were carried out in the absence and the presence of organic solvent and monitored by mass spectrometry. As a measure of enzymatic activity, the respective substrate conversion rates were compared. Figure 1 exemplifies the influences of 0, 10 and 30% MeOH on the activity of Chy. The effect of the organic solvent on the enzymatic assay is already apparent, comparing the positive control assay (0%) and the assays with organic solvent (10 and 30%). Numeric values were obtained by calculating conversion rates (Eq. (2)) using an exponential function (Eq. (1)) which is also shown in Fig. 1.

Table 1 reflects the calculated conversion rates of all studied enzymatic assays in the presence of organic solvents. For assays which already had markedly reduced activity in 10% organic solvent, no measurements were conducted with higher organic solvent contents (as indicated by —). Obviously, the influence of solvents on enzymatic activity differs from enzyme to enzyme. This might be explained by diverse effects of organic solvents on enzymes like binding at the enzyme, competition with substrate binding, conformational changes and changes in charge state distribution due to denaturation effects.[31,32] In the presence of organic solvent, nearly all enzymatic reactions show a decreased conversion rate. Exceptions are the glycosidases HEWL and Chi, exhibiting conversion rates >100% with MeOH (HEWL) or EtOH and ACN (Chi), respectively. Generally, increasing the organic solvent content from 10 to 30% is associated with a decrease of enzymatic activity, except for Chi with MeOH and HEWL with isopropanol where the activity in 30% is distinctly higher than in 10% organic solvent. In fact, it has been reported that there often is no linear correlation between enzymatic activity and concentration of organic solvent

but that at specific concentrations of solvent even a stimulation of enzymatic activity can be observed.[31,33] The proteases NE, PE and Chy show similar responses to the different organic solvents, which may be explained by their similar active sites and similar molecular weights. Adding 10% MeOH to the protease assays results in remaining activities between 52 and 60%, whereas in 30% MeOH the activities are decreased markedly. EtOH, ACN and acetone are quite poorly tolerated; the activity of the proteases is considerably reduced. The influence of organic solvents on Chy activity was also evaluated by Khmelnitsky *et al.*[34] and Ogino *et al.*[35] In their studies, they used parameters such as "c_{50}" or "half-life" values for assessing the enzymatic activity. Thereby, the concentration of the organic solvent is determined at which a half inactivation of the enzyme occurs. Both determined a reduced Chy activity in the presence of MeOH and other organic solvents.

AChE seems to be most susceptible to organic solvents; only in case of 10% MeOH is there a remaining activity of 80%; all other solvents decrease the activity below 25% even in a concentration of 10%. Also Ingkaninan *et al.* as well as Rhee *et al.* showed that the AChE activity is reduced to less than 60 or 90 in 10% MeOH, respectively.[36,37] They also studied the influence of ACN on AChE. The group of Rhee *et al.* detected a remaining activity of 50% in the presence of 10% ACN, whereas Ingkaninan *et al.* only measured 10% residual activity, which is in accordance with the current results. Rhee *et al.* detected higher activities for both solvents; their result may be explained by differences in the substrate solution. In the case of Rhee *et al.* the substrate was dissolved in 30% MeOH, whereas in the cases of Ingkaninan *et al.* and this study, the substrate was dissolved in buffer.

Summing up the results, a low amount of MeOH seems to be the best tolerated organic solvent similar to other biological techniques where, for example, weak influence on the dissociation of noncovalent protein complexes was proved (unpublished data). However, the tested enzymes show distinct differences in their tolerance to MeOH and the other organic solvents. The glycosidases HEWL and Chi seem to be quite unsusceptible to organic modifiers in the set of tested enzymes, with HEWL even showing increased activity in the presence of 30% MeOH. Even in MeOH concentrations of up to 80% the enzyme HEWL still exhibits significant enzymatic activity (data not shown).

Enzymes of the same subclass and with same/similar active sites show similar behavior in the presence of organic solvents *e.g.* the glycosidases (HEWL and Chi) or the proteases Chy, NE and PE, respectively. Unfortunately, no obvious trend can be observed regarding the polarity or the dielectric constant of solvents. The impact of organic solvents on enzymatic activity concerning the polarity and hydrophobicity was discussed in the literature quite contradictory.[34,38,39] In fact, there seems to be some confusion about the use of the terms polarity and hydrophobicity, which complicates the interpretation of the literature data even more. In recent years several research groups attempted to find appropriate approaches to predict the influence of an organic solvent on enzymatic activity. Parameters which describe this effect were for instance the partition coefficient,[34,39] the denaturation capacity[34] or the polarity index.[38] These parameters may be used as reference points, but in accordance with the current data, it also seems to be necessary to study the influence on each enzyme individually. Thus, automated and even better miniaturized reaction systems are a useful tool for screening the solvent tolerance, *e.g.* in direct coupling with mass spectrometry.[16]

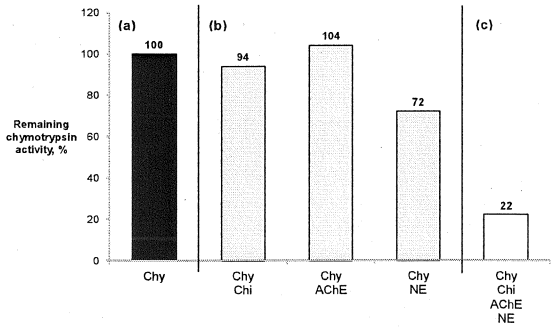

Fig. 2 Remaining activity of Chy in % in multiplexed assays. Chy-assay was conducted as single assay (a) and in combination with a second assay (b) with Chi, AChE and NE as well as in a multiplexed approach with all four assays (c).

Impact of multiplexing on enzymatic conversion

The influence of other enzymatic assays on Chy-activity was tested in order to elucidate the possibility of multiplex approaches. Such multiplexing experiments were performed with two or four enzymatic assays in parallel. Therefore first of all, appropriate reaction conditions for all enzymatic assays have to be chosen, *i.e.* pH, buffer, temperature and concentrations. All parameters have to be adjusted in a way that each single enzymatic assay retains sufficient activity, even if the parameters are not in strict conformity with the enzyme optimum. According to the literature and to preliminary tests, the pH was set at 7.4, the buffer was 10 mM NH_4Ac and the reactions were carried out at room temperature.[8,16,30] The concentrations of enzyme and substrate were adjusted in order to obtain a substrate decrease and product formation within a 20-min reaction time. The assortment of the substrates is a further criterion for multiplexing assays since mass spectrometric detection is dependent on the *m/z* values of the analytes. All used substrates and resulting products have different *m/z* values as described in *Data evaluation*.

In the current study, several multiplexed assays were carried out with the protease Chy and the resulting conversion rates were monitored and calculated (Fig. 2). Control experiments were carried out for all combinations, *i.e.* the substrate for Chy was measured with all available enzymes and substrates separately. In these controls, no decrease of substrate was observed. Initially, combinations of two complete assays were monitored, *i.e.* Chy-assay with Chi-assay, with NE-assay or with AChE-assay, respectively (Fig. 2b). The conversion rate for Chy in the multiplexed assay with Chi is reduced by 6% in comparison to the single Chy-assay. The combination of Chy and AChE leads to a conversion rate 4% higher than the rate in the single Chy-assay. In both cases, the conversion rate differs only marginally from the single Chy-assay. In contrast, the combination of Chy and NE leads to a distinct reduction of the Chy activity by 28% in comparison to the result for single Chy-assay. The diverse impact on Chy-activity may be explained by the characteristics of the used enzymes and substrates. The enzymes Chy, Chi, AChE and NE all belong to the enzyme class of hydrolases. Regarding the subclasses and sub-subclasses, Chy and NE are peptidases (EC 3.4.) or rather serine endopeptidases (EC 3.4.21.). Chi belongs to glycosidases (EC 3.2.) and AChE to the subclass acting on ester bonds (EC 3.1.). Peptidases Chy and NE have the same active sites with the amino acids histidine, aspartic acid and serine whilst the

active sites of the enzymes Chi and AChE consist of completely different amino acid compositions. Chy and NE-assay were conducted with similar substrates, which are comprised of four amino acids and the chromogenic group pNA. The substrate for Chi is a hexasaccharide and that for AChE is the ester acetylcholine. This study found that enzymatic assays with similar enzymes and substrates have greater influences on each other than enzymes of different subclasses and completely different substrates. Measuring the Chy-assay with solely NE or rather substrate for NE led to further information about the NE-influence on Chy activity. Chy-assay in the presence of NE substrate led to a conversion rate for Chy-assay that decreased by 14%, whereas the Chy-assay in the presence of NE leads to conversion rate about three times lower than that in the single assay (conversion rate 37%). Hence Chy activity in the presence of NE-assay seems to be impaired more strongly by the enzyme than by the NE substrate. In the presence of the complete NE assay, the Chy activity is higher (72%) than in the presence of NE alone (37%), so the NE substrate seems to reduce the influence of NE, most possibly due to the binding of the substrate to NE. Regarding the multiplexed experiments of two assays, *vice versa* the same behavior of the enzymes can be observed. In the presence of Chy-assay, the conversion rate of Chi is 78% and for AChE 103%, whereas again multiplexing of the NE-assay with the Chy-assay leads to a conversion rate of 38% for NE (data not shown).

The current results are in accordance with a multiplexing study of Karst and coworkers, who aimed at a mass spectrometric determination of the enzymatic activity of two enzymatic assays in parallel.[19] They used enzymes of different classes and observed very similar development of the reaction product in the single assays as well as in the multiplexed approach. They therewith proved that the two enzymatic reactions do not interfere.

In a next step, four enzymatic assays with Chy, Chi, AChE and NE were performed in a multiplexed assay (Fig. 2c). The conversion rate of Chy is reduced almost fourfold in comparison to the multiplexing of two assays. So the three assays seem to have a synergistic effect on Chy-activity. This observation is in accordance with an experiment of Dixit *et al.*, who developed multiplexed assays for simultaneous determination of the activity of cytochrome P450 (CYP) enzymes.[23] They used specific substrates for seven CYP isoenzymes and detected the resulting metabolites by HPLC-MS. When combining all seven assays in a single experiment they observed an inhibition of 10 and 40% of the activity of two CYP isoenzymes, respectively. The inhibition was eliminated by splitting the assays into two groups of assays. This supports the current results that enzymatic assays, especially with resembling enzymes, cannot be multiplexed in any way. Researchers need to test individually up to which amount assays can be multiplexed and which assays are combinable. On the other hand, systematic studies on the influence and regulation of interfering assays may lead to novel basic mechanistic knowledge of protein activities.

Impact of both organic solvent and multiplexing on enzymatic conversion

Finally, the impact of organic solvent and multiplexing assays on Chy-activity was tested by merging the previous approaches. The four enzymatic assays with Chy, Chi, AChE and NE were conducted in parallel in the presence of 10% MeOH, EtOH, ACN, isopropanol and acetone, respectively (Fig. 3b). In all cases, the conversion rate of Chy is reduced between four- and fivefold compared to the single Chy-assay (Fig. 2a). Addition of 10% MeOH to the combination of all four assays leads to no further reduction of the conversion rate in comparison to the four assays in buffer. Addition of the other organic solvents reduces the conversion rate further in comparison to the multiplexing of four assays in buffer. When adding 10% organic solvent to the single Chy-assay, isopropanol is the best tolerated solvent, followed by MeOH, acetone, EtOH and ACN. The multiplexed assay with all four assays in the presence of 10% organic solvent shows another order of susceptibility, namely MeOH, EtOH, acetone, isopropanol and ACN.

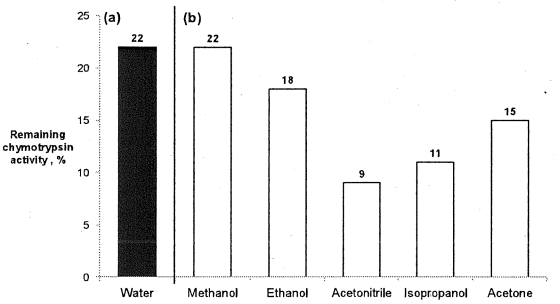

Fig. 3 Remaining activity of Chy in % in multiplexed assays and in the presence of 10% organic solvent. Chy-assay was measured in a multiplexed assay with three other enzymatic assays, *i.e.* Chi, AChE and NE (a). This multiplexed assay was measured in the presence of 10% organic solvent (MeOH, EtOH, ACN, isopropanol and acetone) (b).

This result supports the statement that no general prediction can be made about the influence of organic solvents on enzymatic activity. Only ACN leads to analog results, since as in the single assay, also in the multiplexed approach that is the worst tolerated.

Concluding, simultaneous multiplexing of enzymatic assays and addition of organic solvent impair the enzymatic activity. However, in all cases the substrate consumption and a simultaneous product formation could be monitored. Thus, screening a large number of enzymes is possible for studying reaction pathways or solely determination of enzymatic activity. In this case multiple assays can be carried out in the presence of organic solvent and/or in a multiplexed assay.

Conclusions

The effect of common organic solvents and multiplexed assays on enzymatic activity was studied systematically by calculating the respective conversion rates. Summing up the results, obviously no general rule can be established to predict the susceptibility of an enzyme towards organic solvents, but rather the enzymes and organic solvents have to be tested individually as presented in this study. The obtained information about the suitability of an organic solvent with an enzyme may be useful for diverse analytical systems, *e.g.* for HT-HPLC or hydrophilic interaction chromatography in which 10% MeOH may be sufficient for effective chromatographic separation. Additionally, a small amount of organic modifier represents an improvement for the generation and especially for the desolvation of droplets produced by electrospray sources. In multiplexing experiments the enzymatic activity is marginally reduced in double assays. When multiplexing more than two assays and in the presence of organic solvents, the enzymatic activity is markedly reduced. The data obtained in this study provide an important overview

for further applications in biotechnology and for bioanalytical chemistry with automated nanoESI setups as a basis for screening enzymes.

Acknowledgements

This work was supported by the German Federal Ministry of Economics and Technology within the agenda for the promotion of industrial cooperative research and development based on a decision of the German Bundestag. The access was organized by the Arbeitsgemeinschaft industrieller Forschungsvereinigungen, Köln (Project No. 16203 N). The authors would like to thank Agilent Technologies for the Triple Quadrupole as a loan and Bayerisches Landesamt für Umwelt for the Ion Trap as a gift.

References

1. T. Letzel, *Anal. Bioanal. Chem.*, **2008**, *390*, 257.
2. A. R. de Boer, H. Lingeman, W. M. A. Niessen, and H. Irth, *Trac-Trends Anal. Chem.*, **2007**, *26*, 867.
3. K. D. Greis, *Mass Spectrom. Rev.*, **2007**, *26*, 324.
4. A. Liesener and U. Karst, *Anal. Bioanal. Chem.*, **2005**, *382*, 1451.
5. J. Grassmann, R. K. Scheerle, and T. Letzel, *Anal. Bioanal. Chem.*, **2012**, *2*, 625.
6. T. Letzel, E. Sahmel-Schneider, K. Skriver, T. Ohnuma, and T. Fukamizo, *Carbohydr. Res.*, **2011**, *346*, 863.
7. N. Dennhart, T. Fukamizo, R. Brzezinski, M. E. Lacombe-Harvey, and T. Letzel, *J. Biotechnol.*, **2008**, *134*, 253.
8. N. Dennhart, L. M. M. Weigang, M. Fujiwara, T. Fukamizo, K. Skriver, and T. Letzel, *J. Biotechnol.*, **2009**, *143*, 274.
9. X. Ge, T. L. Sirich, M. K. Beyer, H. Desaire, and J. A. Leary, *Anal. Chem.*, **2001**, *73*, 5078.
10. D. B. Northrop and F. B. Simpson, *Bioorg. Med. Chem.*, **1997**, *5*, 641.
11. S. H. Krishna, *Biotechnol. Adv.*, **2002**, *20*, 239.
12. A. M. Klibanov, *Nature*, **2001**, *409*, 241.
13. H. Ogino and H. Ishikawa, *J. Biosci. Bioeng.*, **2001**, *91*, 109.
14. P. Kebarle and U. H. Verkerk, *Mass Spectrom. Rev.*, **2009**, *28*, 898.
15. A. R. de Boer, T. Letzel, H. Lingeman, and H. Irth, *Anal. Bioanal. Chem.*, **2005**, *381*, 647.
16. R. Scheerle, J. Grassmann, and T. Letzel, *Anal. Methods*, **2011**, *3*, 822.
17. A. R. de Boer, B. Bruyneel, J. G. Krabbe, H. Lingeman, W. M. A. Niessen, and H. Irth, *Lab Chip*, **2005**, *5*, 1286.
18. M. N. Gupta, *Eur. J. Biochem.*, **1992**, *203*, 25.
19. C. Hempen, A. Liesener, and U. Karst, *Anal. Chim. Acta*, **2005**, *543*, 137.
20. S. A. Gerber, C. R. Scott, F. Turecek, and M. H. Gelb, *J. Am. Chem. Soc.*, **1999**, *121*, 1102.
21. A. Liesener and U. Karst, *Analyst*, **2005**, *130*, 850.
22. A. Liesener, A. M. Perchuc, R. Schoni, M. Wilmer, and U. Karst, *Rapid Commun. Mass Spectrom.*, **2005**, *19*, 2923.
23. V. Dixit, N. Hariparsad, P. Desai, and J. D. Unadkat, *Biopharm. Drug Dispos.*, **2007**, *28*, 257.
24. C. F. de Jong, R. J. E. Derks, B. Bruyneel, W. Niessen, and H. Irth, *J. Chromatogr., A*, **2006**, *1112*, 303.
25. J. Kool, M. Giera, H. Irth, and W. M. A. Niessen, *Anal. Bioanal. Chem.*, **2011**, *399*, 2655.
26. T. Schenk, J. Breel, P. Koevoets, S. van den Berg, A. C. Hogenboom, H. Irth, U. R. Tjaden, and J. van der Greef, *J. Biomol. Screen.*, **2003**, *8*, 421.
27. A. R. de Boer, T. Letzel, D. A. van Elswijk, H. Lingeman, W. M. A. Niessen, and H. Irth, *Anal. Chem.*, **2004**, *76*, 3155.
28. A. R. de Boer, J. M. Alcaide-Hidalgo, J. G. Krabbe, J. Kolkman, C. N. V. Boas, W. M. A. Niessen, H. Lingeman, and H. Irth, *Anal. Chem.*, **2005**, *77*, 7894.
29. T. Teutenberg, *High-Temperature Liquid Chromatography—A User's Guide for Method Development*, **2010**, Royal Society of Chemistry.
30. N. Dennhart and T. Letzel, *Anal. Bioanal. Chem.*, **2006**, *386*, 689.
31. L. G. Butler, *Enzyme Microb. Technol.*, **1979**, *1*, 253.
32. M. Samalikova and R. Grandori, *J. Mass Spectrom.*, **2005**, *40*, 503.
33. R. Batra and M. N. Gupta, *Biotechnol. Lett.*, **1994**, *16*, 1059.
34. Y. L. Khmelnitsky, V. V. Mozhaev, A. B. Belova, M. V. Sergeeva, and K. Martinek, *Eur. J. Biochem.*, **1991**, *198*, 31.
35. H. Ogino, Y. Gemba, Y. Yutori, N. Doukyu, K. Ishimi, and H. Ishikawa, *Biotechnol. Prog.*, **2007**, *23*, 155.
36. I. K. Rhee, N. Appels, T. Luijendijk, H. Irth, and R. Verpoorte, *Phytochem. Anal.*, **2003**, *14*, 145.
37. K. Ingkaninan, C. M. de Best, R. van der Heijden, A. J. P. Hofte, B. Karabatak, H. Irth, U. R. Tjaden, J. van der Greef, and R. Verpoorte, *J. Chromatogr., A*, **2000**, *872*, 61.
38. M. N. Gupta, R. Batra, R. Tyagi, and A. Sharma, *Biotechnol. Prog.*, **1997**, *13*, 284.
39. C. Laane, S. Boeren, K. Vos, and C. Veeger, *Biotechnol. Bioeng.*, **1987**, *30*, 81.

Appendix V

Lysozyme Superfamily: Progress in Functional Analysis using ESI-MS and NMR Spectroscopy

Shinya, S., Ohnuma, T., Brzezinski, R., Scheerle, R.K., Grassmann, J., Letzel, T. and Fukamizo, T.

In: Maang, X.G. and Cheung, W.F. (Ed.), Lysozymes: Sources, Functions and Role in Disease, Nova Science Publishers, *2012, 127-154*

The review gives an overview of recent NMR and ESI-MS developments and studies of enzymes belonging to the lysozyme superfamily. The manuscript was a collaborative work with the group of T. Fukamizo. I prepared the part of the manuscript concerning the ESI-MS resarch.

Chapter

LYSOZYME SUPERFAMILY: PROGRESS IN FUNCTIONAL ANALYSIS USING ESI-MS AND NMR SPECTROSCOPY

Shoko Shinya[1], Takayuki Ohnuma[1], Ryszard Brzezinski[2], Romy K. Scheerle[3], Johanna Grassmann[3], Thomas Letzel[3] and Tamo Fukamizo[1]

[1]Department of Advanced Bioscience, Kinki University, Japan
[2]Département de Biologie, Centre d'Étude et de Valorisation de la Diversité Microbienne, Université de Sherbrooke, Canada
[3]Analytical Research Group, Wissenschaftszentrum Weihenstephan, Technische Universität München, Freising, Germany

ABSTRACT

Lysozymes, chitinases, and chitosanases hydrolyze different polysaccharides, cell wall peptidoglycan, chitin, and chitosan, respectively. However, these enzymes have been recognized to represent a lysozyme superfamily, because they share a similar core structure consisting of two α-helices and a three-stranded β-sheet in their catalytic cleft. Recently, the mode of action toward chitin and chitosan oligosaccharides of these enzymes was investigated using a sophisticated ESI-MS system, which enabled speedy determination of the time-course of the oligosaccharide hydrolysis and quantitative determination of the oligosaccharide-binding. The oligosaccharide-binding mode was also examined using modern NMR techniques, including signal assignments based on three-dimensional NMR spectra and chemical shift perturbations of ^{1}H-^{15}N HSQC signals caused by the oligosaccharide-binding. These studies afforded novel information on the molecular mechanism of the substrate-binding of the enzymes belonging to the lysozyme superfamily.

Keywords: lysozyme superfamily, chitinase, chitosanase, ESI-MS, NMR, oligosaccharide binding

ABBREVIATIONS

GlcNAc, *N*-acetyl-D-glucosamine;
MurNAc, *N*-acetyl muramic acid;
$(GlcNAc)_n$, β-1,4-linked oligosaccharide of GlcNAc with a polymerization degree of n;
GlcN, D-glucosamine;
$(GlcN)_n$, β-1,4-linked oligosaccharide of GlcN with a polymerization degree of n;
HEWL, Hen egg white lysozyme;
ESI-MS, electrospray ionization mass spectrometry;
NMR, nuclear magnetic resonance;
HSQC, two-dimensional heteronuclear single quantum correlation;

1. INTRODUCTION

Lysozymes are widely distributed in living organisms, and play an important role in self-defense by destroying the cell walls of pathogenic bacteria upon invasion [1]. The enzymes hydrolyze the β-1,4-glycosidic linkage between *N*-acetylmuramic acid (MurNAc) and *N*-acetyl-D-glucosamine (GlcNAc) of the peptidoglycan chains in bacterial cell walls [2]. Some lysozymes can also hydrolyze β-1,4-glycosidic linkages of chitin, β-1,4-linked polysaccharide of GlcNAc. Three-dimensional structure of a lysozyme from hen egg white (HEWL) was solved by X-ray crystallography and published in 1965 [3]. This was the first visualization of an enzyme structure. The crystal structure of HEWL in a complex with a substrate analogue, the chitin trimer $(GlcNAc)_3$, was also reported in 1967, and the enzymatic mechanism was deduced based on the complex structure [4]. Most researchers working on glycosyl hydrolases have referred to the textbook mechanism for lysozyme catalysis, when they discuss the function of their own enzyme. However, the catalytic mechanism of HEWL has long been controversial [5]. In addition, lysozymes are classified into six types, c(chicken)-type, g(goose)-type, phage-type, i(invertebrate)-type, bacteria-type, and plant-type, based on similarity in amino acid sequences [6-11], and the activity and specificity toward polysaccharide substrates differ according to the lysozyme-type. C-type lysozymes hydrolyze chitin in addition to peptidoglycan, but the phage-type enzymes are active only toward the cell wall substrate [12]. G-type lysozymes hydrolyze both chitin and cell wall polysaccharides, but are much more active toward the cell wall substrate. Transglycosylation activity was found in c-type lysozymes [13], but not in the g-type and phage-type enzymes. Thus, the mechanisms of action of lysozymes should be reviewed based on comparisons between the various types.

Enzymes belonging to GH19 (chitinase), GH22 (c-type lysozyme), GH23 (g-type lysozyme), GH24 (phage-type lysozyme), and GH46 (chitosanase) [14] hydrolyze the β-1,4-glycosidic linkages of related polysaccharides, such as chitin, peptidoglycan, and chitosan (β-1,4-linked polysaccharide of glucosamine (GlcN)), respectively [15-17]. However, these enzymes have been recognized to represent a superfamily, the so-called lysozyme superfamily, because they share a structurally invariant core consisting of two helices and a three-stranded β-sheet which form the catalytic cleft, as shown in Figure 1 [18]. The common structural feature suggests that these enzymes are evolutionarily derived from a common

ancestor, a single enzyme [19, 20]. During this evolutionary process, mutations of the ancestral enzyme would have produced various proteins differing in specificity. Thus, closer examination of the structure-function relationship of these enzymes might afford information on a strategy for producing enzymes possessing desired specificity. On the other hand, these enzymes except GH22 and GH24 enzymes are not fully characterized with respect to the mechanism of substrate-binding and catalysis. Since the 1960s, GH22 and GH24 enzymes have been studied by using X-ray crystallography and a large amount of data including the structures of enzyme-substrate complexes has been accumulated [21-25]. However, reports on the crystal structure of enzyme-ligand complexes of GH19, GH23, and GH46 enzymes are quite limited. A couple of structures for GH19 and GH23 enzyme complexes have been reported very recently [26, 27], but they are in nonproductive complexes, which do not undergo a catalytic reaction. No structural data for GH46 enzyme complexes have been reported yet. This situation has delayed achieving a full understanding of the substrate-binding and recognition mechanisms of the enzymes. In recent years, we have successfully obtained information on the oligosaccharide-binding mode of these enzymes based on the time-course of oligosaccharide hydrolysis obtained by real-time ESI-MS. In addition, oligosaccharide titration experiments using nuclear magnetic resonance (NMR) spectroscopy have successfully produced information on the substrate-binding mode [28, 29]. In this article, we review the ESI-MS and NMR data for the mode of action of the enzymes belonging to the lysozyme superfamily, GH23 g-type lysozymes, GH19 chitinases, and GH46 chitosanases. The data for individual enzymes are discussed based on comparisons between the GH families.

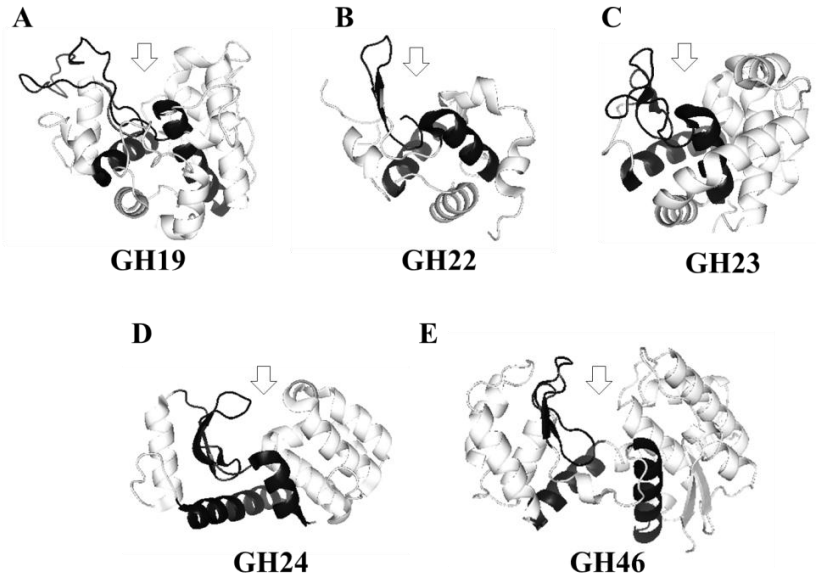

Figure 1. Crystal structures of the enzymes belonging to a lysozyme-superfamily. A, GH19 chitinase (PDB: 2BAA); B, GH22 lysozyme (PDB: 1IEE); C, GH23 goose-type lysozyme (PDB: 153L); D, GH24 phage-type lysozyme (PDB: 3FA0) E, GH46 chitosanase (PDB: 1CHK). The arrows indicate the oligosaccharide-binding cleft of the individual enzymes.

2. ENZYMATIC REACTIONS WITH OLIGOSACCHARIDES DETERMINED BY ESI-MS

Mass spectrometric methods have been used increasingly for analyzing enzymatic reactions [30-38]. In recent years a variety of glycoside hydrolases, such as HEWL, chitinases, and chitosanases, have been investigated by ESI-MS. Mass spectrometric experiments well complement conventional techniques for analyzing enzymatic reactions, such as photometric, fluorimetric, radioisotopic and electrochemical strategies [39]. ESI-MS results are in good agreement with those obtained using the conventional techniques. In conventional spectroscopic detection methods, synthetic substrates labeled with chromophoric groups have to be used, whereas mass spectrometry is independent of substrate labeling. This is of enormous advantage, because chromophoric groups can affect the behavior of enzymatic reactions, especially substrate specificity [33, 40]. In mass spectrometry, oligosaccharide substrates consisting of GlcNAc can be used as "natural" substrates for lysozymes and chitinases, and those consisting of GlcN can be used for chitosanases. Mass spectrometry offers the possibility for simultaneous detection of substrates, intermediates, products, and sometimes the enzyme itself, as well as noncovalently bound complexes. Real-time monitoring using mass spectrometry is therefore an excellent technique, since the amounts of all reaction species participating in the reaction can be monitored during the enzymatic reaction in a continuous-flow strategy [34, 41]. New techniques in coupling continuous-flow assays with a sample introduction part, such as upstream liquid chromatographic separation, have also been developed for studying inhibitors and noncovalent enzyme-ligand complexes [42, 43]. Moreover, high sensitivity of the mass spectrometers enables measurements with low concentrations of the enzyme and the substrate [44].

Table 1 provides an overview of recent ESI-MS studies with glycoside hydrolases. When studying enzymatic assays with GH22 HEWL, GH19 chitinases, and GH46 chitosanases in ESI-MS setups, several parameters, such as the composition and concentration of the salt buffer, pH, reaction temperature, and concentrations of reaction spiecies, were systematically optimized to improve mass spectrometric sensitivity and maintain the enzymatic activity. [41, 44]. These experiments with different setups showed that the enzymes are easy to handle in ESI-MS assays [44-46]. The forthcoming sections review the experimental data for time-course analyses of the enzymatic hydrolysis of different oligosaccharide substrates and determination of noncovalent enzyme-ligand complexes using the enzymes mentioned above.

2.1. Mode of Action of Lysozyme, Chitinases and Chitosanases

2.1.1 Time-Courses of a GH-22 HEWL-Catalyzed Reaction

The hydrolysis of $(GlcNAc)_n$ (n = 3-6) by HEWL was the first reaction with an enzyme of the lysozyme superfamily whose time-course was determined by ESI-MS [41, 47]. The course of the enzymatic reaction was obtained by a single real-time experiment without quenching of the reaction prior to detection. The main products from the hydrolysis of $(GlcNAc)_6$ were $(GlcNAc)_4$ and $(GlcNAc)_2$, with $(GlcNAc)_3$ produced only in a small amount (Figure 2).

Table 1. Overview of researches on lysozyme, chitinases and chitosanases carried out by ESI-MS measurements

Enzyme		Abbreviations	GH Family	Investigations with ESI-MS	References
Lysozymes					
	lysozyme from hen egg white	HEWL	GH22	reaction time-course, systematic optimization of mass spectrometric parameters, noncovalent complexes, experiments in miniaturized and automated systems	[41, 44, 45, 47, 57-61]
Chitinases					
	Nicotiana tabacum	NtChiV*	GH18	reaction time-course	own unpublished data
	Arabidopsios thaliana	AtChiC*	GH18	reaction time-course	own unpublished data
	Cycas revoluta	CrChiA*	GH18	reaction time-course inhibitor studies activity of mutants	[52]
	rye seed	RSC-c	GH19	reaction time-course	own unpublished data
	barley seeds	Chi26	GH19	reaction time-course, noncovalent complexes, activity of mutants, reaction with chromophoric substrate	[40, 47]
	Bryum coronatum	BcChiA	GH19	reaction time-course	own unpublished data
	Streptomyces griseus	ChiC	GH19	reaction time-course	[44, 45]
Chitosanases					
	Streptomyces sp. N174	Csn N174	GH46	reaction time-course, activity of mutants	[55]
	Amycolatopsis orientalis	CsxA*	GH2	reaction time-course	[55]
	Paenibacillus sp. 1794	Csn1794*	GH8	reaction time-course	own unpublished data

*This chapter does not deal with GH18 chitinases, NtChiV and AtChiC, but deals with CrChiA (GH18), CsxA (GH2), and Csn1794 (GH8) for comparison.

HEWL hydrolyzed $(GlcNAc)_5$ mainly into $(GlcNAc)_4$+GlcNAc and less frequently into $(GlcNAc)_2$+$(GlcNAc)_3$. $(GlcNAc)_4$ was cleaved into $(GlcNAc)_3$+GlcNAc and less frequently into $(GlcNAc)_2$+$(GlcNAc)_2$. $(GlcNAc)_3$ was not hydrolyzed by HEWL. The latter result can be explained by the nonproductive complex formed between HEWL and $(GlcNAc)_3$ [48]. The rate of degradation by HEWL depends on substrate chain length, increasing from $(GlcNAc)_4$ to $(GlcNAc)_5$ and $(GlcNAc)_6$ [47]. The time-courses obtained by the single real-time experiments confirmed that the binding cleft of HEWL was composed of subsites from -4 to +2, as demonstrated by X-ray crystallography [4]. The profiles of these time-courses are basically in agreement with results of TLC and HPLC experiments [49].

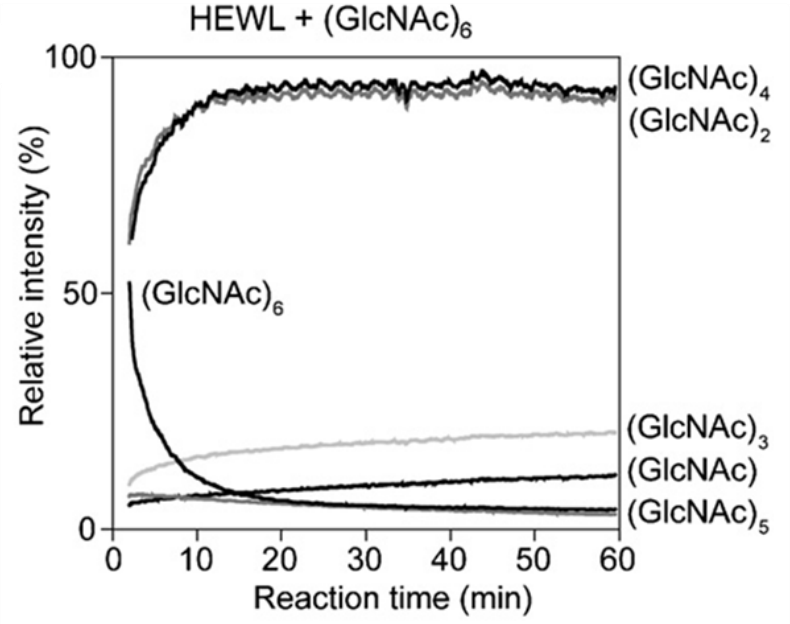

Figure 2. Real-time ESI-MS monitoring of $(GlcNAc)_6$ hydrolysis catalyzed by GH22 HEWL. The enzymatic reaction was carried out in 10 mM ammonium acetate buffer pH 5.2 at 20 ^{o}C. Concentrations of HEWL and the substrate $(GlcNAc)_6$ were 5.0 μM and 25.0 μM, respectively. The relative intensity 100% corresponds to 1.9 x 10^6 counts.

The enzymatic activity in mass spectrometric experiments is typically lower than that obtained in HPLC measurements, probably due to the different assay conditions for ESI-MS, *e.g.* temperature, lower enzyme and substrate concentrations, and buffer conditions [49, 50]. An important difference between ESI-MS and HPLC results is the lack of transglycosylation in ESI-MS experiments [47]. Transglycosylation takes place when the acceptor oligosaccharide molecules attack the transition state formed after cleavage of the β-1,4-glycosidic linkage, instead of a nucleophilic water molecule, and is often found in anomeric form-retaining glycosyl hydrolases including HEWL [16]. The concentration of the substrate $(GlcNAc)_6$ was 1-5 mM in the HPLC experiments with UV detection at 220 nm, whereas in ESI-MS experiments only 10-25 μM (40-fold to hundred-fold lower) is sufficient for the detection of all compounds [44, 45, 49, 50]. This situation might be responsible for the lack of transglycosylation [47].

2.1.2 Time-Courses of GH19 and GH18 Chitinase-Catalyzed Hydrolsyis

Chi26, a GH19 chitinase from barley, *Horduem vulgare* L., seeds, was the first chitinase characterized by an ESI-MS method [47]. The enzyme consists of two α-rich lobes, which bulge out from the "core region" of the enzyme forming a cleft responsible for oligosaccharide-binding and hydrolysis (Figure 1A). The binding cleft of the chitinase appears to be more extended vertically than that of HEWL (Figure 1B), due to the larger molecular mass. Substrate $(GlcNAc)_6$ was cleaved into $(GlcNAc)_3$+$(GlcNAc)_3$ and into $(GlcNAc)_2$+$(GlcNAc)_4$ with almost equal frequency, as shown in Figure 3. Chi26 cleaved $(GlcNAc)_5$ into $(GlcNAc)_3$+$(GlcNAc)_2$, but the oligosaccharides $(GlcNAc)_4$, $(GlcNAc)_3$ and $(GlcNAc)_2$ were not cleaved [47]. The results are consistent with those obtained using an HPLC system with UV detection at 220 nm [51]. For comparative purposes, we determined the time-course of hydrolysis of a GH18 chitinase from cycad (CrChiA) by ESI-MS [52]. In contrast to GH19 chitinases, GH18 chitinases have a $(\alpha/\beta)_8$ barrel fold as a catalytic module [53]. In spite of the structural difference between GH19 and GH18 chitinases, the profile of the time-course obtained for CrChiA (Figure 4) was similar to that for the GH19 enzyme (Figure 3). In this case, however, the splitting to $(GlcNAc)_3$+$(GlcNAc)_3$ appears to be more frequent than that to $(GlcNAc)_2$+$(GlcNAc)_4$. Using $(GlcNAc)_4$ as a substrate, CrChiA produced only $(GlcNAc)_2$. An HPLC analysis of the reaction products from CrChiA revealed that $(GlcNAc)_4$ is converted into $(GlcNAc)_2$ and $(GlcNAc)_3$ without the formation of GlcNAc. Similarly, $(GlcNAc)_6$ was converted into $(GlcNAc)_2$, $(GlcNAc)_3$, $(GlcNAc)_4$, and $(GlcNAc)_5$ without the formation of GlcNAc.

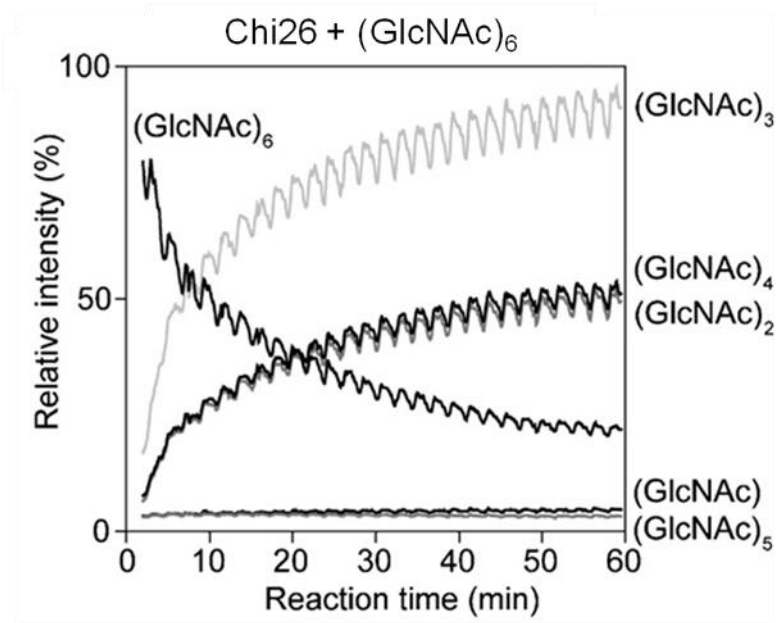

Figure 3. Real-time ESI-MS monitoring of $(GlcNAc)_6$ hydrolysis catalyzed by GH19 Chi26. The enzymatic reaction was carried out in 10 mM ammonium acetate buffer pH 5.2 at 20 ^{o}C. Concentrations of Chi26 and the substrate $(GlcNAc)_6$ were 0.50 μM and 25.0 μM, respectively. The relative intensity 100% corresponds to 8.5 x 10^5 counts.

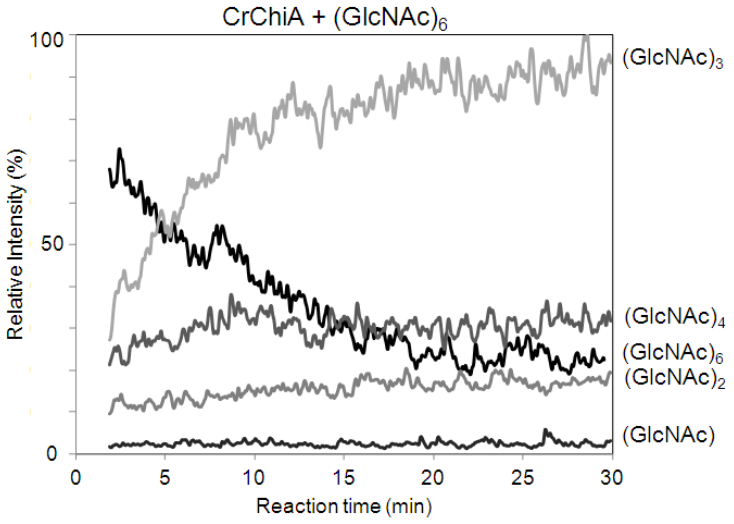

Figure 4. Real-time ESI-MS monitoring of $(GlcNAc)_6$ hydrolysis catalyzed by GH18 CrChiA. The enzymatic reaction was carried out in 10 mM ammonium acetate buffer pH 5.2 at 20 °C. Concentrations of CrChiA and the substrate $(GlcNAc)_6$ were 0.10 μM and 25.0 μM, respectively.

The unusual product distributions obtained by HPLC were explained by a transglycosylation reaction catalyzed by CrChiA [52]. Obviously, the product distribution obtained by HPLC is considerably different from that obtained by ESI-MS. As already described in the last paragraph of section 2.1.1, the ESI-MS results clearly indicate again that no transglycosylation reaction takes place under the ESI-MS conditions. The much lower substrate concentration suppresses the transglycosylation activity.

In recent studies, time-courses of the reaction catalyzed by other GH-19 chitinases, ChiC (chitinase C from *Streptomyces griseus*), RSC-c (chitinase C from rye, *Secale cereal*, seeds), and BcChiA (chitinase A from the moss, *Bryum coronatum*), were analyzed using oligosaccharide substrates $(GlcNAc)_6$ and $(GlcNAc)_4$, [44]. The hexasaccharide $(GlcNAc)_6$ was mainly split into $(GlcNAc)_4$+$(GlcNAc)_2$ by ChiC, whereas the same oligosaccharide was mainly split into $(GlcNAc)_3$+$(GlcNAc)_3$ by RSC-c and BcChiA. $(GlcNAc)_4$ was split symmetrically into two molecules of $(GlcNAc)_2$ by ChiC and BcChiA, whereas the tetramer was not hydrolyzed by RSC-c. The difference in the mode of action between the GH19 enzymes might be partly caused by amino acid substitutions at the substrate-binding cleft. It was also found that RSC-c has loop structures at both ends of the binding cleft but BcChiA does not (Ohnuma et al., unpublished observation). These enzymes are called “loopful” and “loopless” chitinases, respectively. The arrangement of the loop structures might also contribute to the difference in the mode of action. In general, for all enzymes tested, the degradation of the hexamer substrate $(GlcNAc)_6$ proceeded faster than for the tetramer substrate $(GlcNAc)_4$. As already mentioned for HEWL, these results again confirmed the fact that the longer the chain length of oligosaccharide substrates, the higher the degradation rate. This is a typical property of most endo-splitting glycoside hydrolases. [47, 54]

2.1.3. Time-Courses of the Reaction Catalyzed by GH46 and GH2 Chitosanases

Chitosan oligosaccharides, $(GlcN)_n$, have been used as the substrates for chitosanases. Since the oligosaccharides are completely *N*-deacetylated, the absorbancy of ultraviolet light for these oligosaccharides are considerably lower than those for chitin oligosaccharides, $(GlcNAc)_n$. In addition, a convenient HPLC separation system for $(GlcN)_n$ with sufficient durability has not been established probably due to the polycationic properties of $(GlcN)_n$. Consequently, there is a real need to develop an analytical system for determining the reaction time-course of $(GlcN)_n$ hydrolysis using ESI-MS. The first chitosanases investigated by ESI-MS were a GH46 endo-splitting chitosanase from *Streptomyces* sp. N174 (CsnN174) and a GH2 exo-splitting chitosanase from *Amycolatopsis orientalis* (CsxA) [55]. $(GlcN)_6$ was mainly hydrolyzed into $(GlcN)_3$+$(GlcN)_3$ and to a minor extent into $(GlcN)_2$+$(GlcN)_4$ by CsnN174 (Figure 5). The latter product $(GlcN)_4$ was further degraded into two molecules of $(GlcN)_2$. $(GlcN)_5$ was split into $(GlcN)_3$ and $(GlcN)_2$, and $(GlcN)_4$ was symmetrically hydrolyzed into $(GlcN)_2$+$(GlcN)_2$. The results are similar to those obtained with Chi26. The similar product distribution for the GH46 and GH19 enzymes suggests that the subsite arrangement of the binding cleft of the GH46 enzymes is similar to that of the GH19 enzymes. However, GH22 HEWL exhibited a profile different from those of GH19 and GH46 enzymes. Among the enzymes belonging to the lysozyme superfamily, GH22 lysozymes might be an anomaly with respect to the mode of action toward oligosaccharide substrates.

A GH8 chitosanase from *Paenibacillus* sp. 1794 (Csn1794) exhibited a similar cleavage profile toward the $(GlcN)_n$ substrates to that of the GH46 chitosanases.

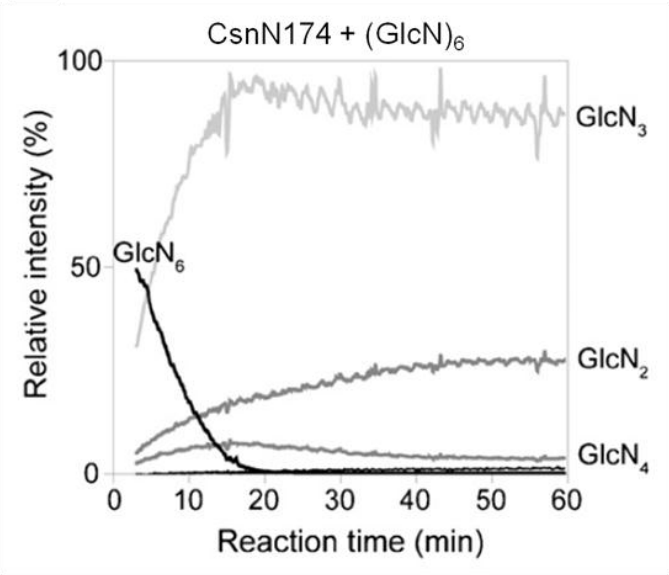

Figure 5. Real-time ESI-MS monitoring of $(GlcN)_6$ hydrolysis catalyzed by GH46 CsnN174. The enzymatic reaction was carried out in 10 mM ammonium acetate buffer pH 5.2. Concentrations of CsnN174 and the substrate $(GlcNAc)_6$ were 10 nM and 25.0 μM, respectively. The relative intensity 100% corresponds to 5.0 x 10^6counts.

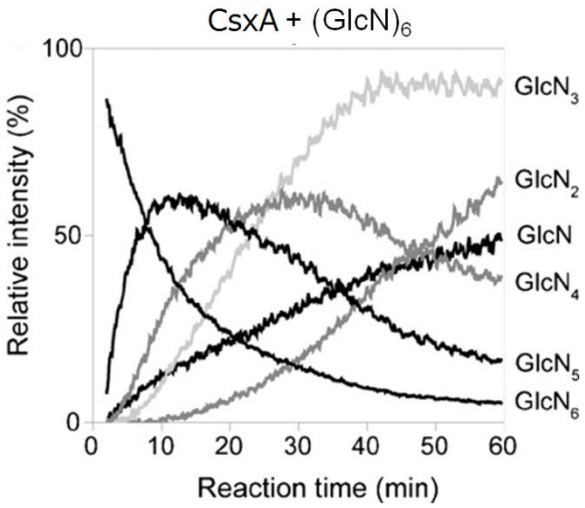

Figure 6. Real-time ESI-MS monitoring of $(GlcN)_6$ hydrolysis catalyzed by GH2 CsxA. The enzymatic reaction was carried out in 10 mM ammonium acetate buffer pH 5.2. Concentrations of CsxA and the substrate $(GlcN)_6$ were 0.96 nM and 25.0 μM, respectively. The relative intensity 100% corresponds to 2.0×10^6 counts for $(GlcN)_6$ and 0.6×10^6 counts for $(GlcN)_n$ (n= 1, 2, 3, 4, and 5).

In contrast, a GH2 chitosanase, CsxA, showed an exo-splitting mechanism; $(GlcN)_6$ was split into GlcN and $(GlcN)_5$, which was further cleaved into GlcN and $(GlcN)_4$, then into GlcN and $(GlcN)_3$ (Figure 6) [55]. When a heterotetramer, $(GlcN)_3$-GlcNAc, was hydrolyzed by CsxA, GlcN and $(GlcN)_2$-GlcNAc were found to be produced in the early stage of the reaction. Thus, the reducing end GlcN residue is split off from the oligosaccharide substrate by CsxA [56].

2.2. Noncovalent Complexes and Dissociation Constants

The quantitative determination of noncovalent protein-ligand complexes is important for understanding the mechanism of action of glycosyl hydrolases. Soft ionization techniques with modern ESI interfaces and the wide detection range of mass spectrometers offer the possibility to study noncovalent complexes. Ganem and colleagues were the first to describe noncovalent enzyme-ligand complexes with HEWL and various oligosaccharides ($(GlcNAc)_n$, n= 2 – 6) [57, 58]. They observed multiple charged ions, ranging from $[HEWL + 7H]^{7+}$ to $[HEWL + 11H]^{11+}$. +8 was the preferred charging state for enzyme-ligand complexes. To date, a variety of HEWL-$(GlcNAc)_n$-complexes with a stoichiometry from 1:1 to 1:4 [$(GlcNAc)_n$:HEWL] have been identified [41, 58]. A well-characterized protein ligand system, the complex of HEWL and $(GlcNAc)_3$, was studied by several research groups for determination of the dissociation constant (K_d) of the complex. Different setups for mixing the enzyme and ligand, as well as different mass spectrometric ionization setups, were used for studying the complex. The mixing of the enzyme and ligand was carried out manually in a simple syringe pump [41, 59] or automatically in a microfluidic chip system [60]. Different electrospray-based ionization methods such as ESI, nanoESI, and electrosonic spray ionization (ESSI) were studied as well and compared by Jecklin and colleagues [61]. The

experiments showed that the K_d obtained for HEWL and $(GlcNAc)_3$ by ESI-MS is in good agreement with previous results from experiments in liquid phase. The K_d values determined by ESI titration experiments are somewhat higher than those obtained in other studies applying fluorescence or UV, probably due to the mass spectrometric setup and ionization technique. [41, 59, 61].

The formation of complexes and simultaneous inhibition of the HEWL reaction with $(GlcNAc)_6$ as a substrate and $(GlcNAc)_3$ as an inhibitor was studied by a continuous-flow mixing analysis [46]. In this setup, $(GlcNAc)_3$ was injected into the system at periodic time-intervals with increasing concentrations. Injection of the inhibitor into the continuous flow of enzyme solution led to a decrease in the product signal and an increase in the substrate signal. Furthermore, the inhibitor-enzyme complexes were also determined by injection of increasingly higher concentrations of $(GlcNAc)_3$ from 1 nM to 40 nM into the continuous-flow system (Figure 7a). The preferred charging state of the HEWL-$(GlcNAc)_3$-complex was found to be +8. The formation of the complexes $[HEWL\text{-}(GlcNAc)_3]^{8+}$, $[HEWL\text{-}((GlcNAc)_3)_2]^{8+}$, $[HEWL\text{-}((GlcNAc)_3)_3]^{8+}$, and $[HEWL\text{-}((GlcNAc)_3)_4]^{8+}$ is shown in Figures 7b-7e.

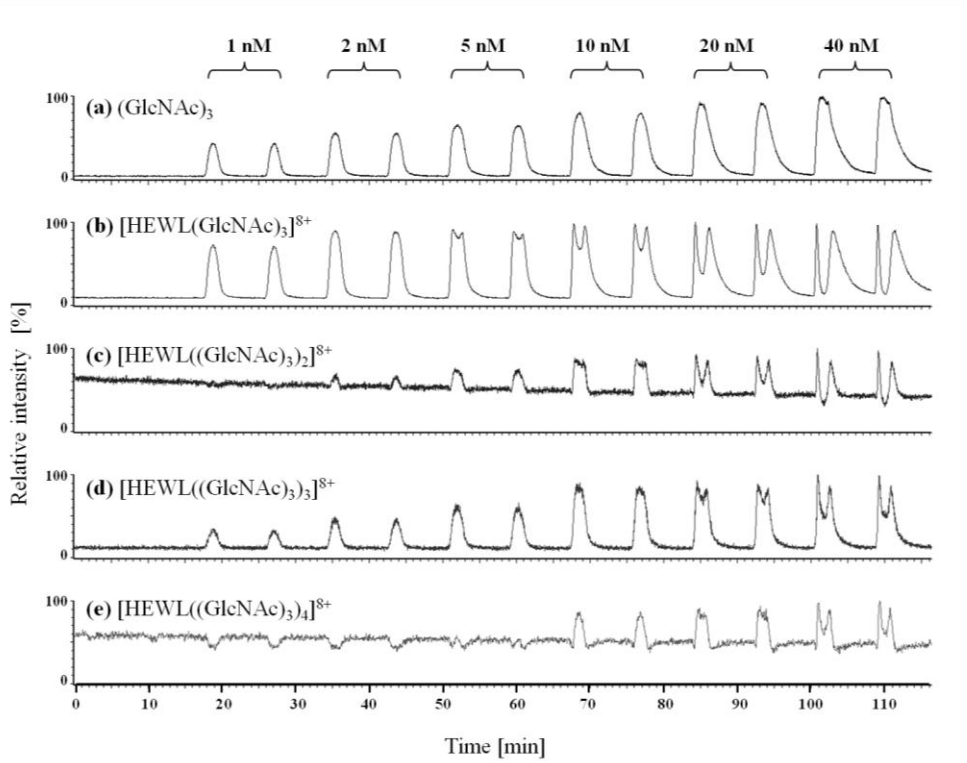

Figure 7. Extracted ion chromatogram upon injection of $(GlcNAc)_3$ into the continuous-flow of the HEWL solution. Various concentrations of $(GlcNAc)_3$ were injected, and the signal responses of $(GlcNAc)_3$ and the enzyme-ligand complexes with charging state +8 were monitored: (a) $(GlcNAc)_3$, (b) $[HEWL\text{-}(GlcNAc)_3]^{8+}$, (c) $[HEWL\text{-}((GlcNAc)_3)_2]^{8+}$, (d) $[HEWL\text{-}((GlcNAc)_3)_3]^{8+}$, and (e) $[HEWL\text{-}((GlcNAc)_3)_4]^{8+}$.

The preferred stoichiometry for the formation of +8 charged complexes was found to be $[HEWL\text{-}(GlcNAc)_3]^{8+}$ > $[HEWL\text{-}((GlcNAc)_3)_3]^{8+}$ > $[HEWL\text{-}((GlcNAc)_3)_2]^{8+}$ > $[HEWL\text{-}((GlcNAc)_3)_4]^{8+}$. In this study, peak splittings were observed due to a shift to a higher stoichiometry (data not shown).

2.3. Enzymatic Activity of Mutated Enzymes and Studying Mutational Effects

We investigated the effects of mutations of chitinases and chitosanases on their reaction time-courses using ESI-MS. Charge state distribution, which provides indirect information about the tertiary structure of enzymes, was also determined by mass spectrometry to evaluate the effects of mutations on the proteins in a folded state. ESI-MS is suitable for estimating whether the effects observed are caused by a local unfolding or a substitution of functional group at the site of the mutation.

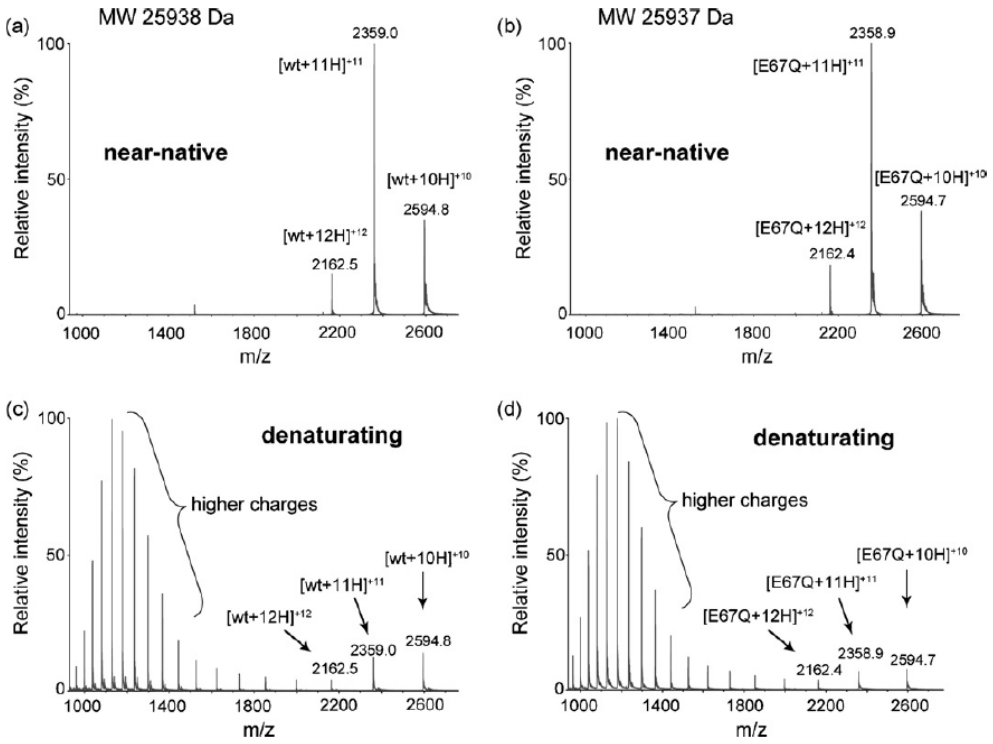

Figure 8. Mass spectra of Chi26 and Chi26-E67Q under folded and unfolded conditions. (a) Mass spectrum of Chi26 (3.65 μM) obtained under folded conditions (10 mM ammonium acetate, pH 5.2). The relative intensity 100 % conrresponds to 1.5 x 10^4 counts; (b) Mass spectrum of Chi26-E67Q (8.46 μM) obtained under folded conditions (10 mM ammonium acetate, pH 5.2). The relative intensity 100 % corresponds to 1.8 x 10^4 counts; (c) Mass spectrum of Chi26 obtained under unfolded conditions (ammonium acetate/methanol/acetic acid). The relative intensity 100 % corresponds to 4.0 x 10^4 counts; (d) Mass spectrum of Chi26-E67Q obtained under unfolded conditions (ammonium acetate/methanol/acetic acid). The relative intensity 100 % corresponds to 9.0 x 10^4 counts.

Dennhart *et al*. found that the charge state distributions of an inactively mutated Chi26, Chi26-E67Q (substitution of Glu67 with Gln) [47], under folded and unfolded conditions were very similar to those of Chi26, as shown in Figure 8, indicating that the inactivity of Chi26-E67Q is caused by a functional group substitution but not by a local unfolding of the enzyme. ESI-MS analysis indicated that Chi26-E67Q degrades neither $(GlcNAc)_6$ nor $(GlcN)_6$, but both oligosaccharides interact with the mutant enzyme. Then we successfully produced reliable data on the association constants for Chi26-E67Q and $(GlcNAc)_n$. The time-courses of $(GlcN)_6$ hydrolysis catalyzed by CsnN174 and two different mutants, CsnN174-D40G (Asp40 is mutated to glycine) and CsnN174-D201A (Asp201 is mutated to alanine), were studied by real-time ESI-MS [55]. The specific activities of the enzymes can be used to evaluate the importance of amino acids in the catalytic reaction. This study showed that the specific activity for CsnN174-D40G was reduced to 2%; indicating that Asp40 is essential for catalysis. Furthermore, the specific activity was hardly affected by the D201A mutation; thus Asp201 participates little in the catalytic reaction. Asp201 was found to be responsible for sugar residue binding at subsite +2, as described later (section 3.3.).

A recent real-time ESI-MS study investigated the time-course of hydrolysis of 4-nitrophenyl penta-*N*-acetyl-β -chitopentaoside $[(GlcNAc)_5$-pNP] by Chi26 [40]. Comparison of the mode of hydrolysis of $[(GlcNAc)_5$-pNP] between the wild-type and Trp72-mutated Chi26 provided information about the role of the mutated tryptophan residue. It was shown that the mutation of Trp72 located at subsite +4 with alanine resulted in a significant change in the substrate-binding mode. The substrate was found to bind predominantly to subsites -2~+4 of the wild type enzyme with the *p*-nitrophenyl moiety located at subsite +4. However, in the mutant enzyme, the preferred binding subsites was -3~+3. Thus, it is most likely that the indole side chain of Trp72 of Chi26 interacts with the 4-nitrophenyl moiety of the substrate.

3. Oligosaccharide Binding Mode of Lysozymes, Chitinases and Chitosanases as Determined by NMR Spectroscopy

Protein NMR spectroscopy has provided a great deal of information about protein structure, stability, interaction, and dynamics [63]. Notably, for determining structure, the hardware and software for NMR measurements have greatly advanced in the last twenty years, and a number of NMR-derived protein structures (more than 8000) have been deposited in the Protein Data Bank (PDB) [64]. NMR-derived structures are now comparable with those determined by X-ray crystallography. However, protein NMR spectroscopy is also an exquisitely powerful tool for accurately determining the protein-ligand interactions [65]. Protein-ligand interactions can be assessed by monitoring changes in chemical shifts and the intensity of specific resonances in an NMR spectrum of a protein (chemical shift perturbation methods). From the changes in resonance, one can simply evaluate whether the protein interacts with a ligand or not, without resonance assignment. Information on the ligand-binding site can be obtained by complete assignment of all resonances in the two-dimensional ^{1}H-^{15}N HSQC spectrum of a target protein, in which the correlations between chemical shifts of directly bound ^{1}H and ^{15}N can be detected. For obtaining a clear ^{1}H-^{15}N HSQC spectrum, however, a target protein should be uniformly labeled with ^{15}N by an appropriate expression

system using a minimal medium in the presence of a ^{15}N-labeled nitrogen source, such as $^{15}NH_4Cl$. For resonance assignment, the protein should be further labeled with ^{13}C uniformly by adding ^{13}C-glucose as a sole carbon sourc into the medium. Using the ^{15}N/^{13}C-double labeled protein, three-dimensional NMR experiments should be conducted to assign the individual resonances in a ^{1}H-^{15}N HSQC spectrum [66]. Thus, for measuring a NMR spectrum, one should install an efficient labeling and purification system. In addition, using the conventional NMR techniques except TROSY experiments in combination with triple-labeling with ^{2}H, ^{13}C, and ^{15}N [67], the upper limit of the molecular mass of proteins is 25-30 kDa. Fortunately, the enzymes belonging to the lysozyme superfamily have a molecular mass of less than 30 kDa, and efficient expression systems for lysozymes, chitinases, and chitosanases available. This situation prompted us to analyze the protein-ligand interactions of the lysozyme superfamily using conventional protein NMR techniques.

3.1. GH-23 Goose-Type Lysozyme

Among the various types of lysozymes, HEWL has been studied most intensively with respect to structure and function [1, 68-71]. As described above, HEWL catalyzes transglycosylation in addition to the hydrolysis of chitin and cell wall peptidoglycan [2, 72]. Lysozymes with such specificity are called chicken-type (c-type) lysozymes and belong to the GH22 family. On the other hand, goose-type (g-type) lysozymes (GH23) are larger (18 kDa) than c-type lysozymes (14 kDa). G-type lysozymes are highly active toward peptidoglycan, but less active toward chitin. Transglycosylation does not take place in the reaction catalyzed by g-type lysozymes [50, 73]. However, the molecular mechanism bringing about the specificity of g-type lysozymes is still unclear. The first g-type lysozyme investigated by X-ray crystallography was from goose egg white (GEWL). Its crystal structure in a complex with $(GlcNAc)_3$ revealed the state of the substrate-binding cleft, especially at subsites -3, -2, and -1 [74]. The crystal structure of a g-type lysozyme from Atlantic cod was also solved in a complex with both $(GlcNAc)_2$ and $(GlcNAc)_3$ [27]. $(GlcNAc)_2$ binds to subsites -3 and -2, while $(GlcNAc)_3$ binds to subsites +1, +2, and +3. Although the crystal structures revealed the mode of binding at a specific subsite, it is difficult to obtain insights into the substrate recognition mechanism of the entire binding cleft including the catalytic center. Thus, we tried to analyze the interaction of a g-type lysozyme with chitin oligosaccharides having longer chain length by chemical shift perturbation methods using protein NMR spectroscopy [28].

We used a g-type lysozyme from ostrich egg white (OEL), because the expression of OEL by the *Pichia pastoris* expression system was found to be much more efficient than that by other expression systems for g-type lysozymes [75]. The OEL-*P. pastoris* system enabled production of a sufficient amount of stable isotope-labeled OEL for NMR measurements. In practice, stable isotope-labeling of OEL was conducted by the OEL-*P. pastoris* system using FMGY and FMMY media containing $^{15}NH_4Cl$, ^{13}C-glucose, and ^{13}C-methanol. Then the labeled protein was purified by cation-exchange chromatography from the culture supernatant. Using the wild type ^{15}N-labeled OEL, we first obtained the ^{1}H-^{15}N HSQC spectrum, which is shown in Figure 9. The individual resonances were well separated, facilitating their assignments. The backbone resonances were assigned sequentially based on a combination of results of three-dimensional NMR experiments, such as HNCO, HNCACO, HNCACB,

CBCA(CO)NH, HNCA and HNCOCA spectra, using $^{13}C/^{15}N$-labeled OEL. The assignments were nearly complete and assigned resonances are labeled in the spectrum (Figure 9). To identify the region interacting with sugar residues at the enzyme's molecular surface, $(GlcNAc)_n$ (n=2, 4, or 6) was titrated, and then chemical shift changes of resonances upon oligosaccharide-binding were monitored. We used an inactive mutant, OEL-E73A, in which Glu73 as a proton donor is mutated to alanine to exclude the hydrolytic activity. The results are shown in Figure 10. The surface model of the protein and the bound $(GlcNAc)_3$ was drawn using a Pymol software based on the crystal structure of GEWL in a complex with $(GlcNAc)_3$ (PDB code: 154L). The amino acid residues, whose resonances were affected upon the addition of $(GlcNAc)_n$ (n=2, 4, and 6), were visualized using a gray-scale. Density represents the magnitude of the chemical shift changes. As seen from the figure, for the binding subsites -3, -2, and -1, the region interacting with $(GlcNAc)_n$ deduced from NMR spectroscopy (Figures 10A and 10B) is consistent with the binding mode determined by crystal structure analysis [74]. However, this NMR study revealed subsites +1, +2, and +3, in which His75, Arg78, Ala79, Asp86, and Asn87 might be involved in binding to the sugar residue (Figure 10C). The result is almost consistent with the $(GlcNAc)_3$-binding site of a g-type lysozyme from Atlantic cod [27]. As expected, the longer the chain length of the oligosaccharide added, the greater the regions affected by $(GlcNAc)_n$. However, the region affected by the binding of $(GlcNAc)_4$ to OEL-E73A appears to be more widely spread over the binding cleft than that presumed from the degree of polymerization of $(GlcNAc)_4$ (Figure 10B). This suggests that $(GlcNAc)_4$ binds to OEL in multiple ways. The binding constants (K_a) were calculated from the titration curves obtained by plotting chemical shift changes of HSQC signals against free sugar concentrations (Figure 11).

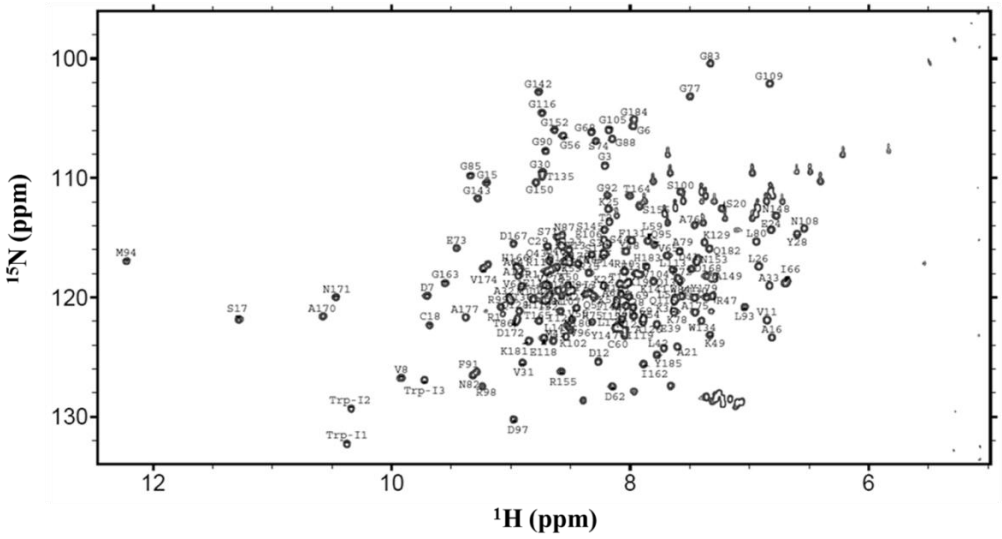

Figure 9. ^{1}H-^{15}N HSQC spectrum of the wild-type OEL. The protein was dissolved in 20mM sodium acetate buffer pH 5.0 containing 10% D_2O to obtain 0.2mM OEL solution. The backbone resonances were assigned by a sequential manner as indicated in the spectrum.

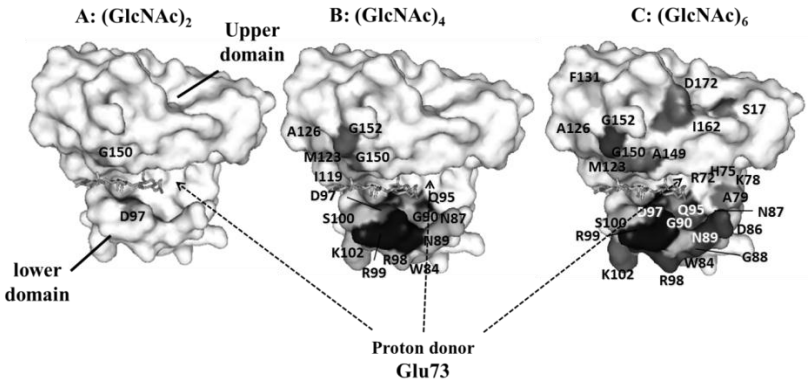

Figure 10. Amino acid residues of OEL-E73A, whose resonances were affected by oligosaccharide binding. The surface model of the enzyme structure was drawn by a PyMOL software based on the crystal structure of GEWL in a complex with $(GlcNAc)_3$ (PDB code: 154L). Concentration of E73A OEL was 0.31mM, and the ligands were 2.9 mM $(GlcNAc)_2$ (A), 1.7 mM $(GlcNAc)_4$ (B) and 1.7 mM $(GlcNAc)_6$ (C). Amino acid residues affected are shown by a gray-scale, and the density represents the magnitude of the shifts induced by the oligosaccharide binding.

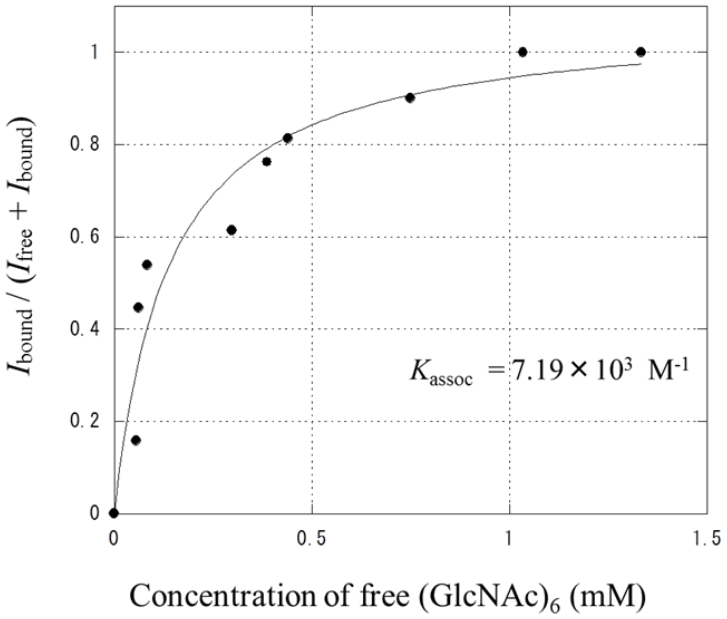

Figure 11. Titration curve of $(GlcNAc)_6$ binding to OEL-E73A determined from the change in the amide backbone resonance of Asp97. The individual experimental points were obtained from integrals of the resonances in the free and bound states using the equation $I_{bound}/ (I_{free}+ I_{bound})$. The solid line indicates the theoretical binding curve best fitted to the experimental points using the scatchard equation.

The K_a value (7.2 x 10^3 M^{-1}) and the unitary binding free energy value (-7.7 kcal/mol) obtained from Figure 11 are consistent with those obtained by means of isothermal titration calorimetry (ITC) [28].

3.2. GH19 Chitinase

As described in section 2.1.2, GH19 chitinases are further divided into "loopful" and "loopless" types. Several loop structures located at both ends of the substrate-binding cleft of the "loopful" GH19 enzymes are missing in the "loopless" chitinases. The bacterial GH19 chitinases investigated thus far are recognized as "loopless", but Chi26 and RSC-c described in section 2.1.2 are "loopful" enzymes. Because of the loop deletions, "loopless" GH19 chitinases have a relatively small molecular weight, 22 kDa. Recently, Taira et al isolated a "loopless" GH19 chitinase from moss, *Brum coronatum* (BcChiA) [76], which was supposed to be appropriate for NMR analysis due to the lower molecular weight. Thus, we expressed $^{13}C/^{15}N$-labeled BcChiA via the *Escherichia coli* expression system using an M9 minimal medium containing ^{13}C-glucose and ^{15}N-NH_4Cl. The amount of the labeled BcChiA produced was similar to that produced by a standard Luria-Broth (LB) medium. Using the $^{13}C/^{15}N$-labeled BcChiA thus obtained, the backbone resonances in the ^{1}H-^{15}N HSQC spectrum of BcChiA (Figure 12) were assigned in a similar manner to those for OEL based on the three-dimensional NMR spectra [29]. As a result, most backbone resonances (99 %) were successfully assigned in a sequential manner. The secondary structural arrangement of BcChiA was estimated based on the chemical shift values of the backbone resonances using a TALOS software [77], and was similar to those for other GH19 chitinases determined by X-ray crystallography. Titration experiments were conducted using BcChiA and $(GlcNAc)_2$ as a ligand. The addition of $(GlcNAc)_2$ into the ^{15}N-labeled BcChiA solution resulted in chemical shift changes of the ^{1}H-^{15}N HSQC resonances as shown in Figure 12 [29]. Based on these changes, amino acid residues whose resonances are affected upon $(GlcNAc)_2$-binding were mapped on the surface of the modeled BcChiA structure, which was obtained with a SWISS-MODEL server [78] using the crystal structure of *Streptomyces coelicolor* A3(2) chitinase as a template (Protein Data Bank code 2CJL) [79]. As shown in the left panel of Figure 13, $(GlcNAc)_2$ interacts strongly with the region surrounding the catalytic center Glu61 of BcChiA (subsites -1 and +1). In the case of OEL-E73A (Figure 10A), however, $(GlcNAc)_2$ tends to bind nonproductively to subsites -1 and -2.

Since OEL is much more active toward peptidoglycan than toward $(GlcNAc)_n$ [15], the enzyme is likely to have a recognition site for the peptidyl moiety of the substrate in the vicinity of the catalytic site. However, the chitin oligosaccharides used for the OEL-binding study have no peptide chain. Therefore, $(GlcNAc)_2$ binds to OEL without any affinity for the peptidyl recognition site close to the catalytic center, resulting in the nonproductive binding to OEL. In contrast, BcChiA prefers $(GlcNAc)_n$ itself as the natural substrate, interacting strongly with $(GlcNAc)_n$ through the catalytic site region (-1 and +1). As seen in the right panel of Figure 13, the region affected by oligosaccharide-binding extended to the back side of the binding cleft. This suggests that the enzyme tightly holds the oligosaccharide chain by clamping motion of the upper and lower domains. Such a domain motion was not suggested from the NMR titration experiments for OEL (section 3.1.). The interface region between the upper and lower domains of BcChiA might be flexible, whereas OEL has a more rigid

structure at the interface. This situation might have resulted in the difference between OEL and BcChiA.

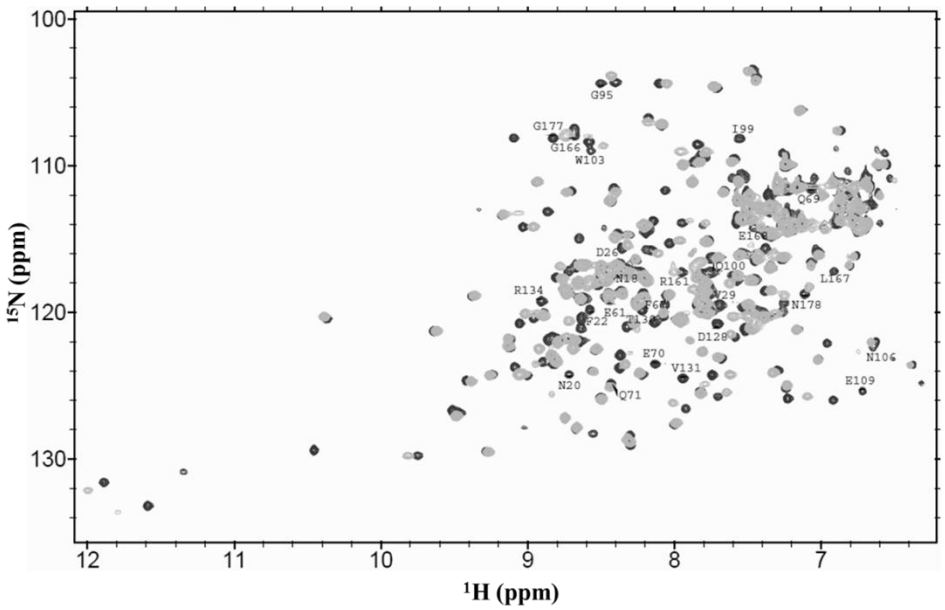

Figure 12. Superimposition of the ^{1}H-^{15}N-HSQC spectra of BcChiA in the presence or absence of $(GlcNAc)_2$. Molar ratios of the enzyme and the ligand are 1:0 (black) and 1:25 (gray). The titration was conducted using 0.4 mM BcChiA solution in 50 mM sodium acetate buffer pH 5.0 containing 10 % D_2O.

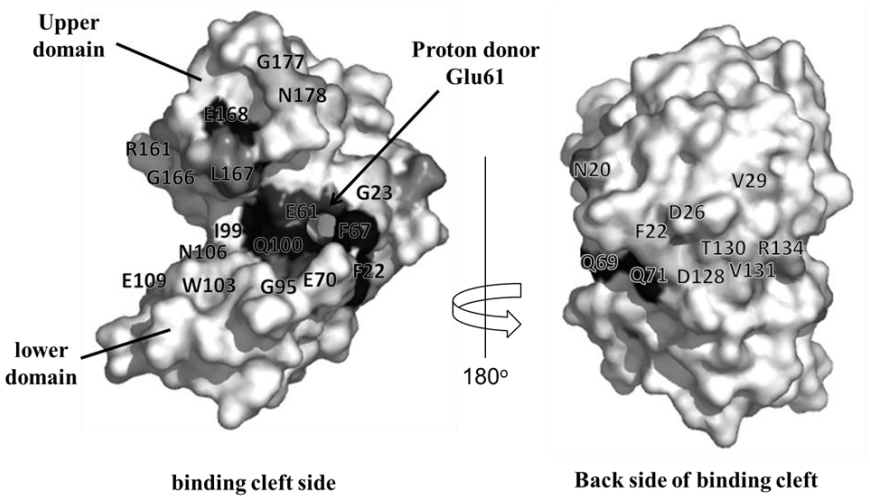

Figure 13. Amino acid residues of BcChiA, whose resonances were affected by the $(GlcNAc)_2$ binding. The modeled structure of BcChiA was constructed by homology-modeling using the crystal structure of *Streptomyce coelicolor* chitinase ChiG (PDB : 2CJL) as a template. Concentration of BcChiA was 0.4 mM, and the $(GlcNAc)_2$ was 20 mM. Amino acid residues affected are shown by a gray-scale, and the density represents the magnitude of the shifts induced by the oligosaccharide binding.

On the other hand, when a Scatchard analysis was performed based on the chemical shift changes obtained by NMR titration experiments, we successfully obtained the binding constant (2.4 x 10^2 M^{-1}) and the unitary binding free energy change (-5.7 kcal/mol) for $(GlcNAc)_2$ binding. Unfortunately, the binding constant of $(GlcNAc)_2$ to BcChiA could not be obtained by ITC [80]. The NMR binding experiments are now in progress using the inactive mutant of BcChiA.

3.3. GH-46 Chitosanase

The first chitosanase, whose structure was solved by X-ray crystallography, was a GH46 endo-splitting chitosanase from *Streptomyces* sp. N174 (CsnN174) [81]. The structure of a chitosanase from *Bacillus circulans* MH-K1 was also solved three years after the publication of the CsnN174 structure [82]. GH46 chitosanases are composed of two domains consisting of several α-helical structures, and the substrate-binding cleft lies between the two domains (Figure 1E). Katsumi et al. examined the binding of the chitosan dimer and trimer [$(GlcN)_2$ and $(GlcN)_3$] to CsnN174 using fluorescence derived from tryptophan side chains [83]. A Scatchard plot based on fluorescence quenching upon oligosaccharide-binding exhibited a biphasic profile which contained two regression lines with different slopes. This indicated that CsnN174 has two sites for the binding of oligosaccharides with a lower degree of polymerization [$(GlcN)_2$ and $(GlcN)_3$], a high-affinity site and a low-affinity site. Unfortunately, the crystal structure of CsnN174 in a complex with the oligosaccharides has not been reported yet, and the mode of binding of the chitosan oligosaccharide to CsnN174 was obtained only from a docking simulation.

The oligosaccharide-binding model obtained by docking simulation based on the crystal structure of free CsnN174 is shown in Figure 14 [81]. Amino acid residues indicated in the figure are estimated to interact with the GlcN residues at the individual subsites of CsnN174.

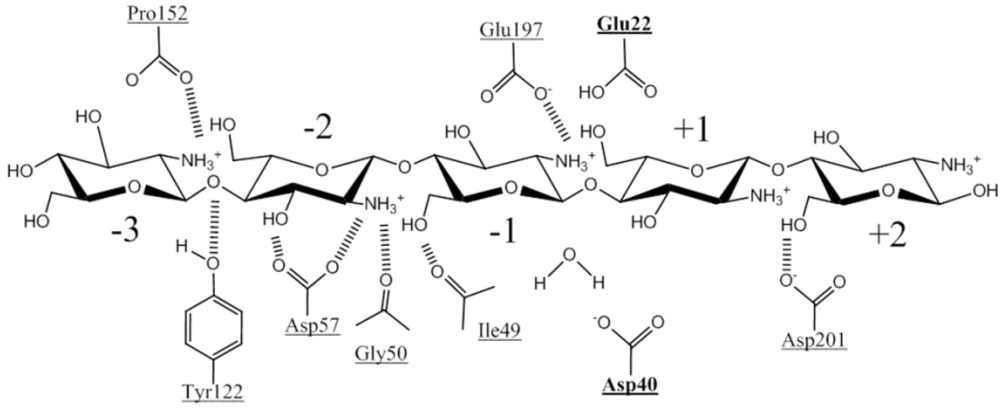

Figure 14. Interaction model between CsnN174 and $(GlcN)_5$ obtained by docking simulation based on the crystal structure of free CsnN174 (PDB: 1CHK). The model was drawn based on the report by Marcotte et al [81]. Glu22 and Asp40 are the catalytic residues.

To confirm the mode of binding, titration experiments were conducted with NMR spectroscopy using CsnN174. Before NMR measurements, $^{13}C/^{15}N$-labeled CsnN174 was

produced by the *Streptomyces lividans* TK24 Δ*csnR* expression system using an M14 minimal medium containing $^{15}NH_4Cl$ and ^{13}C-glucose. The backbone resonances in the ^{1}H-^{15}N HSQC spectrum of CsnN174 were assigned based on three-dimensional NMR spectra in a similar manner to that of OEL. The assignments were not complete, but 70 % of the backbone resonances were assigned. When $(GlcN)_3$ was titrated into CsnN174, several signals, including the resonances of Gly153, Asn23, and His200, were affected by the oligosaccharide-binding (Figure 15). As seen from Figure 14, the Pro152 carbonyl group located in the loop structure between the eighth (136-150) and ninth (158-170) helices interacts with the sugar residue at subsite -3. This interaction is likely to induce the shift of the main chain resonance of Gly153 located in the same loop structure. Since Asn23 is a nearest neighbor of the catalytic proton donor, Glu22, its resonance would have been strongly affected by $(GlcN)_3$-binding. Influence of the $(GlcN)_3$-binding was also seen in the HSQC resonance of His200 (Figure 15). Interaction of Asp201 with the sugar residue at subsite +2 (Figure 14) might affect the resonance of the nearest neighbor, His200. As described above, from the tryptophan fluorescence study, $(GlcN)_3$ was found to bind to two independent binding sites of CsnN174, the high affinity site (-3, -2, and-1) and the low affinity site (+1, +2, and +3) [83].

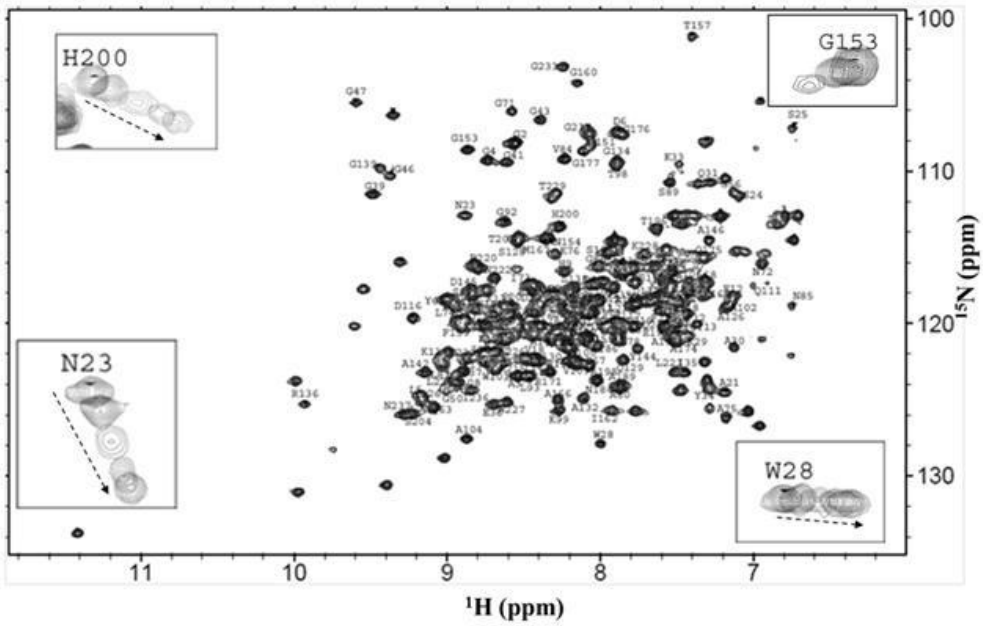

Figure 15. ^{1}H-^{15}N HSQC spectrum of CsnN174 and chemical shift changes of the resonances of CsnN174 in the presence of various concentrations of $(GlcN)_3$ (insets). Molar ratios of CsnN174 and $(GlcN)_3$ were 1:0, 1:5, 1:10, 1:20 and 1:30. The titration was conducted using 0.1 mM CsnN174 solution in 50 mM sodium acetate buffer pH 5.0 containing 10% D_2O.

The NMR data obtained here appear to be consistent with the data obtained from tryptophan fluorescence study; that is, the binding of $(GlcNAc)_3$ to CsnN174 affects simultaneously the resonances of the amino acids, Gly153, Asn23, and His200, located at subsites -3, -1, and +2, respectively. It should be noted that the resonance of Trp28 located in the hinge region connecting the two domains (Figure 1E) was affected by oligosaccharides-

binding. When the enzyme tightly holds the oligosaccharide chain by clamping motion of the two domains, the conformation of the hinge region should be affected by the oligosaccharide-binding. The domain motion might have resulted in the chemical shift change in the Trp28 resonance, as in the case of BcChiA. Furthermore, we calculated the values of K_d and the unitary binding free energy change based on the chemical shift changes of the Trp28 resonance. The unitary binding free energy value (-7.6 kca/mol) obtained by NMR titration experiments is consistent with the value (-7.4 kca/mol) of the high affinity site obtained by tryptophan fluorescence quenching [83]. Taken together, the binding data for the high affinity site obtained by fluorescence quenching is likely derived from Trp28, not from Trp101 and Trp227.

4. IMPLICATIONS

Using a sophisticated ESI-MS system, we obtained the time-courses of the reactions catalyzed by various enzymes belonging to the lysozyme superfamily. The time-course profiles provided information on the cleavage mode of the individual enzymes tested. The results are summarized in Figure 16. When $(GlcNAc)_6$ or $(GlcNAc)_4$ were used as the substrate, most members of the lysozyme superfamily split the oligosaccharides symmetrically, whereas HEWL split the substrates asymmetrically. The binding cleft of HEWL consists of a well-known subsite arrangement, A, B, C, D, E, and F, corresponding to -4, -3, -2, -1, +1, and +2. At subsite -4, the carboxylate of Asp101 interacts with the –NH of an acetamido group of the sugar residue. This interaction brings about the asymmetrical binding of the oligosaccharide substrate. The other enzymes belonging to the superfamily do not exhibit such significant interaction at subsite -4, resulting in the symmetrical cleavage of the oligosaccharides. Thus, HEWL is unique among the superfamily members. The action of HEWL is also distinct when $(GlcNAc)_5$ is used as the substrate. Most enzymes of the lysozyme superfamily catalyze hydrolysis through an inverting mechanism, whereas HEWL does so through a retaining mechanism. HEWL catalyzes a transglycosylation reaction, but the others do not. Thus, HEWL is unique in various respects.

We obtained new insights into the substrate-binding mode of the superfamily members from NMR spectroscopy. A GH23 g-type lysozyme and a GH19 chitinase, both of which split the $(GlcNAc)_6$ substrate symmetrically, exhibited different binding properties toward $(GlcNAc)_n$. $(GlcNAc)_2$ binds to the region surrounding the catalytic center (subsites -1 and +1) of the GH19 enzyme (the left panel of Figure 13), while the oligosaccharide binds nonproductively to the region of subsites -2 and -3 of the GH23 enzyme (Figure 10A). In the case of the GH23 enzyme, $(GlcNAc)_2$ does not correctly bind to the enzyme, because the oligosaccharide does not have the peptidyl moiety, which might be important for the interaction between the GH23 enzyme and the correct substrate, peptidoglycan. In fact, the association constant of the GH23 enzyme for $(GlcNAc)_n$ is lower than that of the GH19 enzyme (Shinya et al., unpublished data). $(GlcNAc)_n$ may be a pseudo-substrate for the GH23 enzyme. In the analysis of GH23 lysozymes, an oligosaccharide substrate containing a peptidyl moiety should be used for correctly understanding the mechanism.

The binding site of $(GlcN)_n$ for the GH46 chitosanase was first identified experimentally using NMR spectroscopy. The binding mode deduced from the chemical shift perturbation

was similar to that obtained from a docking simulation. NMR titration experiments revealed that two binding sites are possible for the interaction of $(GlcN)_3$ with the GH46 enzyme. This is also consistent with the results obtained by fluorescence titration experiments [83].

However, we obtained clear evidence of domain motion upon substrate-binding from the NMR data; that is, chemical shifts of the resonances of amino acids located in the interface between the two domains are significantly affected by the oligosaccharide-binding. Similar effects were also observed in the NMR titration experiments for the GH19 enzyme. It is most likely that such domain motion is common in the enzyme-ligand interaction of members belonging to the lysozyme superfamily. Further information on the enzyme-oligosaccharide interactions will be obtained by more clearly examining the line shape, relaxation, and other behaviors of the NMR signals of the individual reaction species.

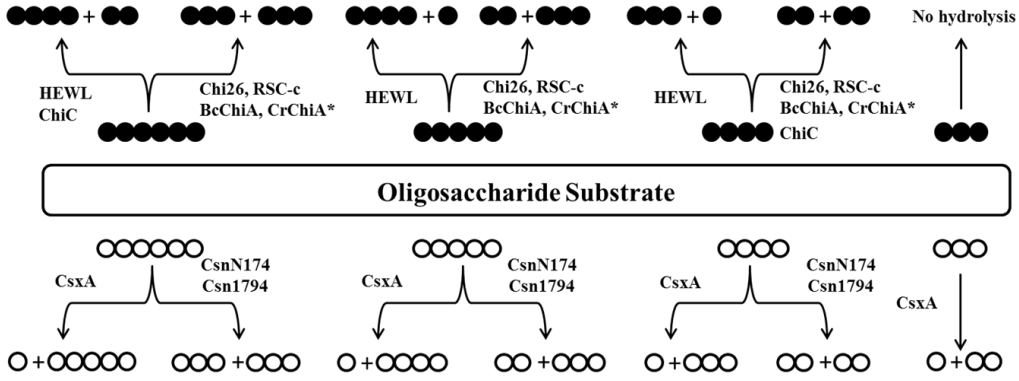

Figure 16. Summary of cleavage profiles of lysozyme, chitinases, and chitosanases with different oligosaccharides determined by ESI-MS experiments. ●, GlcNAc residues; ○, GlcN residues. *CrChiA belongs to the GH18 family, and is not a member of the lysozyme superfamily.

REFERENCES

[1] Jollès, J. and Jollès, P. (1984) What's new in lysozyme research? Always a model system, today as yesterday. Mol. Cell. Biochem., 63, 165-189.

[2] Chipman, D. M., Pollock, J. J., and Sharon, N. (1968) Lysozyme-catalyzed hydrolysis and transglycosylation reactions of bacterial cell wall oligosaccharides. *J. Biol. Chem.*, *243*, 487-496.

[3] Blake, C. C. F., Koenig, D. F., Mair, G. A., North, A. C. T., Phillips, D. C., and Serma, V. R. (1965) Structure of hen egg white lysozyme. A three-dimensional Fourier synthesis at 2 Å resolution. *Nature*, *206*, 757-761.

[4] Phillips, D. C. (1967) The hen egg white lysozyme molecule. *Proc. Natl. Acad. Sci. USA*, *57*, 757-761.

[5] Vocadlo, D. J., Davies, G. J., Laine, R., and Withers, S. G. (2001) Catalysis by hen egg-white lysozyme proceeds via a covalent intermediate. *Nature*, *412*, 835-838.

[6] Canfield, R. E. (1963) The amino acid sequence of egg white lysozyme. *J. Biol. Chem.*, *238*, 2698-2707.

[7] Simpson, R. J. and Morgan, F. J. (1983) Complete amino acid sequence of embden goose (Anwer anwer) egg-white lysozyme. *Biochem. Biophys. Acta., 744*, 349- 351.

[8] Inoue, M., Imada, M., and Tsugita, A. (1970) The amino acid sequence of T4 phage lysozyme. IV. Dilute acid hydrolysis and order of tryptic peptides. *J. Biol. Chem., 245*, 3479-3484.

[9] Ito, Y., Yoshikawa, A., Hotani, T., Fukuda, S., Sugimura, K., and Imoto, T. (1999) Amino acid sequences of lysozymes newly purified from invertebrates imply wide distribution of a novel class in the lysozyme family. *Eur. J. Biochem., 259*, 456-461.

[10] Höltje, J. V. Bacterial lysozymes. In Jollès, P., editor., *Lysozymes: Model Enzymes in Biochemistry and Biology*. Birkhäuser-Verlag, Basel, Switzerland; 1996; 65-74.

[11] Beintema, J. J., Terwisscha, van., and Scheltinga, A. C. Plant lysozymes. In Jollès, P., editor., *Lysozymes: Model Enzymes in Biochemistry and Biology*. Birkhäuser-Verlag, Basel, Switzerland; 1996; 75-86

[12] Mirelma, D., Kleppe, G., and Jensen, H. B., (2008) Studies on the specificity of action of bacteriophage T4 Lysozyme. *Eur. J. Biochem., 55*, 369-373.

[13] Pollock, J. J., and Sharon, N., (1970) Studies on the acceptor specificity of the lysozyme-catalyzed transglycosylation reaction. *Biochemistry, 9*, 3913-3925.

[14] Henrissat, B. and Davies, G. J. (1997) Structural and sequence-based classification of glycoside hydrolases. *Curr. Opin. Struct. Biol., 7*, 637-644.

[15] Arnheim, N., Inouye, M., Law, L., and Laudin, A.,. (1973) Chemical studies on the enzymatic specificity of goose egg white lysozyme. *J. Biol. Chem., 248*, 233-236.

[16] Fukamizo, T. Chitinolytic enzymes: catalysis, substrate binding, and their application. *Curr. Prot. Pept. Sci., 1* (2000), 105-124.

[17] Fukamizo, T., Honda, Y., Goto, S., Boucher, I., and Brzezinski, R. (1995) Reaction mechanism of chitosanase from *Streptomyces* sp. N174. *Biochem. J., 311*, 377-383.

[18] Monzingo, A. F., Marcotte, E. M., Hart, P. J., and Robertus, J. D. (1996) Chitinases, chitosanases, and lysozymes can be divided into procaryotic and eucaryotic families sharing a conserved core. *Nat. Struct. Biol., 3*, 133-140.

[19] Matthews, B. W., Grütter, M. G., Anderson, W. F., and Remington, S. J. (1981) Common precursor of lysozymes of hen egg-white and bacteriophage T4. *Nature, 290*, 334-335.

[20] Grütter, M. G., Weaver, L. H., and Matthews, B. W. (1983) Goose lysozyme structure: an evolutionary link between hen and bacteriophage lysozymes? *Nature, 303*, 828-831.

[21] Strynadka, N. C., and James, M. N., (1996) Lysozyme: a model enzyme in protein crystallography. *EXS., 75*, 185-222.

[22] Lescar, J., Souchon, H., and Alzari, P. M., (1994) Crystal structures of pheasant and guinea fowl egg-white lysozymes. *Protein Sci., 3*, 788-798.

[23] Muraki, M., Goda, S., Nagahora, H., and Harata, K. (1997) Importance of van der Waals contact between Glu 35 and Trp 109 to the catalytic action of human lysozyme. *Protein. Sci., 6*, 473-476.

[24] Kuroki, R., Weaver, L. H., and Matthews, B. W. (1993) A covalent enzyme-substrate intermediate with saccharide distortion in a mutant T4 lysozyme. *Science, 262*, 2030-2033.

[25] Baase, W. A., Liu, L., Tronrud, D. E., and Matthews, B. W., (2010) Lessons from the lysozyme of phage T4. *Protein Sci.,* 19, 631-641.

[26] Huet, J., Rucktooa, P., Clantin, B., Azarkan, M., Looze, Y., Villeret, V., and Wintjens, R. (2008) X-ray structure of papaya chitinase reveals the substrate binding mode of glycosyl hydrolase family 19 chitinases. *Biochemistry, 47*, 8283-8291.

[27] Helland, R., Larsen, R. L., Finstad, S., Kyomuhendo, P., and Larsen, A. N. (2009) Crystal structures of g-type lysozyme from Atlantic cod shed new light on substrate binding and the catalytic mechanism. *Cell. Mol. Life. Sci.*, 66, 2585-2598.

[28] Shinya, S., Ohnuma, T., Kawamura, S., Torikata, T., Nishimura, S., Katoh, E., and Fukamizo, T. (2011) Interaction of a goose-type lysozyme with chitin oligosaccharides as determined by NMR spectroscopy. *J. Biochem.*, *150*, 569-577.

[29] Shinya, S., Nagata, T., Ohnuma, T., Taira, T., Nishimura, S., and Fukamizo, T. (2011) Backbone chemical shifts assignments, secondary structure, and ligand binding of a family GH-19 chitinase from moss, *Bryum coronatum*. *Biomol. NMR. Assign.*, in press.

[30] Ge, X., Sirich, T. L., Beyer, M. K., Desaire, H., and Leary, J. A. (2001) A Strategy for the Determination of Enzyme Kinetics Using Electrospray Ionization with an Ion Trap Mass Spectrometer. *Anal. Chem.*, *73*, 5078-5082.

[31] Northrop, D. B. and Simpson, F. B. (1997) Beyond enzyme kinetics: Direct determination of mechanisms by stopped-flow mass spectrometry. *Bioorgan. Med. Chem.*, *5*, 641-644.

[32] Greis, K. D. (2007) Mass spectrometry for enzyme assays and inhibitor screening: An emerging application in pharmaceutical research. *Mass Spectrom. Rev.*, *26*, 324-339.

[33] Liesener, A. and Karst, U. (2005) Monitoring enzymatic conversions by mass spectrometry: a critical review. *Anal. Bioanal. Chem.*, *382*, 1451-1464.

[34] Lee, E. D., Mueck, W., Henion, J. D., and Covey, T. R. (1989) Real-Time Reaction Monitoring by Continuous-Introduction Ion-Spray Tandem Mass-Spectrometry. *J. Am. Chem. Soc.*, *111*, 4600-4604.

[35] Letzel, T. (2008) Real-time mass spectrometry in enzymology. *Anal. Bioanal. Chem.*, *390*, 257-261.

[36] de Boer, A. R., Lingeman, H., Niessen, W. M., and Irth, H. (2007) Mass spectrometry-based biochemical assays for enzyme inhibitor screening. *Trends. Analyt. Chem.*, *26*, 867-883.

[37] de Boer, A. R., Letzel, T., Lingeman, H., and Irth, H. (2005) Systematic development of an enzymatic phosphorylation assay compatible with mass spectrometric detection. *Anal. Bioanal. Chem.*, *381*, 647-655.

[38] Grassmann, J., Scheerle, R. K., and Letzel, T. (2012) Functional Proteomics: Mass Spectrometric Applications studying Enzymology in Complex Mixtures. *Anal. Bioanal. Chem.*, *402*, 625-645.

[39] Bisswanger, H. *Practical Enzymology*. Wiley-VCH; 2004.

[40] Letzel, T., Sahmel-Schneider, E., Skirver, K., Ohnuma, T., and Fukamizo, T. (2011) Chitinase-catalyzed hydrolysis of 4-nitrophenyl penta-*N*-acetyl-β-chitopentaoside as determined by real-time ESIMS: The 4-nitrophenyl moiety of the substrate interacts with the enzyme binding site. *Carbohydr. Res.*, *346*, 863-866.

[41] Dennhart, N. and Letzel, T. (2006) Mass spectrometric real-time monitoring of enzymatic glycosidic hydrolysis, enzymatic inhibition and enzyme complexes. *Anal. Bioanal. Chem.*, *386*, 689-698.

[42] de Boer, A. R., Letzel, T., van Elswijk, D. A., Lingeman, H., Niessen, W. A., and Irth, H. (2004) On-line coupling of high-performance liquid chromatography to a

continuous-flow enzyme assay based on electrospray ionization mass spectrometry. *Anal. Chem.*, *76*, 3155-3161.

[43] de Boer, A. R., Alcaide-Hidalgo, J. M., Krabbe, J. G. Kolkman, J., van Emde Boas, C. N., Niessen, W. M. A., Lingeman, H., and Irth, H. (2005) High-temperature liquid chromatography coupled on-line to a continuous-flow biochemical screening assay with electrospray ionization mass spectrometric detection. *Anal. Chem.*, *77*, 7894-7900.

[44] Scheerle, R. K., Grassmann, J., and Letzel, T. (2011) Enzymatic conversion continuously monitored with a robotic nanoESI-MS tool: experimental status. *Anal. Methods*, *3*, 822-830.

[45] Scheerle, R. K., Grassmann, J., and Letzel, T. (2012) Real-time ESI-MS of Enzymatic Conversion: Impact of Organic Solvents and Multiplexing. *Anal. Sci.*, *28*, 607-612.

[46] Krappmann, M. and Letzel, T. Functional analysis of proteins, including LC-MS and special freeware. In Letzel, T., editor., *Protein and Peptide Analysis by LC-MS.* Royal Society of Chemistry, Cambridge; 2011; 142-155.

[47] Dennhart, N., Weigang, L. M. M., Fujiwara, M., Fukamizo, T., Skirver, K., and Letzel, T. (2009) 26 kDa endochitinase from barley seeds: Real-time monitoring of the enzymatic reaction and substrate binding experiments using electrospray ionization mass spectrometry. *J. Biotechnol.*, *143*, 274-283.

[48] Lumb, K. J., Cheetham, J. C., and Dobson, C. M. (1994) ^{1}H Nuclear-Magnetic-Resonance studies of hen lysozyme-*N*-acetylglucosamine oligosaccharide complexes in solution: application of chemical-shifts for the comparison of conformational-changes in solution and in the crystal. *J. Mol. Biol.*, *235*, 1072-1087.

[49] Masaki, A., Fukamizo, T., Otakara, A., Torikata, T., Hayashi, K., and Imoto, T. (1981) Lysozyme-Catalyzed Reaction of Chitooligosaccharides. *J. Biochem.*, *90*, 527-533.

[50] Fukamizo, T., Minematsu, T., Yanase, Y., Hayashi, K., and Goto, S. (1986) Substrate Size Dependence of Lysozyme-Catalyzed Reaction. *Arch. Biochem. Biophys.*, *250*, 312-321.

[51] Honda, Y. and Fukamizo, T. (1998) Substrate binding subsites of chitinase from barley seeds and lysozyme from goose egg white. *Biochem. Biophys. Acta.*, *1388*, 53-65.

[52] Taira, T., Fujiwara, M., Dennhart, N., Hayashi, H., Onaga, S., Ohnuma, T., Letzel, T., Sakuda, S., and Fukamizo, T. (2010) Transglycosylation reaction catalyzed by a class V chitinase from cycad, *Cycas revoluta*: A study involving site-directed mutagenesis, HPLC, and real-time ESI-MS. *Biochim. Biophys. Acta.*, *1840*, 668-675.

[53] van Aalten, D.M., Komander, D., Synstad, B., Gåseidnes, S., Peter, M.G., Eijsink, V.G. (2001) Structural insights into the catalytic mechanism of a family 18 exo-chitinase *Proc Natl Acad Sci U S A. 98*, 8979-84.

[54] Ohnuma, T., Numata, T., Osawa, T., Mizuhara, M., Vårum, K. M., and Fukamizo, T. (2011) Crystal structure and mode of action of a class V chitinase from *Nicotiana tabacum*. *Plant. Mol. Biol.*, *75*, 291-304.

[55] Dennhart, N., Fukamizo, T., Brzezinski, R., Lacombe-Harvey, M. E., and Letzel, T. (2008) Oligosaccharide hydrolysis by chitosanase enzymes monitored by real-time electrospray ionization-mass spectrometry. *J. Biotechnol.*, *134*, 253-260.

[56] Fukamizo, T., Fleury, A., Côté, N., Mitsutomi, M., and Brzezinski, R. (2006) Exo-β-D-glucosaminidase from *Amycolatopsis orientalis*: catalytic residues, sugar recognition specificity, kinetics, and synergism. *Glycobiology*, *16*, 1064-1072.

[57] Ganem, B. and Henion, J. D. (2003) Going gently into flight: Analyzing noncovalent interactions by mass spectrometry. *Bioorg. Med. Chem.*, *11*, 311-314.

[58] Ganem, B., Li, Y. T., and Henion, J. D. (1991) Observation of Noncovalent Enzyme Substrate and Enzyme Product Complexes by Ion-Spray Mass-Spectrometry. *J. Am. Chem. Soc.*, *113*, 7818-7819.

[59] Clark, S. M. and Konermann, L. (2004) Determination of ligand-protein dissociation constants by electrospray mass spectrometry-based diffusion measurements. *Anal. Chem.*, *76*, 7077-7083.

[60] Svobodova, J., Mathur, S., Muck, A., Letzel, T., and Svatos, A. (2010) Microchip-ESI-MS determination of dissociation constant of the lysozyme-NAG3 complex. *Electrophoresis.*, *31*, 2680-2685.

[61] Jecklin, M. C., Touboul, D., Bovet, C., Wortmann, A., and Zenobi, R. (2008) Which electrospray-based ionization method best reflects protein-ligand interactions found in solution? A comparison of ESI, nanoESI, and ESSI for the determination of dissociation constants with mass spectrometry. *J. Am. Soc. Mass. Spctrom.*, *19*, 332-343.

[62] Clark, S. M. and Konermann, L. (2004) Screening for noncovalent ligand-receptor interactions by electrospray ionization mass spectrometry-based diffusion measurements. *Anal. Chem.*, *76*, 1257-1263.

[63] Schwalbe, H., (2003) Kurt Wüthrich, the ETH Zürich, and the development of NMR spectroscopy for the investigation of structure, dynamics, and folding of proteins. *ChemBioChem.*, *4*, 135-142.

[64] Kwan, A. H., Mobli, M., Gooley, P. R., King, G. F., and Mackay, J. P. (2011) Macromolecular NMR spectroscopy for the non-spectroscopist. *FEBS J.*, *278*, 687-703.

[65] Bieri, M., Kwan, A. H., Mobli, M., King, G. F., Mackay, J. P., and Gooley, P. R. (2011) Macromolecular NMR spectroscopy for the non-spectroscopist: beyond macromolecular solution structure determination. *FEBS J.*, *278*, 704-715.

[66] Ikura, M., Kay, L. E., and Bax, A. (1990) A novel approach for sequential assignment of ^{1}H, ^{13}C, and ^{15}N spectra of proteins: heteronuclear triple-resonance three-dimensional NMR spectroscopy. Application to calmodulin. *Biochemistry*, *29*, 4695-4667.

[67] Salzmann, M., Pervushin, K., Wider, G., Senn, H., and Wüthrich, K. (1998) TROSY in triple-resonance experiments: New perspectives for sequential NMR assignment of large proteins. *Proc. Natl. Acad. Sci. USA*, *95*, 13585-13590.

[68] Imoto, T., Johnson, L. N., North, A. C. T., Philips, D. C., and Rupley, J. A. Vertebrate lysozyme. In Boyer, P. D., editor., *The Enzymes.* Academic Press, New York; 1972; 665-868.

[69] Imoto, T., (1996) Engineering of lysozyme. *EXS.*, *75*, 163-181.

[70] Kuroki, R., Ito, Y., Kato, Y., and Imoto, T., (1997) A covalent enzyme-substrate adduct in a mutant hen egg white lysozyme (D52E). *J. Biol. Chem*., *272*, 19976-19981.

[71] Fukamizo, T., Torikata, T., Nagayama, T., Minematsu, T., and Hayashi, K., (1983) Enzymatic activity of avian egg-white lysozymes. *J. Biochem.*, *94*, 115-122.

[72] Fukamizo, T., Goto, S., Torikata, T., and Araki, T., (1984) Enhancement of transglycosylation activity of lysozyme by chemical modification *Agric. Biol. Chem.*, *53*, 2641-2651.

[73] Hirakawa, H., Ochi, A., Kawahara, Y., Kawamura, S., Torikata, T., and Kuhara, S., (2008) Catalytic reaction mechanism of goose egg-white lysozyme by molecular modelling of enzyme-substrate complex. *J. Biochem.*, 144, 753-761.

[74] Weaver, L. H., Grütter, M. G., and Matthews, B. W. (1995) The refined structures of goose lysozyme and its complex with a bound trisaccharide show that the "Goose-type" lysozymes lack a catalytic aspartate residue. *J. Mol. Biol., 245*, 54-68.

[75] Kawamura, S., Fukamizo, T., Araki, T., and Torikata, T. (2003) Expression of a synthetic gene coding for ostrich egg-white lysozyme in *Pichia pastoris* and its enzymatic activity. *J. Biochem., 133*, 123-131.

[76] Taita, T., Mahoe, Y., Kawamoto, N., Onaga, S., Iwasaki, H., Ohnuma, T., and Fukamizo, T. (2011) Cloning and characterization of a small family 19 chitinase from moss (*Bryum coronatum*). *Glycobiology, 21*, 644-654.

[77] Cornilescu, G., Delaglio, F., and Bax, A. (1999) Protein backbone angle restraints from searching a database for chemical shift and sequence homology. *J. Biomol. NMR, 13*, 289-302.

[78] Peitsch, M. (1995) Protein modeling by E-mail. *Biotechnology, 13*, 658-660.

[79] Hoell, I. A., Dalhus, B., Heggset, E. B., Aspmo, S. I., and Eijsink, V. G. (2006) Crystal structure and enzymatic properties of a bacterial family19 chitinase reveal differences from plant enzymes. *FEBS J., 273*, 4889-4900.

[80] Ohnuma, T., Sørlie, M., Fukuda, T., Kawamoto, N., Taira, T., and Fukamizo, T. (2011) Chitin oligosaccharide binding to a family GH19 chitinase from the moss *Bryum coronatum*. *FEBS J. 278*, 3991-4001.

[81] Marcotte, E. M., Monzingo, A. F., Emst, S. R., Brzezinski, R., and Robertus, J. D. (1996) X-ray structure of an anti-fungal chitosanase from *Streptomyces* N 174. *Nature Struct. Biol., 3*, 155-162.

[82] Saito, J., Kita, A., Higuchi, Y., Nagata, Y., Ando, A., and Miki, K. (1999) Crystal structure of chitosanase from *Bacillus circulans* MH-K1 at 1.6-A resolution and its substrate recognition mechanism. *J. Biol. Chem., 274*, 30818-30825.

[83] Katsumi, T., Lacombe-Harvey, M. E., Tremblay, H., Brzezinski, R., and Fukamizo, T. (2005) Role of acidic amino acid residues in chitooligosaccharide-binding to *Streptomyces* sp. N174 chitosanase. *Biochem. Biophys. Res. Commun., 338*, 1839-1844.

LCH

Appendix VI

Biochemical and Molecular Characterization of a Thermostable Chitosanase Produced by the Strain *Paenibacillus* sp. 1794 Newly Isolated from Compost

Zitouni, M., Fortin, M., Scheerle, R.K., Letzel, T., Matteau, D., Rodrigue, S. and Brzezinski, R.

Applied Microbiology and Biotechnology, 2013, 97(13), 5801-5813

This article describes the biochemical and molecular characterization of the new thermostable chitosanase Csn 1794 for the first time. The knowledge about the enzyme may be useful for biotechnological applications. The enzyme was isolated in the group of R Brzezinski. The mass spectrometric experiments were planned, conducted and analyzed on my part. I prepared the respective experimental and results section of the manuscript.

Appl Microbiol Biotechnol
DOI 10.1007/s00253-012-4483-4

BIOTECHNOLOGICALLY RELEVANT ENZYMES AND PROTEINS

Biochemical and molecular characterization of a thermostable chitosanase produced by the strain *Paenibacillus* sp. 1794 newly isolated from compost

Mina Zitouni · Mélanie Fortin · Romy K. Scheerle · Thomas Letzel · Dominick Matteau · Sébastien Rodrigue · Ryszard Brzezinski

Received: 1 August 2012 / Revised: 25 September 2012 / Accepted: 29 September 2012

Abstract Chitosan raises a great interest among biotechnologists due to its potential for applications in biomedical or environmental fields. Enzymatic hydrolysis of chitosan is a recognized method allowing control of its molecular size, making possible its optimization for a given application. During the industrial hydrolysis process of chitosan, viscosity is a major problem; which can be circumvented by raising the temperature of the chitosan solution. A thermostable chitosanase is compatible with enzymatic hydrolysis at higher temperatures thus allowing chitosan to be dissolved at higher concentrations. Following an extensive micro-plate screening of microbial isolates from various batches of shrimp shells compost, the strain 1794 was characterized and shown to produce a thermostable chitosanase. The isolate was identified as a novel member of the genus *Paenibacillus*, based on partial 16S rDNA and *rpoB* gene sequences. Using the chitosanase (Csn1794) produced by this strain, a linear time course of chitosan hydrolysis has been observed for at least 6 h at 70 °C. Csn1794 was purified and its molecular weight was estimated at 40 kDa by SDS-PAGE. Optimum pH was about 4.8, the apparent K_m and the catalytic constant k_{cat} were 0.042 mg/ml and 7,588 min^{-1}, respectively. The half-life of Csn1794 at 70 °C in the presence of chitosan substrate was >20 h. The activity of chitosanase 1794 varied little with the degree of *N*-acetylation of chitosan. The enzyme also hydrolyzed carboxymethylcellulose but not chitin. Chitosan or cellulose-derived hexasaccharides were cleaved preferentially in a symmetrical way ("3+3") but hydrolysis rate was much faster for $(GlcN)_6$ than $(Glc)_6$. Gene cloning and sequencing revealed that Csn1794 belongs to family 8 of glycoside hydrolases. The enzyme should be useful in biotechnological applications of chitosan hydrolysis, dealing with concentrated chitosan solutions at high temperatures.

Keywords Chitosan · Chitosanase · Oligosaccharide · Thermostability · Cleavage pattern · *Paenibacillus*

Electronic supplementary material The online version of this article (doi:10.1007/s00253-012-4483-4) contains supplementary material, which is available to authorized users.

M. Zitouni · M. Fortin · D. Matteau · S. Rodrigue · R. Brzezinski (✉)
Centre d'Étude et de Valorisation de la Diversité Microbienne, Département de Biologie, Faculté des Sciences, Université de Sherbrooke, 2500 boulevard de l'Université, Sherbrooke J1K 2R1 Québec, Canada
e-mail: Ryszard.Brzezinski@USherbrooke.ca

R. K. Scheerle · T. Letzel
Analytical Research Group, Wissenschaftszentrum Weihenstephan, Technische Universität München, Weihenstephaner Steig 23, 85354 Freising-Weihenstephan, Germany

Present Address:
M. Fortin
Centre d'expertise en spectrométrie de masse clinique Waters—CHUS, Centre Hospitalier Universitaire de Sherbrooke, 3001, 12e Avenue Nord, Sherbrooke J1H 5N4 Québec, Canada

Introduction

Chitosan is a polysaccharide mainly composed of β-1, 4-linked D-glucosamine units with a variable content of

Published online: 18 October 2012

N-acetyl-D-glucosamine units; lower than 50 % but most often between 0 and 25 % (Crini et al. 2009). Chitosan is found in some natural biomasses; however, its abundance is not sufficient to warrant large-scale exploitation. Thus, at an industrial scale, chitosan is almost exclusively obtained by alkaline treatment of deproteinized, demineralized, and decolorized crustacean shells, resulting in an extensive *N*-deacetylation of chitin (Roberts 1992; Crini et al. 2009). The percentage of D-glucosamine residues in the chitosan thus obtained is defined as the degree of *N*-deacetylation (DDA).

Chitosan is unique among commonly available polysaccharides because it carries amino groups which are protonated in mildly acidic aqueous solutions, at pH values lower than its pK_a (usually 6.3–6.7). Most biological properties of chitosan result from the presence of these positively charged groups. The solubility of chitosan rises with the increase of DDA (Sorlier et al. 2001).

Various forms of chitosan have potential applications in agriculture, biotechnology, in fundamental research, or as health products (recently reviewed in Crini et al. 2009, Aam et al. 2010, Domard 2011, Dai et al. 2011). Two parameters of chitosan molecules were shown to strongly influence its usefulness for a given application: DDA and the molecular weight (MW). Untreated chitosan from commercial sources is composed of polymer chains of very high MW (300–3,000 kDa) (Muzzarelli et al. 1987; Hamdine et al. 2005). Chitosan depolymerization can be achieved by various methods: physical, chemical, or enzymatic. While all three approaches have been used to prepare chitosan forms of low MW (10–100 kDa), only enzymatic or chemical methods seem to be appropriate for the preparation of chitosan oligosaccharides (CHOS) (Aam et al. 2010). Accordingly, the enzymes able to catalyze the hydrolysis of glycoside bonds in chitosan are the subject of many studies (Hoell et al. 2010).

Native chitosan has a high degree of polymerization and yields highly viscous solutions when dissolved at room temperature at relatively low concentrations, such as 4–5% *w/v*. Dissolution at higher concentrations in commonly used acid diluents such as acetic acid is hampered by the occurrence of a sol/gel transition (Rwei et al. 2005). At higher temperatures (50–80 °C), chitosan dissolution is facilitated by the rupture of intra- or intermolecular interactions between chitosan chains (mainly hydrogen bonds) and the point of sol/gel transition is shifted towards higher chitosan concentrations (Desbrieres 2002; Hamdine et al. 2005; Rwei et al. 2005). Thermostable chitosanase enzymes are therefore needed to perform hydrolysis of concentrated chitosan solutions at such high temperatures.

Thermostable chitosanases have been reported in several articles (Yoon et al. 1998, 2001; Ekowati et al. 2006). These examples all originated from bacteria belonging to the genus *Bacillus*. Their maximum activity is around 55–60 °C in standard assay conditions (30 min incubation in chitosan solution at optimal pH). The stability of these enzymes has been evaluated measuring the residual activity after pre-incubation in the absence of substrate. The chitosanases from *Bacillus* sp. KFB-C108 and strain CK4 retained, respectively, 45 and 80 % of their activity after 30 min of incubation at 80 °C (Yoon et al. 1998, 2001) and the chitosanase from *Bacillus licheniformis* MB-2 had a half-life of ~16 min when heated at 90 °C. More recently, a thermostable chitosanase originating from the fungus *Aspergillus fumigatus* and purified from the heterologous host *Pichia pastoris* (Pscheidt and Glieder 2008) has been characterized (Chen et al. 2012). Its maximum activity was at 55–65 °C when determined in a 15-min reaction. The enzyme had a half-life of 150 min at 80 °C when incubated in 50 mM Na-acetate buffer pH 6.5.

However, the half-lives of these enzymes in long-term treatments in the presence of substrate at high temperatures, reflecting their biotechnological usefulness for chitosan hydrolysis, have not been evaluated. We have recently shown that the presence of the substrate chitosan can enhance considerably the thermostability of chitosanases and that this effect must result from a specific interaction of the enzyme with chitosan, as it was much less pronounced with polyethyleneimine, another cationic polymer (Roy et al. 2007; Ghinet et al. 2010). Consequently, the evaluation of chitosanase thermostability in the absence of substrate may not reflect the behavior of the enzyme during a chitosan hydrolysis bioprocess at high temperature.

We report in this study the isolation of a new bacterial strain, *Paenibacillus* sp. 1794 producing a thermostable chitosanase. The enzyme has been purified and its pattern of activity has been characterized with oligosaccharide substrates. We further report the cloning and sequencing of the gene encoding this chitosanase.

Materials and methods

Screening of compost samples and isolation of *Paenibacillus* sp. 1794

The starting material consisted of commercial batches of shrimp shell and peat-based composts. Eight grams of each compost (wet weight) were combined with 1 g of powdered chitosan (number average molecular weight, M_n of 120, 8, or 4 kDa) and thoroughly mixed. The mix was wetted with a solution containing Bushnell Haas salts (Difco; 3.3 g/l) and K_2HPO_4 (6.44 g/l); pH 6.5–6.8, supplemented in some samples with $MgSO_4$ (1 g/L). The mixes were incubated at 30, 37, 45, or 55 °C for 6 weeks with periodic wetting. At the end of this incubation, a further selective treatment with hot phenol (Nonomura and Hayakawa 1988) was applied: 1 g of the mix was dispersed in 10 ml of a 2.5 % aqueous

phenol solution pH 6.0 by vortexing and the suspension was incubated for 30 min at 50 °C.

Following the enrichment procedure, treated or untreated samples were dispersed in 10 ml of peptone water and serial dilutions were plated on an agar medium containing, per liter: 3.27 g Bushnell Haas salts, 2.5 g tryptone, 1.25 g yeast extract, 0.5 glucose, 5 g NaCl, and pH 6.5. After 48 h of incubation at 37 °C, individual colonies were picked up and inoculated within 2 ml wells of a microtiter plate containing 400 μl of tryptic soy broth. After 48 h of growth at 37–50 °C with shaking, the wells were completed with 1.4 ml of medium containing, per liter: 1 g malt extract, 0.5 g K_2HPO_4, 0.2 g $MgSO_4$, 2 g $(NH_4)_2SO_4$, 0.3 g chitosan (M_n~30 kDa), and 2.5 g CHOS (M_n~2 kDa), and further incubated for 72–144 h. Chitosanase activity in the supernatants of the micro-cultures was assayed with the soluble, dyed substrate sRBB-C as described (Zitouni et al. 2010).

The 1794 isolate was routinely propagated in tryptic soy broth (Difco) at 45 °C with shaking. For long-term storage, 1 vol of an overnight culture was combined with an equal volume of sterile glycerol, supplemented with 7 % dimethyl sulfoxide and kept frozen at −80 °C. The strain was deposited in the National Microbiology Laboratory Health Canada Culture Collection (Nr. 110111-01).

Molecular taxonomy

Genomic DNA was extracted from cells using the standard phenol method (Sambrook et al. 1989). The PCR amplification of the variable segment of the 16S rRNA gene was achieved with the universal primers 926/20 BSR (5′-GGGTGAATTYYTTTRAGTTT-3′) and 8/20 BSF (5′-AGAGTTTGATCCTGGCTCAG-3′) and the following program: 5 min at 94 °C followed by 35 cycles of 1 min at 94 °C, 1 min at 48 °C, and 1 min at 72 °C and terminated by elongation for 10 min at 72 °C. The partial *rpoB* sequence, encompassing the so-called "DGGE fragment" (Dahllöf et al. 2000) was determined using primers and PCR conditions as in (da Mota et al. 2004). The PCR products were purified by GFX™ PCR DNA and Gel Band purification kits (GE Healthcare, United Kingdom). Nucleotide sequence has been determined at Genome Québec, Montréal, QC, Canada.

Chitosanase production by *Paenibacillus* sp. 1794

The chitosanase production medium was obtained as follows. First, a 2.5 times concentrated base medium was obtained by dissolving, in distilled water, peptone (12.5 g/l), K_2SO_4 (2.5 g/l), K_2HPO_4 (12.5 g/l), $MgSO_4$ (2.5 g/l), NaCl (0.25 g/l), $CaCl_2$ (0.4 g/l), $FeSO_4$ (25 μM), and 0.5 ml of microelements solution ($ZnSO_4 \cdot 7H_2O$, 1 g/l; $MnCl_2 \cdot 4H_2O$, 1 g/l); this mix was autoclaved; final pH being around 6.5. Separately, solutions (100 g/l) of sucrose, chitosan oligosaccharides (Diversified Natural Products Canada, Granby, QC, Canada), and D-glucosamine were filter sterilized. Still separately, an aqueous suspension of chitosan (Sigma-Aldrich; degree of *N*-acetylation of 84 %) consisting of 5 g of finely ground chitosan powder suspended in 390 ml of distilled water, was autoclaved. To reconstitute the chitosanase production medium (1 l), 400 ml of concentrated base medium were combined with 100 ml of D-glucosamine solution, 70 ml of chitosan oligosaccharides solution, and 40 ml of sucrose solution. This mix was inoculated with a 14–18 h culture (45 °C; 300 rpm shaking) of *Paenibacillus* sp. 1794 in tryptic soy broth (Difco) in a 1/10 proportion. After 10 h of incubation (45 °C; 300 rpm shaking), the culture was combined with the sterile suspension of chitosan (390 ml) and further incubated for 5 to 7 days. This method allowed obtaining 5–12 U of chitosanase per milliliter of culture supernatant.

Chitosanase purification

Protein precipitation After elimination of bacterial cells by centrifugation, the culture supernatant (~1 l) was cooled to 4 °C. The supernatant was then combined with 2 vol of ice-cold acetone with constant mixing. The mixture was left to precipitate for 18 h and supernatant was then removed with a pump. The pellet was suspended in 50 mL of 20 mM Tris–HCl pH 8.0 and left to dissolve overnight at 4 °C. The resulting viscous solution was extracted three times with 20 mL of chloroform and centrifuged to eliminate insoluble particles.

Ion exchange chromatography The enzyme solution obtained after the precipitation step was diluted with 1 vol of 20 mM Tris–HCl pH 8.0 and loaded on a Q-Sepharose Fast Flow column (25 ml of bed volume; GE Healthcare, Baie d'Urfé, QC, Canada). The column was washed with 50 ml of loading buffer and the proteins were eluted with 400 ml of 20 mM Tris–HCl (pH 8) including an NaCl gradient from 0 to 1 M. Fractions of 5 ml were collected. Chitosanase containing fractions were identified by assay with sRBB-C substrate and pooled.

Enzyme concentration This step is facultative. The pooled fractions from the previous step (~25 ml) were diluted with four volumes of 20 mM Tris–HCl buffer pH 8.0 and loaded on a mini-column (1 ml bed volume) Hi-Trap Q (GE Healthcare). Chitosanase was recovered by one-step elution with 0.5 M NaCl in 20 mM Tris–HCl pH 8.0. Fractions of 0.2 ml were collected. The active fractions were identified by assay with sRBB-C substrate and pooled.

Hydroxyapatite chromatography Fractions from the previous step (~1.2 ml) were combined with 10 vol of 1 mM K-phosphate buffer pH 6.8 and loaded on a hydroxyapatite column (DNA grade; bed volume 10 ml, BioRad) equilibrated

with the same buffer. The column was washed with 20 ml of the loading buffer and then with 20 ml of 5 mM unbuffered $MgCl_2$. The proteins were eluted with a 100 ml gradient of 1–300 mM potassium phosphate buffer pH 6.8. Fractions of 0.5 ml were collected. The active fractions were identified by assay with sRBB-C substrate and pooled.

After dialysis against 100 mM Na-acetate buffer pH 5.5, the purified chitosanase was stored at −20 °C after addition of 50% *v*/*v* glycerol. No significant loss of activity was noticed after a 20-month period of storage.

Biochemical procedures and kinetics

In standard assays, the chitosanase activity was measured using, as substrate, 84 % *N*-deacetylated chitosan (0.8 mg/ml) dissolved in 50 mM sodium acetate buffer (pH 4.8). The reaction was started by mixing 480 µl of substrate and 20 µl of appropriately diluted enzyme sample. The mixture was incubated for 10 min at 37 °C. The reaction was then stopped by addition of 1 ml of freshly prepared reagent of Lever (1972) as modified by Schep et al. (1984). The resulting mixture was incubated for 20 min at 100 °C, chilled on ice and centrifuged (5 min, 13,000 rpm) to pull down the unreacted chitosan precipitate. Reducing sugars in the reaction supernatant were determined at 405 nm against a D-glucosamine standard curve. One chitosanase unit was defined as the amount of enzyme that released 1 µmole of D-glucosamine equivalents per minute under the specified conditions.

For the determination of the substrate specificity of chitosanase, chitosan samples of DDAs of 97, 94, and 86 % were obtained respectively from Shanghai Freemen Americas (Piscataway, NJ, USA), Marinard Biotech (Rivière-au-Renard, QC, Canada) and Diversified Natural Products Canada (Granby, QC, Canada). Samples of DDAs of 72, 65, and 62 % were obtained by treating chitosan from Sigma-Aldrich (DDA 84 %) with acetic anhydride, as described by Hirano and Ohe (1975) and Il'ina and Varlamov (2003). The degrees of *N*-deacetylation of all samples were determined by ^{1}H-NMR (Lavertu et al. 2003). Chitosans and other substrates were dissolved in 50 mM sodium acetate buffer, pH 4.8 at 1 mg/ml. Kinetic data were analyzed with GraphPad Prism software.

The half-life time of chitosanase activity at high temperatures was estimated from hydrolysis time-course curves. These experiments were performed at a chitosan substrate concentration of 5 g/L in 0.25 M acetic acid, pH 4.5. Temperature was set up at 70, 75, or 78 °C. After addition of chitosanase (~0.15 mU of enzyme per milligram of substrate), samples were taken periodically for up to 6 h and the accumulation of product was determined by the reducing sugars assay as above. Assuming a first-order inactivation process, the half-life of chitosanase was calculated according to Přenosil et al. (1987) and Fullbrook (1996) using the NLREG program (available at www.nlreg.com).

Protein concentration was determined by the method of Bradford (1976) with bovine serum albumin (Sigma-Aldrich) as standard. The concentration of purified chitosanase was determined from the absorbance at 280 nm assuming an extinction coefficient of 114,773 $cm^{-1}M^{-1}$ estimated from the amino acid sequence of mature protein.

Mass spectrometry studies of hydrolysis patterns of oligosaccharides

Chitosan oligosaccharides of defined length $(GlcN)_n$: β-1,4-linked D-glucosamine oligosaccharides with a polymerization degree of n=2–6 were purchased from Seikagaku Kogyo Co. (Tokyo, Japan). Cello-oligosaccharides $(Glc)_n$: β-1,4-linked D-glucose oligosaccharides with a polymerization degree of n=3, 4, or 6 were purchased from Coring System Diagnostix (Gernsheim, Germany). Ammonium acetate (≥98 %) and acetic acid (≥98 %) were obtained from Sigma-Aldrich (Steinheim, Germany).

Enzyme and substrate solutions were prepared in 10 mM ammonium acetate (pH 5.2). After mixing the enzyme and substrate, the solution was infused into the mass spectrometric interface via syringe (500 µL, Hamilton-Bonaduz, Switzerland) located in a syringe pump (model 11 plus, Harvard Apparatus, Hugo Sachs Elektronik, Hugstetten, Germany) with a flow rate of 10 µL/min (tubing, 1/16″× 0.13 mm i.d., 260 mm length). Samples were measured with a TOF LC/MS 6230 mass spectrometer equipped with a multimode ion source (Agilent Technologies, Santa Clara, USA). Mass spectrometric parameters were as follows: positive ionization mode, 300 °C drying gas temperature, 5 L min^{-1} drying gas flow rate, 85 °C vaporizer temperature, 35 psi nebulizer gas pressure, 1,500 V capillary voltage, 2,000 V charging voltage, 175 V fragmentor voltage, 65 V skimmer voltage, and 750 V octapole RF voltage. The mass range was set to 50–3,200 *m*/*z* and data acquisition was 1.42 cycles/s. System control and data evaluation were performed with MassHunter Workstation Acquisition and Qualitative Analysis software (Agilent Technologies, version B. 04.00, 2011).

Each enzymatic assay was measured for 30 min. The time courses show a delay of 2 min due to the manual mixing step, filling the syringe, and transfer to the source.

Extracted ion chromatogram signal intensities were summed for the following compounds: for $(GlcN)_6/(Glc)_6$ signals $[(GlcN)_6/(Glc)_6+H]^+$, $[(GlcN)_6/(Glc)_6+Na]^+$, $[(GlcN)_6/(Glc)_6+2\ H]^{2+}$, $[(GlcN)_6/(Glc)_6+2Na]^{2+}$, and $[(GlcN)_6/(Glc)_6+H+Na]^{2+}$ and for $(GlcN)_n/(Glc)_n$ (n=1–5) signals $[(GlcN)_n/(Glc)_n+H]^+$ and $[(GlcN)_n/(Glc)_n+Na]^+$. The

time courses were smoothed with a Gaussian function with 15 points function width and 5,000 point Gaussian width.

Fragmentation and rearrangement effects of $(GlcN)_n$ and $(Glc)_n$ free in solution were corrected and ionization factors were determined (Dennhart et al. 2008). Signals were normalized (with substrate signal at $t(2)=100$) for calculating reaction conversion rates. The obtained reaction time courses were extrapolated using an exponential function and substrate conversion rate was calculated (Scheerle et al, 2011). At the stage of about 100 % substrate consumption the symmetrical and asymmetrical, as well as the tetramer re-cleavage for both hexasaccharides $(GlcN)_6$ and $(Glc)_6$ were calculated according to the following equations:

$$\text{frequency of re-cleavage of tetramer: (“2 + 2” cleavage)} = ([\text{dimer}] - [\text{tetramer}])/3$$

$$\text{frequency of symmetrical cleavage: (“3 + 3” cleavage + “2 + 2” cleavage)} = [\text{trimer}]/2 + ([\text{dimer}] - [\text{tetramer}])/3$$

$$\text{frequency of asymmetrical cleavages: (“4 + 2” cleavage)} = [\text{tetramer}] + \text{frequency of “2 + 2” cleavage}$$

Chitosanase gene cloning and sequencing

Partial amino acid sequences of the purified chitosanase were determined by liquid chromatography coupled to tandem mass spectrometry (LC-MS/MS) at the Laboratory of Molecular Biophysics, University of British Colombia, Vancouver, BC, Canada. The sequences have been used to design oligonucleotide primers, synthesized by Integrated DNA Technology (IDT, USA). The longest fragment (0.65 Kb) amplified by PCR from the genomic DNA of *Paenibacillus* sp. 1794 was obtained using the following pair of primers: 5′-AAATGGAACAGCTGGAAA-3′ and 5′-CATCAGATAGTCGGTCGT-3′.

To construct a partial *Paenibacillus* sp. 1794 gene library enriched in the chitosanase gene, Southern blot analysis was first done on restriction enzyme-digested genomic DNA using the PCR-amplified DNA fragment as a probe. The probe was labeled with digoxigenin using the DIG-DNA Labeling Kit (Roche Applied Science, Germany) and used for hybridization with DNA fragments separated by electrophorese on 1 % agarose gel and transferred onto a Hybond-N+ membrane. Staining and detection of hybridized DNA were done according to manufacturer's instructions.

Library construction was pursued by digestion of genomic DNA from *Paenibacillus* sp. with *Bsp*EI enzyme. Fragments of ~6 to 8 Kb were obtained by purification after agarose gel electrophoresis with the GFX™ PCR DNA and Gel Band Purification Kit (GE Healthcare, United Kingdom). The fragments were ligated into *Bsp*EI-digested LITMUS 38i vector (Evans et al. 1995) and used to transform Ultracompetent *E. coli* XL10- Gold® cells (Stratagene, Canada). Approximately 5,000 clones were obtained. They were screened for chitosanolytic activity on nutrient agar plates containing 5 mg/ml of the dyed sRBB-C substrate (Zitouni et al. 2010).

The plasmids recovered from chitosanase-resistant colonies were prepared for sequencing using GenElute TM Plasmid Miniprep Kit DNA purification system (Sigma-Aldrich, Missouri, USA). The nucleotide sequence was determined at the McGill University and Génome Québec Innovation Centre.

Transcription startup determination by rapid amplification of cDNA ends

RNA extraction For RNA isolation, 50 ml of culture of *Paenibacillus* sp. 1794 were grown in tryptic soy broth at 45 °C and exponentially growing cells (OD. 0.8) were collected by centrifugation of 10 ml of culture for 5 min at 5,000×*g* at 4 °C. The pellet was suspended in 1 ml of Trizol (TRI Reagent® RNA Isolation Reagent; Sigma-Aldrich, Missouri, USA). This suspension was transferred to 2 ml screw cap tube with 50 mg of sterile 150 μm glass beads and mixed 10 s by vortexing. The cells were homogenized using Fastprep for 60 s at speed 6.5 then centrifuged 15 s at 17,600×*g* to pellet the beads. The supernatant was transferred in 1.5 ml RNAse-free tube containing 200 μl chloroform then vortexed vigorously for 15 s and incubated 15 min at room temperature. The reaction tubes were centrifuged 15 min at 12,000×*g* at 4 °C. The aqueous phase (≈450 μl) was transferred to 1.5 ml RNAse-free tube and the RNA was precipitated by adding 500 μl of isopropanol. After vortexing, the tubes were incubated 10 min at room temperature then centrifuged 10 min at 12,000×*g* at 4 °C. The pelleted RNA was washed with 1 ml of ethanol 75 %, resuspended in RNAse free water, then transferred to Qiagen RNeasy mini-spin column for DNase treatment and final purification with the Qiagen RNeasy Mini kit, (Hilden, Germany) according to manufacturer's instructions.

5′-RACE A 10-μl reaction containing 300 ng of total RNA, 1 μl of Antarctic phosphatase buffer (10×), 0.5 μl of Antarctic phosphatase (5 U/μl, NEB, Ipswich, USA), and

0.5 μl of RNase inhibitor (40 U/μl, Enzymatics, Beverly, MA, USA) was incubated in a thermal cycler at 37 °C for 30 min, followed by phosphatase heat inactivation at 65 °C for 5 min. Two microliters of 10× T4 polynucleotide kinase buffer (10×), 2 μl of ATP (10 mM), 1 μl of RNase inhibitor (Enzymatics), 1 μl of T4 PNK (10 U/μl, Enzymatics), and 4 μl of nuclease free water were directly added to the tube. The reaction was incubated at 37 °C for 30 min and purified with the clean and concentrator-5′RNA kit according to the manufacturer's instructions (Zymo Research, Irvine, CA, USA).

To 13 μl of purified RNA, the following components were added in a PCR tube: 10 pmoles of "5 hybrid-0" oligo (5′-ACA CGA CGrC rUrCrU rUrCrC rGrArU rCrU-3′), 2 μl of 10× T4 RNA ligase buffer, 2 μl of 100 % DMSO, and 0.6 μl nuclease-free water. The tube was heated to 65 °C for 1 min and put immediately on ice; 0.5 μl of RNAse inhibitor (Enzymatics) and 1.5 μl of T4 RNA ligase 1 (20 U/μl, Enzymatics) were then added, and the reaction was incubated at 37 °C for 60 min. The adaptor-ligated RNA was purified using RNA Clean XP beads (Beckman Coulter, Missisauga, ON, Canada). A reverse transcription was prepared by mixing 10 μl of 5'-adaptor-ligated RNA, 1 μl rapid amplification of cDNA ends (RACE)250 primer (5′-CGCCGCTTGAA TCGTACTTCACAT-3′) (10 pmol), 2 μl dNTPs Mix (10 mM), and incubating at 65 °C for 2 min followed by rapid quenching on ice for 1 min; 2 μl M-MuLV RT buffer (10×), 3 μl H_2O, 1 μl RNase inhibitor, and 1 μl M-MuLV RT (200 U/μl, Enzymatics) were immediately added and the reaction was incubated at 42 to 50 °C for 1 h (42 °C for 10 min, +0.2 °C per min for 40 min, and 50 °C for 10 min), and heated to inactivate at 85 °C for 10 min.

One percent of the cDNA from previous step was used for each PCR reaction with Taq DNA polymerase (NEB) in 10 μl of DMSO, 10 μl dNTPs (10 mM), 10 μl RACE250 primer (10 μM), 10 μl IGA-PE-F primer (5′-AATGATACGGCGA CCACCGAGATCTACACTCTTTCCCTACACGACGCTC TTCCGATCT-3′) (10 μM), 10 μl Taq DNA polymerase buffer (10×), and 49 μl H_2O. The PCR program was 94 °C for 5 min followed by 35 cycles of 94 °C for 1 min, 59.1 °C for 1 min, and 72 °C for 1 min then 72 °C for 10 min. Following the amplification, the PCR product was purified by GFX™ PCR DNA and GEL Band purification Kit, (GE Healthcare). For more specificity a second round of nested PCR was done using the DNA product of the first one and the primers: RACE150 (5′-TTTGACTGCATCGTCCATCGTGGT-3′) (10 μM) and IGA-PE-F using the same conditions. The purified PCR product was cloned into plasmid vector pCR2.1 (Life Technologies, Burlington, ON, Canada). The positive clones were analyzed by DNA sequencing at the McGill University and Génome Québec Innovation Centre.

Nucleotide sequences accession numbers

The nucleotide sequences of 16S rDNA and *rpoB* and *csn1794* genes described in this work were assigned to the GenBank acc. nos. JN688151, JN688152, and JX109837.

Results

Screening and selection of chitosanolytic strains

In order to select a microorganism producing thermostable chitosanase, we used various commercial brands of shrimp shell-based composts as starting material. Samples of compost were enriched with chitosan powder and incubated for 6 weeks at various temperatures with periodic wetting. To maximize the recovery of a large diversity of chitosanolytic bacteria, we used chitosans of various MWs and the salt composition of the wetting solution was also different among enrichments. The variation of these two components that were added to the compost samples allowed us to modulate the antibacterial effect of chitosan during the enrichment step, shown to be dependent on MW and salt concentration (Kong et al. 2010).

At the end of the enrichment step, serial dilutions of these compost suspensions were plated on three types of agar media: a complete medium, an inorganic salt medium with powdered chitosan as sole carbon source, and an inorganic salt medium with peptone and chitosan oligosaccharides. Plates were incubated at three different temperatures: 30, 37, 45, or 55 °C. For some samples, additional treatments (Nonomura and Hayakawa 1988) were performed before plating.

A total number of 2,200 isolates were established from colonies recovered from these agar plates. In order to identify chitosanase-positive strains, the isolates were inoculated in triplicate in microtiter plates with large (2 ml) wells in 400 μl of complete medium. After 48 h of incubation with shaking, the mini-cultures were supplemented with a chitosanase-induction medium containing powdered chitosan as well as chitosan oligosaccharides. At the end of the incubation, chitosanase activity was measured with the soluble dyed substrate sRBB-C by a procedure adapted to microtiter plates (Zitouni et al. 2010).

Among the best chitosanase producers, 25 were chosen for chitosanase thermostability evaluation. To select the best candidates, we determined the half-life of chitosanase activity of crude enzyme preparations during 160-min incubations in chitosan solutions (5 g/L in 0.25 M acetic acid, pH 4.5) at temperatures between 50 and 80 °C. This first round of evaluation allowed selection of seven strains of which the chitosanase activity remained linear for the tested period of time at 70 °C. Among them, three isolates

were selected for their linear behavior in reactions time courses performed at 78 °C. Further discrimination among them was only possible after the third round at 81 °C. The strain 1794 was selected as the isolate producing the chitosanase with the highest thermostability. The choice of the 1794 strain was also confirmed after purification of the three best chitosanases and further thermostability tests (data not shown).

Taxonomic identification of the 1794 isolate

The strain 1794 originated from a composted material based on shrimp shells and peat. It appeared as a Gram-positive, mobile bacterium with bacillary morphology and produced endospores in a variety of media. Optimal growth was observed at 45 °C while slightly slower growth was observed at 55 °C. It gave positive reactions for catalase, oxidase, caseinase, α-amylase, β-galactosidase but negative for tyrosinase. It was negative in the methyl red test, Voges-Proskauer test, gas production from glucose, and hemolysis. Being able to use mannitol and sorbitol, it was also positive for acid production from D-glucosamine, *N*-acetyl-D-glucosamine, L-arabinose, D-ribose, D-xylose, and D-glucose but negative for acid production from glycerol and sorbitol.

The sequence of the hyper variable portion of the 16S rRNA gene (GenBank JN688151) allowed the classification of the isolate 1794 into the genus *Paenibacillus*, being however highly similar to the sequences published for *Paenibacillus favisporus* and *Paenibacillus cineris*. While the strain 1794 could be distinguished from these two species by its biochemical and physiological properties, we further characterized its taxonomical position by partial sequencing of the *rpoB* gene encoding the beta subunit of the RNA polymerase (GenBank JN688152). The sequence was found to be different from all those published to date in GenBank (July 2012), differing by 16 nucleotides among 373 from its closest relative, *P. favisporus*. The strain 1794 represents thus a novel isolate and will be reported as *Paenibacillus* sp. 1794.

Biochemical properties of purified 1794 chitosanase

Chitosanase 1794 (Csn1794) was purified by a three-step process. The first step—precipitation from the supernatant—could be carried out alternatively with ethanol or acetone. In some preparations, the dissolution of the precipitated pellet in acetate buffer led to a very viscous solution. This was probably due to an extracellular polymer secreted by *Paenibacillus* sp. 1794 that co-precipitated with the enzyme. Viscosity could be decreased by extraction with chloroform without significant loss of chitosanase activity (data not shown). After two further chromatographic steps, a homogenous chitosanase preparation was obtained, as estimated from SDS-PAGE and staining with Coomassie Blue (Suppl. Fig. 1). The molecular weight of the protein was estimated to be approximately 40 kDa. In the standard assay at 37 °C, the purified chitosanase had a specific activity of 122 U per milligram of protein.

Variation of activity with pH and temperature change

Maximal chitosanase activity was observed at pH around 4.7–4.8, but the enzyme kept at least 80 % of activity in a wider range of pH values between 3.8 and 6.5 (Fig. 1). The effect of temperature on enzyme activity was determined by running short reactions for 3, 5, or 10 min. Maximal activity was observed at 80 °C for 10 min and at 85 °C for 5- and 3-min incubation times (Fig. 2).

Kinetic parameters

The apparent K_m and the catalytic constant k_{cat} were calculated using a weighted least-square fit approach. Changes in the activity of Csn1794 against increasing concentrations of chitosan substrate were best represented by a model assuming that substrate inhibition influenced the rate of chitosanase-catalyzed reaction (Fig. 3), yielding the following values: K_m=0.042 mg/ml, k_{cat}=7,588 min^{-1}, and K_i=1.66 mg/ml. The occurrence of substrate inhibition was previously observed for a GH46 chitosanase (Boucher et al. 1992).

Substrate specificity

Chitosans with various degrees of *N*-deacetylation were tested as substrates for Csn1794. Besides highly deacetylated commercial samples, a series of chitosans with lower DDAs was synthesized by treatment of chitosan with acetic anhydride according to a published procedure (Hirano and

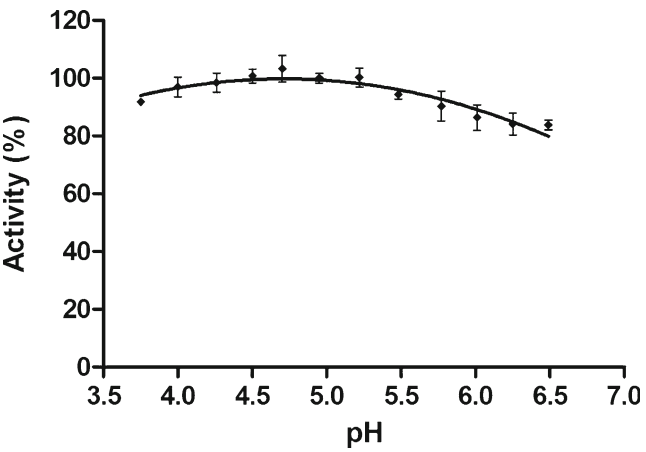

Fig. 1 Determination of pH optimum for activity of Csn1794 chitosanase. Substrate, 84 % *N*-deacetylated chitosan (0.8 mg/ml) dissolved in 50 mM sodium acetate buffer

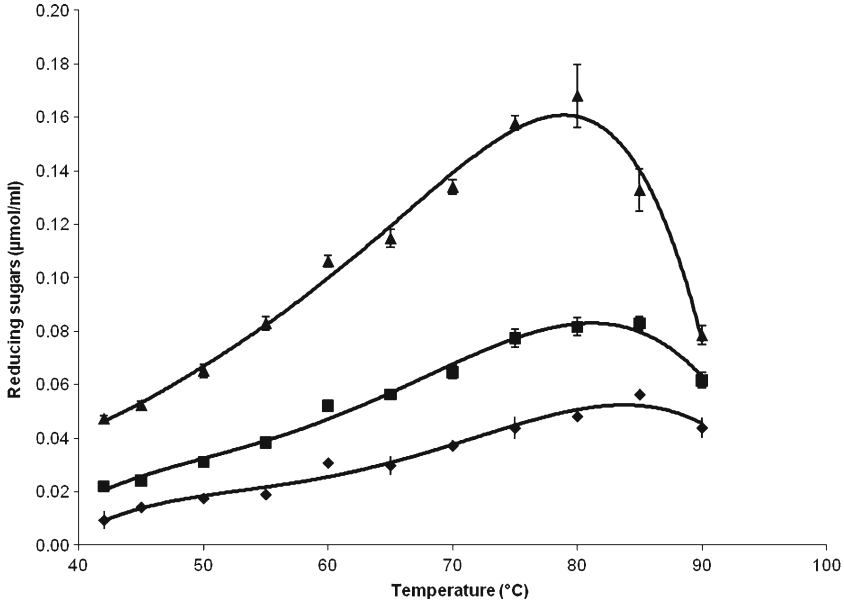

Fig. 2 Effect of temperature on chitosanase Csn1794 activity. Substrate as in Fig. 1; pH 4.5. Reaction time: *triangle* 10 min; *square* 5 min; *diamond* 3 min

Ohe 1975). The activity of Csn1794 varied little with the DDA of the substrate in the studied range (0.62–0.98; Fig. 4). The enzyme is thus able to efficiently hydrolyze a wide spectrum of chitosan substrates.

Using chitosan from Sigma-Aldrich (DDA=84 %) as a reference, we examined the activity of Csn1794 against other types of biopolymers, all dissolved at 1 mg/ml in 50 mM Na-acetate buffer pH 4.8. Csn1794 hydrolyzed carboxymethyl cellulose and methylcellulose with relative activities of 58 and 14 %, respectively. No activity was detected against microcrystalline cellulose, chitin, xylan, laminarin, pustulan, pachyman, mannan, or β-1,3-1,4-glucan.

Pattern of hydrolysis of oligosaccharides

The course of oligosaccharide substrate hydrolysis was monitored in real-time by electrospray ionization mass spectrometry (ESI-MS). Hydrolysis of $(GlcN)_n$ (n=3, 4, 5, and 6) and $(Glc)_n$ (n=3, 4, and 6), respectively, was determined by mixing each substrate with enzyme Csn1794 (Fig. 5). Enzyme concentration was adjusted for every single assay, in order to obtain a sufficient substrate hydrolysis and product signals were detected. $(GlcN)_6$ was hydrolyzed into two molecules $(GlcN)_3$. A very small proportion was hydrolyzed into $(GlcN)_2$ and $(GlcN)_4$ (Fig. 5a). A semi-quantitative estimation of cleavage mode performed at 100 % substrate consumption showed a clear preference to symmetrical cuts ("3+3" and "2+2") over the asymmetrical ones ("4+2") in a 12:1 proportion. $(GlcN)_5$ was hydrolyzed into $(GlcN)_2$ and $(GlcN)_3$ (Fig. 5b). $(GlcN)_4$ was hydrolyzed mainly into dimers $(GlcN)_2$, but $(GlcN)_3$ product was also significant. Trimers should be accompanied by monomers (GlcN) in equivalent amounts which were not observed in the current measurements (Fig. 5c). Measuring the pure GlcN monomer (without enzyme) showed a constant signal, whereas GlcN monomer could not be detected in the presence of enzyme (data not shown). Mass spectrometric signal suppression

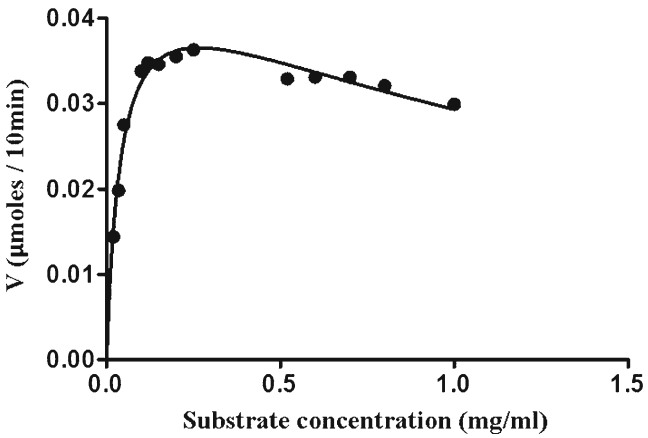

Fig. 3 Effect of substrate concentration of chitosanase Csn1794 activity interpreted according to a substrate inhibition model

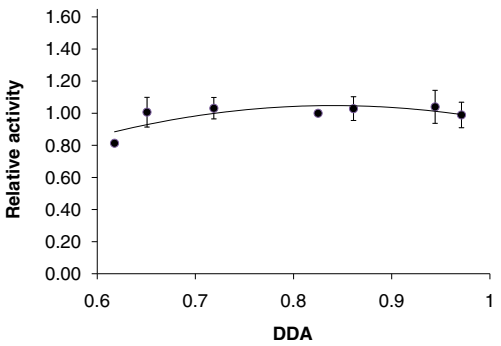

Fig. 4 Relative activity of chitosanase Csn1794 against chitosans of various degrees of *N*-deacetylation. Activity against chitosan from Sigma-Aldrich (DDA=0.84) is taken as a reference (relative activity=1)

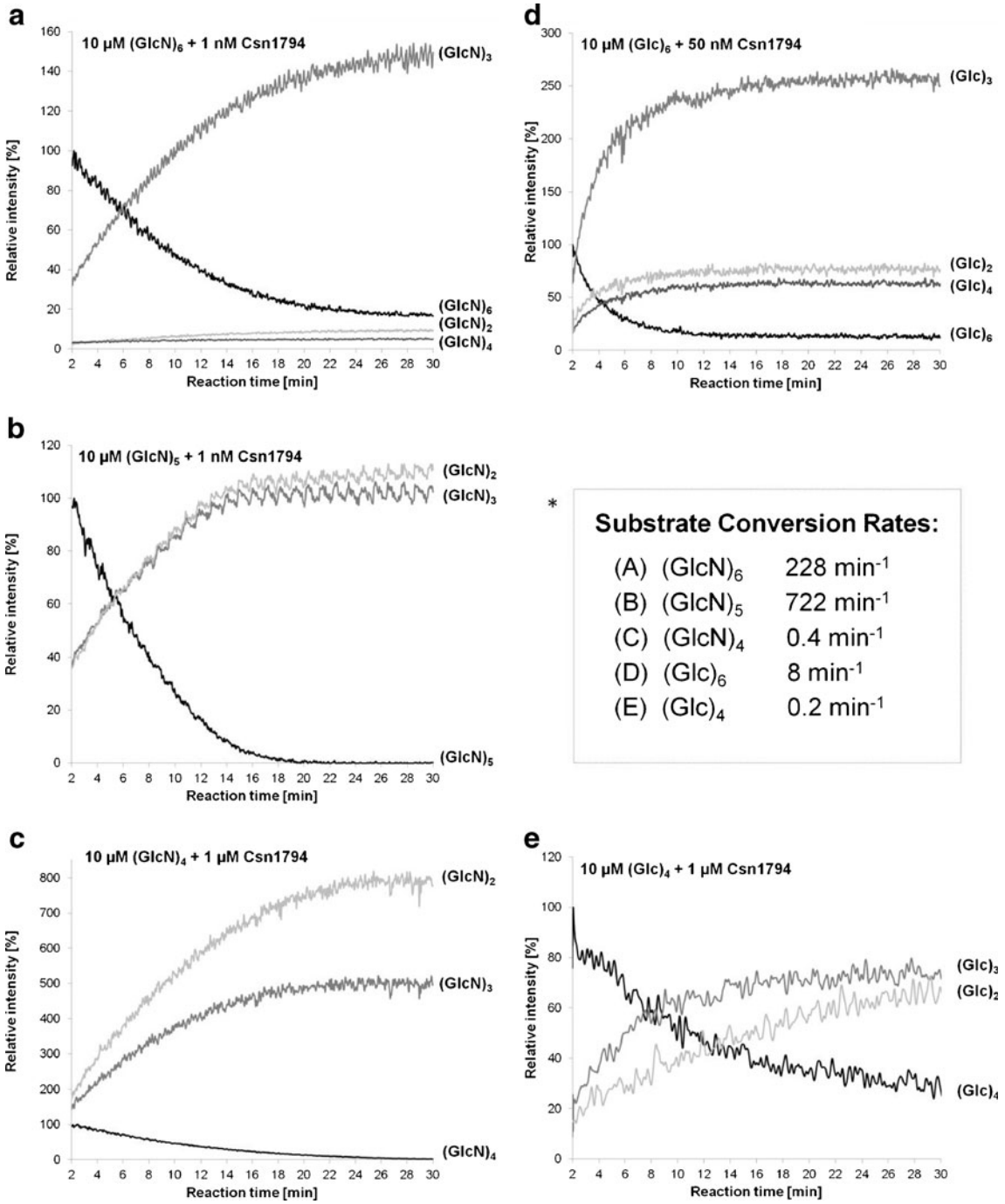

Fig. 5 Real-time ESI-MS monitoring of oligosaccharide hydrolysis by Csn1794. Extracted ion chromatogram time courses for oligosaccharide substrates and products and the corresponding substrate conversion rates (*) are shown. Reactions were performed with 10 μM $(GlcN)_6$ and 1 nM Csn1794 (**a** 100 %≈2.9×10^4 counts), 10 μM $(GlcN)_5$ and 1 nM Csn1794 (**b** 100 %≈1.6×10^4 counts), 10 μM $(GlcN)_4$ and 1 μM Csn1794 (**c** 100 %≈2.3×10^4 counts), 10 μM $(Glc)_6$ and 50 nM Csn1794 (**d** 100 %≈1.3×10^4 counts), and 10 μM $(Glc)_4$ and 500 nM Csn1794 (**e** 100 %≈2.3×10^3 counts)

and/or formation of non-detectable enzyme–substrate complexes may cause this effect. $(GlcN)_3$ was not hydrolyzed by Csn1794 (data not shown).

The cellulose-derived hexasaccharide, $(Glc)_6$, was mainly hydrolyzed into two molecules of $(Glc)_3$, accompanied by a small proportion of $(Glc)_2$ and $(Glc)_4$ (Fig. 5d). Using $(Glc)_4$ as substrate, product signals $(GlcN)_2$ and $(GlcN)_3$ were observed (Fig. 5e). As well as for monomeric GlcN, the signal from Glc could not be detected in the presence of enzyme (data not shown). In contrast with the chitosan-derived hexasaccharide, the ratio of symmetrical/asymmetrical mode of cleavage of $(Glc)_6$ by Csn1794 was only 2:1.

This highlighted a substantial difference in productive substrate binding mode among chitosan and cellulose-derived hexasaccharides.

The conversion rates were calculated to determine Csn1794 activity towards the different substrates (Fig. 5 *): 228 min^{-1} for $(GlcN)_6$, 722 min^{-1} for $(GlcN)_5$, 0.4 min^{-1} for $(GlcN)_4$, 8 min^{-1} for $(Glc)_6$, and 0.2 min^{-1} for $(Glc)_4$. Thus, conversion rates were much faster for hexasaccharides than tetrasaccharides of both origins. Furthermore, hydrolysis was much faster for chitosan hexasaccharide than for cellulose hexasaccharide.

Stability at high temperatures in the presence of chitosan substrate

As shown in our previous work, some chitosanases are stabilized in the presence of chitosan as a result of specific enzyme–substrate interactions (Roy et al. 2007). The stability of the enzyme in the presence of its substrate can be estimated by calculating the chitosanase half-life from the time course of the reaction product accumulation at a given temperature, assuming a first-order deactivation kinetics (Přenosil et al. 1987; Fullbrook 1996; Blanchard et al. 2001; Roy et al. 2007). In these experiments, the enzyme concentration was maintained at low levels, thus avoiding substrate depletion during the 6-h incubations. The following chitosanase half-life values were found by analysis of time-course curves shown in Fig. 6: 1,387 min at 70 °C, 129 min at 75 °C, and 108 min at 78 °C. The time course of hydrolysis at 70 °C was quasi-linear, and Csn1794 kept at least 50 % of its activity for more than 20 h.

Cloning and sequencing of 1794 chitosanase gene

The purified Csn1794 protein was used to determine several partial amino acid sequences. These sequences were used to synthesize degenerate oligonucleotides, which served as primers for PCR amplification of a portion of the chitosanase gene using as template the genomic DNA of *Paenibacillus* sp. 1794. Nucleotide sequencing of the amplified fragment confirmed its similarity to other known chitosanases belonging to the GH8 family of glycoside hydrolases. The PCR-amplified fragment was used as a probe in Southern blotting experiments with genomic DNA digested with various restriction enzymes. The results showed that the chitosanase-encoding gene was localized to a *Bsp*E1 restriction fragment of about 6 kb.

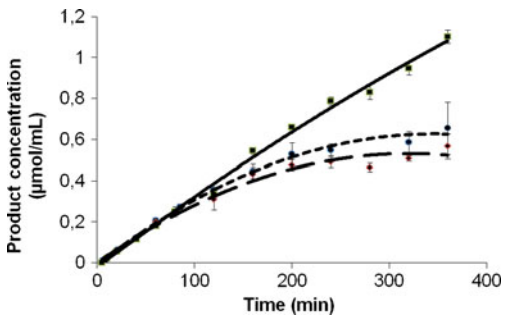

Fig. 6 Time course of chitosan hydrolysis product accumulation at high temperatures. Chitosan (Sigma-Aldrich; DDA=0.84) concentration: 5 g/L in 0.25 M acetic acid; pH 4.5. Product concentration was determined by the reducing sugar assay; *square* 70 °C, *circle* 75 °C, *diamond* 78 °C

A partial genomic library of *Paenibacillus* sp. was constructed ligating *Bsp*E1 fragments of 5–7 kb into *Bsp*E1-digested Litmus 38i vector. Chitosanase-positive clones were selected on a nutrient agar medium supplemented with 5 mg/ml of dyed chitosan sRBB-C (Zitouni et al. 2010). At this concentration, sRBB-C was inhibitory for *Escherichia coli*; however, the clones harboring the chitosanase gene were able to grow in its presence, due to the protective effect of chitosanase against the antimicrobial activity of chitosan (Lacombe-Harvey et al. 2009; Ghinet et al. 2009). Restriction analysis of 18 chitosan-resistant clones showed that they all harbored identical inserts of 5.8 kb. One insert was entirely sequenced (GenBank accession number JX109837); it included an open reading frame of 1,233 bp identifying a chitosanase polypeptide of 410 residues (Suppl. Fig. 2) apparently not localized inside an operon. The ORF began with two potential start codons: GTG followed by ATG, preceded by a well-defined putative ribosome-binding site. No attempts were made to determine which of the two potential start codons was used for translation initiation in vivo. The 5′-RACE method (Bensing et al. 1996) allowed the identification of the transcription start site (nucleotide 44 on Suppl. Fig. 2), revealing relatively well-defined −35 and −10 boxes of a putative SigA-type transcription promoter (Suppl. Fig. 2).

Analysis of the amino acid sequence by SignalP (Petersen et al. 2011) determined a signal peptide with a most probable signal peptidase cleavage site localized after the first 32 residues (Suppl. Fig. 2). The resulting mature extracellular Csn1794 protein is composed of 378 residues with a calculated molecular weight of 41.8 kDa. The predicted *N* terminus of mature Csn1794 enzyme coincided with the experimentally determined *N* terminus of the endoglycanase Pgl8a from *Paenibacillus cooki* (Shinoda et al. 2012). Alignment of primary sequence of Csn1794 with that of the ChoK chitosanase from *Bacillus* sp K17, for which the tertiary structure has been solved (Adachi et al. 2004) suggested Glu64 and Glu254 as catalytic residues.

Discussion

We isolated a novel strain of *Paenibacillus* producing a highly thermostable chitosanase. Our selection and screening procedure differed in several ways from approaches described in the

literature. Most often, chitosanase-producing strains have been found by plating serial dilutions of bacteria from various environmental samples on agar media containing chitosan or a β-glucan. The best producers were thus selected according to the largest degradation areas around their colonies (Boucher et al. 1992; Kimoto et al. 2002; Lee et al. 2006; Shinoda et al. 2012). In our case, we first performed an enrichment procedure, starting with shrimp shells compost mixed with chitosan preparations of various molecular weights, wetted with solutions of varying composition and incubated at various temperatures. After incubation, samples were submitted to additional selective treatments, shown to favor the recovery of spore-producing microorganisms (Nonomura and Hayakawa, 1988). Diverging further from the usual procedures, the best chitosanase producers were chosen following cultures in liquid medium using a chitosanase assay adapted to microtiter plates (Zitouni et al. 2010). The final screening step was focused on chitosanase thermostability, by determination of enzyme half-life in the presence of chitosan substrate. As a result, we selected a microorganism producing a highly thermostable chitosanase with a half-life of approximately 22 h at 70 °C.

While the 1794 isolate seems to be a novel one, the genus *Paenibacillus* to which it belongs is already well represented among known chitosanase producers (Kimoto et al. 2002; Shinoda et al. 2012). So far, most of the chitosanases from paenibacilli belong to GH8 family of glycoside hydrolases. Besides chitosan, GH8 chitosanases can hydrolyze soluble derivatives of cellulose (such as CM-cellulose) or β-1,3-1, 4-glucans and are sometimes designated as chitosanases-glucanases. They catalyze the endo-hydrolysis of their respective substrates with inversion of the anomeric configuration (Adachi et al. 2004). The determination of the tertiary structure of the GH8 chitosanase ChoK from *Bacillus* sp. K17 identified the catalytic residues and revealed the division of the GH8 family into three subfamilies. While all GH8 enzymes share a strictly conserved proton donor residue (Glu64 in Csn1794), the criterion governing the distinction among subfamilies is the localization of the catalytic proton acceptor (Adachi et al. 2004). In the best studied subfamily GH-8a which group cellulases and xylanases, the proton acceptor is an aspartate. The GH8 chitosanases, including Csn1794, belong to subfamily GH-8b and their proton acceptor residue is a glutamate localized on an insertion loop (Adachi et al. 2004). This finding from crystallography was confirmed by site-directed mutagenesis studies of ChoK and of the chitosanase from *Paenibacillus fukuinensis* (Adachi et al. 2004; Isogawa et al. 2009). However, the identification of the proton acceptor in Csn1794 was not immediately evident, as an aspartate (Asp255) and not a glutamate was aligned with the catalytic residue of ChoK using popular algorithms such as T-Coffee (Fig. 7) (Notredame et al. 2000). We however rejected this aspartate as a possible catalytic residue because of the presence of a glycine in the

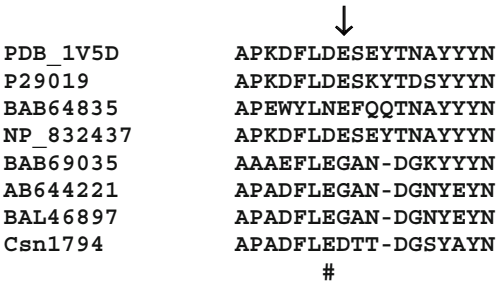

Fig. 7 Alignment of residues surrounding the catalytic proton acceptor in several members of the GH-8b subfamily. Proteins are identified by their GenBank or Protein Data Bank accession numbers. *Downwards arrow* proton acceptor residue of ChoK chitosanase from *Bacillus* sp. K17; *number sign* suggested proton acceptor residue for Csn1794

corresponding position in other chitosanases (Fig. 7). The neighboring glutamate (Glu254) appears to be the best candidate for a catalytic residue. At the same time, this alignment revealed possibility of heterogeneity in the structures of the loop accommodating the proton acceptor residue inside the GH-8b subfamily.

The mode of substrate hydrolysis was studied towards chitosan- and cello-oligosaccharides by real-time ESI-MS. The hexasaccharides $(GlcN)_6$ and $(Glc)_6$ were thereby symmetrically hydrolyzed into two molecules $(GlcN)_3$ and $(Glc)_3$, respectively. A significant amount of $(Glc)_6$ was also hydrolyzed into $(Glc)_4$ and $(Glc)_2$. In case of $(GlcN)_6$ a very small proportion of $(GlcN)_2$ and $(GlcN)_4$ was produced, even in assays with higher enzyme concentrations up to 50 nM (data not shown). $(GlcN)_5$ was hydrolyzed into similar amounts $(GlcN)_3$ and $(GlcN)_2$. Using the tetramers as substrates, trimers $(GlcN)_3$ and $(Glc)_3$ as well as dimers $(GlcN)_2$ and $(Glc)_2$ were observed. Main product of $(GlcN)_4$ was $(GlcN)_2$ with a smaller amount of $(GlcN)_3$, whereas $(Glc)_4$ was split in similar parts $(Glc)_3$ and $(Glc)_2$. As already described in the "Results" section, the monomers (GlcN) and (Glc) could not be detected in mass spectrometric experiments (Dennhart et al. 2008). Trimers $(GlcN)_3$ and $(Glc)_3$ were not hydrolyzed by the enzyme, even with 1 μM Csn1794. They thus bind unproductively to the enzyme. The hydrolysis profiles show that the enzyme needs at least three units on one of the two sides of the catalytic site to hydrolyze efficiently. On the basis of the substrate time courses the conversion rates were calculated to compare the specific activity of Csn1794 towards the various substrates. Conversion rates for $(GlcN)_6$ and $(GlcN)_5$ are about 500 to 1,000 times higher than the rate observed for $(GlcN)_4$. Thus, regarding the chain length of the substrates, the enzyme needs at least five sugar residues for efficient substrate hydrolysis, binding three units on one of the sides of the catalytic center, corroborating the above conclusion based on hydrolysis profiles.

On the other hand, the substrate with the glucosamine units shows higher conversion rates than the substrate with

glucose units. The conversion of $(GlcN)_6$ is about 30 times faster than for $(Glc)_6$. Hydrolysis of $(Glc)_6$ could not be significantly increased, even with higher substrate concentration of 25 μM $(Glc)_6$ with 10 or 50 nM Csn1794, which led to conversion rates of 20 and 21 min^{-1}, respectively (data not shown). Accordingly, the presence of charged amino groups in the substrate is important for substrate binding and enzyme activity. Interestingly, while the conversion for chitosan hexasaccharide is ~30× faster than that for cellulose hexasaccharide, the enzyme activity measured with high MW chitosan is only ~2× higher than on carboxymethyl cellulose. Again, the presence of charged groups could be responsible for the relatively fast hydrolysis of this soluble derivative of cellulose.

The cleavage mode observed for Csn1794 is in contrast with that of the GH46 chitosanase from *Streptomyces* sp. N174 (CsnN174), studied earlier by our group (Dennhart et al, 2008). Regarding the hydrolysis profile of $(GlcN)_n$ oligosaccharides with CsnN174, the cleavage of $(GlcN)_6$ into $(GlcN)_2$ and $(GlcN)_4$, was relatively more important (Dennhart et al. 2008). CsnN174 split $(GlcN)_4$ predominantly into $(GlcN)_2$ and only a negligible amount of $(GlcN)_3$. In the last study for the CsnN174 the substrate degradation rates were calculated as well: 290 min^{-1} for $(GlcN)_6$, 385 min^{-1} for $(GlcN)_5$, and 140 min^{-1} for $(GlcN)_4$. Calculation procedure in the current experiments is based on the newly introduced exponential function whereas for CsnN174 the calculation was based on the time point of complete substrate consumption (Dennhart et al. 2008; Scheerle et al. 2011). However, similar tendencies were observed. For both enzymes $(GlcN)_5$ showed the highest conversion rate, followed by $(GlcN)_6$. $(GlcN)_4$ gave the slowest conversion rate, whereby $(GlcN)_4$ was hydrolyzed much more effectively by CsnN174 than with Csn1794. Both enzymes did not hydrolyze $(GlcN)_3$. The lack of hydrolysis of trimers as well as the absence of a "5+1" type of cleavage of hexasaccharides indicates that both enzymes are essentially *endo*-type chitosanases.

The closest relatives of Csn1794 are the endoglycanase Pgl8a from *P. cookii* (85 % identity, 94 % similarity) and the glucanase from *Bacillus circulans* WL-12 (82 % identity, 89 % similarity) (Shinoda et al. 2012; Bueno et al. 1990). First identified as an endocellulase and a β-1,3-1,4-glucanase, respectively, both enzymes have chitosanase activity. As far as thermostability is concerned, these enzymes have been characterized by methods different from ours, so direct comparison is not possible. rPgl8a chitosanase, purified from a recombinant strain of *E. coli*, had maximal activity at 70 °C in a 20-min reaction with glycol chitosan (5 mg/ml) at pH 4.3, while Csn1794 had maximal activity at 80 °C in a 10-min reaction with chitosan (0.8 mg/ml) at pH 4.5. Interestingly, the maximal activity of rPgl8a in slightly alkaline conditions (pH 8) was observed at a much lower temperature of 50 °C. This suggested that the enzyme was stabilized by the presence of chitosan at acidic pH (Shinoda et al. 2012), corroborating our own observations on GH46 chitosanases (Roy et al. 2007). These findings emphasize again our choice to measure the thermostability of chitosanases in the presence of chitosan substrate as necessary to evaluate their real usefulness for large-scale hydrolysis of chitosan.

Acknowledgments Work at Université de Sherbrooke was supported by a Strategic Grant to RB and Discovery Grants to RB and SR from Natural Science and Engineering Council of Canada. Work at TU München was supported by the Arbeitsgemeinschaft industrieller Forschungsvereinigungen, Köln, Germany (project no. 16203N). The authors thank Dr. Brian Talbot for critical reading of the manuscript. A provisional patent on behalf the Université de Sherbrooke, involving MZ, MF, and RB has been filed regarding the application of this enzyme for chitosan hydrolysis.

References

Aam BB, Heggset EB, Norberg AL, Sørlie M, Vårum KM, Eijsink VGH (2010) Production of chitooligosaccharides and their potential applications in medicine. Mar Drugs 8:1482–1517. doi:10.3390/md8051482

Adachi W, Sakihama Y, Shimizu S, Sunami T, Fukazawa T, Suzuki M, Yatsunami R, Nakamura S, Takénaka A (2004) Crystal structure of family GH-8 chitosanase with subclass II specificity from *Bacillus* sp. K17. J Mol Biol 343:785–795. doi:10.1016/j.jmb.2004.08.028

Bensing BA, Meyer BJ, Dunny GM (1996) Sensitive detection of bacterial transcription initiation sites and differentiation from RNA processing sites in the pheromone-induced plasmid transfer system of *Enterococcus faecalis*. Proc Natl Acad Sci U S A 93:7794–7799

Blanchard J, Fukamizo T, Boucher I, Brzezinski R (2001) High level expression of the chitosanase from *Streptomyces* sp. N174 and study of its intramolecular interactions. Recent Res Dev Microbiol 5:111–121

Boucher I, Dupuy A, Vidal P, Neugebauer WA, Brzezinski R (1992) Purification and characterization of a chitosanase from *Streptomyces* N174. Appl Microbiol Biotechnol 38:188–193

Bradford MM (1976) A rapid and sensitive method for the quantitation of microgram quantities of protein utilizing the principle of protein-dye binding. Anal Biochem 72:248–254. doi:10.1016/0003-2697(76)90527-3

Bueno A, Vazquez de Aldana CR, Correa J, del Rey F (1990) Nucleotide sequence of a 1,3-1,4-β-glucanase-encoding gene in *Bacillus circulans* WL-12. Nucl Acids Res 18:4248

Chen X, Zhai C, Kang L, Li C, Yan H, Zhou Y, Yu X, Ma L (2012) High-level expression and characterization of a highly thermostable chitosanase from *Aspergillus fumigatus* in *Pichia pastoris*. Biotechnol Lett 34:689–694. doi:10.1007/s10529-011-0816-0

Crini G, Guibal É, Morcellet M, Torri G, Badot P-M. (2009) Chitine et chitosane. Préparation, propriétés et principales applications. In : Crini G, Badot P-M, Guibal É (ed) Chitine et chitosane. Du biopolymère à l'application, Presses universitaires de Franche-Comté, pp 19–54

Dahllöf I, Baillie H, Kjelleberg S (2000) *rpoB*-based microbial community analysis avoids limitations inherent in 16S rRNA gene

intraspecies heterogeneity. Appl Environ Microbiol 66:3376–3380. doi:10.1128/AEM.66.8.3376-3380.2000

Dai T, Tanaka M, Huang Y-Y, Hamblin MR (2011) Chitosan preparations for wounds and burns: antimicrobial and wound-healing effects. Expert Rev Anti Infect Ther 9:857–879. doi:10.1586/eri.11.59

Da Mota FF, Gomes EA, Paiva E, Rosado AS, Seldin L (2004) Use of *rpoB* gene analysis for identification of nitrogen-fixing *Paenibacillus* species as an alternative to the 16S rRNA gene. Lett Appl Microbiol 39:34–40. doi:10.1111/j.1472-765X.2004.01536.x

Dennhart N, Fukamizo T, Brzezinski R, Lacombe-Harvey M-È, Letzel T (2008) Oligosaccharide hydrolysis by chitosanase enzymes monitored by real-time electrospray ionization-mass spectrometry. J Biotechnol 134:253–260. doi:10.1016/j.jbiotec.2008.02.004

Desbrieres J (2002) Viscosity of semiflexible chitosan solutions: influence of concentration, temperature and role of intermolecular interactions. Biomacromolecules 3:342–349. doi:10.1021/bm010151+

Domard A (2011) A perspective on 30 years research on chitin and chitosan. Carbohydr Pol 84:696–703. doi:10.1016/j.carbpol.2010.04.083

Ekowati E, Hariyadi P, Witarto AB, Hwang JK, Suhartono MT (2006) Biochemical characteristics of chitosanase from the Indonesian *Bacillus licheniformis* MB-2. Mol Biotechnol 33:93–102. doi:10.1385/MB:33:2:93

Evans PD, Cook SN, Riggs PD, Noren CJ (1995) LITMUS: multipurpose cloning vector with a novel system for bidirectional *in vitro* transcription. Biotechniques 19:130–135

Fullbrook PD (1996) Practical limits and prospects (kinetics). In: Godfrey T, West S (eds) Industrial enzymology. Macmillan Press, London, pp 503–540

Ghinet MG, Gagnon J, Lacombe-Harvey M-È, Brzezinski R (2009) Molecular weight modulates the antimicrobial effect of chitosan on *Escherichia coli*. In: Rustichelli F, Caramella C, Şenel S, Vårum KM (eds) Advances in chitin sciences, vol. XI, Venice, Italy

Ghinet MG, Roy S, Poulin-Laprade D, Lacombe-Harvey M-E, Morosoli R, Brzezinski R (2010) Chitosanase from *Streptomyces coelicolor* A3(2): biochemical properties and role in protection against antibacterial effect of chitosan. Biochem Cell Biol 88:907–916. doi:10.1139/o10-109

Hamdine M, Heuzey M-C, Bégin A (2005) Effect of organic and inorganic acids on concentrated chitosan solutions and gels. Int J Biol Macromol 37:134–142

Hirano S, Ohe Y (1975) A facile *N*-acylation of chitosan with carboxylic anhydrides in acidic solutions. Carbohydr Res 41:C1–C2

Hoell IA, Vaaje-Kolstad G, Eijsink VGH (2010) Structure and function of enzymes acting on chitin and chitosan. Biotechnol Genet Eng Rev 27:331–366

Il'ina AV, Varlamov VP (2003) Effect of the degree of acetylation of chitosan on its enzymatic hydrolysis with the preparation celloviridin G20kh. Appl Biochem Microbiol 39:239–242. doi:10.1023/A:1023515308584

Isogawa D, Fukuda T, Kuroda K, Kusaoke H, Kimoto H, Suye S, Ueda M (2009) Demonstration of catalytic proton acceptor of chitosanase from *Paenibacillus fukuinensis* by comprehensive analysis of mutant library. Appl Microbiol Biotechnol 85:95–104. doi:10.1007/s00253-009-2041-5

Kimoto H, Kusaoke H, Yamamoto I, Fujii Y, Onodera T, Taketo A (2002) Biochemical and genetic properties of *Paenibacillus* glycosyl hydrolase having chitosanase activity and discoidin domain. J Biol Chem 277:14695–14702. doi:10.1074/jbc.M108660200

Kong M, Chen XG, Xing K, Park HJ (2010) Antimicrobial properties of chitosan and mode of action: a state of the art review. Int J Food Microbiol 144:51–63. doi:10.1016/j.ijfoodmicro.2010.09.012

Lacombe-Harvey M-È, Fukamizo T, Gagnon J, Ghinet MG, Dennhart N, Letzel T, Brzezinski R (2009) Accessory active site residues of *Streptomyces* sp. N174 chitosanase: variations on a common theme in the lysozyme superfamily. FEBS J 276:857–869

Lavertu M, Xia Z, Serreqi AN, Berrada M, Rodrigues A, Wang D, Buschmann MD, Gupta A (2003) A validated ^{1}H NMR method for the determination of the degree of deacetylation of chitosan. J Pharm Biomed Anal 32:1149–1158. doi:10.1016/S0731-7085(03)00155-9

Lee YS, Yoo JS, Chung SY, Lee YC, Cho YS, Choi YL (2006) Cloning, purification, and characterization of chitosanase from *Bacillus* sp. DAU101. Appl Microbiol Biotechnol 73:113–121. doi:10.1007/s00253-006-0444-0

Lever M (1972) A new reaction for colorimetric determination of carbohydrates. Anal Biochem 47:273–279. doi:10.1016/0003-2697(72)90301-6

Muzzarelli RAA, Lough C, Emanuelli M (1987) The molecular weight of chitosans studied by laser light-scattering. Carbohydr Res 164:433–442. doi:10.1016/0008-6215(87)80146-5

Nonomura H, Hayakawa M (1988) New methods for selective isolation of soil actinomycetes. In: Okami Y, Beppu T, Ogawara H (eds) Biology of actinomycetes '88. Japan Scientific Societies Press, Tokyo, pp 288–293

Notredame C, Higgins DG, Heringa J (2000) T-Coffee: a novel method for fast and accurate multiple sequence alignment. J Mol Biol 302:205–217. doi:10.1006/jmbi.2000.4042

Petersen TN, Brunak S, von Heijne G, Nielsen H (2011) SignalP 4.0: discriminating signal peptides from transmembrane regions. Nature Methods 8:785–786. doi:10.1038/nmeth.1701

Přenosil JE, Dunn IJ, Heinzle E (1987) Biocatalyst reaction engineering. In: Kennedy JF (ed) Biotechnology, vol 7a, Enzyme technology. VCH, Weinheim, pp 489–545

Pscheidt B, Glieder A (2008) Yeast cell factories for fine chemical and API production. Microb Cell Fact 7:25. doi:10.1186/1475-2859-7-25

Roberts GAF (1992) Chitin chemistry. MacMillan, London

Roy S, Gagnon J, Fortin M, Ghinet MG, LeHoux J-G, Dupuis G, Brzezinski R (2007) Quantitative fluorometric analysis of the protective effect of chitosan on thermal unfolding of catalytically active native and genetically-engineered chitosanases. Biochim Biophys Acta—Proteins Proteom 1774:975–984. doi:10.1016/j.bbapap. 2007.05.016

Rwei SP, Chen TY, Cheng YY (2005) Sol/gel transition of chitosan solutions. J Biomater Sci Polymer Edn 16:1433–1445. doi:10.1163/156856205774472290

Sambrook J, Fritsch EF, Maniatis T (1989) Molecular cloning, a laboratory manual, 2nd edn. Cold Spring Harbor Laboratory, Cold Spring Harbor

Scheerle RK, Grassmann J, Letzel T (2011) Enzymatic conversion continuously monitored with a robotic nanoESI-MS tool: experimental status. Anal Methods 3:822–830. doi:10.2116/analsci.28.607

Schep GP, Shepherd MG, Sullivan PA (1984) Purification and properties of a β-1,6-glucanase from *Penicillium brefeldianum*. Biochem J 223:707–714

Shinoda S, Kanamasa S, Arai M (2012) Cloning of an endoglycanase gene from *Paenibacillus cookii* and characterization of the recombinant enzyme. Biotechnol Lett 34:281–286. doi:10.1007/s10529-011-0759-5

Sorlier P, Denuzière A, Viton C, Domard A (2001) Relation between the degree of acetylation and the electrostatic properties of chitin and chitosan. Biomacromolecules 2:765–772. doi:10.1021/bm015531+

Yoon H-G, Ha S-C, Lim Y-H, Cho H-Y (1998) New thermostable chitosanase from *Bacillus* sp.: purification and characterization. J Microbiol Biotechnol 8:449–454

Yoon H-G, Kim H-Y, Kim H-K, Hong B-S, Shin D-H, Cho H-Y (2001) Thermostable chitosanase from *Bacillus* sp. strain CK4: its purification, characterization and reaction pattern. Biosci Biotechnol Biochem 65:802–809

Zitouni M, Fortin M, Thibeault J-S, Brzezinski R (2010) A dye-labelled soluble substrate for the assay of endo-chitosanase activity. Carbohydr Polym 80:522–525. doi:10.1016/j.carbpol.2009.12.012